



*ugr*

Universidad  
de **Granada**

**DOCTORAL THESIS**

**INTEGRATED TECHNOLOGIES BASED ON THE USE OF  
ACTIVATED CARBON AND RADIATION TO REMOVE  
CONTAMINANTS PRESENT IN LANDFILL LEACHATES**

**TECNOLOGÍAS INTEGRADAS BASADAS EN EL USO DE  
CARBÓN ACTIVADO Y RADIACIÓN PARA LA ELIMINACIÓN  
DE CONTAMINANTES PRESENTES EN LIXIVIADOS DE  
VERTEDEROS**

Presented by

**Mahmoud Mohamed Mohamed**

**Granada, 2012**

Editor: Editorial de la Universidad de Granada  
Autor: Mahmoud Mohamed Mohamed  
D.L.: GR 588-2013  
ISBN: 978-84-9028-402-5



**TECNOLOGÍAS INTEGRADAS BASADAS EN EL USO DE  
CARBÓN ACTIVADO Y RADIACIÓN PARA LA  
ELIMINACIÓN DE CONTAMINANTES PRESENTES EN  
LIXIVIADOS DE VERTEDEROS**

**Por**

**Mahmoud Mohamed Mohamed**

Memoria presentada para aspirar al grado de Doctor  
por la Universidad de Granada

Fdo.: Mahmoud Mohamed Mohamed

Los Directores de la Tesis:

Dr. José Rivera Utrilla  
Catedrático de Química Inorgánica  
de la Universidad de Granada

Dr. Manuel Sánchez Polo  
Prof. Titular de Química Inorgánica  
de la Universidad de Granada

Dr. Raúl Ocampo Pérez  
Investigador del Dpto. de Química Inorgánica  
de la Universidad de Granada





José Rivera Utrilla, Catedrático de Química Inorgánica, Manuel Sánchez Polo, Profesor Titular de Química Inorgánica y Raúl Ocampo Pérez, Investigador del departamento de Química Inorgánica,

**CERTIFICAN QUE,**

Mahmoud Mohamed Mohamed, titulado en Ingeniería Civil, ha realizado la Tesis Doctoral **“Tecnologías integradas basadas en el uso de carbón activado y radiación para la eliminación de contaminantes presentes en lixiviados de vertederos”** en el Departamento de Química Inorgánica de la Facultad de Ciencias de la Universidad de Granada para aspirar al grado de Doctor, reuniendo las condiciones necesarias para ser presentada y defendida ante el tribunal correspondiente.

Y para que conste a los efectos oportunos, en cumplimiento de la legislación vigente, firmamos el presente certificado en Granada, a 21 de Septiembre del 2012.

Fdo.: José Rivera Utrilla  
Catedrático de Química Inorgánica de  
la Universidad de Granada

Fdo.: Manuel Sánchez Polo  
Prof. Titular de Química Inorgánica de  
la Universidad de Granada

Fdo.: Raúl Ocampo Pérez  
Investigador del Dpto. de Química Inorgánica  
de la Universidad de Granada



## **DEDICATION**

*This dissertation is dedicated to my parents and family, and to the people who dedicate their lives to seek for the truth...*



## ACKNOWLEDGEMENTS

*Praise be to ALLAH, the Cherisher and Sustainer of the worlds, who with his grace this work has been done...*

This thesis would have not been possible without the support of my supervisors, colleagues, family and friends who in different ways encouraged me and shared this long way. To all of you, I express my grateful acknowledgment and sincerely thank for bringing this thesis to a successful end.

With greatest appreciation, I acknowledge the friendship, support, insight and guidance of my supervisors: Prof. José Rivera Utrilla, for providing scientific consultation advice in all phases of my work and especially for his personal support always believing in my capabilities, being present at all times and giving me the needed strength to carry on when difficulties appeared and encouraging me to study earnestly and for his fatherly role inside and outside the work throughout my Ph.D. years; Dr. Manuel Sánchez Polo for his relentless efforts and I was lucky to work with a researcher like him who has a spirit of innovation with new ideas and applications in the scientific research; and to Dr Raúl Ocampo Pérez for his continuous assistance and constant hard work inspired me to better myself and to reach to higher aim.

My sincere thanks to Dr. José Diego Méndez for his support and valuable comments on both my thesis and future research career plans. I would like to express my gratitude to Dr. Isidora Bautista Toledo for her dedication, valuable advices, for being present and helping me in every ways possible, for her motherly role through the thesis period and her gifts (wonderful toys) to my daughter. I really thank you so much for your kindness.

I would also like to thank Dr. Jesús J. López Peñalver for his contributions of time, ideas and continuous assistant in the radyolsis work. Furthermore, I want to thank Dr. Alegría Carrasco from Analytic Chemistry Department for her collaboration to identify the byproduct compounds from different processes which were studied in this thesis. Moreover, to express my gratefulness to Dr. Rafael Robles from Organic Chemistry Department for invaluable discussions on the reaction mechanisms and special gratitude

to Dr. Antonio Mota from Inorganic Chemistry Department for his efforts in the energetic calculations to form radicals in the photooxidation work.

I am indebted to many of my colleagues who supported me and help me since the first day I was here: Gonzalo, Carla, Inma, Valente, Jacob, Jorge, Elmouwahidi, Zula, David, Esther, José, Paulina, Saied, Ibrahim, Adel, Elena, Santiago, Marta, Abdelhakim, Abdullah, and Drs. Carlos Moreno, María Angeles, Francisco Carrasco, Francisco Maldonado, Agustín Francisco, Montserrat Zamorano, Miguel Ángel, Sahar El-Shatoury, Ihsan, Amani, Maria, Antonio and Angel.

Acknowledgements are also owed to my friends in Granada from different countries who have been the best friends during my stay in Granada: Mohamed, Yassir, Nabil, Mariam, Omar, Siddiq, Chakib, Boubker, Kitani, Obid, Tarek, Mustafa, Abdel aziz, Ibrahim, Elena, Ridwan, Idres, Sidi Hamida, Segad, Wanda, Inma, Itgar, Hassan, Lala, Mohamed, Conchi, Francisco, Hanan, Walid, Ismail and many more.

I dedicate this work to my father, my mother, my sisters, and my brothers. Without their care and support from childhood to now, I would never have made it through this process or any of the tough times in my life.

A special thanks to my wife for helping me throughout my life, making me believe that I am capable of everything, giving me important advices and listening to me and special thanks to her patience and her extreme efforts.

A very special thanks to ALLAH for his gift, my daughter Mariam, who makes me happy in the tough times and for letting me sleep during some nights in the last period of this work.

Finally, I would like to thank everybody who was important to the successful realization of my thesis, as well as expressing my apology for every one that I unfortunately forgot to mention.

This doctoral thesis has been achieved through financial support provided by Ministry of Science and Innovation of Spain and funds from FEDER (CTQ2007-97792-C02-01 and CTQ2011-29035-C02-02), and the Junta de Andalucía (RNM7522 and 3823).



**CONTENIDOS Y ESTRUCTURA  
DE LA TESIS**





## CONTENIDOS Y ESTRUCTURA DE LA TESIS

En esta Tesis Doctoral se estudia la eliminación de cinco contaminantes presentes en los lixiviados (ácido ftálico, bisfenol A, ácido difenólico, ácido 2,4-diclorofenoxiacético y ácido 4-cloro-2-metilfenoxiacético), en fase acuosa, mediante las técnicas de adsorción sobre carbones activados, fotooxidación y radiólisis. Los resultados experimentales obtenidos y la discusión de los mismos se presentan en esta Memoria divididos en siete Capítulos.

El **primer Capítulo**, dedicado a la introducción del trabajo desarrollado en la Tesis, comienza analizando la problemática actual de la contaminación de las aguas por los contaminantes seleccionados para este estudio y los métodos más idóneos para su eliminación. A continuación, se exponen los fundamentos de los tratamientos utilizados y, al final del Capítulo, se indican los objetivos de la Tesis.

En el **segundo Capítulo** se analiza el comportamiento de dos carbones activados comerciales de diferentes características texturales y químicas en los procesos de adsorción de los cinco contaminantes seleccionados. Este Capítulo se centra, fundamentalmente, en el estudio de las cinéticas de adsorción de estos compuestos aplicando diferentes modelos cinéticos y difusionales y relacionando los resultados obtenidos con las características físicas y químicas de los carbones activados y de los adsorbatos.

En el **tercer Capítulo** se estudia el proceso de adsorción del ácido ftálico sobre carbones activados tanto en régimen estático como dinámico. Concretamente, en este Capítulo, se analizan las isotermas de adsorción y las curvas de rotura de las columnas y se evalúa la influencia de diferentes parámetros como son: pH de la disolución, fuerza iónica, tipo de agua (ultrapura, subterránea, superficial y residual) y presencia de microorganismos en el medio (bioadsorción).

El **cuarto Capítulo** aborda el estudio de la eficiencia de la radiación UV en la fotodegradación directa e indirecta (en presencia de generadores de radicales hidroxilo,

sulfato o carbonato/bicarbonato) del bisfenol A. Para ello, se realiza un estudio cinético y se analiza la influencia de las distintas variables operacionales, así como la evolución de la concentración del carbono orgánico total y la toxicidad del sistema durante la fotodegradación del contaminante, tanto en agua ultrapura como aguas naturales (subterránea, superficial y residual).

El **quinto Capítulo** estudia el papel que juega el carbón activado en la fotodegradación catalítica del ácido 2, 4-diclorofenoxiacético mediante el Proceso de Oxidación Avanzada basado en radiación UV/TiO<sub>2</sub>/carbón activado. Se evalúa la influencia de las características texturales y químicas de los carbones activados, tanto originales como oxidados, en el rendimiento de la degradación y se propone el mecanismo a través del cual se potencia la degradación del contaminante en presencia de carbón.

El **sexto Capítulo** se centra en el uso de la radiación gamma, como Proceso Avanzado de Oxidación/Reducción, para la eliminación de los cinco contaminantes seleccionados. Se estudian las cinéticas de descomposición y se determinan los valores de las constantes de velocidad de degradación de cada uno de los compuestos con el radical hidroxilo, electrón y átomo de hidrógeno generados por la radiólisis del agua. Los valores de estas constantes se relacionan con la composición química de las correspondientes moléculas de los contaminantes.

En el **séptimo Capítulo** se exponen los resultados obtenidos al tratar, con radiación gamma, aguas contaminadas con ácido difenólico. Se estudia el efecto de los parámetros operacionales (velocidad de dosis, concentración inicial de contaminante, pH y contenido de oxígeno de la disolución) y de la presencia de diferentes aniones inorgánicos en la degradación del contaminante. Además, se evalúa la influencia de la matriz del agua (ultrapura, superficial y residual) y la evolución del carbono orgánico total y la toxicidad del medio acuoso en función de la dosis de radiación adsorbida. Esta Memoria termina con un apartado donde se resumen las conclusiones globales obtenidas de la presente Tesis Doctoral.

Los resultados del trabajo de investigación realizado durante el desarrollo de esta Tesis se recogen en los siguientes artículos:

- José Rivera-Utrilla, Manuel Sánchez-Polo, Mahmoud M. Abdel daiem, Raúl Ocampo-Pérez. *Role of activated carbon in the photocatalytic degradation of 2, 4- dichlorophenoxyacetic acid by the UV/TiO<sub>2</sub>/activated carbon system*. Journal of Applied Catalysis B: Environmental, **126**, 100–107 (2012) (I.F. 5.625).
- Raúl Ocampo-Pérez, Mahmoud M. Abdel daiem, José Rivera-Utrilla, José D. Méndez-Díaz, Manuel Sánchez-Polo. *Modeling adsorption rate of organic micropollutants present in landfill leachates onto granular activated carbon*. Journal of Colloid and Interface Science, **385**, 174–182 (2012) (I.F. 3.070).
- Mahmoud M. Abdel daiem, Raúl Ocampo-Pérez, José Rivera-Utrilla, Manuel Sánchez-Polo, José D. Méndez-Díaz. *Environmental impact of phthalate acid esters and their removal from water and sediments by different technologies - A review*. Journal of Environmental Management, **109**, 164–178 (2012) (I.F. 3.245).
- José D. Méndez-Díaz, Mahmoud M. Abdel daiem, José Rivera-Utrilla, Manuel Sánchez-Polo, Isidora Bautista-Toledo. *Adsorption/Bioadsorption of Phthalic Acid, an Organic Micropollutant Present in Landfill Leachates, on Activated Carbons*. Journal of Colloid and Interface Science, **369**, 358–365 (2012) (I.F. 3.070).
- Mahmoud M. Abdel daiem, Raúl Ocampo-Pérez, José Rivera-Utrilla, Manuel Sánchez-Polo, Jesús J. López-Peñalver. *Rate constants for reactions of hydrated electrons, hydrogen atoms, and hydroxyl radicals in aqueous solution with organic micropollutants detected in landfill leachates*. Submitted for publication.

- Manuel Sánchez-Polo, Mahmoud M. Abdel daiem, Raúl Ocampo-Pérez, José Rivera-Utrilla. *Comparative study of the photodegradation of bisphenol a by  $HO^\bullet$ ,  $SO_4^{\bullet-}$  AND  $CO_3^{\bullet-}/HCO_3^{\bullet-}$  radicals in aqueous phase*. Submitted for publication.
- Mahmoud M. Abdel daiem, José Rivera-Utrilla, Raúl Ocampo-Pérez, Manuel Sánchez-Polo, Jesús J. López-Peñalver. *Treatment of water contaminated with diphenolic acid by gamma radiation in the presence of different compounds*. Submitted for publication.

Los resultados más relevantes de esta Tesis se han presentado, además, en los siguientes congresos científicos:

- [1] XXX VII Reunión Ibérica de Adsorción (RIA). Sevilla, España, Septiembre 2012.
- [2] VIII International Congress of Chemical Engineering (ANQUE). Sevilla, Spain, June 2012.
- [3] The Annual World Conference on Carbon (CARBON). Krakow, Poland, June 2012.
- [4] X<sup>th</sup> International Symposium on Environment, Catalysis and Process Engineering (ECGP'10). Fez, Morocco, April 2012.
- [5] XI Reunión del Grupo Español del Carbón (GEC). Badajoz, España, Octubre 2011.
- [6] VII International Congress of Chemical Engineering (ANQUE). Oviedo, Spain, June 2010.
- [7] X Reunión del Grupo Español del Carbón (GEC). Gerona, España, Mayo 2010.



# ÍNDICE



## **CAPÍTULO 1. INTRODUCCIÓN**

27

|  |     |
|--|-----|
| <b>1. ENVIRONMENTAL IMPACT AND TREATMENT OF CONTAMINANTS PRESENT IN LANDFILL LEACHATES STUDIED IN THE PRESENT DOCTORAL THESIS</b>        | 29  |
| <b>1.1. Bisphenol A</b>  | 30  |
| <b>1.2. Diphenolic acid</b>  | 31  |
| <b>1.3. 2,4- Dichlorophenoxyacetic acid</b>  | 31  |
| <b>1.4. 4-chloro-2-methylphenoxyacetic acid</b>  | 31  |
| <b>1.5. Removal of BPA, DPA, 2,4-D, and MCPA from aqueous solution by means of different technologies</b>                                | 32  |
| <b>1.6. References</b>   | 42  |
| <b>1.7. ENVIRONMENTAL IMPACT OF PHTHALIC ACID ESTERS AND THEIR REMOVAL FROM WATER AND SEDIMENTS BY DIFFERENT TECHNOLOGIES - A REVIEW</b> | 49  |
| 1.7.1. Introduction  | 51  |
| 1.7.2. Phthalic acid esters  | 53  |
| <i>1.7.2.1. Properties, classification and applications of phthalates (PAEs)</i>   | 53  |
| <i>1.7.2.2. PAEs in the environment</i>  | 55  |
| <i>1.7.2.3. Toxicity and effects on human health</i>   | 58  |
| <i>1.7.2.4. Legislations and restrictions</i>  | 60  |
| 1.7.3. Removal of PAEs from water and sediments by means of different technologies   | 62  |
| <i>1.7.3.1. Physical/Chemical treatments</i>   | 62  |
| <i>1.7.3.2. Biological treatments</i>  | 64  |
| <i>1.7.3.3. Advanced oxidation processes</i>   | 68  |
| <i>1.7.3.4. Wastewater and sludge treatment plants</i>   | 69  |
| 1.7.4. Conclusions   | 81  |
| 1.7.5. References  | 82  |
| <b>2. FUNDAMENTOS QUÍMICOS DE LOS SISTEMAS DE TRATAMIENTO APLICADOS</b>  | 101 |



|   |     |
|---|-----|
| <b>2.1. Adsorción sobre carbón activado</b>   | 101 |
| 2.1.1. Textura porosa de los carbones activados   | 102 |
| 2.1.2. Química superficial de los carbones activados  | 103 |
| 2.1.3. Uso del carbón activado como agente depurador de las aguas   | 105 |
| 2.1.4. Adsorción de compuestos aromáticos sobre carbón activado en fase acuosa  | 106 |
| <b>2.2. Procesos avanzados de oxidación</b>   | 107 |
| 2.2.1. Procesos avanzados de oxidación basados en la radiación UV   | 109 |
| 2.2.2. Fotocatálisis heterogénea  | 111 |
| 2.2.3. Procesos avanzados de oxidación basados en la radiación gamma  | 113 |
| <b>2.3. Bibliografía</b>  | 117 |
| <b>3. OBJETIVOS DEL TRABAJO DESARROLLADO EN LA PRESENTE TESIS DOCTORAL</b>  | 125 |
| <br>  |     |
| <b><u>CAPÍTULO 2. MODELADO DE LA VELOCIDAD DE ADSORCIÓN DE MICROCONTAMINANTES ORGÁNICOS PRESENTES EN LOS LIXIVIADOS DE VERTEDERO SOBRE CARBÓN ACTIVADO GRANULAR</u></b> | 127 |
| <br>  |     |
| <b>1. INTRODUCTION</b>  | 133 |
| <b>2. DIFFUSIONAL AND KINETIC MODELS</b>  | 134 |
| <b>2.1. Diffusional model</b>   | 134 |
| <b>2.2. Kinetics models</b>   | 135 |
| <b>3. EXPERIMENTAL</b>  | 136 |
| <b>3.1. Reagents</b>  | 136 |
| <b>3.2. Activated carbons</b>   | 137 |
| <b>3.3. Adsorption isotherms</b>  | 137 |
| <b>3.4. Adsorption kinetics</b>   | 139 |
| <b>4. RESULTS AND DISCUSSION</b>  | 139 |
| <b>4.1. Characterization of activated carbons</b>   | 139 |

|   |     |
|---|-----|
| 4.2. Adsorption isotherm of micropollutants on activated carbon                   | 142 |
| 4.3. Calculation of mass transport parameters                                     | 144 |
| 4.4. Pore volume diffusion model (PVDM)   | 145 |
| 4.5. Pore volume and surface diffusion model (PVSDM)                              | 148 |
| 4.6. Effect of the mass external transport on overall adsorption rate             | 150 |
| 4.7. Effect of the adsorbed pollutant mass on the effective diffusion coefficient | 150 |
| 4.8. Interpretation of the adsorption rate data with the kinetic models           | 154 |
| 5. CONCLUSIONS  | 155 |
| 6. REFERENCES   | 157 |

**CAPÍTULO 3. ADSORCIÓN/BIOADSORCIÓN DE ÁCIDO FTÁLICO, UN MICROCONTAMINANTE ORGÁNICO PRESENTE EN LOS LIXIVIADOS DE VERTEDERO, SOBRE CARBONES ACTIVADOS**

|   |     |
|---|-----|
| 1. INTRODUCTION   | 165 |
| 2. EXPERIMENTAL   | 166 |
| 2.1. Reagents   | 166 |
| 2.2. Activated carbon   | 166 |
| 2.3. PA adsorption on activated carbon  | 167 |
| 3. RESULTS AND DISCUSSION   | 169 |
| 3.1. Characterization of activated carbon   | 169 |
| 3.2. Phthalic acid adsorption process   | 173 |
| 3.3. Influence of both medium pH and solution ionic strength on PA adsorption       | 175 |
| 3.4. Influence of the presence of microorganisms on PA adsorption (bioadsorption)   | 177 |
| 3.5. Influence of the chemical characteristics of the water matrix on PA adsorption | 179 |
| 3.6. PA adsorption on activated carbon in dynamic regime                            | 181 |

|                       |     |
|-----------------------|-----|
| <b>4. CONCLUSIONS</b> | 182 |
| <b>5. REFERENCES</b>  | 184 |

**CAPÍTULO 4. ESTUDIO COMPARATIVO DE LA FOTODEGRADACIÓN DEL BISFENOL A CON RADICALES HO<sup>•</sup>, SO<sub>4</sub><sup>•-</sup>, Y CO<sub>3</sub><sup>•-</sup>/HCO<sub>3</sub><sup>•</sup> EN FASE ACUOSA** 189

|   |     |
|---|-----|
| <b>1. INTRODUCTION</b>  | 193 |
| <b>2. MATERIALS AND METHODS</b>   | 195 |
| <b>2.1. Reagents</b>  | 195 |
| <b>2.2. Experimental methodology</b>  | 195 |
| <b>2.3. Bisphenol A degradation by UV, UV/H<sub>2</sub>O<sub>2</sub>, UV/K<sub>2</sub>S<sub>2</sub>O<sub>8</sub>, and UV/Na<sub>2</sub>CO<sub>3</sub> systems</b> | 196 |
| <b>2.4. Analytical methods</b>  | 197 |
| <b>3. RESULTS AND DISCUSSION</b>  | 199 |
| <b>3.1. Photolysis of BPA</b>   | 199 |
| <b>3.2. Indirect photodegradation of BPA</b>  | 202 |
| 3.2.1. BPA photodegradation by UV/H <sub>2</sub> O <sub>2</sub> system  | 202 |
| 3.2.2. BPA photodegradation by UV/K <sub>2</sub> S <sub>2</sub> O <sub>8</sub> system   | 207 |
| 3.2.3. BPA photodegradation by UV/Na <sub>2</sub> CO <sub>3</sub> system  | 210 |
| <b>3.3. Time course of TOC and toxicity</b>   | 213 |
| <b>3.4. Comparison among UV/H<sub>2</sub>O<sub>2</sub>, UV/K<sub>2</sub>S<sub>2</sub>O<sub>8</sub>, and UV/Na<sub>2</sub>CO<sub>3</sub> systems</b>               | 215 |
| <b>4. CONCLUSIONS</b>   | 218 |
| <b>5. REFERENCES</b>  | 220 |

**CAPÍTULO 5. PAPEL DEL CARBÓN ACTIVADO EN LA DEGRADACIÓN FOTOCATALÍTICA DEL ÁCIDO 2,4-DICLOROFENOXIACÉTICO MEDIANTE EL SISTEMA UV/TiO<sub>2</sub>/CARBÓN ACTIVADO** 225

|                        |     |
|------------------------|-----|
| <b>1. INTRODUCTION</b> | 229 |
|------------------------|-----|

|  |     |
|--|-----|
| <b>2. EXPERIMENTAL METHOD</b>  | 231 |
| <b>2.1. Reagents</b>   | 231 |
| <b>2.2. Activated carbon</b>   | 231 |
| <b>2.3. Titanium dioxide</b>   | 233 |
| <b>2.4. Adsorption isotherms of 2,4-D on both activated carbon and TiO<sub>2</sub></b>                     | 233 |
| <b>2.5. Photoreactor design</b>  | 233 |
| <b>2.6. Photocatalytic degradation of 2,4-D in the presence of activated carbon and/or TiO<sub>2</sub></b> | 234 |
| <b>2.7. Determination of 2,4-D concentration in aqueous solution</b>                                       | 234 |
| <b>2.8. Determination of total organic carbon</b>  | 235 |
| <b>2.9. Determination of degradation byproduct toxicity</b>  | 235 |
| <b>3. RESULTS AND DISCUSSION</b>   | 235 |
| <b>3.1. Adsorption isotherms and adsorption kinetics of 2,4-D on activated carbon</b>                      | 235 |
| <b>3.2. Photocatalytic degradation of 2,4-D in the presence of the activated carbons</b>                   | 238 |
| <b>3.3. Effect of the mass of activated carbon and TiO<sub>2</sub> on 2,4-D photocatalytic degradation</b> | 242 |
| <b>3.4. 2,4-D photocatalytic degradation in the presence of radical scavengers</b>                         | 244 |
| <b>3.5. Time course of TOC and toxicity during 2,4-D degradation</b>                                       | 247 |
| <b>4. CONCLUSIONS</b>  | 249 |
| <b>5. REFERENCES</b>   | 250 |

|  |     |
|--|-----|
| <b><u>CAPÍTULO 6. CONSTANTES DE VELOCIDAD DE REACCIÓN DEL ELECTRÓN HIDRATADO, ÁTOMO DE HIDRÓGENO Y RADICAL HIDROXILO GENERADOS MEDIANTE RADIACIÓN GAMMA EN DISOLUCIÓN ACUOSA CON MICROCONTAMINANTES ORGÁNICOS DETECTADOS EN LIXIVIADOS DE VERTEDEROS</u></b> | 253 |
|--|-----|

|  |     |
|--|-----|
| <b>1. INTRODUCTION</b>   | 257 |
| <b>2. MATERIALS AND METHODS</b>  | 258 |
| <b>2.1. Reagents</b>   | 258 |
| <b>2.2. Irradiation sources</b>  | 258 |
| <b>2.3. Analytical methods</b>   | 259 |
| <b>2.4. Determination of radiation-chemical yields and dose constants</b>  | 260 |
| <b>2.5. Determination of reaction rate constants (<math>k_{H\cdot}</math>, <math>k_{HO\cdot}</math> and <math>k_{e_{aq}^-}</math>)</b>           | 260 |
| 2.5.1. Determination of $k_{H\cdot}$   | 260 |
| 2.5.2. Determination of reaction rate constants ( $k_{HO\cdot}$ and $k_{e_{aq}^-}$ )   | 261 |
| <b>3. RESULTS AND DISCUSSION</b>   | 262 |
| <b>3.1. Degradation induced by gamma irradiation</b>   | 262 |
| <b>3.2. Determination of the radical reaction rate constants <math>k_{HO\cdot}</math>, <math>k_{e_{aq}^-}</math> and <math>k_{H\cdot}</math></b> | 264 |
| <b>4. CONCLUSIONS</b>  | 267 |
| <b>5. REFERENCES</b>   | 269 |

**CAPÍTULO 7. TRATAMIENTO DE AGUA CONTAMINADA CON  
ÁCIDO DIFENÓLICO MEDIANTE RADIACIÓN GAMMA  
EN PRESENCIA DE DIFERENTES COMPUESTOS**

|  |     |
|--|-----|
| <b>1. INTRODUCTION</b>   | 277 |
| <b>2. MATERIALS AND METHODS</b>  | 279 |
| <b>2.1. Reagents</b>   | 279 |
| <b>2.2. Irradiation sources</b>  | 279 |
| <b>2.3. Collection and characterization of water samples</b>   | 280 |
| <b>2.4. Analytical methods</b>   | 280 |
| <b>2.5. Determination of radiation-chemical yields and dose constant</b>   | 281 |
| <b>3. RESULTS AND DISCUSSION</b>   | 282 |
| <b>3.1. Radiolytic degradation of DPA in aqueous solution</b>  | 282 |
| <b>3.2. Effect of the presence of <math>O_2</math> on DPA degradation</b>  | 288 |
| <b>3.3. Effect of the presence of <math>Br^-</math>, <math>Cl^-</math>, <math>CO_3^{2-}</math>, <math>NO_2^-</math>, <math>NO_3^-</math>, or <math>SO_4^{2-}</math> on</b> |     |

|  |     |
|--|-----|
| <b>DPA degradation</b>   | 288 |
| <b>3.4. Effect of water matrix on DPA degradation</b>            | 293 |
| <b>3.5. Evolution of TOC and toxicity during DPA degradation</b> | 294 |
| <b>4. CONCLUSIONS</b>  | 297 |
| <b>5. REFERENCES</b>   | 298 |
| <b>CONCLUSIONES GENERALES</b>                                    | 303 |
| <b>PUBLICACIONES</b>   | 309 |









## **1. ENVIRONMENTAL IMPACT AND TREATMENT OF CONTAMINANTS PRESENT IN LANDFILL LEACHATES STUDIED IN THE PRESENT DOCTORAL THESIS**

This section analyzes the environmental problems created by the presence of compounds used as plasticizers and herbicides in landfill leachates. Given the large number of contaminants in this type of aqueous effluent, model compounds were selected for each group: bisphenol A (BPA) and diphenolic acid (DPA), representing plasticizers; and 2,4-dichlorophenoxyacetic acid (2,4-D) and 4-chloro-2-methylphenoxyacetic acid (MCPA), representing herbicides. Phthalic acid (PA) was also studied as a plasticizer of interest, therefore, an extensive review on its adverse environmental effects was published in the *Journal of Environmental Management* (see Section 1.7).

Landfills remain a prime concern of waste management systems throughout the world, including Europe (Salem et al., 2008), and have been identified as one of the main threats to groundwater resources (Fatta et al., 1999). The two most serious environmental effects of landfills are related to the leachate formed during decomposition from the percolation of rainwater through the waste layer and to the toxic byproducts generated by chemical and biological processes during waste leaching (Primo et al., 2008). Once landfill leachate is released into the environment, it can pollute soils (Hernández et al., 1999; Islam and Singhal, 2002), surface water (Mangimbulude et al., 2009; North et al., 2006), groundwater (Mikac et al., 1998; Reyes-López et al., 2008), and wildlife, due to its toxicity (Clément and Merlin, 1995; Pivato and Raga, 2006; Silva et al., 2004).

Various organic pollutants and chemical species have been detected in the composition of landfill leachates, including: i) plasticizers and organic esters added to polymers in order to improve the properties of the final product (Nascimento Filho et al., 2003), ii) antioxidants or stabilizers used to improve the durability of materials (Marttinen et al., 2003), and iii) herbicides/pesticides or other widely-used anti-pest compounds (Slack et al., 2005).

The most common monomeric plasticizers are BPA and DPA, which have been detected in landfill leachates and in different aqueous systems (Laganá et al., 2004; Smith and Weber Jr., 1990; Öman and Hynning, 1993). Due to their very large production and wide distribution, they have become ubiquitous environmental pollutants; moreover, they are considered to be endocrine disruptors (Gültekin and Ince, 2007; Tanaka et al., 2001).

Novel effects of herbicides at environmentally relevant concentrations were recently reported (Orton et al., 2009). 2,4-D is a widely used herbicide (Han et al., 2010) that is commonly preferred worldwide because of its low cost and good selectivity (Aksu and Kabasakal, 2004). MCPA is frequently utilized to control a wide variety of broadleaf weeds in crops, including corn, grapes, flax, sugarcane, and pulses, and in grasses and orchards, as well as in non-cultivated areas. Both compounds have frequently been detected in drinking water (Peixoto et al., 2009).

The following sections provide a brief description of the above pollutants and outline the treatments commonly used for their removal from aqueous solutions.

### **1.1. Bisphenol A**

BPA is a representative compound among endocrine disruptors. It causes reproductive damage to aquatic organisms and is widely used as a raw material in the production of polycarbonate plastics and epoxy resins. Due to the widespread utilization of BPA, there is increasing interest in effective remediation technologies for its removal from contaminated water (Laganá et al., 2004). BPA has been detected in all types of environmental waters at varying concentrations: up to 17.2 mg/L in hazardous waste landfill leachate (Yamamoto et al., 2001), 12 µg/L in stream water (Liu et al., 2009), and 0.1 µg/L in drinking water (MHLWJ, 2000).

The production and application of BPA is rising with the increasing use of plastics, and the global production of BPA was 3.9 million tons in 2006 and increased to 4.7 million tons in 2008 (Nempo and Chosa-Kai, 1997; Morgan, 2006; Jiao et al., 2008). EU countries are responsible for nearly 30 % of world production.

The US National Institute for Occupational Safety and Health's Registry of Toxic Effects of Chemical substances describes BPA as a primary irritant, a mutagen, and an agent that affects the reproductive system (NIOHS 1998).

### **1.2. Diphenolic acid**

In the recent decade, it has been observed much attention from researchers to synthesize new polyesters and polycarbonates using DPA instead of BPA (Cerbai et al., 2008; Fischer and Hartraxft, 1966; Zhang and Moore, 2002; Zhang and Moore, 2003), because DPA is commercially available and much cheaper than BPA and it can introduce functional carboxyl groups into the polymer structure (Ping et al., 2009). DPA has the same environmental risks of BPA because it is one of BPA derivatives. Both pollutants cause not only strong estrogenic endocrine disrupting effect but also various diseases including carcinogenesis, liver damage and obesity-promoting effects.

### **1.3. 2,4- Dichlorophenoxyacetic acid**

Among the herbicides, 2,4-D is the most widely used herbicide in the world (Han et al., 2010), due to its low cost and good selectivity (Aksu and Kabasakal, 2004). It is used in cultivated agriculture, in pasture and rangeland applications, forest management, home gardens, and to control aquatic vegetation (Benli et al., 2007). It has been detected in water systems in various regions (Gold et al., 1988). It is considered moderately toxic, with a maximum allowed concentration in drinking water of 100 µg/L. The toxicity of 2,4-D and its degradation products make this chemical substance a potential hazard by contaminating our environment (Hameed et al., 2009). The removal of 2,4-D from water, therefore, is one of the major environmental concerns these days (Aksu and Kabasakal, 2004).

### **1.4. 4-chloro-2-methylphenoxyacetic acid**

MCPA, which was developed in the 1940s, is one of the most frequently detected herbicides in drinking water, with contamination levels up to 0.4 µg/L (Cabral et al., 2003; Peixoto et al., 2009; Sun et al., 1995). MCPA belongs to the family of phenoxyacetic acids, which are considered highly carcinogenic. Moreover, although it generally causes low-to-moderate toxicity, poisoning can have serious and sometimes

fatal sequelae, including coma, renal dysfunction, and central nervous system depression (Bradberry et al., 2000; Roberts et al., 2005).

### **1.5. Removal of BPA, DPA, 2,4-D, and MCPA from aqueous solution by means of different technologies**

Numerous studies have addressed the removal of BPA, DPA, 2,4-D, and MCPA from aqueous solution by means of different technologies. Tables 1-4 summarize some of the most representative studies on the removal of these contaminants from water.

Physical, chemical, and biological processes have been used in systems for eliminating BPA from aqueous solution (Bautista-Toledo et al., 2005; Gattullo et al., 2012; Zhou et al., 2011). Activated carbons have a high BPA adsorption capacity, which depends on the characteristics of the activated carbon, the solution pH, and the presence of electrolytes in the water (Bautista-Toledo et al., 2005).

Biological treatment is effective to eliminate BPA from aqueous solution but requires a long treatment time, and its application is limited to very low concentrations of BPA (Gattullo et al., 2012). However, BPA biodegradation is enhanced by the presence of natural organic matter (NOM), which acts as a substrate for the microorganisms (e.g., green alga) in the system, increasing their growth (Gattullo et al., 2012). The presence of  $\text{Fe}^{3+}$  in an anaerobic system was also found to improve the bioremediation of BPA, attributed to the action of  $\text{Fe}^{3+}$  as an alternative electron acceptor (Li et al., 2012).

Technologies based on advanced oxidation processes (AOPs) have proven highly effective in the degradation of organic compounds in aqueous solution. BPA photodegradation of up to 100% has been reported using electrocatalytic, electrochemical, ultrasonic, gamma radiation, photo Fenton, UV,  $\text{O}_3$ , UV/ $\text{O}_3$ , UV/ $\text{TiO}_2$ ,  $\text{O}_3$ / $\text{TiO}_2$ , UV/ $\text{O}_3$ /carbon, UV/ $\text{O}_3$ / $\text{TiO}_2$ , and UV/ $\text{O}_3$ / $\text{TiO}_2$ /carbon processes (Cui et al., 2009; Guo et al., 2012; Ju et al., 2012; Katsumata et al., 2004; Rivas et al., 2009; Wang et al., 2009; Zhang et al., 2011). However, the mineralization levels are rather low, except in the case of UV/ $\text{O}_3$ /activated carbon, UV/ $\text{O}_3$ / $\text{TiO}_2$ /activated carbon, and UV/ $\text{O}_3$ / $\text{TiO}_2$ , which completely mineralize the organic matter after 2 h of treatment

(Rivas et al., 2009). Table 1 summarizes the key studies on the technologies commonly used to remove BPA from aqueous solution.

Few studies have been published on the elimination of DPA from aqueous solution by adsorption or photocatalytic processes (Guo et al., 2009a; Guo et al., 2009b; Guo et al., 2009c). These have shown a low effectiveness in DPA degradation in aqueous solution, and there is a need for research into other processes that could mineralize DPA and completely remove it from waters. Table 2 summarizes the most representative studies on the removal of DPA from aqueous phase by different processes.

Activated carbons have a high capacity to adsorb 2,4-D from aqueous solution, which is attributable to their large surface area (Aksu and Kabasakal, 2004; Hameed et al., 2009). However, UV radiation was found to be inadequate to completely degrade or mineralize 2,4-D in water in either the absence or presence of promoter agents (Alfano et al., 2001; Kundu et al., 2005).

Photocatalysis has been proposed as a good option for the degradation of 2,4-D, and UV/TiO<sub>2</sub> and UV/TiO<sub>2</sub>/activated carbon processes achieved removal percentages of 75% and 100%, respectively (Akpan and Hameed, 2011; Matos et al., 2001). The improved 2,4-D photodegradation obtained with the presence of activated carbon in the photocatalytic process can be attributed to its synergistic effects with TiO<sub>2</sub>. Table 3 summarizes some of the most representative articles on 2,4-D removal from aqueous solution.

The MCPA degradation percentage was only 1% with UV radiation and 12% with adsorption on TiO<sub>2</sub> particles, but it was 90% when UV radiation and TiO<sub>2</sub> were combined (Zertal et al., 2001).

Garcia-Segura et al. (2011) removed around 80% of MCPA from aqueous solution after a 2-h of treatment with a solar photoelectron-Fenton process and obtained 75% mineralization. On the other hand, MCPA degradation percentages were 74% with ozonation and 94% with the combined UV/O<sub>3</sub> system (Benoit-Guyod et al., 1986).

Gamma radiation obtained an optimal percentage MCPA removal (up to 100%) at a solution pH of 1.5 and dose of 3000 Gy, MCPA can be completely removed by gamma radiation and partially removed by photooxidation and photocatalytic processes (Bojanowska-Czajka et al., 2006). Table 4 summarizes the main studies on the elimination of MCPA from water.

**Table 1.** Removal of BPA from aqueous solution.

| Type of treatment   | Concentration | Experimental conditions  | Removing ratio   | Ref                            | Observations  |
|---|---------------|--|--|--------------------------------|---|
| Adsorption onto activated carbon  | [50-350 mg/L] | Three activated carbons with different chemical nature were used to adsorb BPA from aqueous solution. The influence of solution pH (2-12), ionic strength (NaCl (0.01 M and 0.10 M)), and the presence of mineral matter in carbons on the adsorption of BPA was analyzed. | 129.6-263.1 mg/g   | (Bautista-Toledo et al., 2005) | The adsorption of BPA fundamentally depends on the chemical nature of the carbon surface and the solution pH. Furthermore, the presence of electrolytes in solution favored the adsorption process due to a screen effect; however, the presence of mineral matter in carbons reduced their adsorption capacity because of the hydrophilic nature of this matter  |
| Electrocatalytic degradation (Ti-based PbO <sub>2</sub> -ionic liquids (ILs) electrode) | [30-80 mg/L]  | The influence of solution current density, solution pH, concentration of supporting electrolyte, and initial concentration of BPA was studied on the BPA degradation.  | 100% within 150 min  | (Ju et al., 2012)              | The electrode showed a high stability and reusability due to the better electroconductivity and reusability of ILs. The hydroxyl radicals (HO <sup>•</sup> ) generated in the electrocatalytic process played a key role in oxidizing BPA to form CO <sub>2</sub> and H <sub>2</sub> O. Moreover, these results illustrated that PbO <sub>2</sub> -ILs/Ti electrode was effective for pollutants degradation and had a great potential application. The optimal conditions were (current density (30mA/cm <sup>2</sup> ), solution pH (9), and supporting catalyst (0.07 mol/L)). |
| Electrochemical (EC) degradation  | [100 mg/L]    | EC degradation of BPA was tested for four types of anode materials: Pt, Ti/Boron-doped diamond (BDD), Ti/Sb-SnO <sub>2</sub> and Ti/RuO <sub>2</sub> .   | Pt (100%)<br>Ti/BDD (100%)<br>Ti/Sb-SnO <sub>2</sub> (100%)<br>Ti/RuO <sub>2</sub> (75%) | (Cui et al., 2009)             | BPA was readily destructed at the Ti/Sb-SnO <sub>2</sub> and Ti/BDD anodes, the Pt anode had a high ability to remove BPA, and the Ti/RuO <sub>2</sub> anode was incapable of effectively oxidising BPA. The BPA degradation was based on the HO <sup>•</sup> radicals produced by water electrolysis. In comparison, with its high durability and good reactivity for organic oxidation, the Ti/BDD anode appears to be the more promising one for the effective EC treatment of BPA and similar endocrine disrupting chemical (EDCs) pollutants.                                |



**Table 1.** Removal of BPA from aqueous solution (continued).

| Type of treatment   | Concentration | Experimental conditions   | Removing ratio  | Ref                  | Observations  |
|---|---------------|---|---|----------------------|---|
| Ultrasonic irradiation  | [1 mg/L]      | The presence of different additives (H <sub>2</sub> O <sub>2</sub> , air bubbles and humic acid) were investigated on the ultrasonic degradation of BPA under various operating conditions, i.e., ultrasonic frequency, power intensity and power density.  | (70-100%)   | (Zhang et al., 2011) | The ultrasonic irradiation is directly related to the HO• production as a result of BPA degradation. The optimal experimental conditions were determined to be the frequency of 800 kHz and the power intensity of 3.0 W/cm <sup>2</sup> . The addition of a low concentration of H <sub>2</sub> O <sub>2</sub> could facilitate BPA ultrasonic degradation efficiently. However, further increased dosage of H <sub>2</sub> O <sub>2</sub> was shown to decrease the degradation efficiency of BPA. It was also found that the BPA ultrasonic degradation was inhibited by aeration and the presence of humic acids. |
| Advanced oxidation processes  | [0.10 mmol/L] | The elimination and mineralization of BPA by using several technologies such as UV, O <sub>3</sub> , UV/O <sub>3</sub> , UV/TiO <sub>2</sub> , O <sub>3</sub> /TiO <sub>2</sub> , UV/O <sub>3</sub> /activated carbon (AC), UV/O <sub>3</sub> /TiO <sub>2</sub> , UV/O <sub>3</sub> /TiO <sub>2</sub> /AC were studied.                             | BPA:<br>(100%) for all treatments<br>TOC:<br>UV (15%)<br>O <sub>3</sub> (25%)<br>UV/O <sub>3</sub> (75%)<br>UV/TiO <sub>2</sub> (80%)<br>O <sub>3</sub> /TiO <sub>2</sub> (60%)<br>UV/O <sub>3</sub> /AC,<br>UV/O <sub>3</sub> /TiO <sub>2</sub> , and<br>UV/O <sub>3</sub> /TiO <sub>2</sub> /AC<br>(100%) | (Rivas et al., 2009) | The processes such as ozonation or photooxidation are capable of efficiently removing BPA from water, however, mineralization levels are rather low. The combination of UV/O <sub>3</sub> /AC, UV/O <sub>3</sub> /TiO <sub>2</sub> /AC, and UV/O <sub>3</sub> /TiO <sub>2</sub> completely mineralized the organic matter   |
| Photocatalytic (UV /TiO <sub>2</sub> ) in a self-designed horizontal circulating bed photocatalytic reactor (HCBPR) | [10-50 mg/L]  | Photocatalytic degradation of BPA in the presence of TiO <sub>2</sub> and UV radiation was performed in HCBPR. TiO <sub>2</sub> catalyst was immobilized on the surface of polyurethane foam (PF). The effects of initial BPA concentration, initial solution pH, TiO <sub>2</sub> dosage and temperature on BPA photodegradation were investigated | BPA (97%)<br>TOC (95%)<br>within 6 h  | (Wang et al., 2009)  | The BPA degradation efficiency can be effectively improved by increasing solution pH from 3.4 to 12.3. The optimum TiO <sub>2</sub> carrier dosage was about 1%. The effect of temperature on BPA photodegradation was found to be unremarkable in the range of 21.2-30.5 °C.   |

**Table 1.** Removal of BPA from aqueous solution (continued).

| Type of treatment   | Concentration | Experimental conditions   | Removing ratio    | Ref                      | Observations  |
|---|---------------|---|-------------------|--------------------------|---|
| Gamma radiation   | [10-100 mg/L] | The effects of different additives (CHCl <sub>3</sub> , CH <sub>3</sub> OH or fulvic acid), absorbed dose (1-8 kGy), BPA initial concentration, solution pH (5.2-9.0), dissolved oxygen (DO) (1.9-6.8 mg/L), and organic matter (10-100 mg/L) on BPA removal were investigated. | 100%              | (Guo et al., 2012)       | Gamma radiation was feasible and effective to remove BPA from aqueous solution. However, TOC removal was not as effective as that of BPA. High absorbed dose, low solution pH, high DO concentration and the addition of CHCl <sub>3</sub> were favorable for BPA removal, but BPA removal was reduced by adding fluvic acid and CH <sub>3</sub> OH. The mechanism of gamma radiation-induced BPA removal in aqueous solution was mainly attributed to HO <sup>•</sup> radical oxidation. |
| Photo-Fenton  | [10 mg/L]     | The effects of solution pH (2.0-4.5), Fe(II) concentration (0.00-0.04 mmol/L) and H <sub>2</sub> O <sub>2</sub> concentration (0.0-0.4 mmol/L) on BPA degradation were investigated.  | 100% within 9 min | (Katsumata et al., 2004) | The degradation rate of BPA was strongly influenced by the pH and by initial H <sub>2</sub> O <sub>2</sub> and Fe (II) concentrations. The degree of BPA conversion to CO <sub>2</sub> was more than 90% in 36 h of treatment.  |
| Biodegradation, green alga ( <i>Monoraphidium braunii</i> ) | [2-10 mg/L]   | <i>Monoraphidium braunii</i> ( <i>M. braunii</i> ) was tested after 2 and 4 days of its growth to remove BPA, either in the presence of natural organic matter (NOM (2-50 mg/L)) or in the absence of NOM.  | 35%-48%           | (Gattullo et al., 2012)  | After 2 and 4 days, BPA at low concentrations was not toxic for alga, whereas at the highest concentration it reduced alga growth and photosynthetic efficiency. The sole NOM and its combinations with BPA at the lowest concentrations increased the cell number. Moreover, NOM, at any concentration, scarcely influenced the BPA removal.   |
| Adsorption on peat and modified peat                        | [5-55 mg/L]   | Fibric peat was modified with hexadecyltrimethylammonium bromide (HTAB).  | 31.4 mg/g         | (Zhou et al., 2011)      | The HTAB modified peat displayed a faster initial BPA sorption and a higher capacity than the unmodified peat over a wide concentration range. It showed that the improved hydrophobic interactions are the dominant mechanism and the chemical modification of the peat surface greatly enhanced the sorption capacity toward organic compound dissolved in water.   |

**Table 2.** Removal of DPA from aqueous solution.

| Type of treatment   | Concentration        | Experimental conditions   | Removing ratio  | Ref                 | Observations  |
|---|----------------------|---|---|---------------------|---|
| Photocatalytic (UV/ $\beta$ -cyclodextrin ( $\beta$ -CD)) | [10-100 $\mu$ mol/L] | The influence of $\beta$ -CD on the photodegradations of DPA radiated under UV lamp was investigated. The potential of $\beta$ -CD photocatalysis for treatment and removal of EDCs from aqueous solution was investigated. | UV (20%)<br>UV/ $\beta$ -CD (33.5%)   | (Guo et al., 2009a) | The photocatalytic degradation was enhanced in the presence of $\beta$ -CD mainly as a result of the moderate inclusion depth of DPA molecule in the $\beta$ -CD cavity, this kind of inclusion structure allows the DPA molecule sufficient proximity to secondary hydroxyl groups of the $\beta$ -CD cavity, and these hydroxyl groups could be activated and converted to hydroxyl radicals under UV irradiation, which can enhance the photooxidation of DPA. |
| Photochemical ( $\beta$ -CD/TiO <sub>2</sub> )            | [10-80 $\mu$ mol/L]  | The influence of $\beta$ -CD on the photochemical behaviour of DPA in the presence of TiO <sub>2</sub> suspensions under a 250 W metal halide lamp (MHL) was studied.   | MHL (2%)<br>MHL/TiO <sub>2</sub> (58%)<br>MHL/ $\beta$ -CD (68%)<br>TiO <sub>2</sub> (2.93 $\mu$ mol/g)<br>TiO <sub>2</sub> / $\beta$ -CD (30.00 $\mu$ mol/g) | (Guo et al., 2009b) | The enhancement of DPA photochemical degradation in the presence of TiO <sub>2</sub> and $\beta$ -CD was mainly due to the adsorption of DPA on TiO <sub>2</sub> , which makes DPA degradation more easily in the presence of hydroxyl radicals photoproduced by TiO <sub>2</sub>   |
| Adsorption and photodecomposition                         | [10-80 $\mu$ mol/L]  | The comparison between the influence of $\beta$ -CD or $\alpha$ -CD on the adsorption and photodecomposition of DPA in the presence of TiO <sub>2</sub> suspensions under a 250 W (MHL) was investigated.                   | MHL/TiO <sub>2</sub> / $\beta$ -CD (78%)<br>MHL/TiO <sub>2</sub> / $\alpha$ -CD (40%)<br>TiO <sub>2</sub> / $\alpha$ -CD (0.63 $\mu$ mol/g)                   | (Guo et al., 2009c) | The inhibition of photodegradation of DPA with $\alpha$ -CD was mainly because $\alpha$ -CD and DPA did not form a stable inclusion compound, as well as the decrease of the adsorption amount of DPA on the TiO <sub>2</sub> surface.  |

**Table 3.** Removal of 2,4 -D from aqueous solution.

| Type of treatment                               | Concentration  | Experimental conditions  | Removing ratio   | Ref                        | Observations  |
|---|----------------|--|--|----------------------------|---|
| Adsorption (activated carbon)                   | [50-400 mg/L]  | Adsorbent: activated carbon derived from date stones. Solution pH (2-11) and adsorption temperature: 30 °C.  | 238.10 mg/g  | (Hameed et al., 2009)      | The equilibrium data were fitted to the Langmuir, Freundlich and Temkin isotherm models, and they were best described by the Langmuir isotherm model. The adsorption kinetics of 2,4-D obeyed pseudo-first-order adsorption kinetics.   |
| Adsorption (activated carbon)                   | [100-600 mg/L] | Adsorption equilibrium, kinetics and thermodynamics of 2,4-D onto granular activated carbon were studied in aqueous solution in a batch system with respect to solution pH, temperature and initial 2,4-D concentration.   | 518.00 mg/g at 45 °C and pH = 2  | (Aksu and Kabasakal, 2004) | Equilibrium data were very well fitted to the Freundlich and Koble-Corrigan isotherm models. It was found that both the boundary layer and intraparticle diffusion played important roles in the adsorption mechanisms of 2,4-D. The activation energy of adsorption was determined using the Arrhenius equation obtaining a value of as 8.46 kJ/mol.   |
| Photooxidation (UV)                             | [5-40 mg/L]    | The effects of various parameters such as light intensity, exposure time, the presence of O <sub>2</sub> , wavelength of light, pH, other commonly occurring ions (e.g. Cl <sup>-</sup> , SO <sub>4</sub> <sup>2-</sup> , Ca <sup>2+</sup> /Mg <sup>2+</sup> , Fe <sup>3+</sup> , NO <sub>3</sub> <sup>-</sup> ) were studied.   | 81%  | (Kundu et al., 2005)       | The percentage of degradation of 2,4-D can be increased either by increasing the light intensity or by irradiating the sample for longer time. Moreover, the presence of O <sub>2</sub> improved the degradation of 2,4-D and, at pH up to 7, however, the presence of different ions decreased the degradation of 2,4-D.   |
| Photocatalytic (UV/(Ca-Ce-W-TiO <sub>2</sub> )) | [10-50 mg/L]   | Preparation of (Ca-Ce-W-TiO <sub>2</sub> ): solution A: was prepared by dissolving an appropriate amount of Ca, Ce, and W in ethanol and water. Solution B: the doped TiO <sub>2</sub> was prepared by the sol-gel method using [Ti(OBu) <sub>4</sub> ] as the precursor, which was dissolved in ethanol under stirring. Solution A was gradually poured into solution B until sols were formed. | 100% at reaction time (hr):<br>10 mg/L (1.0)<br>20 mg/L (1.5)<br>30 mg/L (2.5)<br>40 mg/L (2.5)<br>50 mg/L (3.5) | (Akpan and Hameed, 2011)   | The degradation of 2,4-D was a result of the properties of the composite photocatalyst (large surface area, reduced band gap which also inhibited electron-hole recombination, high crystallinity). A comparison of the efficiency of the photocatalyst with a commercially available photocatalyst, TiO <sub>2</sub> -Sigma product and other photocatalysts in literature placed the composite photocatalyst used in this study above the rest. |

**Table 3.** Removal of 2,4 -D from aqueous solution (continued).

| Type of treatment                                  | Concentration | Experimental conditions   | Removing ratio  | Ref                   | Observations  |
|--|---------------|---|---|-----------------------|---|
| Photocatalytic (UV/TiO <sub>2</sub> /AC)           | [94 mg/L]     | The photocatalytic degradation experiments were carried out in the presence of TiO <sub>2</sub> and two different AC (L and H) for 60 minutes in dark (adsorption) and 600 minutes in the presence of UV/TiO <sub>2</sub> /AC (photocatalytic). | UV/TiO <sub>2</sub> (75%)<br>UV/TiO <sub>2</sub> /AC (100%) | (Matos et al., 2001)  | The presence of AC-H improved the photocatalytic degradation of 2,4-D with a synergistic factor of 1.3 (TiO <sub>2</sub> /AC-H) = (50 mg/10 mg). It has been explained by an important adsorption of 2,4-D on AC followed by a mass transfer to photocatalytic degradation.   |
| Photooxidation (UV/H <sub>2</sub> O <sub>2</sub> ) | [30-90 mg/L]  | The experimental work was performed in a batch, well-stirred tank reactor irradiated from its bottom using a low power, germicidal, tubular lamp placed at the focal axis of a cylindrical reflector of parabolic cross-section.                | 70% after 6 h   | (Alfano et al., 2001) | 2,4-D degradation initial rates (UV/H <sub>2</sub> O <sub>2</sub> ) were twenty times faster than those obtained employing UV radiation alone. Immediately after the initiation of the degradation reaction, equally toxic intermediate products such as 2,4-dichlorophenol (DCP) and chlorohydroquinone (CHQ) can be detected. |

**Table 4.** Removal of MCPA from aqueous solution.

| Type of treatment                       | Concentration   | Experimental conditions   | Removing ratio   | Ref                   | Observations   |
|---|-----------------|---|--|-----------------------|--|
| Photochemical<br>1<br>(UV and sunlight) | [0.11- 0.55 μM] | The phototransformation of MCPA in aqueous solution irradiated at 254 nm and in the range of solar light ( $\lambda > 300$ nm) as direct photolysis and indirect photolysis in the presence of silica and TiO <sub>2</sub> was studied. | UV (1%)<br>TiO <sub>2</sub> (12%)<br>UV/TiO <sub>2</sub> (90%) | (Zertal et al., 2001) | Direct photolysis of MCPA on silica and the phototransformation in the presence of TiO <sub>2</sub> are almost specific. The phototransformation of MCPA is not significantly affected by O <sub>2</sub> nor by the irradiation wave length between 254 and 310 nm, but it is highly depending on the solution pH. |

**Table 4.** Removal of MCPA from aqueous solution (continued).

| Type of treatment                                    | Concentration  | Experimental conditions  | Removing ratio                                    | Ref                               | Observations   |
|--|----------------|--|---|-----------------------------------|--|
| Solar photoelectro-Fenton                            | [186 mg/L]     | To optimize the degradation of MCPA, Fe <sup>2+</sup> concentration and solution pH were selected as independent variables, where TOC, degradation, and energy consumption were taken as responses.      | 23% to 80% after 120 min                          | (Garcia-Segura et al., 2011)      | The optimum variables found were 5.0 ampere, 1.0 mM Fe <sup>2+</sup> , and pH 3.0, after 120 min of electrolysis. Under these conditions, 75% of mineralization with 71% of current efficiency and 87.7 kWh/kg TOC of energy consumption were obtained. Hydroxyl radicals also destroyed 4-chloro-2-methylphenol, methylhydroquinone and methyl-p-benzoquinone detected as aromatic by-products. |
| Photooxidation (KrCl and XeBr excilamps irradiation) | [0.2- 2.0 M]   | The photodegradation of MCPA was carried out in the presence of UV radiation and (KrCl and a XeBr excilamps). The biodegradability (COD/BOD) of phototreated MCPA solutions was studied.                 | Up to 55%   | (Tchaik ovskaya et al., 2012)     | The application of excilamps significantly improved the efficiency of MCPA phototransformation in aqueous solutions. Irradiation of MCPA with a KrCl excilamp emitting at 222 nm, and with a XeBr excilamp emitting at 283 nm was carried out. Biological processes are not suitable for MCPA removal due to low or total absence of biodegradability of this class of pollutants                |
| Ozonation (O <sub>3</sub> and UV/O <sub>3</sub> )    | [0.01- 0.22 M] | The degradation of MCPA by ozone has been examined in the presence and absence of UV radiation.  | O <sub>3</sub> (74 %)<br>UV/O <sub>3</sub> (95 %) | (Benoit-Guyod et al., 1986)       | In the dark, ozonolysis rapidly proceeded, and few aromatic products were detected. Under irradiation, MCPA degradation occurred even more rapidly, and a series of benzenoid intermediates could be isolated. Two distinct ozonolysis pathways: ring-hydroxylation and cleavage by molecular ozone in the dark, and side-chain oxidation by hydroxyl radicals under irradiation were indicated. |
| Gamma radiation                                      | [100 mg/L]     | The radiolytic degradation of MCPA was carried out using gamma radiation and it was optimized in terms of irradiation dose, solution pH (1.5, 7.0, and 11.5) and H <sub>2</sub> O <sub>2</sub> addition. | 100 % at a 3000 Gy dose                           | (Bojano wska-Czajka et al., 2006) | Radiolytic degradation of MCPA should be carried out in solution pH 1.5. The presence of H <sub>2</sub> O <sub>2</sub> during irradiation of MCPA did not affect the efficiency of decomposition of MCPA, however, it increased the efficiency of formation of carboxylic acids.   |

## 1.6. References

- Akpan UG, Hameed BH (2011) Photocatalytic degradation of 2,4-dichlorophenoxyacetic acid by Ca–Ce–W–TiO<sub>2</sub> composite photocatalyst. *Chem Eng J* 173:369-375
- Aksu Z, Kabasakal E (2004) Batch adsorption of 2,4-dichlorophenoxy-acetic acid (2,4-D) from aqueous solution by granular activated carbon. *Sep Purif Technol* 35:223-240
- Alfano OM, Brandi RJ, Cassano AE (2001) Degradation kinetics of 2,4-D in water employing hydrogen peroxide and UV radiation. *Chem Eng J* 82:209-218
- Bautista-Toledo I, Ferro-García MA, Rivera-Utrilla J, Moreno-Castilla C, Vegas Fernández FJ (2005) Bisphenol A removal from water by activated carbon. Effects of carbon characteristics and solution chemistry. *Environ Sci Technol* 173:6246-625
- Benli AÇK, Sarıkaya R, Sepici-Dincel A, Selvi M, Şahin D, Erkoç F (2007) Investigation of acute toxicity of (2,4-dichlorophenoxy)acetic acid (2,4-D) herbicide on crayfish (*Astacus leptodactylus* Esch. 1823). *Pestic Biochem Physiol* 88:296-299
- Benoit-Guyod JL, Crosby DG, Bowers JB (1986) Degradation of MCPA by ozone and light. *Water Res* 20:67-72
- Bojanowska-Czajka A, Drzewicz P, Kozyra C, Nałęcz-Jawecki G, Sawicki J, Szostek B, Trojanowicz M (2006) Radiolytic degradation of herbicide 4-chloro-2-methyl phenoxyacetic acid (MCPA) by  $\gamma$ -radiation for environmental protection. *Ecotoxicol Environ Saf* 65:265-277
- Bradberry SM, Watt BE, Proudfoot AT, Vale JA (2000) Mechanisms of toxicity, clinical features, and management of acute chlorophenoxy herbicide poisoning: a review. *J Toxicol Clin Toxicol* 38:111–122.

- Cabral MG, Viegas CA, Teixeira MC, Sá-Correia I (2003) Toxicity of chlorinated phenoxyacetic acid herbicides in the experimental eukaryotic model *Saccharomyces cerevisiae*: role of pH and of growth phase and size of the yeast cell population. *Chemosphere* 51:47-54
- Cerbai B, Solaro R, Chiellini E (2008) Synthesis and characterization of functional polyesters tailored for biomedical applications. *J Polym Sci Part A* 46:2459-2476
- Clément B, Merlin G (1995) The contribution of ammonia and alkalinity to landfill leachate toxicity to duckweed. *Sci Total Environ* 170:71-79
- Cui Y, Li X, Chen G (2009) Electrochemical degradation of bisphenol A on different anodes. *Water Res* 43:1968-1976
- Fatta D, Papadopoulos A, Loizidou M (1999) A Study on the landfill leachate and its impact on the ground water quality of the greater area. *Environ Geochem Hlth* 21:175-190.
- Fischer P, Hartraxft GR (1966) Diphenolic acid ester polycarbonates. *J Appl Polym Sci* 10:245–252
- Gattullo CE, Bährs H, Steinberg CEW, Loffredo E (2012) Removal of bisphenol A by the freshwater green alga *Monoraphidium braunii* and the role of natural organic matter. *Sci Total Environ* 416:501-506
- Gold AJ, Morton TG, Sullivan WM, McClory J (1988) Leaching of 2,4-D and dicamba from home lawns. *Water Air Soil Poll* 37:121-129
- Garcia-Segura S, Almeida LC, Bocchi N, Brillas E (2011) Solar photoelectro-Fenton degradation of the herbicide 4-chloro-2-methylphenoxyacetic acid optimized by response surface methodology. *J Hazard Mater* 194:109-118
- Gültekin I, Ince NH (2007) Synthetic endocrine disruptors in the environment and water remediation by advanced oxidation processes. *J Environ Manage* 85:816-832



- Guo L, Wang B, Huang W, Wu F, Huang J (2009a) Photocatalytic degradation of diphenolic acid in the Presence of beta-Cyclodextrin under UV Light. *E S I A T* 322-324.
- Guo L, Liu Y, Wang B, Wu F, Li Y (2009b) Photochemical behavior of diphenolic acid in  $\beta$ -Cyclodextrin and TiO<sub>2</sub> suspensions. *I C B B E* 1-4.
- Guo L, Wang B, Huang W, Wu F, Li Y (2009c) Adsorption and photodecomposition of diphenolic acid  $\alpha$ - or  $\beta$ - cyclodextrins and TiO<sub>2</sub> suspensions. *S O P O* 1-4.
- Guo Z, Dong Q, He D, Zhang C (2012) Gamma radiation for treatment of bisphenol A solution in presence of different additives. *Chem Eng J* 183:10-14
- Hameed BH, Salman JM, Ahmad AL (2009) Adsorption isotherm and kinetic modeling of 2,4-D pesticide on activated carbon derived from date stones. *J Hazard Mater* 163:121-126
- Han D, Jia W, Liang H (2010) Selective removal of 2,4-dichlorophenoxyacetic acid from water by molecularly-imprinted amino-functionalized silica gel sorbent. *J Environ Sci* 22:237-241
- Hernández AJ, Adarve MJ, Gil A, Pastor J (1999) Soil salivation from landfill leachates: Effects on the macronutrient content and plant growth of four grassland species. *Chemosphere* 38:1693-1711
- Islam J, Singhal N (2002) A one-dimensional reactive multi-component landfill leachate transport model. *Environ Model Softw* 17:531-543
- Ju P, Fan H, Guo D, Meng X, Xu M, Ai S (2012) Electrocatalytic degradation of bisphenol A in water on a Ti-based PbO<sub>2</sub>-ionic liquids (ILs) electrode. *Chem Eng J* 179:99-106
- Jiao FR, Sun XJ, Pang ZT (2008) Production and market analysis of Bisphenol A. *Chem Ind* 26:21-33

- Katsumata H, Kawabe S, Kaneco S, Suzuki T, Ohta K (2004) Degradation of bisphenol A in water by the photo-Fenton reaction. *J Photochem Photobiol A* 162:297-305
- Kundu S, Pal A, Dikshit AK (2005) UV induced degradation of herbicide 2,4-D: kinetics, mechanism and effect of various conditions on the degradation. *Sep Purif Technol* 44:121-129
- Laganá A, Bacaloni A, De Ieva I, Faberi A, Fago G, Marino A (2004) Analytical methodologies for determining the occurrence of endocrine disrupting chemicals in sewage treatment plant and natural waters. *Anal Chem Acta* 501:79- 88.
- Li G, Zu L, Wong P, Hui X, Lu Y, Xiong J, An T (2012) Biodegradation and detoxification of bisphenol A with one newly-isolated strain *Bacillus* sp. GZB: Kinetics, mechanism and estrogenic transition. *Bioresour Technol* 114:224-230
- Liu G, Ma J, Li X, Qin Q (2009) Adsorption of bisphenol A from aqueous solution onto activated carbons with different modification treatments. *J Hazard Mater* 164:1275-1280
- Mangimbulude JC, Breukelen BMv, Krave AS, Straalen NMv, Röling WFM (2009) Seasonal dynamics in leachate hydrochemistry and natural attenuation in surface run-off water from a tropical landfill. *Waste Manage* 29:829-838
- Marttinen SK, Kettunen RH, Rintala JA (2003) Occurrence and removal of organic pollutants in sewages and landfill leachates. *Sci Total Environ* 301:1-12
- Matos J, Laine J, Herrmann J- (2001) Effect of the Type of Activated Carbons on the Photocatalytic Degradation of Aqueous Organic Pollutants by UV-Irradiated Titania. *J Catal* 200:10-20
- Mikac N, Cosovic B, Ahel M, Andreis S, Toncic Z (1998) Assessment of groundwater contamination in the vicinity of a municipal solid waste landfill (Zagreb, Croatia). *Water Sci Technol* 37:37-44

- Ministry of health, labour and welfare of Japan (MHLWJ) (2000) Exposure and behavior researches of endocrine disrupting chemicals in tap water
- Morgan M (2006) Phenol/acetone-facts, figures and future. The 4<sup>th</sup> ICIS World Phenol/Acetone Conference, Prague, June 6-7, 2006. Available online at: <http://WWW.icis.com/v2/chemicals/9075165/bisphenol-a/uses.html2006>
- Nascimento Filho Id, von Mühlen C, Schossler P, Bastos Caramão E (2003) Identification of some plasticizers compounds in landfill leachate. *Chemosphere* 50:657-663
- Nemoto K, Chosa-Kai T (1997) Ministry of international trade and industry of Japan. Japan
- North JC, Frew RD, Hale RV (2006) Can stable isotopes be used to monitor landfill leachate impact on surface waters?. *J Geochem Explor* 88:49-53
- Öman C, Hynning P (1993) Identification of organic compounds in municipal landfill leachates. *Environ Pollut* 80:265-271
- Orton F, Lutz I, Kloas W, Routledge EJ (2009) Endocrine Disrupting Effects of Herbicides and Pentachlorophenol: In Vitro and in Vivo Evidence. *Environ Sci Tech* 43:2144-2150.
- Peixoto FP, Lopes ML, Madeira VMC, Vicente JAF (2009) Toxicity of MCPA on non-green potato tuber calli. *Acta physiol Plant* 31:103-109.
- Ping Z, Linbo W, Bo-Geng L (2009) Thermal stability of aromatic polyesters prepared from diphenolic acid and its esters. *Polym Degrad Stab* 94:1261-1266
- Pivato A, Raga R (2006) Tests for the evaluation of ammonium attenuation in MSW landfill leachate by adsorption into bentonite in a landfill liner. *Waste Manage* 26:123-132

- Primo O, Rivero MJ, Ortiz I (2008) Photo-Fenton process as an efficient alternative to the treatment of landfill leachates. *J Hazard Mater* 153:834-842
- Registry of toxic effects of chemical substances (1998) National Institute for Occupational safety and health (NIOHS)
- Reyes-López JA, Ramírez-Hernández J, Lázaro-Mancilla O, Carreón-Díazconti C, Garrido MM (2008) Assessment of groundwater contamination by landfill leachate: A case in México. *Waste Manage* 28:S33-S39
- Rivas FJ, Encinas Á, Acedo B, Beltrán FJ (2009) Mineralization of bisphenol A by advanced oxidation processes. *J Chem Technol Biotechnol* 84:589-594
- Roberts DM, Seneviratne R, Mohammed F, Patel R, Senarathna L, Hittarage A, Buckley NA, Dawson AH, Eddleston M (2005) Intentional self-poisoning with the chlorophenoxy herbicide 4-chloro-2-methylphenoxyacetic acid (MCPA). *Ann Emerg Med* 46:275–284
- Salem Z, Hamouri K, Djemaa R, Allia K (2008) Evaluation of landfill leachate pollution and treatment. *Desalination* 220:108-114
- Silva AC, Dezotti M, Sant'Anna GL (2004) Treatment and detoxification of a sanitary landfill leachate. *Chemosphere* 55:207-214
- Slack RJ, Gronow JR, Voulvoulis N (2005) Household hazardous waste in municipal landfills: contaminants in leachate. *Sci Total Environ* 337:119-137
- Smith EH, Weber Jr. WJ (1990) Comparative assessment of the chemical and adsorptive characteristics of leachates from a municipal and an industrial landfill. *Water Air Soil Pollut* 53:279-295
- Sun Y, Pignatello J (1995) Evidence for a surface dual hole-radical mechanism in the TiO<sub>2</sub> photocatalytic oxidation of 2,4-Dichlorophenoxyacetic acid. *Environ Sci Technol* 29:2065-2072

- Tanaka S, Nakata Y, Kimura T, Yustiawati, Kawasaki M, Kuramitz H (2001) Electrochemical decomposition of bisphenol A using Pt/Ti and SnO<sub>2</sub>/Ti anodes. *J Appl Electrochem* 32:197-201.
- Tchaikovskaya ON, Karetnikova EA, Sokolova IV, Mayer GV, Shvornev DA (2012) The phototransformation of 4-chloro-2-methylphenoxyacetic acid under KrCl and XeBr excilamps irradiation in water. *J Photochem Photobiol A* 228:8-14
- Wang R, Ren D, Xia S, Zhang Y, Zhao J (2009) Photocatalytic degradation of Bisphenol A (BPA) using immobilized TiO<sub>2</sub> and UV illumination in a horizontal circulating bed photocatalytic reactor (HCBPR). *J Hazard Mater* 169:926-932
- Yamamoto T, Yasuhara A, Shiraishi H, Nakasugi O (2001) Bisphenol A in hazardous waste landfill leachates. *Chemosphere* 42:415-418
- Zertal A, Sehili T, Boule P (2001) Photochemical behaviour of 4-chloro-2-methylphenoxyacetic acid: Influence of pH and irradiation wavelength. *J Photochem Photobiol A* 146:37-48
- Zhang RF, Moore JA (2002) Synthesis, characterization and properties of polycarbonate containing diphenolic acid. *Polym Prepr* 43:1007-1008
- Zhang R, Moore JA (2003) Synthesis, Characterization and Properties of Polycarbonate Containing Carboxyl Side Groups. *Macromol Sympos* 199:375-390
- Zhang K, Gao N, Deng Y, Lin TF, Ma Y, Li L, Sui M (2011) Degradation of bisphenol-A using ultrasonic irradiation assisted by low-concentration hydrogen peroxide. *J Environ Sci* 23:31-36
- Zhou Y, Chen L, Lu P, Tang X, Lu J (2011) Removal of bisphenol A from aqueous solution using modified fibric peat as a novel biosorbent. *Sep Purif Technol* 81:184-190

# 1.7. ENVIRONMENTAL IMPACT OF PHTHALIC ACID ESTERS AND THEIR REMOVAL FROM WATER AND SEDIMENTS BY DIFFERENT TECHNOLOGIES A REVIEW - AREVIEW

Article published in Journal of Environmental Management 109, 164-178 (2012)



## Highlights

- The properties of phthalic acid esters (PAEs) were described.
- The persistence of PAEs in the environment was evaluated.
- The most recent methods to remove PAEs from water and sediments were analyzed.
- The selection of the appropriate removal treatment depends on the type of PAEs.

## ABSTRACT

This article describes the most recent methods developed to remove phthalic acid esters (PAEs) from water, wastewater, sludge, and soil. In general, PAEs are considered to be endocrine disrupting chemicals (EDCs), whose effects may not appear until long after exposure. There are numerous methods for removing PAEs from the environment, including physical, chemical and biological treatments, advanced oxidation processes and combinations of these techniques. This review largely focuses on the treatment of PAEs in aqueous solutions but also reports on their treatment in soil and sludge, as well as their effects on human health and the environment.



### 1.7.1. Introduction

Legislation on the quality of wastewater discharged into the environment has become increasingly strict and wastewater reutilization more widespread over recent years, leading to the development of novel technologies for treating wastewater and removing new and emerging pollutants (Arévalo et al., 2009). There is a constant generation of new contaminants with unknown short-, medium-, or long-term effects on human health and the environment, whose maximum permissible concentrations have yet to be established. Industrial and pharmaceutical pollutants are causing particular concern due to their continuous discharge into water and their persistence, even at low concentrations (Klavarioti et al., 2009).

Industrial waste has been poorly managed and is becoming a major problem in industrialized regions. Agriculture, chemical, textile and metallurgic industries consume large amounts of water that are released into the environment after processing and contain dissolved toxic substances such as acids, bases, toxic chemical compounds and heavy metals, all potentially harmful to the environment (Navarro and Font, 1993).

Industrial activity has led to the release of a large number of synthetic organic chemicals into the environment, including plasticizers and organic esters, which are added to polymers to facilitate their processing and increase the flexibility and toughness of the final product by internal modification of the polymer molecules (Bauer and Herrmann, 1997; Nascimento-Filho et al., 2003). They are widely used in numerous products, such as medical equipment, food film, upholstery, flooring, mouldings, gaskets, piping, rainwear, electrical wire insulation, roofing systems, vehicle trim/undercoating, and pond liners, among others. They also serve to endow paints with special coating properties.

The most widely used primary plasticizers have a low molecular weight and are designated monomeric plasticizers, distinguishing them from polymeric plasticizers, which are generally saturated polyesters. The most common monomeric plasticizers are esters derived from phthalic acid, although others are derived from different organic



acids, such as phosphates, trimetillates, citrates, sebacates, and adipates, among others (Titow, 1990; Wickson, 1993). The content of phthalate in a finished plastic product ranges from 10 to 60% by weight (IARC, 2000).

Polyvinylchloride (PVC) is an excellent example of the industrial importance of plasticizers (Horn et al., 2004). PVC is one of the most frequently used polymers because it is easily processed, the raw materials involved in its production have a relatively low cost, and a wide range of properties can be obtained. The annual production of PVC is in the tens of millions of tons, and approximately 87% of the phthalate esters produced are used in soft PVC (Mersiowsky et al., 2001).

In many applications, the plasticizer may migrate from a plastic item to the medium (gas, liquid or solid) with which it is in contact. The migration depends on the properties of the polymer (e.g., molecular weight), the nature and amount of the plasticizer, the plasticization process, and the homogeneity of the compound and the surrounding media (e.g., nature, compatibility with the plasticizer) among other factors, as well as on the temperature and contact area. The permanence of a plasticizer in a flexible plastic material depends on three main factors: structure, molecular weight/viscosity, and polarity. Branched plasticizers are more permanent than equivalent linear plasticizers, since branching tends to hinder movement or entangle the plasticizer within the polymer matrix, hampering its migration or removal by volatilization or extraction. However, although linear structures provide less permanence, they yield superior low temperature properties (Marcilla et al., 2004).

In landfills, the leachate is formed from refractory organic contents during biological degradation. The leachate has high biochemical oxygen (BOD) and chemical oxygen (COD) demands and passes down through the layers of the landfill through the action of rainwater, thereby potentially contaminating the soil and drinking waters (Kuch and Ballschmiter, 2001). Analyses of landfills have revealed alkylphenols (APs), Bisphenol A (BPA), phthalic acid esters (PAEs), organotin compounds (OTs), styrene and estradiol (Asakura et al., 2004).

Conventional treatments of landfill leachate are not able to remove plasticizers due to their resistance to microbial decomposition, and the widespread presence of PAEs is raising concerns about their toxicological effects on living organisms (Alatríste-Mondragon et al., 2003).

According to the above observations, the objective of this study was to review and analyze the most important aspects of PAEs such as: properties and classification, development and applications, their presence in the environment, toxicity and effects on human health, legislations and restrictions, as well as their removal from landfills leachates by means of different technologies.

### 1.7.2. Phthalic acid esters

#### *1.7.2.1. Properties, classification and applications of phthalates (PAEs)*

Phthalates are non-halogenated esters of phthalic acid that find wide spread utilization in various industrial and consumer-orientated applications. Commonly produced PAEs are colorless or yellowish oil like liquids and almost odourless. PAEs have a melting point below  $-25^{\circ}\text{C}$ , with the exception of DMP ( $+5.5^{\circ}\text{C}$ ) and DUP ( $-9^{\circ}\text{C}$ ). The boiling point of PAEs ranges from  $230^{\circ}\text{C}$  to  $486^{\circ}\text{C}$ . The low melting point and high boiling point of these PAEs contribute to their applicability as plasticizers, heat transfer fluids and carriers.

The water solubility of a chemical compound influences its biodegradation, bioaccumulation potential and environmental distribution. Leachate from wastewater treatment facilities, landfill and sludge-amended soils is also affected by aqueous solubility. Hydrophobicity, indicated by the octanol-water partitioning factor,  $K_{\text{OW}}$ , and vapour pressure, play an important role in the fate of emissions and other releases of PAEs into the atmosphere. This chemical family exhibits an increase in  $K_{\text{OW}}$  of eight orders of magnitude and a decrease in vapour pressure of four orders of magnitude with lengthening of the alkyl chain from 1 to 13 carbon atoms (Stales et al., 1997). The most common PAEs found in the environment and their physico-chemical properties are listed in Table 1.

**Table 1.** Physico-chemical properties of selected phthalates

| Phthalic acid ester            | Acronym      | M.W. (g/mol) <sup>1</sup> | Solubility in water<br>25°C (g/L) | LogK <sub>OW</sub> <sup>2</sup> | Structural formula  | CAS N <sup>o</sup> <sup>3</sup> |
|--------------------------------|--------------|---------------------------|-----------------------------------|---------------------------------|---|---------------------------------|
| Phthalic acid                  | PA           | 166.1                     | 0.625                             | 0.81                            | C <sub>6</sub> H <sub>4</sub> (COOH) <sub>2</sub>   | 88-99-3                         |
| Dimethyl phthalate             | DMP          | 194.2                     | < 0.100                           | 1.64                            | C <sub>6</sub> H <sub>4</sub> (COOCH <sub>3</sub> ) <sub>2</sub>  | 131-11-3                        |
| Dimethyl Terephthalate         | DMTP         | 194.2                     | 0.019-0.034                       | 2.25                            | C <sub>6</sub> H <sub>4</sub> (COOCH <sub>3</sub> ) <sub>2</sub>  | 120-61-6                        |
| Diethyl phthalate              | DEP          | 222.2                     | 1.000                             | 2.70                            | C <sub>6</sub> H <sub>4</sub> (COOC <sub>2</sub> H <sub>5</sub> ) <sub>2</sub>  | 84-66-2                         |
| Diallyl phthalate              | DAP          | 246.2                     | 0.182                             | 3.29                            | C <sub>6</sub> H <sub>4</sub> (COOCH <sub>2</sub> CH=CH <sub>2</sub> ) <sub>2</sub>   | 131-17-9                        |
| Butyl 2-Ethylhexyl phthalate   | BOP          | 334.4                     | 0.001                             | 6.77                            | CH <sub>3</sub> (CH <sub>2</sub> ) <sub>3</sub> OOCC <sub>6</sub> H <sub>4</sub> COOCH <sub>2</sub> CH<br>(C <sub>2</sub> H <sub>5</sub> )(CH <sub>2</sub> ) <sub>3</sub> CH <sub>3</sub> | 85-69-8                         |
| Di- <i>n</i> -propyl phthalate | DPP,<br>DPrP | 250.3                     | 0.060                             | 3.57                            | C <sub>6</sub> H <sub>4</sub> [COO(CH <sub>2</sub> ) <sub>2</sub> CH <sub>3</sub> ] <sub>2</sub>  | 131-16-8                        |
| Di- <i>n</i> -nonyl phthalate  | DnNP         | 418.6                     | <0.001                            | 10.14                           | C <sub>6</sub> H <sub>4</sub> [COO(CH <sub>2</sub> ) <sub>8</sub> CH <sub>3</sub> ] <sub>2</sub>  | 84-76-4                         |
| Di- <i>n</i> -butyl phthalate  | DnBP,<br>DBP | 278.4                     | 0.015                             | 4.83                            | C <sub>6</sub> H <sub>4</sub> [COO(CH <sub>2</sub> ) <sub>3</sub> CH <sub>3</sub> ] <sub>2</sub>  | 84-74-2                         |
| Diisobutyl phthalate           | DIBP         | 278.3                     | 0.011                             | 4.46                            | C <sub>6</sub> H <sub>4</sub> [COOCH <sub>2</sub> CH(CH <sub>3</sub> ) <sub>2</sub> ] <sub>2</sub>  | 84-69-5                         |
| Butylcyclohexyl phthalate      | BCP          | 304.4                     | <0.002                            | 5.29                            | CH <sub>3</sub> (CH <sub>2</sub> ) <sub>3</sub> OOCC <sub>6</sub> H <sub>4</sub> COOC <sub>6</sub> H <sub>11</sub>  | 84-64-0                         |
| Di- <i>n</i> -pentyl phthalate | DnPP         | 306.4                     | <0.001                            | 5.89                            | C <sub>6</sub> H <sub>4</sub> [COO(CH <sub>2</sub> ) <sub>4</sub> CH <sub>3</sub> ] <sub>2</sub>  | 131-18-0                        |
| Dicyclohexyl phthalate         | DCP          | 330.4                     | <0.002                            | 5.76                            | C <sub>6</sub> H <sub>4</sub> [COOC <sub>6</sub> H <sub>11</sub> ] <sub>2</sub>   | 84-61-7                         |
| Butyl benzyl phthalate         | BBP          | 312.4                     | <0.002                            | 5.00                            | CH <sub>3</sub> (CH <sub>2</sub> ) <sub>3</sub> OOCC <sub>6</sub> H <sub>4</sub> COOCH <sub>2</sub> C <sub>6</sub> H <sub>5</sub>   | 85-68-7                         |
| Di- <i>n</i> -hexyl phthalate  | DnHP         | 334.5                     | <0.001                            | 6.95                            | C <sub>6</sub> H <sub>4</sub> [COO(CH <sub>2</sub> ) <sub>5</sub> CH <sub>3</sub> ] <sub>2</sub>  | 84-75-3                         |
| Diisohexyl phthalate           | DIHxP        | 334.4                     | <0.001                            | 6.58                            | C <sub>6</sub> H <sub>4</sub> [COO(CH <sub>2</sub> ) <sub>3</sub> CH(CH <sub>3</sub> ) <sub>2</sub> ] <sub>2</sub>  | 146-50-9                        |
| Di- <i>n</i> -heptyl phthalate | DIHpP        | 362.5                     | <0.001                            | 7.65                            | C <sub>6</sub> H <sub>4</sub> [COO(CH <sub>2</sub> ) <sub>4</sub> CH(CH <sub>3</sub> ) <sub>2</sub> ] <sub>2</sub>  | 3648-21-3                       |
| Butyl decyl phthalate          | BDP          | 362.5                     | <0.001                            | 8.01                            | CH <sub>3</sub> (CH <sub>2</sub> ) <sub>3</sub> OOCC <sub>6</sub> H <sub>4</sub> COO(CH <sub>2</sub> ) <sub>9</sub> CH <sub>3</sub>   | 89-19-0                         |
| Di(2-ethylhexyl) phthalate     | DEHP         | 390.6                     | <0.001                            | 8.71                            | C <sub>6</sub> H <sub>4</sub> [COOCH <sub>2</sub> CH(C <sub>2</sub> H <sub>5</sub> )(CH <sub>2</sub> ) <sub>3</sub> CH <sub>3</sub> ] <sub>2</sub>  | 117-81-7                        |
| Di- <i>n</i> -octyl phthalate  | DOP,<br>DnOP | 390.6                     | <0.001                            | 9.08                            | C <sub>6</sub> H <sub>4</sub> [COO(CH <sub>2</sub> ) <sub>7</sub> CH <sub>3</sub> ] <sub>2</sub>  | 117-84-0                        |
| Diisooctyl phthalate           | DIOP         | 390.6                     | <0.001                            | 8.71                            | C <sub>6</sub> H <sub>4</sub> [COO(CH <sub>2</sub> ) <sub>5</sub> CH(CH <sub>3</sub> ) <sub>2</sub> ] <sub>2</sub>  | 27554-26-3                      |
| Di( <i>n</i> -decyl) phthalate | DnDP         | 446.7                     | <0.001                            | 11.20                           | C <sub>6</sub> H <sub>4</sub> [COO(CH <sub>2</sub> ) <sub>9</sub> CH <sub>3</sub> ] <sub>2</sub>  | 84-77-5                         |
| Diisononyl phthalate           | DINP         | 418.6                     | <0.001                            | 9.77                            | C <sub>6</sub> H <sub>4</sub> [COO(CH <sub>2</sub> ) <sub>6</sub> CH(CH <sub>3</sub> ) <sub>2</sub> ] <sub>2</sub>  | 28553-12-0                      |
| Diisodecyl phthalate           | DIDP         | 446.7                     | <0.001                            | 10.47                           | C <sub>6</sub> H <sub>4</sub> [COO(CH <sub>2</sub> ) <sub>7</sub> CH(CH <sub>3</sub> ) <sub>2</sub> ] <sub>2</sub>  | 26761-40-0                      |
| Diundecyl phthalate            | DUP          | 474.7                     | <0.001                            | 12.26                           | C <sub>6</sub> H <sub>4</sub> [COO(CH <sub>2</sub> ) <sub>10</sub> CH <sub>3</sub> ] <sub>2</sub>   | 3648-20-2                       |
| Diisoundecyl phthalate         | DIUP         | 474.7                     | <0.001                            | 12.26                           | C <sub>6</sub> H <sub>4</sub> [COO(CH <sub>2</sub> ) <sub>8</sub> CH(CH <sub>3</sub> ) <sub>2</sub> ] <sub>2</sub>  | 85507-79-5                      |
| Ditridecyl phthalate           | DTDP         | 530.8                     | <0.010                            | 14.39                           | C <sub>6</sub> H <sub>4</sub> [COO(CH <sub>2</sub> ) <sub>12</sub> CH <sub>3</sub> ] <sub>2</sub>   | 119-06-2                        |
| Diisotridecyl phthalate        | DIUP         | 530.8                     | <0.001                            | 14.02                           | C <sub>6</sub> H <sub>4</sub> [COO(CH <sub>2</sub> ) <sub>10</sub> CH(CH <sub>3</sub> ) <sub>2</sub> ] <sub>2</sub>   | 27253-26-5                      |
| Terephthalic acid              | TPA          | 166.1                     | 0.017                             | 1.16-2.00                       | C <sub>6</sub> H <sub>4</sub> (COOH) <sub>2</sub>   | 100-21-0                        |

<sup>1</sup> Molecular weight, <sup>2</sup> LogK<sub>OW</sub> (ChemSpider Database), <sup>3</sup> Chemistry Abstracts Service registry number.

Low-molecular-weight phthalates (e.g., DMP, DEP and DBP) are widely used in cosmetics and personal care products. For example, DMP and DEP allow perfume fragrances to evaporate more slowly, lengthening the duration of the scent, and a small amount of DBP gives nail polish a chip-resistant property. DEP is used as an ethanol denaturant and DBP in cellulose esters, printing inks, and specialized adhesive formulations. Longer phthalate molecules, such as di (2-ethylhexyl) phthalate (DEHP), diisononyl phthalate (DINP) and BBP, have a wide application as plasticizers in the polymer industry to improve flexibility, workability, and general handling properties; around 80% of all phthalates are used for this purpose (IARC, 2000).

DINP and DEHP have been used in recent decades for PVC plasticization (including toy manufacture) due to their low cost and the flexibility and durability of the final product, among other properties. Flexible PVC is widely used in medical applications (e.g., catheters and bottles) due to its excellent physical properties and low cost (Shin et al., 2002).

Worldwide production of PAEs is approximately 6 million tons per year (Mackintosh et al., 2006). Similar to other products present in plastics, the majorities of PAEs ends up in at municipal landfills together with waste PVC and are able to migrate into groundwater through the soil (Castillo and Barceló, 2001).

#### *1.7.2.2. PAEs in the environment*

The major portion of phthalate acid esters found in the environment is as a result of the slow release of phthalates from plastics and other phthalate containing materials due to weathering. These pollutants are refractory to the environmental microorganisms, and their accumulation in natural waters causes their wide distribution within aqueous systems like rivers, lakes, and ground waters, as well as a noticeable influence on the ecological environment. In recent times, the behaviour of PAEs in the environment has attracted considerable attention because they are considered endocrine-disrupting chemicals (Chang et al., 2006; Colón et al., 2001). For these reasons, several research groups have addressed the identification of PAEs in several kinds of environmental samples, like municipal solid waste compost (Farrell and Jones, 2009), sludge of

sewage and wastewater treatment (Gibson et al., 2007; Huang et al., 2008; Marttinen et al., 2003a; Marttinen et al., 2004a; Rhind et al., 2007; Roslev et al., 2007), river sediments (Chang et al., 2005; Chi, 2009; Lin et al., 2009; McDowell and Metcalfe, 2001; Otton et al., 2008; Xu and Li, 2008; Zhou and Liu, 2000) and landfill leachate (Albaiges et al., 1986; Buszka et al., 2009; Fang et al., 2009a; Fang et al., 2009b; Furtmann and Seifert, 1990; Kotzias et al., 1975; Marttinen et al., 2003b; Öman and Hynning, 1993; Rodrigues et al., 2002; Smith and Weber Jr., 1990).

PAEs are usually determined by means of chromatographic techniques, involving a pre-treatment step with liquid-liquid extraction (LLE) (Mori, 1976), ultrasonic extraction (USE) (Ma et al., 2003), microwave-assisted extraction (MAE) (Bartolomé et al., 2005), liquid-phase micro extraction (LPME), (Batlle and Nerín, 2004; Psillakis and Kalogerakis, 2003) solid-phase micro extraction (SPME) (Cortazar et al., 2002; Peñalver et al., 2001), or solid phase extraction (SPE). SPE is the most widely used technique because of its high recovery rate, elevated pre-concentration factors, low consumption of organic solvents, simplicity, and its easy automation and operation, among other advantages (Zhao et al., 2007; Zhou et al., 2006). Detection limits for some PAEs are given in Table 2.

**Table 2.** Detection limits of phthalates in wastewater and sludge (Dargnat et al., 2009).

| <b>Location</b>          | <b>DMP</b> | <b>DEP</b> | <b>DnBP</b> | <b>BBP</b> | <b>DEHP</b> | <b>DnOP</b> |
|--------------------------|------------|------------|-------------|------------|-------------|-------------|
| <b>Wastewater (ng/L)</b> | 20         | 30         | 30          | 10         | 40          | 20          |
| <b>Sludge (ng/L dw)</b>  | 50         | 80         | 80          | 100        | 500         | 150         |

Phthalates are not chemically bound to polymer matrixes and can be readily dispersed into the environment during their production and use and after their disposal. Phthalate plasticizers have become ubiquitous contaminants because they are not covalently bound to PVC and can leach, migrate or evaporate into foodstuffs or any other material, indoor air and the atmosphere (Pant et al., 2008). Because of their low solubility, phthalates tend to be concentrated from wastewater into sewage sludge, which is then used as a soil amendment, implying the exposure of soil microbial communities, plants, and animals to these compounds and their introduction into the food chain.

The extensive use of PAEs in industrial processes and consumer products has resulted in their ubiquitous presence in the environment. As an example of their universal presence, one study in Guangzhou city (China) detected 16 PAEs (DMP, DEP, DnBP, DIBP, DMPP, DMGP, DEEP, DnAP, DnHP, BBP, HEHP, DBEP, DCHP, DEHP, DnNP and DnOP) in all samples from water and sediments of urban lakes. Sources of these compounds included urban storm water runoff, atmospheric deposition and the discharge of untreated industrial wastewater and municipal sewage. Concentrations of the PAEs ranged from 1.69 to 4.72  $\mu\text{g/L}$  in water and from 2.27 to 74.94  $\mu\text{g/g dw}$  in sediments (Zeng et al., 2008).

Other studies have reported phthalate concentrations from 0.3 to 77  $\text{ng/m}^3$  in the atmosphere, from 0.3 to 98  $\mu\text{g/L}$  in surface waters, from 0.2 to 8.4  $\text{mg/kg dw}$  in sediments and from 28 to 154  $\text{mg/kg dw}$  in sewage sludge (Fromme et al., 2002; Stales et al., 1997). The presence of phthalates was observed in water samples during a 5-year (2000-2004) survey of micro-pollutants in rivers and small streams in the Han River basin, Korea (Ko et al., 2008). They have been detected in freshwater fish species, e.g., bream (*Abramis brama*, 1900–3120  $\text{ng/g dw}$  of DEHP and 720–800  $\text{ng/g dw}$  of DEP) and in marine species, e.g., flounder (*Platichthys flesus*, 40–70  $\text{ng/g dw}$  of DEHP and 100-200  $\text{ng/g dw}$  of DEP (Dargnat et al., 2009).

It is common practice to dispose of biosolids by treating the sludge and using it for soil conditioning (biosolids represent half of European sludge production), and the resulting accumulation of persistent toxic organic compounds, as PAEs, in the soil poses a growing threat to ecosystems and human health. The use of sewage sludge in agriculture can produce human exposure during its application or through the resulting introduction of these compounds into the food chain. There is an urgent need to ensure that sludge is free from these contaminants before its utilization (Amir et al., 2005).

PAEs have been found in sewage sludge at levels of 12-1250  $\text{mg/Kg}$  (Stales et al., 1997). Table 3 reports the PAE findings in 10 raw leachate samples from three landfills. The presence of phthalates was analyzed in leachates from 17 landfills in Sweden,

Denmark, Germany, and Italy, detecting PAEs and the presence of their degradation products phthalic acid monoesters (PMEs) and ortho-phthalic acid (PA) in 11 of them; PME concentrations ranged from 1-20  $\mu\text{g/L}$  and PA concentrations from 2-880  $\mu\text{g/L}$  (Jonsson and Borén, 2002). Concentrations of DMP, DEP, DnBP, DIBP, BBP, and DEHP in water and sediment have been routinely reported, but there are limited data on many other PAEs (Table 4).

PAEs have been found in sewage sludge at levels of 12-1250 mg/Kg (Stales et al., 1997). Table 3 reports the PAE findings in 10 raw leachate samples from three landfills. The presence of phthalates was analyzed in leachates from 17 landfills in Sweden, Denmark, Germany, and Italy, detecting PAEs and the presence of their degradation products phthalic acid monoesters (PMEs) and ortho-phthalic acid (PA) in 11 of them; PME concentrations ranged from 1-20  $\mu\text{g/L}$  and PA concentrations from 2-880  $\mu\text{g/L}$  (Jonsson and Borén, 2002). Concentrations of DMP, DEP, DnBP, DIBP, BBP, and DEHP in water and sediment have been routinely reported, but there are limited data on many other PAEs (Table 4).

**Table 3.** Concentration of PAEs in ten leachate samples from three landfills ( $\mu\text{g/L}$ ) (Zhang and Wang, 2009).

| Landfill No    | DMP  | DEP  | DIBP  | DBP   | BBP   | DEHP   | DnOP   |
|----------------|------|------|-------|-------|-------|--------|--------|
| R <sub>1</sub> | 0.14 | 0.11 | 1.65  | 0.96  | 19.32 | 88.86  | 521.11 |
| R <sub>2</sub> | 0.75 | 0.25 | 5.45  | 3.30  | 21.80 | 97.55  | 514.70 |
| R <sub>3</sub> | 1.35 | 0.70 | 15.15 | 5.95  | 8.50  | 232.50 | 280.30 |
| R <sub>4</sub> | 2.80 | 1.80 | 63.65 | 59.75 | 0.54  | 121.42 | 15.35  |
| R <sub>5</sub> | 0.24 | 0.44 | 28.44 | 24.69 | 0.50  | 72.49  | -      |
| J <sub>1</sub> | 0.02 | 0.35 | 1.09  | 1.28  | 4.37  | 7.91   | 113.02 |
| J <sub>2</sub> | -    | -    | 0.44  | 0.35  | 0.19  | 1.61   | 5.59   |
| J <sub>3</sub> | 0.03 | 0.03 | 62.58 | 2.43  | -     | 72.55  | -      |
| J <sub>4</sub> | 0.61 | 5.66 | 81.55 | 40.61 | -     | 81.59  | -      |
| H              | 0.02 | 0.04 | 2.71  | 2.67  | -     | 1.71   | -      |
| Mean           | 0.60 | 0.94 | 26.27 | 14.20 | 5.52  | 77.82  | 145.01 |

### 1.7.2.3. Toxicity and effects on human health

The toxicity of phthalates remains under debate, characterised by tensions between the commercial importance of phthalates and their impact on human health and the

environmental. Some research groups have described some phthalates as hazardous to human health, while other groups, usually associated with phthalate producers, have argued that dose levels are low and pose only a minimal threat to health (IARC, 2000). It has been reported that phthalates may affect blood components in humans and guinea pigs (Guess and Haberman, 1968) and exert a teratogenic effect on rats (Singh et al., 1972; Singh et al., 1974), and there is evidence that di-2-ethylhexyl and bis (2-methoxyethyl) phthalates have potential mutagenic effects in male mice (Calley et al., 1966). A study of the biological activity of eight phthalate acid esters indicated that the degree of their toxicity was low when administered parentally and paralleled their water solubility (Autian, 1973). Animal toxicology studies found that DEHP, DBP and DEP decreased testicular and epididymal weight, semen quality and fertility while increasing cryptorchidism, testis damage, and leydig cell hyperplasia (Pant et al., 2008).

Phthalates exhibit low acute toxicity with LD 50 values of 1–30 g/kg bodyweight or with even higher concentrations. In short- and long-term rodent studies, dose-related adverse effects were found in liver, kidney and in thyroid gland tissue and testes. All phthalates have been tested negative for mutagenicity and/or genotoxicity. With regard to carcinogenicity, the activity of DEP is questionable, for DINP no hints for carcinogenicity were obtained (Heudorf et al., 2007).

The exposure of adult humans to DEHP in everyday life has been estimated to be 0.71 µg/kg/d. Reports include the detection of 15- 83.2 µg/L of DEHP in human blood and of 2.1 to 44.5 µg/L of MEHP in human urine, among other DEHP by-products. Some phthalate esters are known to be toxic to the developing male reproductive system, and low-molecular-weight phthalates (e.g., DEP) have been found to cause irritation of eyes, nose and throat (Benson, 2009).

Mixtures of phthalate esters and other anti-androgenic compounds were shown to have cumulative, largely dose additive effects on male reproductive tract development when administered during sexual differentiation *in utero*, potentially affecting human reproductive development (Howdeshell et al., 2008). In humans, multivariate analyses



demonstrated that the concentrations of phthalate metabolites in the mother were significantly associated with the concentrations found in the infant (Sathyanarayana et al., 2008). One study found that relatively short-term exposure to DEHP had no adverse effects on reproduction, but BBP was named as a suspected endocrine-disrupting compound in a pilot field study carried out by the EPA (Peñalver et al., 2002). The most frequently detected PAE was reported to be DBP, found at highest levels in venous blood followed by breast milk, umbilical cord blood and urine; this order depends on metabolic factors (Chen et al., 2008).

#### *1.7.2.4. Legislations and restrictions*

The potential risk to human and animal health of PAEs has become a matter of considerable worldwide concern. They have been included in the list of priority pollutants compiled by both the USA Environmental Protection Agency (USEPA) and the EU, and in the list of priority pollutants in Chinese waters (Yuan et al., 2008; Zhao et al., 2008). In 1998, the Scientific Committee on Toxicity, Ecotoxicity and the Environment (CSTEE) of the European Union proposed the setting of new permissible levels for extractable phthalates in toys (Proceedings of the Third Plenary Meeting of CSTEE, 1998). The next year, in the absence of a reproducible test to determine migration levels for regulatory purposes, the EU banned phthalates in products designed for children under the age of 3 years that could be put in their mouths (Official Journal of the European Communities. L 315/46, 1999). This EU prohibition on their use in children's toys remains in place (Bette, 2007). In California, some phthalates have been banned from children's toys since 2009 (Bette, 2007). NASA banned the use of phthalates in spacecrafts due to their ability to volatilize and condense on viewports and other areas (Gross and Colony 1973).

Although the risk for humans has not been established, various Consumers Associations and Ecologist Groups have called for the removal of phthalates in PV, especially in PVC items designed for oral use. Serious questions have been raised about toy and child-care applications, especially if they are susceptible to be chewed or sucked by children (Marcilla et al., 2004).

**Table 4.** Comparison among concentrations of major PAEs in water/sediment.

| <b>Location</b>               | <b>DMP</b> | <b>DEP</b> | <b>DiBP</b> | <b>DnBP</b> | <b>BBP</b> | <b>DEHP</b> | <b>Ref</b>                      |
|-------------------------------|------------|------------|-------------|-------------|------------|-------------|---------------------------------|
| <i><b>Water (mg/L)</b></i>    |            |            |             |             |            |             |                                 |
| Taiwan, China                 | -----      | 0.500      | -----       | 4.900       | <0.100     | 9.300       | (Yuan et al., 2002)             |
| Guangzhou, China              | 0.009      | 0.031      | 0.430       | 1.990       | <0.001     | 0.170       | (Zeng et al., 2008)             |
| Klang River Basin, Malaysia   | <0.050     | <0.050     | 0.250       | 1.600       | -----      | 16.600      | (Tan, 1995)                     |
| Rieti District, Italy         | <0.012     | <0.010     | 0.300       | 1.600       | <0.010     | 4.300       | (Vitali et al. 1997)            |
| Berlin, Germany               | -----      | -----      | -----       | 0.500       | -----      | 2.700       | (Fromme et al., 2002)           |
| Dutch coast, the Netherlands  | 0.017      | 0.430      | -----       | 0.250       | 0.077      | 0.320       | (Vethaak et al., 2005)          |
| Fresh water, the Netherlands  | -----      | -----      | -----       | 0.210       | -----      | 0.330       | (Peijnenburg and Struijs, 2006) |
| <i><b>Sediment (mg/g)</b></i> |            |            |             |             |            |             |                                 |
| Taiwan, China                 | -----      | 0.200      | -----       | 6.300       | 0.200      | 4.600       | (Yuan et al., 2002)             |
| Guangzhou, China              | 0.039      | 0.130      | 5.800       | 0.280       | 0.034      | 1.300       | (Zeng et al., 2008)             |
| Klang River Basin, Malaysia   | 0.003      | 0.003      | 0.056       | 0.250       | -----      | 1.630       | (Tan, 1995)                     |
| Rieti District, Italy         | <0.0002    | 0.002      | 0.013       | 0.008       | 0.002      | 0.069       | (Vitali et al., 1997)           |
| Berlin, Germany               | -----      | -----      | -----       | 0.450       | -----      | 0.700       | (Fromme et al., 2002)           |
| Dutch coast, the Netherlands  | 0.014      | 0.133      | -----       | 0.390       | 0.014      | 0.600       | (Vethaak et al., 2005)          |
| Fresh water, the Netherlands  | -----      | -----      | -----       | 0.088       | -----      | 4.300       | (Peijnenburg and Struijs, 2006) |

### 1.7.3. Removal of PAEs from water and sediments by means of different technologies

As noted above, large amounts of PAEs are leached from plastics dumped at municipal landfills (Bauer et al., 1998). PAE concentrations ranged from 10 to 300  $\mu\text{g/L}$  in wastewater (WW) from a number of chemicals plants and nearby rivers and reached 30 mg/L in WW near a plasticiser-producing factory (Mailhot et al., 2002). Numerous studies have addressed the removal of PAEs from water and sediments, and treatments can be classified into three general groups: i) physical/chemical treatments, ii) biological treatments, and iii) advanced oxidation processes. Each group is analyzed below, discussing the treatment of PAEs in WW and sludge plants in a final section.

#### *1.7.3.1. Physical/Chemical treatments*

Physical and chemical processes include the reduction of suspended solids, colloid particles, floating material, colour and toxic compounds by floatation, coagulation/flocculation, and adsorption (Metcalf et al., 2003).

Floatation is widely used to separate solid particles from a liquid phase mainly to reduce colloids, ions, macromolecules, microorganisms or fibres (Rubio et al., 2002). In coagulation/flocculation, a floc-forming chemical reagent is added to a water or wastewater to enmesh or combine with non-settleable colloidal solids and slow-settling suspended solids to produce a fast-settling floc that can then be removed, usually by sedimentation (Reynolds, 1982).

Zhang and Wang (2009) investigated the removal of dissolved organic matter (DOM) and phthalic acid esters from landfill leachate through a complexation–flocculation process by using ferric chloride, aluminum sulfate and poly aluminum chloride as coagulants. The results revealed that hydrophobic contaminants with  $\log K_{OW}$  greater than 4 and DOM in wastewater can be removed simultaneously through the complexation–flocculation process. Zheng et al. (2009) evaluate the feasibility of removing PAEs from fresh and partially stabilized landfill leachates by a coagulation and flocculation process and found that less than 30% of the PAEs in the fresh leachate could be removed.

Adsorption is an efficient method to remove organic compounds from drinking water. In fact, the USA Environmental Protection Agency has acknowledged that adsorption on activated carbon, one of the oldest water treatments, is one of the best methods available to remove organic and inorganic compounds from water intended for human consumption.

Adsorption of landfill leachate onto granular or powder activated carbon yields a higher reduction in dissolved organic carbon in comparison to chemical methods and has proven to be the most effective and reliable physicochemical non-destructive technique for PAEs removal (Fettig et al., 1996; Imai et al., 1998; Kargi and Pamukoglu, 2004; Kargi and Yunus-Pamukoglu, 2003; Morawe et al., 1995; Welander and Henrysson, 1998; Zamora et al., 2000).

Activated carbons are very effective adsorbents due to their large surface area and chemical nature (Bautista-Toledo et al., 2008; Méndez-Díaz et al., 2010). In aqueous phase, the solution pH has an important effect on the adsorption yield because it determines the charge density of the activated carbon (Radovic et al., 2001) and the chemical form of ionizable compounds (e.g., PAEs) (Rivera-Utrilla et al., 2009). Venkata-Mohan et al. (2007) studied the adsorption of DEP from aqueous phase onto commercial activated carbon demonstrating that adsorption of DEP is highly dependent on the solution pH, diminishing as the pH of the solution was increased from 2.0 to 10.5. The same trend was found by Ayranci and Bayram (2005) for the adsorption of PA on activated carbon cloth. Thus, the solution pH was found to be important in the adsorption of PA due to ionization. At pH values higher than the  $pH_{pzc}$  of carbon-cloth, phthalic acid was not adsorbed due to possession of the same negative charge that the carbon surface. Other adsorbents have been also employed to remove PAEs from aqueous solutions e.g. chitosan, manganese oxides, clays, multiwalled carbon nanotubes, polymeric resins and others.

Julínová and Slavík (2012) present a detailed revision of the removal of phthalates from aqueous solution by different adsorbents. Méndez-Díaz et al. (2012) investigated the adsorption of PA in aqueous solution on two activated carbons with different chemical

natures, and analyzed the influence of solution pH and ionic strength. They reported that the activated carbons used had a high capacity to adsorb PA due to their phenolic groups content, moreover, the adsorption capacity was favored at acidic pHs and it was not affected by the presence of electrolyte.

Table 5 summarizes key studies on the removal of PAEs by physical/chemical treatments.

#### *1.7.3.2. Biological treatments*

By means of biological treatments of water, organic pollutants, they are mainly transformed into carbon dioxide, nitrates, sulphate, and end-products in aerobic procedures, and into ammonia, methane and hydrogen sulphate in anaerobic treatments (Metcalf et al., 2003).

Abundant data are available on the biodegradation of PAEs (Xu et al., 2005). Some studies on the environmental fate of DBP and DEHP demonstrated that microbial activity is the main degradation mechanism for their degradation in aquatic and terrestrial systems, including surface waters, soils and sediments (Juneson et al., 2001; Sello et al., 2004). The hydrolysis and photolysis of these compounds is slow (Zhou et al., 1995), confirming the importance of the biological pathway (Xu et al., 2008). Other studies reported that PAEs with short ester hydrocarbon chains are more readily biodegraded and mineralized than those with long ester chains, some of which are considered recalcitrant (Ejlertsson et al., 1997; Jianlong et al., 2000; O'Grady et al., 1985).

Bioremediation offers a potential solution for the conversion of PAEs into harmless by-products such as CO<sub>2</sub> and H<sub>2</sub>O by the use of different electron acceptors (Wu et al., 2008). The biodegradation of PAEs under aerobic conditions has been widely studied (Ng, 2005; Oliver et al., 2007; Vega and Bastide, 2003; Wang et al., 2006), but few data are available on the biotransformation of PAEs under anoxic conditions (Cheung et al., 2007).

**Table 5.** A summary of key studies on physical/chemical treatments to remove PAEs.

| Type of treatment                               | PAEs   | Experimental conditions   | Removing ratio  | Ref                          | Observations   |
|---|--|---|---|------------------------------|--|
| Adsorption by activated carbon                  | DEP<br>[0.5-3.0 mg/L]  | A commercial activated carbon was used. The pH of aqueous solution ranged from 2 to 10.5 at temperature 30°C.   | 82.6 – 53.2%  | (Venkata-Mohan et al., 2007) | Adsorption kinetics of DEP onto activated carbon obeyed the pseudo second order rate equation. Experimental data showed good fit with both the Langmuir and Freundlich adsorption isotherm models. DEP sorption was found to be dependent on the aqueous phase pH and the uptake was observed to be greater at acidic pH.  |
| Coagulation-flocculation (CF)                   | DMP<br>DEP<br>DOP<br>DIBP<br>DnBP<br>BBP<br>DEHP<br>[0.5 – 7.8 µg/L]   | Samples were storing at 4°C, and passing through 0.45-µm filter, using aluminium chloride as coagulant. Fresh leachate (AlCl <sub>3</sub> dose 4.8 mg/g, pH 8.0, fast agitation 350 rpm for 30 s and gentle agitation 60 rpm for 55 min). Partial leachate (AlCl <sub>3</sub> dose 3.6 mg/g, pH 7.0, fast agitation 200 rpm for 30 s and gentle agitation 60 rpm for 55 min). | Fresh Leachate<br><br>< 30%<br><br>Partial Leachate<br><br>≈50% | (Zheng et al., 2009)         | PAEs were not adequately removed by CF. DEHP showed higher removal efficacy versus DnBP in fresh leachate; PAE removal was closely related to PAE hydrophobic adsorption. It decreased to a similar level in partial leachate; the reduction in DIBP, DnBP, and DEHP during CF did not correlate with their K <sub>ow</sub> . Findings suggest that sorption mechanisms other than non-specific hydrophobic interaction play a more important role in PAE removal. Humic substances in partially stabilized leachate facilitate PAE removal by CF. |
| Adsorption by hyper-cross-linked polymer resins | DMP-DEP<br>[50- 500 mg/L]  | Two commercial hyper-cross-linked resins, NDA-150 and NDA-99, and granular activated carbon AC-750 were used at pH 7 and T = 25°C.  | Adsorption capacity in order:<br><br>NDA-150> NDA 99> AC-750    | (Xu et al., 2008)            | The greater adsorption performances of the two resins (NDA-99 and NDA-150) were assumed to result from their more abundant micro- and mesopore structure, where phthalates can be intensively adsorbed by pore-filling mechanism.  |
| Adsorption on chitosan beads                    | PAEs:<br>DBP, DEHP,<br>DMP<br>MPEs <sup>a)</sup> :<br>MBP <sup>b)</sup> , MMP <sup>c)</sup> ,<br>MEHP <sup>d)</sup><br>PA<br>[15 mg/L] | The chitosan was in the form of spherical uniform beads with a relatively uniform size distribution of ≈4 mm diameter at pH 7 and T 25°C.   | Adsorption capacity in the order<br>PA>PAEs>MPEs                | (Salim et al., 2010)         | Results showed that chitosan adsorbed PAEs mainly due to hydrophobic interactions, and interacted with PA mainly due to interactions between polar active groups. For the monoesters, especially for MMP and MEHP, lower hydrophobicity than PAEs and higher hydrophilicity than PA made them less adsorbable.   |

**Table 5.** A summary of key studies on physical/chemical treatments to remove PAEs (continued).

| Type of treatment                               | PAEs  | Experimental conditions  | Removing ratio  | Ref                        | Observations   |
|---|---|--|-----------------|----------------------------|--|
| Adsorption on high-area activated carbon cloth. | PA<br>DEP<br>DMP<br>DAP<br><br>[0.239-0.241 mmol/L] | The carbon cloth used in this study has a specific surface area of 2500m <sup>2</sup> /g. Solutions of phthalic acid were prepared in water, 1M H <sub>2</sub> SO <sub>4</sub> and 0.005 M NaOH to examine the ionization effect on adsorption, while the phthalate solutions were prepared only in water to avoid dissociation into ions. | 90 % in 125 min | (Ayranci and Bayram, 2005) | Phthalic acid and its esters can be largely removed from aqueous solutions by adsorption onto high-area activated carbon cloth. The removal rate was of first order. Adsorption equilibrium data obtained for phthalic acid and its esters were successfully fitted by both Langmuir and Freundlich equations. |

a) Phthalate monoesters.  
b) Monobutyl phthalate.  
c) Monomethyl phthalate.  
d) Monoethylhexyl phthalate.

Metabolic breakdown of PAEs by microorganisms is considered one of the major routes of their environmental degradation in soil, natural waters and wastewaters (Chauret et al., 1995; Inman et al., 1984; Jianlong et al., 2000; Johnson et al., 1984; Pujar and Ribbons, 1985; Ribbons et al., 1984; Wang et al., 1997), in which the biodegradation of several PAEs has been observed under aerobic conditions (Ribbons et al., 1984). Shelton et al. (1984) found that DMP, DEP, DBP, BBP were mineralized in digested sludge but DEHP and DnOP persisted. Banat et al. (1999) investigated the influence of sludge temperature and aeration rate on the reduction of DEHP concentration as well as the reduction of the organic dry solid (ODS), and they found that it was possible to achieve up to 70% reduction of the DEHP concentration and 61% of ODS within 96 hours with a specific air flow rate of 16 m<sup>3</sup>/m<sup>3</sup>.h and a thermophilic temperature of 63 °C. Standardized aerobic biodegradation tests in inoculated sewage sludge showed that phthalate esters degraded 50% within 28 days (Jonsson et al., 2003).

Sugatt et al. (1984) studied the biodegradation of fourteen commercial PAEs widely used as plasticizers by means of an acclimated shake flask CO<sub>2</sub> evolution test showing that all of the commercial phthalate esters were susceptible to biodegradation by mixed populations of microorganisms from natural sources.

Saeger and Tucker (1976) studied the primary and ultimate biodegradation of phthalic acid, monobutyl phthalate and five structurally diverse PAE plasticizers in river water and activated sludge samples by using ultraviolet spectrophotometer, gas chromatography and CO<sub>2</sub> evolution and demonstrated that the phthalic acid ester plasticizers and intermediate degradation products readily undergo ultimate degradation in different mixed microbial systems at concentrations ranging from 1 to 83 mg/L.

Biodegradation is not effective for long-chain PAEs or landfill leachate, although some authors reported that the primary and sometimes ultimate degradation of PAEs occurred during sludge treatments (Battersby and Wilson, 1989; Subba-Rao, 1982). The problem with landfill leachate is its complex composition, which also changes over time (He et al., 2009). PAE compounds with lower molecular weight (e.g. DMP, DEP, DBP and BBP) were easier to degrade than members with higher molecular weight (e.g. DOP and



DEHP) (Alatríste-Mondragón et al., 2003). Hence, PAEs can be degraded by microorganisms under various conditions (Jianlong et al., 2000), but it is a long time-consuming process that cannot readily biodegrade long-chain PAEs (Xu et al., 2005). Table 6 summarizes some of the most representative studies on the biological treatment of PAEs.

#### *1.7.3.3. Advanced oxidation processes*

Advanced oxidation processes (AOPs) are used in wastewater to oxidize complex organic compounds that are difficult to biologically degrade into simpler by-products. AOPs involve the generation of hydroxyl and other free radicals (Metcalf et al., 2003) that enhance the degradation process, achieving the complete conversion of the target pollutant species to CO<sub>2</sub>, H<sub>2</sub>O and mineral acids (Joseph et al., 2009). Because of the ability of AOPs to convert contaminants into less harmful chemicals, they have been proposed as a potential alternative approach for the treatment of bio-recalcitrant organic pollutants (Chen et al., 2009). AOPs include different combinations of ozone, hydrogen peroxide, sonolysis, ultraviolet (UV) radiation and photocatalysis, among other treatments.

Several researchers have addressed the photolysis of PAEs by using artificial irradiation sources such as mercury lamps (Mailhot et al., 2002), Xenon arc lamps (Bajt et al., 2001), and ultraviolet light (Lau et al., 2005), but there is limited information on the utilization of sunlight irradiation (Lertsirisopon et al., 2009).

The removal percentage of PAEs by AOPs has ranged from 0.0 to 99.9% depending on the type of PAE and its chemical and physical characteristics. Although some treatments, such as direct UV radiation and single H<sub>2</sub>O<sub>2</sub>, produce no PAE degradation, combined UV/H<sub>2</sub>O<sub>2</sub> treatment has proven effective, reducing an initial concentration of 1 mg/L DEP by 98.6% after 60 min under UV radiation of 133.9 μW/cm<sup>2</sup> and H<sub>2</sub>O<sub>2</sub> dose of 20 mg/L (Xu et al., 2007). Similar results were found for DMP (Xu et al., 2009). The photo-Fenton process (UV/H<sub>2</sub>O<sub>2</sub>/Fe<sup>2+</sup>) effectively degrades aqueous DEP, observing a maximum percentage degradation of 75.8% after 120 min at pH 3 (DEP concentration of 10 mg/L, H<sub>2</sub>O<sub>2</sub> of 5.44×10<sup>-4</sup> mol/L, and Fe<sup>2+</sup> of 1.67×10<sup>-4</sup> mol/L)

(Yang et al., 2005). The combined use of UV and activated carbon cloth to remove DMP, DEP and DAP (initial concentrations of  $2.4 \times 10^{-4}$  mol) achieved high removal rates, with the adsorption following first-order kinetics (Ayranci and Bayram, 2005).

Gledhill et al. (1980) obtained less than 5% degradation of BBP after exposure to sunlight irradiation for 28 days. According to results yielded by a mathematical model, Wolfe et al. (1980) considered photolysis to be the primary PAE degradation pathway in oligotrophic lakes. Further research on biotic degradation with natural solar irradiation is warranted to improve our knowledge of its effects on PAEs in waters (Lertsirisophon et al., 2009). Table 7 summarizes some representative articles on PAEs oxidation by AOPs technologies.

#### *1.7.3.4. Wastewater and sludge treatment plants*

Table 8 summarizes the main studies on the elimination of PAEs in water, wastewater and sludge treatment plants. In conventional wastewater plants, PAEs removal rates are very high in aerated sludge. PAEs can be settled by physical/chemical precipitation and adsorbed on the sludge surface, enhancing their removal. Some researchers found biodegradation rates of 9% for MBP and BBP, 78% for DEHP, and 45% for DUP (Staples., 2003). The fate of PAEs in anaerobic sewage sludge is important, since many wastewater treatment plants use anaerobic digestion processes prior to sludge disposal (Edgar et al., 2001). The removal rate and biodegradation rate of PAEs depend on their physical and chemical properties (Ziougou et al., 1989).

**Table 6.** Studies on biological treatments to remove PAEs

| Type of treatment  | PAEs  | Experimental conditions  | Removing ratio  | Ref                     | Observations  |
|--|---|--|---|-------------------------|---|
| Microbial degradation under anaerobic digestion of sludge. | DMP<br>DBP<br>DOP<br>[10 mg/L]  | Mixed digested sludge collected from primary anaerobic digester (local wastewater treatment plant) was used. PAEs were dissolved in acetone, added to the sludge for each compound. Aliquots of sludge (200 mL, 10%) were transferred into the conical flasks, while continuously purging with oxygen-free nitrogen.   | DMP > 90%<br>4 days<br>DBP > 90%<br>7 days<br>DOP < 20%<br>10 days<br><br>Theoretical CH <sub>4</sub> recovered (%)<br><br>DMP = 78 %<br>DBP = 75%<br>DOP = 10% | (Jianlong et al., 2000) | The biodegradation rate of three phthalates under anaerobic conditions appeared to be related to the length of the alkyl-side chains. The amounts of methane produced were measured, showing that ester groups and phthalate ring were mineralized at a significant rate. The kinetics study demonstrated that the biodegradation of three phthalates conformed to the first order model.   |
| Biodegradation by anaerobic digested sludge                | DMP<br>[20 mg/L]  | The anaerobic digested sludge used as inoculum in this study was collected from a WW treatment plant. The culture was purged with oxygen free argon gas for 10 min and then incubated at 30°C. The minimal medium was composed of CaCl <sub>2</sub> ·2H <sub>2</sub> O (0.3 g/L), Na <sub>2</sub> HPO <sub>4</sub> ·2H <sub>2</sub> O (0.065 g/L), MgCl <sub>2</sub> ·6H <sub>2</sub> O (0.165 g/L), and 1.25 mg/L of trace elements. Medium was replaced at least every 3 days. | DMP after 12 days with fermentation was 100%.<br><br>COD 70.6%<br><br>The volume of methane produced was 3.65 mL over the period of 20 days.                    | (Wu et al., 2008)       | First-order kinetic model has previously been used to describe PAE biodegradation under various environmental conditions, but it was not suitable for DMP. A modified Gompertz Model was used to explain the kinetics of phthalic acid degradation. The free energy is greater for DMP biodegradation to PA than for PA degradation to benzoate explaining the PA accumulation observed throughout the reaction. Methane production results demonstrated that DMP is not completely mineralized under fermentation conditions |
| Biodegradation by <i>Pseudomonas fluorescens</i> FS1       | DMP, DEP,<br>DnBP<br>[25-400 mg/L]<br>DIBP<br>[25-300 mg/L]<br>DnOP DEHP<br>[12.5-200 mg/L] | FS1 isolated from activated sludge at a petrochemical were used under aerobic conditions.  | After 3 days<br>99% of DMP, DEP,<br>DnBP, DIBP<br>30% DnOP<br>20% DEHP  | (Zeng et al., 2004)     | Optimum biodegradation temperature, pH, inoculum age and inoculum concentration were 20–35 °C, 6.5–8.0, 18–24 h and 4–8% v/v, respectively. PAE biodegradation rates decreased and PAE inhibition effects markedly increased with greater alkyl chain length and alkyl branch chains.   |

**Table 6.** Studies on biological treatments to remove PAEs (continued).

| Type of treatment                                   | PAEs  | Experimental conditions  | Removing ratio   | Ref                 | Observations  |
|---|---|--|--|---------------------|---|
| Lagooning sludge (LS) and activated sludge (AS)     | A mix of (DEHP, BBP, DBP, DEP, DMP) [500 ng/ $\mu$ L]   | LS from anaerobic lagoon of an experimental WWTP. AS from a municipal WWTP. The selected times of sampling were for LS (initial mixture, after 30, 60, 90 and 180 days) and for AS (initial mixture, after 15, 30, 45, 75, 90 and 135 days).   | Half life for LS<br>45.4 day<br><br>Half life for AS<br>28.9 day   | (Amir et al., 2005) | Biodegradation rate of DEHP was found higher for AS compared with LS due to a high microbial activity in AS. During decomposition, removal of PAEs is suggested to occur through degradation by microbial communities. The microbial metabolism seems to begin by the decomposition of alkyl side- chains before aromatic ring-cleavage. PAEs with long alkyl side- chains cannot be interpreted as an increase of toxicity but as an intermediate stage of detoxification. |
| Biodegradation of PAEs in typical agriculture soils | DBP<br>In fluve-aquic [3.18-29.37 mg/Kg]<br>In black soil [2.75-14.62 mg/Kg]<br>DEHP<br>In fluve-aquic [1.15-7.99 mg/Kg]<br>In black soil [0.44-4.20 mg/Kg] | Each sample consisted of a composite of six samples collected within the sampling unit. The initial sample was collected at a starting point, with the five additional samples collected 25 m from the first point (12 m from greenhouse fields) at azimuth intervals of 72°. The samples were collected from a depth of 0 –20 cm below the surface layer. | -In fluve-aquic<br>DBP average 14.06 mg/kg<br>DEHP average 4.86 mg/kg<br>-In black soil<br>DBP average 7.60 mg/kg<br>DEHP average 2.35 mg/kg | (Xu et al., 2008)   | The degradation of DBP >DEHP, with higher degradation rates in the fluve-aquic. DBP biodegradation might begin by esters hydrolysis to form monobutyl (MBP) and the corresponding alcohol, then MBP degrades to phthalic acid or butyl benzoate, which might be possibly caused by microbial decarboxylation, the two derivatives of MBP degrade to form protocatechuate through ring cleavage.   |
| Degradation by acclimated activated sludge          | DBP [50-200 mg/L]   | Activated sludge obtained from a wastewater treatment plant was acclimated and used as seeding microbes to investigate the kinetics of DBP biodegradation. The sludge was acclimated by a fill-and-draw operation of the cycle every day in a 2.0 litre reactor at 25°C.   | > 90%  | (Wang et al., 1997) | DBP can be rapidly degraded by acclimated activated sludge. DBP was not oxidized without biological aids; therefore, it is also reasonable to speculate that the increase in respiration rate is attributable to biological oxidation of DBP. The amount of biogas-adsorbed DBP is low and can be neglected.  |

**Table 6.** Studies on biological treatments to remove PAEs (continued).

| Type of treatment  | PAEs  | Experimental conditions   | Removing ratio                | Ref                          | Observations  |
|--|---|---|-------------------------------|------------------------------|---|
| Biodegradation by using <i>Pseudomonas fluorescens</i> B-1 | DBP<br>[2.5-10 mg/L]                              | Microbial degradation of DBP was studied in batch experiments and the effect of initial DBP concentrations on the degradation was investigated. The samples were incubated at 30° C on a rotary shaker operated at 150 rpm.                                   | 94.9%                         | (Xu et al., 2005)            | The biodegradation process followed a first-order kinetic. The pH value of the culture medium played an important role in the biodegradation of DBP. The optimum pH was 7.0.  |
| Biodegradation by <i>A Bacillus</i> sp                     | DMTP  | The organism was isolated from garden soil by an enrichment culture technique.  |                               | (Sivamurthy and Pujar, 1989) | Pathway of DMTP degradation was proposed.   |
| Fixed film bioreactor                                      | PA<br>DMP<br>[10-500 mg/L]                        | Synthetic wastewater was used (COD: N: P=100: 7: 1). The effect of two operating factors: hydraulic retention time and initial concentration of PA and DMP were studied.  | > 95%                         | (Pirsaheb et al., 2009)      | Remarkable amount of DMP (398 mg/Kg of sludge) was adsorbed on the biomass due to its higher hydrophobicity compared to PA (171 mg/Kg of sludge). The kinetic parameters were determined and compared for both pollutants, PA and DMP.  |
| Trickling filter STW                                       | DEP<br>[0.10-25 µg/L]<br>DEHP<br>[14.6-30.2 µg/L] | Sewage samples were collected during one year in glass Winchester bottles with polytetrafluoroethylene lined caps. Suspended solids, biochemical oxygen demand, chemical oxygen demand, and ammoniacal nitrogen concentrations were obtained for each sample. | DEP (94-99%)<br>DEHP (<1-44%) | (Oliver et al., 2005)        | DEHP was the most recalcitrant phthalate. Low molecular weight phthalates such as DEP were biodegraded at constantly high rates by the trickle filter. The results of this study can be used to optimise and design wastewater treatments and processes to improve sewage effluent and sludge quality that may be required under EU regulations.            |
| Biodegradation by white rot fungi                          | DBP<br>[100 µM]                                   | Three fungi, <i>D. concentrica</i> , <i>P. chrysosporium</i> and <i>T. versicolor</i> were used in this study   | > 90%                         | (Lee et al., 2004)           | The three fungi, <i>D. concentrica</i> , <i>P. chrysosporium</i> and <i>T. versicolor</i> showed high resistance to DBP with a little inhibition depending on concentration. The degradation efficiency was 94% for <i>D. concentrica</i> , 83% for <i>T. versicolor</i> after first day of incubation, and completely degraded after 6 days of incubation. |

**Table 6.** Studies on biological treatments to remove PAEs (continued).

| Type of treatment                                     | PAEs   | Experimental conditions  | Removing ratio   | Ref                          | Observations   |
|---|--|--|--|------------------------------|--|
| Biotic degradation under natural sunlight irradiation | BBP [0.44 mmol/L]<br>DBP [0.52 mmol/L]<br>DEHP [0.35 mmol/L]<br>DINP [0.32 mmol/L] | Experiment were evaluated over a wide pH range 5-9, the PAE solutions in glass test tubes were placed either in the dark or under the natural sunlight irradiation at ambient temperature for 140 days from autumn to winter. The daily average radiation and ambient temperature widely varied from 17.1 to 242.8 W/m <sup>2</sup> (107.9 W/m <sup>2</sup> ), and 0.40 to 27.4°C (10.8 °C), study the effect of pH (5-9). | In dark<br>All PAEs 20%<br>Under sun light<br>DINP (50%)<br>BBP, DBP (20%)<br>DEHP (20%) | (Lertsirisopon et al., 2009) | Biotic degradation of the PAEs with relatively short alkyl chains, such as BBP and DBP, at neutral pH, was significantly lower than that in acidic or alkaline condition. Photolysis was considered to contribute to the total biotic degradation at all pHs. The degradation rate of DINP was much higher than those of the other PAEs, and it was almost completely removed during the experimental period at pH 5 and 9.  |
| Anoxic biodegradation                                 | DMP [102 mg/L]   | DMP biodegradation by activated sludge cultures under nitrate-reducing conditions was investigated. The effect of pH (5-9) and temperature (20-40 ° C) was studied.  | 100%   | (Wu et al., 2007)            | Under the optimized condition, DMP was biodegraded in 56 h under anoxic conditions and its degradation rate followed a first-order kinetic. The biodegradation pathway was proposed as DMP → MMP → PA → ... → CO <sub>2</sub> + H <sub>2</sub> O. The molar ratio of DMP to nitrate consumed was found to be 9.0:1. The biodegradation rate constant decreased when pH was higher than 9.0 or lower than 6.0. This constant increased by augmenting the temperature from 20 to 32°C. |

**Table 7.** Degradation of PAEs by advanced oxidation processes.

| Type of treatment                             | PAEs                      | Experimental conditions   | Removing ratio  | Ref                 | Observations  |
|---|---------------------------|---|---|---------------------|---|
| UV/H <sub>2</sub> O <sub>2</sub>              | DMP<br>[0.35-8.04 mg/L]   | Photoreactor was equipped with ten 30W commercial low pressure-Hg UV lamps (emitting wavelength: 253.7 nm), I <sub>0</sub> = 133.9 μW/cm <sup>2</sup> . The effects of H <sub>2</sub> O <sub>2</sub> concentration (2.5-40 mg/L), UV radiation intensity (21.2, 50.1, 77.2, 107.6 and 133.9 μW/cm <sup>2</sup> ), and initial solution pH (2-11) were investigated.                                   | 87-99%<br>I <sub>0</sub> = 133.9 μW/cm <sup>2</sup> , pH 6.8<br>[H <sub>2</sub> O <sub>2</sub> ] <sub>0</sub> = 40 mg/L | (Xu et al., 2009)   | DMP degradation in UV/H <sub>2</sub> O <sub>2</sub> advanced oxidation process follows pseudo-first order kinetics and the rate constant (k <sub>app</sub> ) is affected by the UV radiation intensity, H <sub>2</sub> O <sub>2</sub> concentration, solution pH (optimal pH 4) and initial concentration of DMP.   |
| O <sub>3</sub> /H <sub>2</sub> O <sub>2</sub> | DMP<br>DEP<br>DPrP<br>DBP | Experiments were performed in a 1 L bench-scale glass reactor. Ozone delivered into the reactor was kept constant concentration across the whole experiment process (4–5 mg/L). The second-order rate constants of the four types of PAEs compounds with HO• were determined using competitive kinetic. Determination of TOC and toxicity of PAEs was carried out using natural water.                | 40-80%  | (Wen et al., 2011)  | The measured second-order rate constants for the reaction of the PAEs with HO• were 2.67×10 <sup>9</sup> , 3.98×10 <sup>9</sup> , 4.47×10 <sup>9</sup> and 4.64×10 <sup>9</sup> M <sup>-1</sup> s <sup>-1</sup> , respectively. After 30 min oxidation, the TOC decreased from 3.76 to 3.22 mg/L, indicating that only 14.4% of TOC was mineralized, whereas the toxicity was slightly reduced.   |
| Electrochemical Oxidation                     | DEP<br>[100 mg/L]         | Experiments were carried out by using a self-made Pd/C gas-diffusion electrode as the cathode and a Ti/IrO <sub>2</sub> /RuO <sub>2</sub> anode. The cathode generated H <sub>2</sub> O <sub>2</sub> through two electron reduction of fed molecule oxygen in the electrolysis. At the same time, HO• was determined in the electrochemical systems by ESR  | 80.9 -40.2% after 9 h   | (Wang et al., 2010) | The electrochemical oxidation enhanced the biodegradation character of the DEP solution. Hence, the degradation of DEP was attributed to the cooperatively oxidation processes including electrochemical oxidation at the anode and H <sub>2</sub> O <sub>2</sub> and HO• produced by the reduction of oxygen at the cathode<br>The electrolysis products determined by GC–MS indicated that the main aromatic intermediates were MEP and PA acids. |
| Sonolytic<br>Photolytic<br>Sonophotolytic     | DEP                       | The degradation of DEP (45 μM) was carried out in a capped cylindrical glass batch reactor equipped with four UVC lamps (λ = 254nm and power of 10W) or two UVC and two VUV lamps at 15-18 °C. Ultrasounds with a frequency of 283 kHz with a nominal power of 40, 65 and 85 W/L were applied. The concentrations of DEP, total organic carbon (TOC) and H <sub>2</sub> O <sub>2</sub> were analyzed. | (Sonolytic)<br>58%<br>(Photolytic)<br>70-100<br>(Sonophotolytic)<br>90-100%   | (Na et al., 2012)   | Sonophotolytic degradation of DEP resulted in a significantly faster degradation than the photolytic and sonolytic processes due to the higher photon energy and higher hydroxyl radical generation by homolysis of water. Significant degradation and mineralization (TOC) of DEP were observed with the combined sonophotolytic processes.  |

**Table 7.** Degradation of PAEs by advanced oxidation processes.

| Type of treatment   | PAEs                  | Experimental conditions  | Removing ratio                     | Ref                 | Observations   |
|---|-----------------------|--|------------------------------------|---------------------|--|
| UV/Si-FeOOH/H <sub>2</sub> O <sub>2</sub>   | DMP<br>[7.7 mg/L]     | The catalyst Si-FeOOH was synthesized by adding Si to the amorphous FeOOH. The experiment was carried out in home-made photo-catalytic reactor using UV <sub>365</sub> (125 W)/Si-FeOOH/H <sub>2</sub> O <sub>2</sub> .  | 70-98%<br>pH 10-5                  | (Yuan et al., 2011) | The prepared catalyst exhibited a high catalytic activity and 97% degradation of DMP with 0.5 g/L Si-FeOOH (Si/Fe = 0.2) and 2 mmol/L H <sub>2</sub> O <sub>2</sub> could be obtained at 30 min reaction and initial solution pH of 5.0.   |
| Pulse radiolysis<br>Electron beam   | DMP<br>[0.12-1.23 mM] | Pulse radiolysis experiments were carried out with 10 ns pulses of 10 MeV electrons from a linear electron accelerator. Electron beam experiments were performed using a GJ-2-II electron accelerator with beam energy of 1.8 MeV at the applied radiation. The experiments were carried out mainly at absorbed doses of 1–20 kGy and the dose rate was kept at 0.045 kGy/s.   | >95% at<br>absorbed dose<br>20 kGy | (Wu et al., 2011)   | The bimolecular rate constants for the reaction of hydroxyl radical and hydrated electron with DMP were measured to be $3.4 \times 10^9 \text{ M}^{-1} \text{ s}^{-1}$ and $1.6 \times 10^{10} \text{ M}^{-1} \text{ s}^{-1}$ , respectively, under pulse radiolysis experiments. Hydroxyl radicals were found to attack aromatic ring while hydrated electrons attacked the ester group of DMP. Among the byproducts detected, dimethylhydroxy phthalate and benzoquinone are included. |
| UV/TiO <sub>2</sub> /O <sub>3</sub>   | DMP<br>[10 mg/L]      | A glass tubular photoreactor with UV lamp (15W), with wavelength of 365 nm, was used. At solution pH = 5.5 and 1.0 g of TiO <sub>2</sub> . Ozone was produced from pure oxygen (air flow rate = 1.0 L min <sup>-1</sup> ) by using a DHX-SS-03C ozone generator.   | 90-100%                            | (Jing et al., 2011) | The combination of ozone with photocatalytic oxidation was more efficient than other oxidation processes, especially for DMP mineralization. The rate constants for TiO <sub>2</sub> /UV/O <sub>3</sub> process were 2.5 times higher than that in TiO <sub>2</sub> /UV/O <sub>2</sub> . The system UV/O <sub>3</sub> implies a synergistic effect between the photocatalysis and ozonation. TOC removal at 45 min was 89.9% with 100 mg h <sup>-1</sup> ozone dosage                    |
| O <sub>3</sub> /UV/TiO <sub>2</sub> supported in $\gamma$ -Al <sub>2</sub> O <sub>3</sub> | DMP                   | The TiO <sub>2</sub> /Al <sub>2</sub> O <sub>3</sub> catalyst was prepared with $\gamma$ -Al <sub>2</sub> O <sub>3</sub> particles using a wet impregnation method followed by an incineration procedure. An airtight reactor with an effective volume of 5.5 L was used. The ozone was supplied at flow rate of 1.95 L/min. Semi-batch ozonation was performed under various experimental conditions including the fed ozone concentration, catalyst type, catalyst dosage, and ultraviolet radiation | 90-100 %                           | (Chen et al., 2011) | The complete removal of DMP was efficiently achieved by both sole and catalytic ozonation; meanwhile, the presence of the catalysts slightly accelerated the elimination rate of DMP. The mineralization efficiency, in terms of total organic carbon (TOC) removal, was substantially enhanced by employing the TiO <sub>2</sub> /Al <sub>2</sub> O <sub>3</sub> catalyst.  |



**Table 7.** Degradation of PAEs by advanced oxidation processes (continued).

| Type of treatment                         | PAEs              | Experimental conditions   | Removing ratio               | Ref                        | Observations  |
|---|-------------------|---|------------------------------|----------------------------|---|
| UV/Si-FeOOH/H <sub>2</sub> O <sub>2</sub> | DMP<br>[7.7 mg/L] | The catalyst Si-FeOOH was synthesized by adding Si to the amorphous FeOOH. The experiment was carried out in home-made photo-catalytic reactor using UV <sub>365</sub> (125 W)/Si-FeOOH/H <sub>2</sub> O <sub>2</sub> .   | 70-98%<br>pH 10-5            | (Yuan et al., 2011)        | The prepared catalyst exhibited a high catalytic activity and 97% degradation of DMP with 0.5 g/L Si-FeOOH (Si/Fe = 0.2) and 2 mmol/L H <sub>2</sub> O <sub>2</sub> could be obtained at 30 min reaction and initial solution pH of 5.0.  |
| ozone/activated carbon                    | DEP<br>[200 mg/L] | The ACs used in this study (L27, X17, F22 and S21) were commercial activated carbons provided by Pica. Experiments were carried out at pH 2.5, 3.5, 5.6, 6.2 or 7.2 and 2 g of AC. The initial ozone concentrations was 0.23 mmol/L   | >90% at all pHs              | (de Oliveira et al., 2011) | Results show that degradation efficiency depends both on textural properties (microporous and external surfaces favour this treatment) and chemical functions (both acid and basic functions improve radical hydroxyl generation). It was demonstrated that AC acts more as a radical initiator and promoter and a reaction support than as an adsorbent material.  |
| O <sub>3</sub> /Fe-Silica (SBA-15)        | DMP<br>[10 mg/L]  | SBA-15 was synthesized by a hydrothermal method and Fe/SBA-15 was prepared by an incipient wetness impregnation method. Ozone was produced in situ from pure oxygen, pH = 5.7 and 0.28 g catalyst were added into the reactor, and ozone (50 mg h <sup>-1</sup> ) was continuously fed to the solution through a porous glass plate at the bottom of the reactor. | 90-100%<br>T 25°C, pH 5.7    | (Huang et al., 2011)       | Fe/SBA-15/O <sub>3</sub> process improved DMP and total organic carbon (TOC) removal efficiency due to the generation of hydroxyl radical (HO <sup>•</sup> ). The rate constant when using Fe/SBA-15/O <sub>3</sub> was 0.0058 min <sup>-1</sup> , 3.9 times higher than that of O <sub>3</sub> alone, 3.4 and 1.9 times higher than those of SBA-15/O <sub>3</sub> and Fe <sub>2</sub> O <sub>3</sub> /O <sub>3</sub> processes, respectively. |
| ZrOx/ZnO /UV/ Microwave (MW)              | DMP<br>[50 mg/L]  | ZrOx/ZnO was prepared through a surfactant-assisted hydrothermal method. ZrOx/ZnO/UV/MW degradation of DMP was conducted with an integrated microwave and UV reaction facility, equipped with a microwave discharged electrodeless lamp. The microwave power for the UV/MW process was 400W, and the light intensity was 9.79 mW/cm <sup>2</sup> .                | ≈100% after 60 min at pH 5.6 | (Liao et al., 2010)        | The TOC removal efficiency of DMP was 88% after 30 min reaction. It was found that the removal process of DMP by microwave-assisted photocatalytic followed pseudo first order kinetics in all cases, and ZrOx/ZnO significantly accelerated the degradation of DMP.  |
| O <sub>3</sub> /UV                        | DEP<br>[100μM]    | An UV lamp with an intensity of I <sub>0</sub> = 8.84×10 <sup>-7</sup> Einstein L <sup>-1</sup> s <sup>-1</sup> was used. The net ozone dose was set at 1.5 and 4 mg/L min with the flow rate fixed at 0.5 L/min.   | > 95 %<br>pH=7, T=20°C       | (Oh et al., 2006)          | The ozone/UV process was shown to have the highest efficiency for the elimination of DEP and its by-products, leading to the complete mineralization of DEP.  |

**Table 7.** Degradation of PAEs by advanced oxidation processes (continued).

| Type of treatment                                  | PAEs                | Experimental conditions  | Removing ratio  | Ref                   | Observations   |
|--|---------------------|--|---|-----------------------|--|
| O <sub>3</sub> / Ru-Al <sub>2</sub> O <sub>3</sub> | DMP<br>[6.0 mg/L]   | The Ru/Al <sub>2</sub> O <sub>3</sub> catalysts with different Ru loading were prepared by the dipping method. The experiments were conducted in a 1 L glass reactor. Catalyst and ozone dosage were 10 g/L and 116 mg O <sub>3</sub> /h, respectively.  | 100%<br>T = 15°C  | (Yunrui et al., 2007) | Ru/Al <sub>2</sub> O <sub>3</sub> significantly increased the effect of ozonation. TOC removal in 120 min reached 72% while only 24% with ozone alone. The optimal catalyst preparing condition was 0.1 wt% Ru content.  |
| UV/H <sub>2</sub> O <sub>2</sub>                   | DEP<br>[1.0 mg/L]   | The experiment was carried out under the following conditions: (1) self photolysis of DEP solution with different initial concentrations and UV radiations; (2) H <sub>2</sub> O <sub>2</sub> oxidation alone with DEP solution in dark; (3) DEP solution oxidation with UV-light and H <sub>2</sub> O <sub>2</sub> ; (4) effects of different impact factors in UV-H <sub>2</sub> O <sub>2</sub> process. | 16.8%-99.8%<br>[H <sub>2</sub> O <sub>2</sub> ] = 2.5-30 mg/L | (Xu et al., 2007)     | DEP cannot be effectively removed by UV radiation and H <sub>2</sub> O <sub>2</sub> oxidation alone, while UV-H <sub>2</sub> O <sub>2</sub> combination process proved to be effective and could completely degrade this compound. More than 98.6% of DEP can be removed after 60 min under intensity of UV radiation of 133.9 μW/cm <sup>2</sup> and H <sub>2</sub> O <sub>2</sub> dosage of 20 mg/L.               |
| UV/TiO <sub>2</sub>                                | BBP<br>[1.0 mg/L]   | The photocatalytic degradation experiments were carried out in a laboratory-scale photoreactor equipped with sixteen 350 nm black blue fluorescent UV lamps, each one with approximately 8W maximum output. Titanium dioxide (P25, Degussa), a mixture of 70% anatase and 30% rutile, was used as a photocatalyst.   | 75-85%  | (Xu et al., 2009)     | The optimal TiO <sub>2</sub> dosage and pH value for the BBP degradation were 2.0 g/L and 7.0, respectively. The effects of co-existing substances on the degradation rate of BBP revealed that some anions (such as BrO <sub>3</sub> <sup>-</sup> , ClO <sub>4</sub> <sup>-</sup> and Cr <sub>2</sub> O <sub>7</sub> <sup>2-</sup> ) could enhance BBP degradation, and other anions would restrain BBP degradation |
| O <sub>3</sub> /UV<br>O <sub>3</sub> /zeolite      | DMP<br>[0.4-5.6 mM] | Semibatch ozonation experiments were performed under various reaction conditions to examine the effects of inlet gas ozone concentration, high silica zeolite dosage, and UV radiation intensity on the decomposition of DMP.  | >98% in both treatments                                       | (Chen et al., 2008)   | The complete removal of DMP can be efficiently achieved via both O <sub>3</sub> and O <sub>3</sub> /UV treatments. The presence of high silica zeolites accelerates the decomposition rate of DMP in the O <sub>3</sub> process. The removal efficiencies of both chemical oxygen demand (COD) and total organic carbons (TOC) are significantly enhanced by employing the ozonation combined with UV radiation.     |

**Table 7.** Degradation of PAEs by advanced oxidation processes (continued).

| Type of treatment  | PAEs                 | Experimental conditions   | Removing ratio                    | Ref                              | Observations   |
|--|----------------------|---|-----------------------------------|----------------------------------|--|
| UV/TiO <sub>2</sub><br>UV/H <sub>2</sub> O <sub>2</sub><br>UV/H <sub>2</sub> O <sub>2</sub> /Fe<br>O <sub>3</sub><br>O <sub>3</sub> /Fe<br>O <sub>3</sub> /TiO <sub>2</sub><br>UV/O <sub>3</sub> /H <sub>2</sub> O <sub>2</sub> /Fe<br>UV/O <sub>3</sub> /H <sub>2</sub> O <sub>2</sub> /Fe/TiO <sub>2</sub> | TPA<br>[50 mg/L]     | Ferric sulfate and TiO <sub>2</sub> particles were used as photocatalysts. The irradiation intensity was 144 μW/cm <sup>2</sup> and the wavelength was 253.7 nm. Constant amount of ozone (2.4 mg/h) was introduced.                              | 40-100%<br>Depending of treatment | (Thiruvenkatachari et al., 2007) | The time required for the complete destruction of TPA can be minimized from 10 h using UV/TiO <sub>2</sub> system, to less than 10 min by UV/H <sub>2</sub> O <sub>2</sub> /Fe/O <sub>3</sub> system. Some of the likely organic intermediates identified during TPA destruction include benzoquinone, benzene, maleic acid and oxalic acid.   |
| UV/TiO <sub>2</sub><br>UV/H <sub>2</sub> O <sub>2</sub><br>UV/H <sub>2</sub> O <sub>2</sub> /Fe<br>O <sub>3</sub><br>O <sub>3</sub> /Fe<br>O <sub>3</sub> /TiO <sub>2</sub><br>UV/O <sub>3</sub> /H <sub>2</sub> O <sub>2</sub> /Fe<br>UV/O <sub>3</sub> /H <sub>2</sub> O <sub>2</sub> /Fe/TiO <sub>2</sub> | TPA<br>[50 mg/L]     | Ferric sulfate and TiO <sub>2</sub> particles were used as photocatalysts. The irradiation intensity was 144 μW/cm <sup>2</sup> and the wavelength was 253.7 nm. Constant amount of ozone (2.4 mg/h) was introduced.                              | 40-100%<br>Depending of treatment | (Thiruvenkatachari et al., 2007) | The time required for the complete destruction of TPA can be minimized from 10 h using UV/TiO <sub>2</sub> system, to less than 10 min by UV/H <sub>2</sub> O <sub>2</sub> /Fe/O <sub>3</sub> system. Some of the likely organic intermediates identified during TPA destruction include benzoquinone, benzene, maleic acid and oxalic acid.   |
| UV/TiO <sub>2</sub> /mPMMA <sup>a)</sup><br>UV/Pt-TiO <sub>2</sub> /mPMMA <sup>a)</sup><br>poly(methyl methacrylate)   | DMP<br>[0.05-0.4 mM] | The photocatalytic experiments of DMP under various experimental conditions were conducted to examine the effects of the initial DMP concentration, photocatalyst dosage, UV radiation intensity and Pt doping content on the degradation of DMP. | >99%                              | (Chen et al., 2009)              | The elimination rate of DMP concentration significantly increased with increasing photocatalyst dosage, UV radiation intensity at 254 nm and Pt doping content while decreased with increasing initial DMP concentration. Pt-TiO <sub>2</sub> /mPMMA microspheres offer better photocatalytic performance than the TiO <sub>2</sub> /mPMMA microspheres, especially with respect to mineralization efficiency. |

a) Magnetic poly (methyl methacrylate)

**Table 8.** Removal of PAEs in wastewater and sludge treatment plants.

| Type of treatment                 | PAEs  | Experimental conditions   | Removing ratio   | Ref                                | Observations  |
|-----------------------------------|---|---|--|------------------------------------|---|
| An aerobic digestion of WW sludge | DBP<br>DEHP<br>[5-500 mg/L]                               | Two digesters were used for the experiments. A hot water jacket and a water recirculation bath were used to maintain the temperature of the digesters at 35°C.<br>Digesters were operated with a 20 days HRT.   | DBP<br>73.1-99.5%<br>DEHP<br>n.d -79.0%<br>The biogas production was<br>0.9-0.94 L/g | (Alatríste-Mondragon et al., 2003) | PAEs with longside-chains such as DEHP can only be biodegraded at low rates during anaerobic digestion of wastewater sludge with a consequent accumulation in the reactor and a toxic level when sewage sludge with high concentrations of PAEs is digested.  |
| Complexation-flocculation         | DEHP<br>[1.71-232.5 µg/L]                                 | The optimum stirring conditions to remove DOM in leachate by coagulation were: flocculants added during fast stirring at 200 rpm for 4 min, followed by slow stirring at 60 rpm for 20 min.<br>Three coagulant agents were used:<br>1- Ferric chloride<br>2- Aluminium sulphate<br>3- Poly aluminium chloride (PAC) | 1. 20%<br>2. 25%<br>3. 50%   | (Zhang and Wang, 2009)             | Biodegradation was not effective for long chain PAEs in the landfill leachate.<br>PAC was the most efficient coagulant.<br>Hydrophobic contaminants with log $K_{ow}$ greater than 4 are removed through the complexation-flocculation process.   |
| Batch anaerobic digestion         | DMP<br>DEP<br>DBP<br>BBP<br>DEHP<br>DOP<br>[0.50-10 mg/L] | Mixed digested sludge from Hogsmill Valley Water Pollution Control Works (London, U.K.) was used.   | DBP>DMB>B<br>BP>DEP<br>50-100%   | (Ziogou et al., 1989)              | PAEs were rapidly degraded during batch anaerobic digestion of sewage sludge. First order reaction kinetics was found to apply to their degradation rates. DEHP and DOP appeared to be persistent under the same experimental conditions and their fate during sludge disposal needs to be further investigated, given their universal and widespread occurrence. |
| Aerobic/anoxic treatment          | DEHP<br>[98-122 µg/L]                                     | Removal of DEHP from reject water from sewage sludge was studied in two sequencing batch reactors (SBRs) with different aerobic/anoxic periods during a 6-h total cycle period.   | 95%  | (Marttinen et al., 2004b)          | SBRs treatment had the potential to remove DEHP biologically from reject water but this removal was restricted by the poor bioavailability of DEHP as a result of sorption to solids  |

**Table 8.** Removal of PAEs in wastewater and sludge treatment plants (continued).

| Type of treatment  | PAEs  | Experimental conditions   | Removing ratio   | Ref                         | Observations   |
|--|---|---|--|-----------------------------|--|
| Wastewater treatment plant   | <p><i>-Wastewater [<math>\mu\text{g/L}</math>]</i><br/>           DEHP=[9-44],<br/>           DMP =[0.02],<br/>           DEP=[ 1.6-25],<br/>           DnBP=[0.03],<br/>           BBP=[0.01],<br/>           DnOP=[0.02]</p> <p><i>-Sludge [<math>\mu\text{g/L}</math>]</i><br/>           DEHP=[72],<br/>           DEP=[0.08],<br/>           DMP=[0.05],<br/>           DnOP=[0.1],<br/>           DnBP=[0.15],<br/>           BBP=[0.01].</p> | The WWTP capacity is about 30000 m <sup>3</sup> /day (from 20000 m <sup>3</sup> /day under dry weather to 55000 m <sup>3</sup> /day under rainy periods)                        | DEHP (78%)<br>DMP, DEP,<br>DnBP, and BBP<br>(68-96%)   | (Dargnat et al., 2009)      | The DEHP removal seemed to proceed rather from particle settling than from biodegradation, whereas the rest of PAEs were easily biodegraded.   |
| Aerobic/anoxic treatment   | DEHP<br>[98-122 $\mu\text{g/L}$ ]   | Removal of DEHP from reject water from sewage sludge was studied in two sequencing batch reactors (SBRs) with different aerobic/anoxic periods during a 6-h total cycle period. | 95%  | (Marttinen et al., 2004b)   | SBRs treatment had the potential to remove DEHP biologically from reject water but this removal was restricted by the poor bioavailability of DEHP as a result of sorption to solids   |
| Aeration (AR)<br>Coagulation and sedimentation (CS)<br>Activated carbon (AC)<br>Advanced oxidation process (AOP) | DEHP<br>[50-100 $\mu\text{g/L}$ ]   | Leachate treatments<br>(Adsorption and oxidation)   | DEP: AR>50%,CS <50%<br>DBP: AC>50%, AR>90%,CS <50%<br>BBP: AC>50%,AOP > 99% AR>90%,CS <50%<br>DEHP AC>50%, AR<50%, CS >50%<br>AC>50%, AOP >99% | (Asakura and Matsuto, 2009) | Both DBP and BBP can be treated by aeration and DEHP by advanced oxidation processes. The removal ratios of DEHP in leachate of 100 m <sup>3</sup> /d with 100 Kg of activated carbon were 50-70%, assuming a complete mixing model. |

#### 1.7.4. Conclusions

The extended use of materials containing PAEs has led to their spread in the environment. Thus, these compounds have been detected in different types of water (surface, ground, drinking, and wastewater), sludge, and soils.

Although there are many publications related to the impact of PAEs on human health, more research effort is needed to clarify the toxicity level of these potential pollutants.

The removal of PAEs can be efficiently addressed by means of technologies such as adsorption, coagulation-flocculation, biodegradation, and advanced oxidation processes. The highest yields were detected for the following systems: adsorption on high-area activated carbon cloth, biological treatments (mainly for short alkyl chain PAEs), pulse radiolysis, electron beam, UV/H<sub>2</sub>O<sub>2</sub>, UV/TiO<sub>2</sub>/O<sub>3</sub>, O<sub>3</sub>/activated carbon, O<sub>3</sub>/UV, and O<sub>3</sub>/Ru-Al<sub>2</sub>O<sub>3</sub>.

### 1.7.5. References

- Alatríste-Mondragón, F., Iranpour, R., Ahring, B.K., 2003. Toxicity of di-(2-ethylhexyl) phthalate on the anaerobic digestion of wastewater sludge. *Water Res.* 37, 1260-1269.
- Albaiges, J., Casado, F., Ventura, F., 1986. Organic indicators of groundwater pollution by a sanitary landfill. *Water Res.* 20, 1153-1159.
- Amir, S., Hafidi, M., Merlina, G., Hamdi, H., Jouraiphy, A., El Gharous, M., Revel, J.C., 2005. Fate of phthalic acid esters during composting of both lagooning and activated sludges. *Process Biochemistry* 40, 2183-2190.
- Arévalo, J., Moreno, B., Pérez, J., Gómez, M.A., 2009. Applicability of the Sludge Biotic Index (SBI) for MBR activated sludge control. *J. Hazard. Mater.* 167, 784-789.
- Asakura, H., Matsuto, T., 2009. Experimental study of behavior of endocrine-disrupting chemicals in leachate treatment process and evaluation of removal efficiency. *Waste Manage.* 29, 1852-1859.
- Asakura, H., Matsuto, T., Tanaka, N., 2004. Behavior of endocrine-disrupting chemicals in leachate from MSW landfill sites in Japan. *Waste Manage.* 24, 613-622.
- Autian, J., 1973. Toxicity and health threats of phthalate esters: review of the literature. *Environ. Health Perspect.* 4, 3-26.
- Ayranci, E., Bayram, E., 2005. Adsorption of phthalic acid and its esters onto high-area activated carbon-cloth studied by in situ UV-spectroscopy. *J. Hazard. Mater.* 122, 147-153.
- Bajt, O., Mailhot, G., Bolte, M., 2001. Degradation of dibutyl phthalate by homogeneous photocatalysis with Fe(III) in aqueous solution. *Applied Cat. B: Environmental* 33, 239-248.

- Banat, F.A., Prechtel, S., Bischof, F., 1999. Experimental assessment of bio-reduction of Di-2-thylhexyl phthalate (DEHP) under aerobic thermophilic conditions. *Chemosphere* 39, 2097-2106.
- Bautista-Toledo, M.I., Méndez-Díaz, J.D., Sánchez-Polo, M., Rivera-Utrilla, J., Ferro-García, M.A., 2008. Adsorption of sodium dodecylbenzenesulfonate on activated carbons: Effects of solution chemistry and presence of bacteria, *J. Colloid Interface Sci.* 317, 11-17.
- Bartolomé, L., Cortazar, E., Raposo, J.C., Usobiaga, A., Zuloaga, O., Etxebarria, N., Fernández, L.A., 2005. Simultaneous microwave-assisted extraction of polycyclic aromatic hydrocarbons, polychlorinated biphenyls, phthalate esters and nonylphenols in sediments. *J. Chromatogr. A* 1068, 229-236.
- Battle, R., Nerín, C., 2004. Application of single-drop microextraction to the determination of dialkyl phthalate esters in food simulants. *J. Chromatogr. A* 1045, 29-35.
- Battersby, N.S., Wilson, V., 1989. Survey of the anaerobic biodegradation potential of organic chemicals in digesting sludge. *Appl. Environ. Microbiol.* 55, 433-439.
- Bauer, M.J., Herrmann, R., 1997. Estimation of the environmental contamination by phthalic acid esters leaching from household wastes. *Sci. Total Environ.* 208, 49-57.
- Bauer, M.J., Herrmann, R., Martin, A., Zellmann, H., 1998. Chemodynamics, transport behaviour and treatment of phthalic acid esters in municipal landfill leachates. *Water Sci. Technol.* 38, 185-192.
- Benson, R., 2009. Hazard to the developing male reproductive system from cumulative exposure to phthalate esters-dibutyl phthalate, diisobutyl phthalate, butylbenzyl phthalate, diethylhexyl phthalate, dipentyl phthalate, and diisononyl phthalate. *Regul. Toxicol. Pharm.* 53, 90-101.



- Bette, H., 2007. California Bans Phthalates In Toys For Children. Chemical and Engineering News, P. 12. <http://pubs.acs.org/cen/news/85/i43/8543news4.html>.
- Buszka, P.M., Yeskis, D.J., Kolpin, D.W., Furlong, E.T., Zaugg, S.D., Meyer, M.T., 2009. Waste-indicator and pharmaceutical compounds in landfill-leachate-affected ground water near Elkhart, Indiana, 2000-2002. Bull. Environ. Contam. Toxicol. 82, 653-659.
- Calley, D., Autian, J., Guess, W.L., 1966. Toxicology of a series of phthalate esters. J. Pharm. Sci. 55, 158-162.
- Castillo, M., Barceló, D., 2001. Characterisation of organic pollutants in textile wastewaters and landfill leachate by using toxicity-based fractionation methods followed by liquid and gas chromatography coupled to mass spectrometric detection. Anal. Chim. Acta 426, 253-264.
- Chang, B.V., Liao, C.S., Yuan, S.Y., 2005. Anaerobic degradation of diethyl phthalate, di-n-butyl phthalate, and di-(2-ethylhexyl) phthalate from river sediment in Taiwan. Chemosphere 58, 1601-1607.
- Chang, M., Liu, X., Nelson, P.J., Munzing, G.R., Gegan, T.A., Kissin, Y.V., 2006. Ziegler-Natta catalysts for propylene polymerization: Morphology and crystal structure of a fourth-generation catalyst. J. Cat. 239, 347-353.
- Chauret, C., Mayfield, C.I., Inniss, W.E., 1995. Biotransformation of di-n-butyl phthalate by a psychrotrophic *Pseudomonas fluorescens* (BGW) isolated from subsurface environment. Can. J. Microbiol. 41, 54-63.
- Chen, C., Wu, P., Chung, Y., 2009. Coupled biological and photo-Fenton pretreatment system for the removal of di-(2-ethylhexyl) phthalate (DEHP) from water. Bioresour. Technol. 100, 4531-4534.
- Chen, J., Liu, H., Qiu, Z., Shu, W., 2008. Analysis of di-n-butyl phthalate and other organic pollutants in Chongqing women undergoing parturition. Environ. Pollut. 156, 849-853.

- Chen, Y., Chen, L., Shang, N., 2009. Photocatalytic degradation of dimethyl phthalate in an aqueous solution with Pt-doped TiO<sub>2</sub>-coated magnetic PMMA microspheres. *J. Hazard. Mater.* 172, 20-29.
- Chen, Y., Hsieh, D., Shang, N., 2011. Efficient mineralization of dimethyl phthalate by catalytic ozonation using TiO<sub>2</sub>/Al<sub>2</sub>O<sub>3</sub> catalyst. *J. Hazard. Mater.* 192, 1017-1025.
- Chen, Y., Shang, N., Hsieh, D., 2008. Decomposition of dimethyl phthalate in an aqueous solution by ozonation with high silica zeolites and UV radiation. *J. Hazard. Mater.* 157, 260-268.
- Cheung, J.K.H., Lam, R.K.W., Shi, M.Y., Gu, J., 2007. Environmental fate of endocrine-disrupting dimethyl phthalate esters (DMPE) under sulfate-reducing condition. *Sci. Total Environ.* 381, 126-133.
- Chi, J., 2009. Phthalate acid esters in *Potamogeton crispus* L. from Haihe River, China. *Chemosphere* 77, 48-52.
- Colón, L.A., Maloney, T.D., Fermier, A.M., 2001. Chapter 4 Packed bed columns, in: Zdeněk Deyl and Frantiaek `vec (Ed.), *Journal of Chromatography Library*. Elsevier, pp. 111-164.
- Cortazar, E., Zuloaga, O., Sanz, J., Raposo, J.C., Etxebarria, N., Fernández, L.A., 2002. MultiSimplex optimisation of the solid-phase microextraction-gas chromatographic-mass spectrometric determination of polycyclic aromatic hydrocarbons, polychlorinated biphenyls and phthalates from water samples. *J. Chromatogr. A* 978, 165-175.
- Dargnat, C., Teil, M., Chevreuil, M., Blanchard, M., 2009. Phthalate removal throughout wastewater treatment plant: Case study of Marne Aval station (France). *Sci. Total Environ.* 407, 1235-1244.
- de Oliveira, T.F., Chedeville, O., Fauduet, H., Cagnon, B., 2011. Use of ozone/activated carbon coupling to remove diethyl phthalate from water: Influence of activated carbon textural and chemical properties. *Desalination* 276, 359-365.

- Edgar, K.J., Buchanan, C.M., Debenham, J.S., Rundquist, P.A., Seiler, B.D., Shelton, M.C., Tindall, D., 2001. Advances in cellulose ester performance and application. *Prog. Polym. Sci.* 26, 1605-1688.
- Ejlertsson, J., Alnervik, M., Jonsson, S., Svensson, B.H., 1997. Influence of water solubility, side-chain degradability, and side-chain structure on the degradation of phthalic acid esters under methanogenic conditions. *Environ. Sci. Technol.* 31, 2761-2764.
- Fang, C., Long, Y., Lu, Y., Shen, D., 2009a. Behavior of dimethyl phthalate (DMP) in simulated landfill bioreactors with different operation modes. *Int. Biodeterior. Biodegrad.* 63, 732-738.
- Fang, C., Long, Y., Wang, W., Feng, H., Shen, D., 2009b. Behavior of dibutyl phthalate in a simulated landfill bioreactor. *J. Hazard. Mater.* 167, 186-192.
- Farrell, M., Jones, D.L., 2009. Critical evaluation of municipal solid waste composting and potential compost markets. *Bioresour. Technol.* 100, 4301-4310.
- Fettig, J., Stapel, H., Steinert, C., Geiger, M., 1996. Treatment of landfill leachate by preozonation and adsorption in activated carbon columns. *Water Sci. Technol.* 34, 33-40.
- Fromme, H., Kuchler, T., Otto, T., Pilz, K., Müller, J., Wenzel, A., 2002. Occurrence of phthalates and bisphenol A and F in the environment. *Water Res.* 36, 1429-1438.
- Mackintosh, C.E., Maldonado, J.A., Ikonomou, M.G., Gobas, F.A.P.C., 2006. Sorption of Phthalate esters and PCBs in a Marine Ecosystem. *Environ. Sci. Technol.* 40, 3481-3488.
- Furtmann, K., Seifert, D., 1990. On the routine determination of chromium (VI) in soils. *Fresenius J. Anal. Chem.* 338, 73-74.
- Gibson, R.W., Wang, M., Padgett, E., Lopez-Real, J.M., Beck, A.J., 2007. Impact of drying and composting procedures on the concentrations of 4-nonylphenols, di-(2-

ethylhexyl)phthalate and polychlorinated biphenyls in anaerobically digested sewage sludge. *Chemosphere* 68, 1352-1358.

Gledhill, W.E., Kaley, R.G., Adams, W.J., Hicks, O., Michael, P.R., Saeger, V.W., LeBlanc, G.A., 1980. An environmental safety assessment of butyl benzyl phthalate. *Environ. Sci. Technol.* 14, 301-305.

Gross, F.C., Colony, J.A., 1973. The ubiquitous nature and objectionable characteristics of phthalate esters in aerospace technology. *Environ. Health Perspect.* 3, 37-48.

Guess, W.L., Haberman, S., 1968. Toxicity profiles of vinyl and polyolefinic plastics and their additives. *J. Biomed. Mater. Res.* 2, 313-335.

He, P., Zheng, Z., Zhang, H., Shao, L., Tang, Q., 2009. PAEs and BPA removal in landfill leachate with Fenton process and its relationship with leachate DOM composition, *Sci. Total Environ.* 407, 4928-4933.

Heudorf, U., Mersch-Sundermann, V., Angerer, J., 2007. Phthalates: Toxicology and exposure. *Int. J. Hyg. Environ. Health* 210, 623-634.

Horn, O., Nalli, S., Cooper, D., Nicell, J., 2004. Plasticizer metabolites in the environment. *Water Res.* 38, 3693-3698.

Howdeshell, K.L., Rider, C.V., Wilson, V.S., Gray Jr., L.E., 2008. Mechanisms of action of phthalate esters, individually and in combination, to induce abnormal reproductive development in male laboratory rats. *Environ. Res.* 108, 168-176.

Huang, M., Li, Y., Gu, G., 2008. The effects of hydraulic retention time and sludge retention time on the fate of di-(2-ethylhexyl) phthalate in a laboratory-scale anaerobic-anoxic-aerobic activated sludge system. *Bioresour. Technol.* 99, 8107-8111.

Huang, R., Yan, H., Li, L., Deng, D., Shu, Y., Zhang, Q., 2011. Catalytic activity of Fe/SBA-15 for ozonation of dimethyl phthalate in aqueous solution. *Appl. Catal. B Environ.* 106, 264-271.

- IARC, 2000. Monographs on the Evaluation of Carcinogenic Risks to Humans. Some Industrial Chemicals. International Agency for Research on cancer, Lyon, France, 77.
- Imai, A., Onuma, K., Inamori, Y., Sudo, R., 1998. Effects of pre-ozonation in refractory leachate treatment by the biological activated carbon fluidized bed process. *Environ. Technol.* 19, 213-221.
- Inman, J.C., Strachan, S.D., Sommers, L.E., Nelson, D.W., 1984. The decomposition of phthalate esters in soil. *J. Environ. Sci. Health, Part B* 19, 245-257.
- Jianlong, W., Lujun, C., Hanchang, S., Yi, Q., 2000. Microbial degradation of phthalic acid esters under anaerobic digestion of sludge. *Chemosphere* 41, 1245-1248.
- Jing, Y., Li, L., Zhang, Q., Lu, P., Liu, P., Lü, X., 2011. Photocatalytic ozonation of dimethyl phthalate with TiO<sub>2</sub> prepared by a hydrothermal method. *J. Hazard. Mater.* 189, 40-47.
- Johnson, B.T., Heitkamp, M.A., Jones, J.R., 1984. Environmental and chemical factors influencing the biodegradation of phthalic acid esters in freshwater sediments. *Environ. Pollut. Ser. B Chem. Phys.* 8, 101-118.
- Jonsson, S., Borén, H., 2002. Analysis of mono- and diesters of o-phthalic acid by solid-phase extractions with polystyrene-divinylbenzene-based polymers. *J. Chromatogr. A* 963, 393-400.
- Jonsson, S., Ejlertsson, J., Svensson, B.H., 2003. Behaviour of mono- and diesters of o-phthalic acid in leachates released during digestion of municipal solid waste under landfill conditions. *Adv. Environ. Res.* 7, 429-440.
- Joseph, C.G., Li Puma, G., Bono, A., Krishnaiah, D., 2009. Sonophotocatalysis in advanced oxidation process: A short review. *Ultrason. Sonochem.* 16, 583-589.
- Julinová, M., Slavík, R., 2012. Removal of phthalates from aqueous solution by different adsorbents: A short review. *J. Environ. Manage.* 94, 13-24.

- Junesson, C., Ward, O.P., Singh, A., 2001. Biodegradation of bis(2-ethylhexyl)phthalate in a soil slurry-sequencing batch reactor. *Process Biochem.* 37, 305-313.
- Kargi, F., Pamukoglu, M.Y., 2004. Adsorbent supplemented biological treatment of pre-treated landfill leachate by fed-batch operation. *Bioresour. Technol.* 94, 285-291.
- Kargi, F., Yunus Pamukoglu, M., 2003. Simultaneous adsorption and biological treatment of pre-treated landfill leachate by fed-batch operation. *Process Biochem.* 38, 1413-1420.
- Klavarioti, M., Mantzavinos, D., Kassinos, D., 2009. Removal of residual pharmaceuticals from aqueous systems by advanced oxidation processes. *Environ. Int.* 35, 402-417.
- Ko, K.B., Park, C.G., Moon, T.H., Ahn, Y.H., Lee, J.K., Ahn, K.H., Park, J.H., Yeom, I.T., 2008. Advanced H<sub>2</sub>O<sub>2</sub> oxidation for diethyl phthalate degradation in treated effluents: Effect of nitrate on oxidation and a pilot-scale AOP operation. *Water Sci. Technol.* 58, 1031-1037.
- Kotzias, D., Klein, W., Korte, F., 1975. Beiträge zur ökologischen Chemie CVI : Vorkommen von Xenobiotika im Sickerwasser von Mülldeponien. *Chemosphere* 4, 301-306.
- Kuch, H.M., Ballschmiter, K., 2001. Determination of endocrine-disrupting phenolic compounds and estrogens in surface and drinking water by HRGC-(NCI)-MS in the picogram per liter range. *Environ. Sci. Technol.* 35, 3201-3206.
- Lau, T.K., Chu, W., Graham, N., 2005. The degradation of endocrine disruptor di-n-butyl phthalate by UV irradiation: A photolysis and product study. *Chemosphere* 60, 1045-1053.
- Lee, S., Koo, B., Lee, S., Kim, M., Choi, D., Hong, E., Jeung, E., Choi, I., 2004. Biodegradation of dibutylphthalate by white rot fungi and evaluation on its estrogenic activity. *Enzyme Microb. Technol.* 35, 417-423.

- Lertsirisopon, R., Soda, S., Sei, K., Ike, M., 2009. Abiotic degradation of four phthalic acid esters in aqueous phase under natural sunlight irradiation. *J. Environ. Sci.* 21, 285-290.
- Liao, W., Zheng, T., Wang, P., Tu, S., Pan, W., 2010. Efficient microwave-assisted photocatalytic degradation of endocrine disruptor dimethyl phthalate over composite catalyst ZrOx/ZnO. *J. Environ. Sci.* 22, 1800-1806.
- Lin, C., Lee, C., Mao, W., Nadim, F., 2009. Identifying the potential sources of di-(2-ethylhexyl) phthalate contamination in the sediment of the Houjing River in southern Taiwan. *J. Hazard. Mater.* 161, 270-275.
- Ma, L.L., Chu, S.G., Xu, X.B., 2003. Organic contamination in the greenhouse soils from Beijing suburbs, China. *J. Environ. Monit.* 5, 786-790.
- Mailhot, G., Sarakha, M., Lavedrine, B., Cáceres, J., Malato, S., 2002. Fe(III)-solar light induced degradation of diethyl phthalate (DEP) in aqueous solutions. *Chemosphere* 49, 525-532.
- Marcilla, A., García, S., García-Quesada, J.C., 2004. Study of the migration of PVC plasticizers. *J. Anal. Appl. Pyrolysis* 71, 457-463.
- Marttinen, S.K., Kettunen, R.H., Rintala, J.A., 2003a. Occurrence and removal of organic pollutants in sewages and landfill leachates. *Sci. Total Environ.* 301, 1-12.
- Marttinen, S.K., Hänninen, K., Rintala, J.A., 2004a. Removal of DEHP in composting and aeration of sewage sludge. *Chemosphere* 54, 265-272.
- Marttinen, S.K., Kettunen, R.H., Sormunen, K.M., Rintala, J.A., 2003b. Removal of bis(2-ethylhexyl) phthalate at a sewage treatment plant. *Water Res.* 37, 1385-1393.
- Marttinen, S.K., Ruissalo, M., Rintala, J.A., 2004b. Removal of bis (2-ethylhexyl) phthalate from reject water in a nitrogen-removing sequencing batch reactor. *J. Environ. Manage.* 73, 103-109.

- McDowell, D.C., Metcalfe, C.D., 2001. Phthalate Esters in Sediments Near a Sewage Treatment Plant Outflow in Hamilton Harbour, Ontario: SFE Extraction and Environmental Distribution. *J. Great Lakes Res.* 27, 3-9.
- Méndez-Díaz, J.D., Abdel daiem, M.M., Rivera-Utrilla, J., Sánchez-Polo, M., Bautista-Toledo, I., 2012. Adsorption/bioadsorption of phthalic acid, an organic micropollutant present in landfill leachates, on activated carbons, *J. Colloid Interface Sci.* 369, 358-365.
- Méndez-Díaz, J.D., Prados-Joya, G., Rivera-Utrilla, J., Leyva-Ramos, R., Sánchez-Polo, M., Ferro-García, M.A., Medellín-Castillo, N.A., 2010. Kinetic study of the adsorption of nitroimidazole antibiotics on activated carbons in aqueous phase, *J. Colloid Interface Sci.* 345, 481-490.
- Mersiowsky, I., Brandsch, R., Ejlertsson, J., 2001. Screening for organotin compounds in European landfill leachates. *J. Environ. Qual.* 30, 1604-1611.
- Metcalf, Eddy, Inc., 2003. *Wastewater Engineering: Treatment, Disposal, and Reuse*, 3rd Edition. McGraw-Hill, New York.
- Morawe, B., Ramteke, D.S., Vogelpohl, A., 1995. Activated carbon column performance studies of biologically treated landfill leachate. *Chem. Eng. Proc.* 34, 299-303.
- Mori, S., 1976. Identification and determination of phthalate esters in river water by high-performance liquid chromatography. *J. Chromatogr.* 129, 53-60.
- Na S, Jinhua C, Mingcan C, Khim J., 2012. Sonophotolytic Diethyl phthalate (DEP) Degradation with UVC or VUV Irradiation. *Ultrason. Sonochem.* 19, 1094-1098.
- Nascimento Filho, I.d., von Mühlen, C., Schossler, P., Bastos Caramão, E., 2003. Identification of some plasticizers compounds in landfill leachate. *Chemosphere* 50, 657-663.



- Navarro, A., Font, X., 1993. Discriminating different sources of groundwater contamination caused by industrial wastes in the Besós River Basin, Barcelona, Spain. *Appl. Geochem.* 8, 277-279.
- Ng, S.W., 2005. Rerefinement of catena-poly [[tetraaquacobalt(II)- $\mu$ -pyrazine] phthalate] in a lower-symmetry space group. *Acta Crystallogr. Sect. E Struct. Rep. Online* 61.
- Official Journal of the European Communities, 1999. L 315/46, 9 December 1999.
- O'Grady, D.P., Howard, P.H., Werner, A.F., 1985. Activated sludge biodegradation of 12 commercial phthalate esters. *Appl. Environ. Microbiol.* 49, 443-445.
- Oh, B.S., Jung, Y.J., Oh, Y.J., Yoo, Y.S., Kang, J., 2006. Application of ozone, UV and ozone/UV processes to reduce diethyl phthalate and its estrogenic activity. *Sci. Total Environ.* 367, 681-693.
- Oliver, R., May, E., Williams, J., 2007. Microcosm investigations of phthalate behaviour in sewage treatment biofilms. *Sci. Total Environ.* 372, 605-614.
- Oliver, R., May, E., Williams, J., 2005. The occurrence and removal of phthalates in a trickle filter STW. *Water Res.* 39, 4436-4444.
- Öman, C., Hynning, P., 1993. Identification of organic compounds in municipal landfill leachates. *Environ. Pollut.* 80, 265-271.
- Otton, S.V., Sura, S., Blair, J., Ikonomou, M.G., Gobas, F.A.P.C., 2008. Biodegradation of mono-alkyl phthalate esters in natural sediments. *Chemosphere* 71, 2011-2016.
- Pant, N., Shukla, M., Kumar Patel, D., Shukla, Y., Mathur, N., Kumar Gupta, Y., Saxena, D.K., 2008. Correlation of phthalate exposures with semen quality. *Toxicol. Appl. Pharmacol.* 231, 112-116.
- Peijnenburg, W.J.G.M., Struijs, J., 2006. Occurrence of phthalate esters in the environment of the Netherlands. *Ecotoxicol. Environ. Saf.* 63, 204-215.

- Peñalver, A., Pocurull, E., Borrull, F., Marcé, R.M., 2002. Method based on solid-phase microextraction–high-performance liquid chromatography with UV and electrochemical detection to determine estrogenic compounds in water samples. *J. Chromatogr. A* 964, 153-160.
- Peñalver, A., Pocurull, E., Borrull, F., Marcé, R.M., 2001. Comparison of different fibers for the solid-phase microextraction of phthalate esters from water. *J. Chromatogr. A* 922, 377-384.
- Proceedings of the Third Plenary Meeting of CSTEE, 1998. Phthalate migration from soft PVC toys and children care articles, Brussels.
- Pirsaheb, M., Mesdaghinia, A., Shahtaheri, S.J., Zinatizadeh, A.A., 2009. Kinetic evaluation and process performance of a fixed film bioreactor removing phthalic acid and dimethyl phthalate. *J. Hazard. Mater.* 167, 500-506.
- Psillakis, E., Kalogerakis, N., 2003. Hollow-fibre liquid-phase microextraction of phthalate esters from water. *J. Chromatogr. A* 999, 145-153.
- Pujar, B.G., Ribbons, D.W., 1985. Phthalate metabolism in *Pseudomonas fluorescens* PHK: Purification and properties of 4,5-dihydroxyphthalate decarboxylase. *Appl. Environ. Microbiol.* 49, 374-376.
- Radovic, L.R., Moreno-Castilla, C., Rivera-Utrilla, J., 2001. Carbon materials as adsorbents in aqueous solutions. *Chemistry and Physics of Carbon* 27, 227-405.
- Reynold, T.D., 1982. *Unit operation and processes in environmental engineering*, Boston, Massachusetts.
- Rivera-Utrilla, J., Prados-Joya, G., Sánchez-Polo, M., Ferro-García, M.A., Bautista-Toledo, I., 2009. Removal of nitroimidazole antibiotics from aqueous solution by adsorption/bioadsorption on activated carbon, *J. Hazard. Mater.* 170, 298-305.
- Rhind, S.M., Kyle, C.E., Mackie, C., Telfer, G., 2007. Effects of exposure of ewes to sewage sludge-treated pasture on phthalate and alkyl phenol concentrations in their milk. *Sci. Total Environ.* 383, 70-80.

- Ribbons, D.W., Keyes, P., Kuna, D.A., Taylor, B.F., Etaon, R.W., Anderson, B.N., 1984. Microbial degradation of phthalates. Microbial degradation of organic compounds. New York, Marcel Dekker.
- Rodrigues, L.S., Antunes, I.F., Teixeira, M.G., Da Silva, J.B., 2002. Genetic divergence in bean land races and research-developed cultivars. *Pesqui. Agropecu. Bras.* 37, 1275-1284.
- Roslev, P., Vorkamp, K., Aarup, J., Frederiksen, K., Nielsen, P.H., 2007. Degradation of phthalate esters in an activated sludge wastewater treatment plant. *Water Res.* 41, 969-976.
- Rubio, J., Souza, M.L., Smith, R.W., 2002. Overview of flotation as a wastewater treatment technique. *Minerals Eng* 15, 139-155.
- Saeger, V.W., Tucker, E.S., 1976. Biodegradation of phthalic acid esters in river water and activated sludge. *Appl. Environ. Microbiol.* 31, 29-34.
- Salim, C.J., Liu, H., Kennedy, J.F., 2010. Comparative study of the adsorption on chitosan beads of phthalate esters and their degradation products. *Carbohydr. Polym.* 81, 640-644.
- Sathyanarayana, S., Calafat, A.M., Liu, F., Swan, S.H., 2008. Maternal and infant urinary phthalate metabolite concentrations: Are they related?. *Environ. Res.* 108, 413-418.
- Sello, G., Bernasconi, S., Orsini, F., Tansi, M., Galli, E., Di Gennaro, P., Bestetti, G., 2004. Organic phase effect in the biphasic bioconversion of substituted naphthalenes by engineered *E. coli* containing *P. fluorescens* N3 dioxygenase. *J. Molec. Cat. B* 29, 181-186.
- Shelton, D.R., Boyd, S.A., Tledje, J.M., 1984. Anaerobic biodegradation of phthalic acid esters in sludge. *Environ. Sci. Technol.* 18, 93-97.

- Shin, S.M., Jeon, H.S., Kim, Y.H., Yoshioka, T., Okuwaki, A., 2002. Plasticizer leaching from flexible PVC in low temperature caustic solution. *Polym. Degrad. Stab.* 78, 511-517.
- Singh, A.R., Lawrence, W.H., Autian, J., 1974. Mutagenic and antifertility sensitivities of mice to di 2 ethylhexyl phthalate (DEHP) and dimethoxyethyl phthalate (DMEP). *Toxicol. Appl. Pharmacol.* 29, 35-46.
- Singh, A.R., Lawrence, W.H., Autian, J., 1972. Teratogenicity of phthalate esters in rats. *J. Pharm. Sci.* 61, 51-55.
- Sivamurthy, K., Pujar, B.G., 1989. Bacterial Degradation of Dimethylterephthalate. *J. Ferment. Bioeng.* 68, 375-377.
- Smith, E.H., Weber Jr., W.J., 1990. Comparative assessment of the chemical and adsorptive characteristics of leachates from a municipal and an industrial landfill. *Water Air Soil Pollut.* 53, 279-295.
- Stales, C.A., Peterson, D.R., Parkerton, T.F., Adams, W.J., 1997. The environmental fate of phthalate esters: A literature review. *Chemosphere* 35, 667-749.
- Staples, C.A., 2003. *The Handbook of Environmental Chemistry (Phthalates Esters)*. Springer-Verlag, Berlin-Heidelberg-New York.
- Subba-Rao, R.V., Rubin, H.E., Alexander, M., 1982. Kinetics and extent of mineralization of organic chemicals at trace levels in freshwater and sewage. *Appl. Environ. Microbiol.* 43, 1139-1150.
- Sugatt, R.H., O'Grady, D.P., Banerjee, S., 1984. Toxicity of organic mixtures saturated in water to . Effect of compositional changes. *Chemosphere* 13, 11-18.
- Tan, G.H., 1995. Residue levels of phthalate esters in water and sediment samples from the Klang River basin. *Bull. Environ. Contam. Toxicol.* 54, 171-176.

- Thiruvengkatachari, R., Kwon, T.O., Jun, J.C., Balaji, S., Matheswaran, M., Moon, I.S., 2007. Application of several advanced oxidation processes for the destruction of terephthalic acid (TPA). *J. Hazard. Mater.* 142, 308-314.
- Titow W V., 1990. *PVC Plastics. Properties Processing and Applications*, Elsevier Applied Science.
- Vega, D., Bastide, J., 2003. Dimethylphthalate hydrolysis by specific microbial esterase. *Chemosphere* 51, 663-668.
- Venkata-Mohan, S., Shailaja, S., Rama Krishna, M., Sarma, P.N., 2007. Adsorptive removal of phthalate ester (Di-ethyl phthalate) from aqueous phase by activated carbon: A kinetic study. *J. Hazard. Mater.* 146, 278-282.
- Vethaak, A.D., Lahr, J., Schrap, S.M., Belfroid, A.C., Rijs, G.B.J., Gerritsen, A., De Boer, J., Bulder, A.S., Grinwis, G.C.M., Kuiper, R.V., Legler, J., Murk, T.A.J., Peijnenburg, W., Verhaar, H.J.M., De Voogt, P., 2005. An integrated assessment of estrogenic contamination and biological effects in the aquatic environment of The Netherlands. *Chemosphere* 59, 511-524.
- Vitali, M., Guidotti, M., Macilenti, G., Cremisini, C., 1997. Phthalate esters in freshwaters as markers of contamination sources - A site study in Italy. *Environ. Int.* 23, 337-347.
- Wang, H., Sun, D.-., Bian, Z.-., 2010. Degradation mechanism of diethyl phthalate with electrogenerated hydroxyl radical on a Pd/C gas-diffusion electrode. *J. Hazard. Mater.* 180, 710-715.
- Wang, J., Liu, P., Shi, H., Qian, Y., 1997. Kinetics of phthalic acid ester degradation by acclimated activated sludge. *Process Biochemistry* 32, 567-571.
- Wang, J., Jiang, D., Gu, Z., Yan, X., 2006. Multiwalled carbon nanotubes coated fibers for solid-phase microextraction of polybrominated diphenyl ethers in water and milk samples before gas chromatography with electron-capture detection. *J. Chromatogr. A* 1137, 8-14.

- Welander, U., Henrysson, T., 1998. Physical and chemical treatment of a nitrified leachate from a municipal landfill. *Environ. Technol.* 19, 591-599.
- Wen, G., Ma, J., Liu, Z., Zhao, L., 2011. Ozonation kinetics for the degradation of phthalate esters in water and the reduction of toxicity in the process of  $O_3/H_2O_2$ . *J. Hazard. Mater.* 195, 371-377.
- Wickson J., 1993. *Handbook of Polyvinyl Chloride Formulating*, Wiley, New York.
- Wolfe, N.L., Burns, L.A., Steen, W.C., 1980. Use of linear free energy relationships and an evaluative model to assess the fate and transport of phthalate esters in the aquatic environment. *Chemosphere* 9, 393-402.
- Wu, D., Hu, B., Zheng, P., Qaisar, M., 2007. Anoxic biodegradation of dimethyl phthalate (DMP) by activated sludge cultures under nitrate-reducing conditions. *J. Environ. Sci.* 19, 1252-1256.
- Wu, D., Mahmood, Q., Wu, L., Zheng, P., 2008. Activated sludge-mediated biodegradation of dimethyl phthalate under fermentative conditions. *J. Environ. Sci.* 20, 922-926.
- Wu, M., Liu, N., Xu, G., Ma, J., Tang, L., Wang, L., Fu, H., 2011. Kinetics and mechanisms studies on dimethyl phthalate degradation in aqueous solutions by pulse radiolysis and electron beam radiolysis. *Radiat. Phys. Chem.* 80, 420-425.
- Xu, B., Gao, N., Cheng, H., Xia, S., Rui, M., Zhao, D., 2009. Oxidative degradation of dimethyl phthalate (DMP) by UV/ $H_2O_2$  process. *J. Hazard. Mater.* 162, 954-959.
- Xu, B., Gao, N., Sun, X., Xia, S., Rui, M., Simonnot, M., Causserand, C., Zhao, J., 2007. Photochemical degradation of diethyl phthalate with UV/ $H_2O_2$ . *J. Hazard. Mater.* 139, 132-139.
- Xu, G., Li, F., Wang, Q., 2008. Occurrence and degradation characteristics of dibutyl phthalate (DBP) and di-(2-ethylhexyl) phthalate (DEHP) in typical agricultural soils of China. *Sci. Total Environ.* 393, 333-340.

- Xu, X., Li, S., Li, X., Gu, J., Chen, F., Li, X., Li, H., 2009. Degradation of n-butyl benzyl phthalate using TiO<sub>2</sub>/UV. *J. Hazard. Mater.* 164, 527-532.
- Xu, X., Li, H., Gu, J., 2005. Biodegradation of an endocrine-disrupting chemical di-n-butyl phthalate ester by *Pseudomonas fluorescens* B-1. *Int. Biodeterior. Biodegrad.* 55, 9-15.
- Xu, Z., Zhang, W., Pan, B., Hong, C., Lv, L., Zhang, Q., Pan, B., Zhang, Q., 2008. Application of the Polanyi potential theory to phthalates adsorption from aqueous solution with hyper-cross-linked polymer resins. *J. Colloid Interface Sci.* 319, 392-397.
- Yang, G., Zhao, X., Sun, X., Lu, X., 2005. Oxidative degradation of diethyl phthalate by photochemically-enhanced Fenton reaction. *J. Hazard. Mater.* 126, 112-118.
- Yuan, B., Li, X., Graham, N., 2008. Aqueous oxidation of dimethyl phthalate in a Fe(VI)-TiO<sub>2</sub>-UV reaction system. *Water Res.* 42, 1413-1420.
- Yuan, B., Li, X., Li, K., Chen, W., 2011. Degradation of dimethyl phthalate (DMP) in aqueous solution by UV/Si-FeOOH/H<sub>2</sub>O<sub>2</sub>. *Colloids Surf. Physicochem. Eng. Aspects* 379, 157-162.
- Yuan, S.Y., Liu, C., Liao, C.S., Chang, B.V., 2002. Occurrence and microbial degradation of phthalate esters in Taiwan river sediments. *Chemosphere* 49, 1295-1299.
- Yunrui, Z., Wanpeng, Z., Fudong, L., Jianbing, W., Shaoxia, Y., 2007. Catalytic activity of Ru/Al<sub>2</sub>O<sub>3</sub> for ozonation of dimethyl phthalate in aqueous solution. *Chemosphere* 66, 145-150.
- Zamora, R.M.R., Moreno, A.D., De Velásquez, M.T.O., Ramírez, I.M., 2000. Treatment of landfill leachates by comparing advanced oxidation and coagulation-flocculation processes coupled with activated carbon adsorption. *Water Sci. Technol.* 41, 231-235.

- Zeng, F., Cui, K., Li, X., Fu, J., Sheng, G., 2004. Biodegradation kinetics of phthalate esters by *Pseudomonas fluorescens* FS1. *Process Biochem.* 39, 1125-1129.
- Zeng, F., Cui, K., Xie, Z., Liu, M., Li, Y., Lin, Y., Zeng, Z., Li, F., 2008. Occurrence of phthalate esters in water and sediment of urban lakes in a subtropical city, Guangzhou, South China. *Environ. Int.* 34, 372-380.
- Zhang, C., Wang, Y., 2009. Removal of dissolved organic matter and phthalic acid esters from landfill leachate through a complexation–flocculation process. *Waste Manage.* 29, 110-116.
- Zhao, R., Wang, X., Yuan, J., Lin, J., 2008. Investigation of feasibility of bamboo charcoal as solid-phase extraction adsorbent for the enrichment and determination of four phthalate esters in environmental water samples. *J. Chromatogr. A* 1183, 15-20.
- Zhao, X., Li, J., Shi, Y., Cai, Y., Mou, S., Jiang, G., 2007. Determination of perfluorinated compounds in wastewater and river water samples by mixed hemimicelle-based solid-phase extraction before liquid chromatography–electrospray tandem mass spectrometry detection. *J. Chromatogr. A* 1154, 52-59.
- Zheng, Z., Zhang, H., He, P.-., Shao, L.-., Chen, Y., Pang, L., 2009. Co-removal of phthalic acid esters with dissolved organic matter from landfill leachate by coagulation and flocculation process. *Chemosphere* 75, 180-186.
- Zhou, C.Y., Wu, J., Chi, H., Wong, M.K., Koh, L.L., Wee, Y.C., 1995. High performance liquid chromatographic determination of aluminium in natural waters in the form of its lumogallion chelate. *Talanta* 42, 415-422.
- Zhou, J.L., Liu, Y.P., 2000. Kinetics and equilibria of the interactions between diethylhexyl phthalate and sediment particles in simulated estuarine systems. *Mar. Chem.* 71, 165-176.
- Zhou, Q., Xiao, J., Wang, W., 2006. Using multi-walled carbon nanotubes as solid phase extraction adsorbents to determine dichlorodiphenyltrichloroethane and its



metabolites at trace level in water samples by high performance liquid chromatography with UV detection. *J. Chromatogr. A* 1125, 152-158.

Ziougou, K., Kirk, P.W.W., Lester, J.N., 1989. Behaviour of phthalic acid esters during batch anaerobic digestion of sludge. *Water Res.* 23, 743-748

## 2. FUNDAMENTOS QUÍMICOS DE LOS SISTEMAS DE TRATAMIENTOS DE AGUAS APLICADOS

### 2.1. Adsorción sobre carbón activado

En los tratamientos de aguas, el proceso de adsorción consiste en la concentración de sustancias solubles en la superficie de un sólido. Este proceso se considera un tratamiento terciario, y, por ello, se aplica al final de los tratamientos secundarios. Dado que el compuesto soluble a eliminar se ha de concentrar en la superficie del sólido, un parámetro determinante del proceso será el área superficial del sólido. Sin embargo, existen otros factores que, según el sistema, también pueden afectar a su eliminación y contribuir a aumentar su efectividad en la extracción de un determinado contaminante, éstos son:

- Solubilidad del adsorbato
- Hidrofobicidad
- Estructura y volumen molecular
- Peso molecular
- Problemas de difusión
- Polaridad
- Concentración (grado de saturación)
- Naturaleza química del adsorbente
- Química de la disolución (pH, presencia de electrolitos u otras especies)

Las aplicaciones de la adsorción de compuestos químicos sobre un sólido son muchas, desde la eliminación de un amplio abanico de sustancias orgánicas (colorantes, fenoles, mercaptanos, etc.) hasta sustancias inorgánicas como las especies metálicas. En la actualidad, el sólido universalmente utilizado como adsorbente en el tratamiento de aguas es el carbón activado, el cual ha ido sustituyendo al uso del filtro de arena, debido a su mayor capacidad para la extracción de compuestos orgánicos e inorgánicos que no han sido completamente separados en etapas anteriores. Los carbones activados son materiales que poseen un alto poder de adsorción, como resultado, entre otras

características, de una importante y variada red de poros. Un carbón activado se puede definir como un material que se ha fabricado a partir de una materia prima de elevado contenido en carbono y que desarrolla su porosidad mediante un proceso de activación específica. La materia prima para la preparación de estos materiales es muy variada, abarcando desde turba, lignito, hulla, breas, huesos de aceituna, hasta cáscaras de fruta y cualquier tipo de residuo lignocelulósico; actualmente, también se están obteniendo carbones activados a partir de diversos polímeros sintetizados artificialmente.

### 2.1.1. Textura porosa de los carbones activados

Una de las características más importantes de los carbones activados es su estructura porosa, la cual se debe a la presencia de pequeñas láminas de grafito con numerosos defectos estructurales y apilados de forma muy desordenada. Los huecos que quedan entre el entrecruzamiento de dichas láminas constituyen la porosidad del carbón (Stoeckli, 1990), siendo ésta la responsable de su elevada superficie y de su aplicación como adsorbente universal.

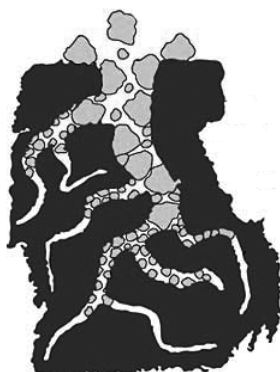


**Figura 1.** Representación de la estructura porosa del carbón activado.

Atendiendo a su diámetro, los poros de un sólido pueden clasificarse, de acuerdo con la IUPAC, en tres grupos:

- Microporos: Poros de diámetro inferior a 2 nm
- Mesoporos: Poros con un diámetro comprendido entre 2-50 nm
- Macroporos: Poros con un diámetro superior a los 50 nm

Los microporos son los responsables de los elevados valores de área superficial que presentan los carbones activados, que, en general, oscilan entre 500 y 1500 m<sup>2</sup>/g (Gregg and Sing, 1982), y de su elevada capacidad de adsorción de moléculas de pequeñas dimensiones, especialmente gases. Los mesoporos son importantes para la adsorción de moléculas de gran tamaño y, junto con los macroporos, actúan como canales de transporte y acceso hasta los microporos (Rodríguez-Reinoso and Linares-Solano, 1989).

### 2.1.2. Química superficial de los carbones activados

Las propiedades de los materiales de carbón no sólo están determinadas por su textura porosa sino que las características químico-superficiales también desempeñan un papel fundamental (Boehm, 1966). La composición elemental media de un carbón activado es aproximadamente de un 90% C, 0.5% H, 6% O, 0.5% S y el resto de materia mineral, pudiendo diferir el contenido de algunos elementos dependiendo de la naturaleza del material de partida y de las condiciones del proceso de activación.

Los carbones activados presentan un carácter anfótero, es decir, se comportan como bases o como ácidos en función del pH del medio (Figura 2). La carga superficial de los mismos va a depender del pH de la disolución. Así, el pH para el que la densidad superficial de carga positiva es igual a la densidad superficial de carga negativa recibe el nombre de pH del punto cero de carga (pH<sub>PZC</sub>). En aquellos casos en los que el pH de la disolución sea superior al pH<sub>PZC</sub>, el carbón presentará carga negativa superficial, mientras que para valores de pH inferiores al pH<sub>PZC</sub>, el carbón presentará carga superficial positiva. Atendiendo a la densidad de carga de los carbones, éstos pueden ser clasificados en carbones básicos, también denominados H (pH<sub>pzc</sub> > 7) o carbones ácidos, denominados L (pH<sub>pzc</sub> < 7).

Los carbones ácidos se caracterizan por presentar elevadas concentraciones de grupos oxigenados superficiales y, aunque no se ha precisado con exactitud la naturaleza de todas las estructuras de estos grupos químicos superficiales, las principales especies presentes son ácidos carboxílicos, fenoles, lactonas, quinonas, anhídridos carboxílicos y peróxidos cíclicos (Boehm, 1966; Figueiredo et al., 1999; Leon y Leon and Radovic,



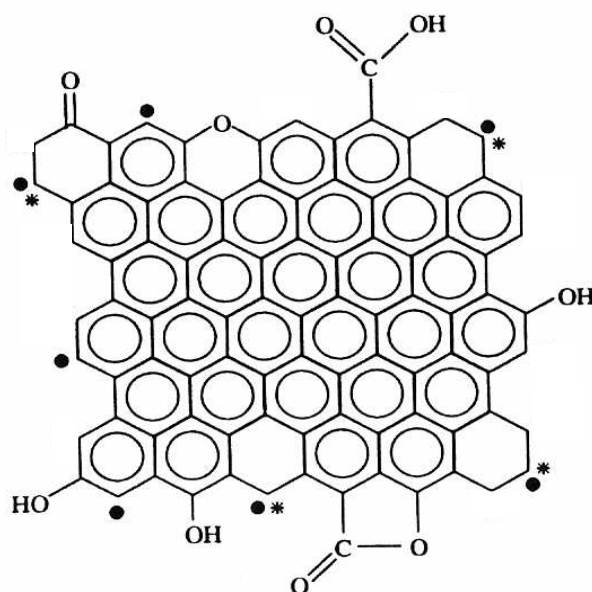


**Figura 3.** Representación de algunos de los grupos químicos superficiales presentes en un carbón activado. ●) electrón  $\sigma$  desapareado; \*) electrón  $\pi$  localizado.

### 2.1.3. Uso del carbón activado como agente depurador de las aguas

El uso de carbón activado es una de las tecnologías más antiguas aplicadas en el tratamiento de aguas. Su empleo como agente depurador comenzó en 1883, con el uso de filtros de carbón activado en plantas a escala piloto en Estados Unidos para eliminar el olor y sabor del agua destinada al consumo humano. Los resultados obtenidos en estos estudios provocaron la implantación, a comienzos de 1930, de columnas de carbón activado en la mayoría de las plantas depuradoras estadounidenses. Actualmente, la adsorción sobre carbón activado está reconocida por la United States Environmental Protection Agency (USEPA) como una de las mejores tecnologías disponibles para la eliminación de compuestos orgánicos e inorgánicos de las aguas destinadas a consumo humano (Radovic et al., 2001).

La utilización del carbón activado en el tratamiento de aguas superficiales se ha extendido como el método de emergencia más eficaz para eliminar contaminantes orgánicos tras los episodios de contaminación, como el caso del vertido en la ría de Arousa en Caldas (Galicia), en Septiembre de 2006, producida por el incendio de un almacén de productos químicos de la empresa alemana Brenntag, o bien, el caso del

pantano de Iznajar (Córdoba), en Julio de 2005, por contaminación difusa de plaguicidas en embalses (terbutilamina, simazina, etc.), o el vertido en el río Lagares y en la playa de Samil (Vigo), producido por un incendio en una nave industrial de productos químicos en Septiembre de 2008.

#### 2.1.4. Adsorción de compuestos aromáticos sobre carbón activado en fase acuosa

El uso del carbón activado es una alternativa muy interesante para la depuración de aguas residuales y aguas destinadas al consumo humano. La adsorción de compuestos aromáticos en disolución acuosa por carbones activados ha sido ampliamente estudiada (Aksu and Kabasakal, 2004; Ayranci and Bayram, 2005; Bautista-Toledo et al., 2008; Bilgili, 2006; Coughlin and Ezra, 1968; Ferro-García et al., 1990a; Ferro-García et al., 1990b; Hameed et al., 2009; Leyva Ramos et al., 2002; Lim et al., 2009; Liu et al., 2009; Mattson et al., 1969; Moreno-Castilla et al., 1995; Moreno-Castilla, 2004; Radovic et al., 1997; Rivera-Utrilla et al., 2009; XU et al., 2009); sin embargo, para mejorar su eficiencia en el proceso de eliminación de estos contaminantes, es necesario conocer el mecanismo responsable del mismo. Existe una cierta controversia con relación al mecanismo que gobierna este proceso, así, se han propuesto diferentes mecanismos como son:

- La existencia de interacciones dispersivas entre los electrones  $\pi$  del anillo aromático del adsorbato y los electrones  $\pi$  de los planos grafénicos de la superficie del carbón activado (Coughlin and Ezra, 1968; Radovic et al., 1997).
- Formación de un complejo donador-aceptor que involucra a los grupos superficiales tipo carbonilo, los cuales actúan como donantes, y el anillo aromático del compuesto orgánico que actúa como aceptor (Mattson et al., 1969; Moreno-Castilla et al., 1995).
- Establecimiento de interacciones electrostáticas/dispersivas y formación de enlaces por puente de hidrógeno (Franz et al., 2000).

Al existir cierta incertidumbre acerca de la contribución de las diferentes interacciones implicadas en estos procesos de adsorción, no es posible establecer un mecanismo general, siendo necesario un estudio exhaustivo para cada sistema en particular. No obstante, tras una extensa revisión bibliográfica acerca de la adsorción de estos compuestos aromáticos, se ha llegado a las siguientes conclusiones (Radovic et al., 2001):

- Este proceso sigue un modelo complejo con interacciones electrostáticas y dispersivas adsorbente-adsorbato.
- El rendimiento del proceso viene determinado por la solubilidad del adsorbato, hidrofobicidad del adsorbato y del adsorbente y, por último, por la fortaleza de las interacciones dispersivas  $\pi$ - $\pi$ . La fortaleza de estas interacciones  $\pi$ - $\pi$  se pueden modificar por los sustituyentes de los anillos aromáticos del adsorbato o del carbón activado.
- El pH del medio desempeña un papel muy importante en el proceso de adsorción.

## 2.2. Procesos avanzados de oxidación

La oxidación supone la transferencia de uno o más electrones desde un donante (reductor) a un aceptor (oxidante) que tiene afinidad por electrones. La transferencia de estos electrones supone una transformación química para ambos compuestos y, en algunos casos, se producen especies radicalarias muy reactivas y, por lo tanto, muy inestables debido a su configuración electrónica. A la producción de radicales le sigue una reacción de oxidación entre los radicales oxidantes y otros reactivos, orgánicos o inorgánicos, hasta que se forman productos termodinámicamente estables. Los productos finales de una oxidación completa de compuestos orgánicos son dióxido de carbono, agua y, en algunos casos, sales.

Los procesos avanzados de oxidación (PAOs) se producen en dos etapas: 1) la formación de un potente oxidante, generalmente radicales  $\text{HO}^\bullet$ , y 2) reacción de ese oxidante con los contaminantes orgánicos del agua. Inicialmente se entendía por PAOs los procesos en los que intervenían  $\text{O}_3$ ,  $\text{H}_2\text{O}_2$  y/o luz ultravioleta, UV; sin embargo, esa denominación se ha ido ampliando a procesos en los que intervienen la catálisis con



TiO<sub>2</sub>, la cavitación, la irradiación con haz de electrones de alta energía, las reacciones Fenton, etc. Todos estos procesos producen radicales hidroxilo que reaccionan y destruyen un amplio abanico de contaminantes orgánicos. Aunque los procesos indicados pueden tener otros mecanismos de destrucción de contaminantes, en general, la eficacia de un PAO es proporcional a su capacidad para generar radicales.

De acuerdo con lo expuesto, la base de los PAOs es la generación de radicales libres (HO•, O<sub>2</sub>•-, HO<sub>2</sub>•), siendo el principal responsable el radical hidroxilo, HO•. Estos radicales libres son especies altamente reactivas, capaces de atacar con éxito a la mayor parte de las moléculas orgánicas, con constantes de velocidad de reacción muy elevadas que oscilan entre 10<sup>6</sup>-10<sup>9</sup> M<sup>-1</sup>s<sup>-1</sup>. Así pues, los PAOs se definen como: “aquellos procesos de oxidación que implican la generación de radicales hidroxilo en cantidad suficiente para interaccionar con los contaminantes del medio”. El elevado número de sistemas que pueden generar estos radicales (Tabla 1) hace que estos procesos avanzados de oxidación sean muy versátiles (Andreozzi et al., 1999; Brillas et al., 1998).

**Tabla 1.** Tecnologías basadas en procesos avanzados de oxidación usadas para el tratamiento de aguas.

| Procesos no fotoquímicos   | Procesos fotoquímicos   |
|--|---|
| <ul style="list-style-type: none"> <li>• Oxidación en agua sub/supercrítica</li> <li>• Reactivo Fenton (Fe<sup>2+</sup>/H<sub>2</sub>O<sub>2</sub>)</li> <li>• Oxidación electroquímica</li> <li>• <b>Radiólisis</b></li> <li>• Plasma no térmico</li> <li>• Ultrasonidos</li> <li>• Ozonización:               <ul style="list-style-type: none"> <li>○ en medio alcalino (O<sub>3</sub>/OH<sup>-</sup>)</li> <li>○ en presencia de peróxido de hidrógeno (O<sub>3</sub>/H<sub>2</sub>O<sub>2</sub>)</li> <li>○ catalítica</li> </ul> </li> </ul> | <ul style="list-style-type: none"> <li>• UV de vacío (UVV)</li> <li>• <b>UV/ (reactivo químico)</b></li> <li>• Foto-Fenton (UV/Fe<sup>2+</sup>/H<sub>2</sub>O<sub>2</sub>)</li> <li>• UV/O<sub>3</sub></li> <li>• <b>Fotocatálisis heterogénea</b></li> </ul> |

De las tecnologías expuestas en la Tabla 1, en el desarrollo de la presente Tesis Doctoral se han analizado las posibilidades que presentan para eliminar y degradar plastificantes, herbicidas y plaguicidas los siguientes PAOs: UV/peróxido de hidrógeno, UV/peroxodisulfato de potasio, UV/carbonato de sodio, UV/dióxido de titanio, UV/dióxido de titanio/carbón activado y radiólisis. A continuación se presentan los fundamentos químicos de los PAOs estudiados en esta Tesis Doctoral.

### 2.2.1. Procesos avanzados de oxidación basados en la radiación UV

La excelente capacidad de los radicales hidroxilos para oxidar compuestos orgánicos ha hecho que se invierta un gran esfuerzo por parte de los investigadores para explorar su generación fotoquímica. En la naturaleza es común encontrar compuestos que pueden descomponerse mediante reacciones fotoquímicas por aplicación de luz solar. Esta degradación depende de la longitud de onda de la radiación ( $\lambda$ ), de la capacidad de absorción molar del compuesto ( $\epsilon$ ) y de su rendimiento cuántico ( $\Phi$ ) (Kari et al., 1995). Estos parámetros están relacionados por la siguiente ecuación:

$$\Phi_{\lambda} = \frac{k_{\lambda}}{2.303 \cdot E_{\lambda} \cdot \epsilon_{\lambda}} \quad (1)$$

$k_{\lambda}$ : Constante cinética de degradación a una determinada  $\lambda$  (1/s)

$E_{\lambda}$ : Energía emitida por la fuente (Einstein/s/m<sup>2</sup>)

$\epsilon_{\lambda}$ : Coeficiente de absorción del compuesto a la  $\lambda$  considerada (m<sup>2</sup>/mol)

$\Phi_{\lambda}$ : Rendimiento cuántico a la  $\lambda$  considerada (mol/Einstein)

La radiación más utilizada para la fotólisis es aquella con una  $\lambda$  comprendida entre 200-400 nm; ésta pertenece a la región del espectro ultravioleta. La estructura de la molécula determinará si ésta es capaz de absorber un tipo de radiación e incrementar su energía de forma que alcance un estado excitado, pudiendo llegar a la ruptura de enlaces y, por lo tanto, a su degradación.

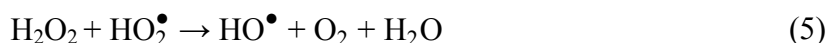
En el caso de que los compuestos no lleguen a ser degradados por fotólisis directa, sigue existiendo la posibilidad de lograrlo, mediante vía indirecta, por generación de

radicales. El uso de estas tecnologías para un proceso avanzado de oxidación tiene múltiples ventajas frente a las no fotoquímicas:

- En ocasiones, algunos de los contaminantes sufren fotólisis directa.
- No es necesario añadir reactivos químicos.
- Reduce la cantidad requerida de ciertos oxidantes en sistemas combinados.
- Se ven afectados en menor medida por cambios drásticos de pH.

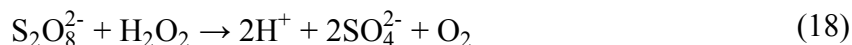
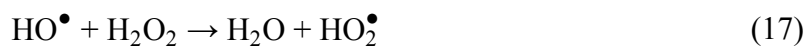
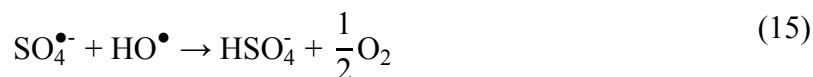
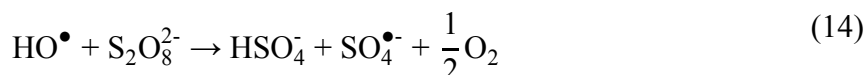
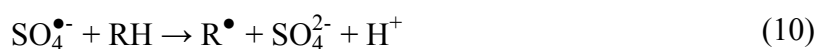
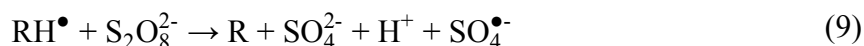
En el sistema UV/H<sub>2</sub>O<sub>2</sub>, la ruptura de la molécula de H<sub>2</sub>O<sub>2</sub> mediante el uso de fotones tiene un gran rendimiento cuántico ( $\Phi_{HO^\bullet} = 0.98$ ), por lo que produce, prácticamente, dos radicales HO<sup>•</sup> por cada molécula de H<sub>2</sub>O<sub>2</sub> (Reacción 2) (Glaze et al., 1987). Un inconveniente a tener en cuenta es el bajo coeficiente de absorción molar del H<sub>2</sub>O<sub>2</sub>, lo que hace necesario establecer condiciones de flujo turbulento para evitar que zonas de la disolución queden sin tratar. El proceso fotoquímico es más eficiente en medio alcalino, ya que el anión hidropéroxido (HO<sub>2</sub><sup>-</sup>) presenta una absorptividad mayor que el H<sub>2</sub>O<sub>2</sub> (Glaze et al., 1987).

El bajo coeficiente de absorción molar del H<sub>2</sub>O<sub>2</sub> podría compensarse aumentando la cantidad del reactivo, sin embargo, los radicales HO<sup>•</sup> generados también pueden reaccionar con el H<sub>2</sub>O<sub>2</sub>, sobre todo si éste se encuentra en altas concentraciones (Reacciones 3-6). Por lo tanto, un exceso de H<sub>2</sub>O<sub>2</sub> inhibe el proceso de degradación de contaminantes en disolución.



El peroxodisulfato (S<sub>2</sub>O<sub>8</sub><sup>2-</sup>) es un fuerte oxidante con un potencial de reducción de E<sup>0</sup>=2.05 V. Esta especie se usa en la industria del petróleo para la descontaminación de fluidos hidráulicos (Salari et al., 2009); también se usa para la degradación de algunos

contaminantes orgánicos. Sin embargo, debido a que las reacciones con  $S_2O_8^{2-}$  son muy lentas a temperatura ambiente, se han propuesto diferentes métodos para activar o acelerar la descomposición de moléculas orgánicas (Khataee y Mirzajani, 2010). Los métodos de activación más frecuentemente usados consisten en la generación de radicales sulfatos  $SO_4^{\bullet-}$  ( $E^0 = 2.6$  V) por medio de la descomposición fotoquímica, térmica o química del  $S_2O_8^{2-}$  (Criquet et al., 2009; Ito et al., 2009; Mora et al., 2009). El ion sulfato generado como producto final es prácticamente inerte y no es considerado un contaminante como el  $H_2O_2$ , el cual debe ser eliminado después de su aplicación, por lo cual, el uso del radical  $SO_4^{\bullet-}$  para la degradación de contaminantes se ha incrementado en los últimos años. Las reacciones (7) a (18) muestran la activación fotoquímica del  $S_2O_8^{2-}$  (Khataee and Mirzajani, 2010)



### 2.2.2. Fotocatálisis heterogénea

Una alternativa para generar radicales libres es llevar a cabo la fotólisis sobre la superficie de un semiconductor; ésta es la base de la fotocatálisis heterogénea, que consiste en la absorción, directa o indirecta, de energía radiante, visible o ultravioleta, por un sólido que, en su forma excitada, actúa como catalizador para producir

reacciones de degradación de los compuestos situados en la interfase. Existen varios semiconductores con las características apropiadas para ser empleados como fotocatalizadores; sin embargo, los semiconductores utilizados son aquellos que son estables, baratos, que requieran una radiación no demasiado energética, interesando aquellos que pueden ser activados con radiación visible. Los fotocatalizadores más utilizados para degradar compuestos orgánicos son  $\text{TiO}_2$ ,  $\text{ZnO}$ ,  $\text{SnO}_2$ ,  $\text{WO}_3$ ,  $\text{ZrO}_2$ ,  $\text{CeO}_2$ ,  $\text{ZnS}$ ,  $\text{CdS}$  y óxidos de Fe (Antoniadou et al., 2011; Ashkarran et al., 2010; Faisal et al., 2011; Gao et al., 2011; Kim et al., 2011; Ohno et al., 1998).

El principio fundamental de este sistema se basa en la fotogeneración de electrones en la banda de conducción (BC) del catalizador y, consecuentemente, “huecos” positivos ( $h^+$ ) en la banda de valencia (BV), por la aplicación de radiación de energía igual o mayor que la diferencia energética entre ambas bandas. Para los catalizadores mencionados, este  $\Delta E$  es del orden de 3.2 eV, que corresponde a la energía de la radiación UV, que incluso puede ser suministrada por la luz solar. Los radicales hidroxilos son formados en la superficie del fotocatalizador por reacción directa del agua adsorbida y los huecos generados, mientras que en la banda de conducción los electrones generados reaccionan con el  $\text{O}_2$  adsorbido generando el radical superóxido ( $\text{O}_2^{\bullet-}$ ).

El dióxido de titanio es el semiconductor más utilizado como fotocatalizador para la eliminación de contaminantes orgánicos e inorgánicos, tanto en fase líquida como en fase gas, debido a su alta disponibilidad, bajo costo, alta estabilidad química y nula toxicidad (Amama et al., 2002; Araña et al., 2007; Brugnera et al., 2010; Chen et al., 2009; Sun et al., 2008). En la Figura 4 se muestra, a modo de ejemplo, la activación del  $\text{TiO}_2$  mediante luz UV.

En los últimos años se ha comprobado que los materiales de carbono contribuyen, en gran medida, a la mejora del proceso fotocatalítico fundamentalmente a través de uno de los tres mecanismos siguientes: 1) minimización de la recombinación de los pares electrón-hueco fotogenerados, 2) modificación del “band gap” del fotocatalizador hacia mayores longitudes de onda y 3) presencia de centros de adsorción que aceleran el contacto entre el contaminante y el catalizador. Este cambio en la velocidad de

degradación de los contaminantes en presencia del material de carbono se ha descrito en la literatura como un efecto sinérgico entre el  $\text{TiO}_2$  y el material carbonoso para la degradación de compuestos aromáticos (Cordero et al., 2007; Matos et al., 1998; Xue et al., 2011).

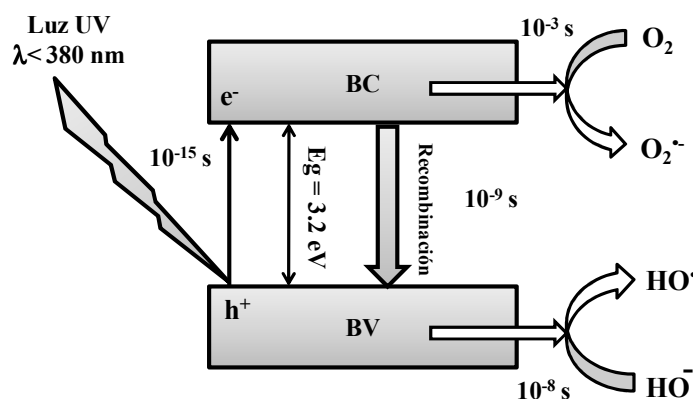


**Figura 4.** Activación del  $\text{TiO}_2$  mediante luz UV

### 2.2.3. Procesos avanzados de oxidación basados en la radiación gamma

La eliminación de contaminantes del agua mediante radiólisis se basa en la generación de radicales, electrones altamente reactivos, iones y moléculas neutras, por exposición del agua a radiaciones electromagnéticas de alta energía (Arslan-Alaton and Gurses, 2004; Buens and Sims, 1981; Ferradini, 1961). Para ello, se suelen utilizar rayos X o radiación gamma emitida por fuentes radiactivas de  $^{60}\text{Co}$  ( $t_{1/2} = 5,271$  años,  $E_\gamma = 1,173$  y  $1,332 \text{ MeV}$ ) y  $^{137}\text{Cs}$  ( $t_{1/2} = 30,170$  años,  $E_\gamma = 0,661 \text{ MeV}$ ), o bien aceleradores lineales de electrones.

Al irradiar el agua con radiaciones ionizantes, éstas van perdiendo paulatinamente su energía a través de colisiones inelásticas con las moléculas de agua, produciéndose la ionización o excitación de estas moléculas. A través de un complejo mecanismo, se forman especies muy activas como son:  $e_{\text{aq}}^-$ ,  $\text{H}^{\bullet}$  y  $\text{HO}^{\bullet}$ , iones como  $\text{H}_3\text{O}^+$  y moléculas estables como:  $\text{O}_2$ ,  $\text{H}_2$ ,  $\text{H}_2\text{O}_2$ , (Figura 5). Todas estas especies químicas son productos radiolíticos primarios que van a ser los que, posteriormente, originen modificaciones en las moléculas de contaminante y den lugar a su degradación. Por lo tanto, el proceso de

degradación o mineralización de los microcontaminantes presentes en el agua costa de las siguientes etapas:

- Formación de radicales libres activos (sucede en tiempos del orden de  $10^{-10}$  s).
- Difusión de los radicales (tiempo del orden de  $10^{-3}$  s).
- Reacciones inducidas entre los productos radiolíticos primarios y las moléculas de contaminante.

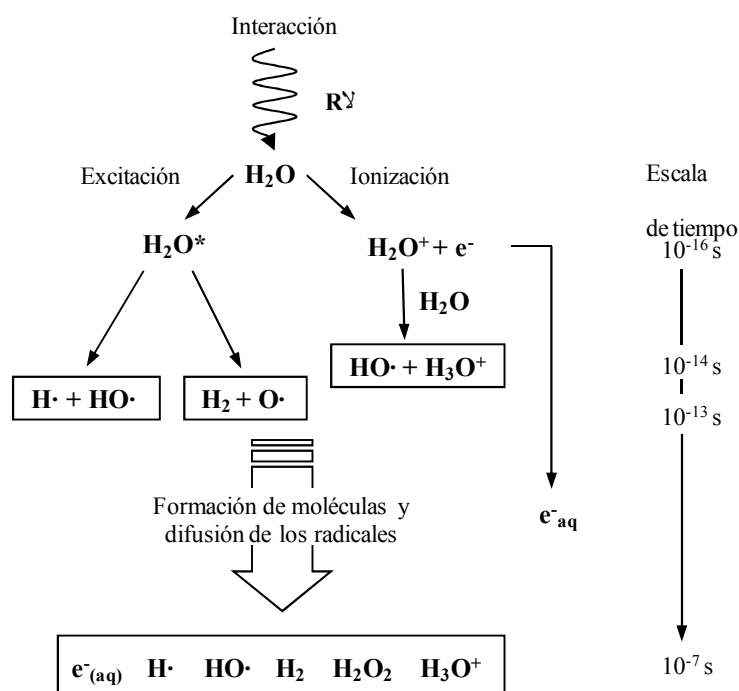


**Figura 5.** Especies generadas en la radiólisis del agua pura a pH neutro.

Los procesos químicos involucrados en la radiólisis del agua por radiaciones ionizantes han sido estudiados y documentados con el fin de que este tratamiento pueda ser utilizado eficazmente en el tratamiento de aguas (Getoff, 1996). La radiólisis del agua también ha sido ampliamente estudiada para conocer los efectos biológicos producidos por las radiaciones ionizantes sobre los seres vivos (Woods and Pikaev, 1994), ya que la molécula de agua es la más abundante en el cuerpo humano, del orden del 65% del peso de un adulto, y, por lo tanto, la que presenta una mayor probabilidad de interacción con la citada radiación gamma.

Estos procesos, basados en radiaciones electromagnéticas de alta energía, resultan más económicos y eficientes a gran escala que otros procesos usados para la eliminación de microcontaminantes persistentes de las aguas (Bolton et al., 1998; Choppin et al., 2002; Woods and Pikaev, 1994). A diferencia de las radiaciones UV, en las que parte de los fotones son absorbidos por el contaminante, la radiación gamma presenta una gran probabilidad de que su energía sea absorbida por las moléculas de agua, produciendo la radiólisis de la misma y generando las especies mencionadas anteriormente (Figura 5).

De las especies primarias originadas por la interacción de la radiación gamma con las moléculas de agua,  $e_{aq}^-$ ,  $H^\bullet$  y  $HO^\bullet$ , las dos primeras actúan como fuertes agentes reductores y el radical hidroxilo, como oxidante fuerte. Por esta razón, algunos autores se refieren a estos tratamientos como Procesos Avanzados de Oxidación/Reducción (PAO/Rs) (Kurucz et al., 1995). En la Tabla 2 se muestra una estimación de la concentración de las especies reactivas más importantes que se generan durante la radiólisis del agua pura en función de la dosis absorbida (Mezyk et al., 2008).

**Tabla 2.** Concentración de especies reactivas generadas en agua pura en función de las dosis habituales de irradiación gamma.

| Dosis absorbida<br>(kGy) | Concentración<br>(mM) |             |              |          |
|--------------------------|-----------------------|-------------|--------------|----------|
|                          | $e_{aq}^-$            | $H^\bullet$ | $HO^\bullet$ | $H_2O_2$ |
| 0.1                      | 0.03                  | 0.01        | 0.03         | 0.01     |
| 0.5                      | 0.14                  | 0.03        | 0.14         | 0.04     |
| 1.0                      | 0.27                  | 0.06        | 0.28         | 0.07     |
| 5.0                      | 1.35                  | 0.30        | 1.40         | 0.35     |
| 10.0                     | 2.70                  | 0.60        | 2.80         | 0.70     |

La gran eficiencia que presenta esta tecnología en la eliminación de microcontaminantes persistentes en las aguas está despertando una especial atención en la aplicación de estos sistemas de tratamiento en la eliminación de una gran variedad de contaminantes (Basfar et al., 2005; Kurucz et al., 1995; Mezyk et al., 2008). El desconocimiento de esta tecnología, de sus rendimientos y de las condiciones de seguridad con las que se



debe trabajar, hace que no esté totalmente difundida (Basfar et al., 2005; Mezyk et al., 2008). Hoy en día existen algunas plantas de tratamiento de aguas en varios países que aplican este sistema, sin embargo, su utilización no está demasiado extendida.

### 2.3. REFERENCIAS

- Aksu Z, Kabasakal E (2004) Batch adsorption of 2,4-dichlorophenoxy-acetic acid (2,4-D) from aqueous solution by granular activated carbon. *Sep Purif Technol* 35:223-240
- Amama PB, Itoh K, Murabayashi M (2002) Gas-phase photocatalytic degradation of trichloroethylene on pretreated TiO<sub>2</sub>. *Appl Catal B: Environ* 37:321-330
- Andreozzi R, Caprio V, Insola A, Marotta R (1999) Advanced oxidation processes (AOP) for water purification and recovery. *Catal Today* 53:51-59
- Antoniadou M, Daskalaki VM, Balis N, Kondarides DI, Kordulis C, Lianos P (2011) Photocatalysis and photoelectrocatalysis using (CdS-ZnS)/TiO<sub>2</sub> combined photocatalysts. *Appl Catal B: Environ* 107:188-196
- Araña J, Pulido Melián E, Rodríguez López VM, Peña Alonso A, Doña Rodríguez JM, González Díaz O, Pérez Peña J (2007) Photocatalytic degradation of phenol and phenolic compounds: Part I. Adsorption and FTIR study. *J Hazard Mater* 146:520-528
- Arslan-Alaton I, Gurses F (2004) Photo-Fenton-like and photo-fenton-like oxidation of Procaine Penicillin G formulation effluent. *J Photochem Photobiol A* 165:165-175
- Ashkarran AA, Afshar SAA, Aghigh SM, kavianipour M (2010) Photocatalytic activity of ZrO<sub>2</sub> nanoparticles prepared by electrical arc discharge method in water. *Polyhedron* 29:1370-1374
- Ayranci E, Bayram E (2005) Adsorption of phthalic acid and its esters onto high-area activated carbon-cloth studied by in situ UV-spectroscopy. *J Hazard Mater* 122:147-153
- Basfar AA, Khan HM, Al-Shahrani AA, Cooper WJ (2005) Radiation induced decomposition of methyl tert-butyl ether in water in presence of chloroform: Kinetic modelling. *Water Res* 39:2085-2095

- Bautista-Toledo MI, Méndez-Díaz JD, Sánchez-Polo M, Rivera-Utrilla J, Ferro-García MA (2008) Adsorption of sodium dodecylbenzenesulfonate on activated carbons: Effects of solution chemistry and presence of bacteria. *J Colloid Interface Sci* 317:11-17
- Bilgili MS (2006) Adsorption of 4-chlorophenol from aqueous solutions by xad-4 resin: Isotherm, kinetic, and thermodynamic analysis. *J Hazard Mater* 137:157-164
- Boehm HP (1966) Chemical Identification of Surface Groups. In: *Advances in Catalysis*. Academic Press, New York:179-274
- Bolton JR, Valladares JE, Zanin JP, Cooper WJ, Nickelsen MG, Kajdi DC, Waite TD, Kurucz CN (1998) Figures-of-Merit for Advanced Oxidation Processes - A Comparison of Homogeneous UV/H<sub>2</sub>O<sub>2</sub>, Heterogeneous TiO<sub>2</sub> and Electron Beam Processes. *J Adv Oxid Technol* 3:174-185
- Brillas E, Mur E, Sauleda R, Sánchez L, Peral J, Domènech X, Casado J (1998) Aniline mineralization by AOP's: anodic oxidation, photocatalysis, electro-Fenton and photoelectro-Fenton processes. *Appl Catal B: Environ* 16:31-42
- Brugnera MF, Rajeshwar K, Cardoso JC, Zanoni MVB (2010) Bisphenol A removal from wastewater using self-organized TiO<sub>2</sub> nanotubular array electrodes. *Chemosphere* 78:569-575
- Burns WG, Sims HE (1981) Effect of Radiation Type in Water Radiolysis. *Journal of the Chemical Society - Faraday Transactions 1: Physical Chemistry in condensed Phases* 77:2803-2813
- Busset C, Mazellier P, Sarakha M, De Laat J (2007) Photochemical generation of carbonate radicals and their reactivity with phenol. *J Photochem Photobiol A* 185:127-132
- Canonica S, Kohn T, Mac M, Real FJ, Wirz J, Gunten UV (2005) Photosensitizer Method to Determine Rate Constants for the Reaction of Carbonate Radical with Organic Compounds. *Environ Sci Technol* 39:9182-9188

- Chen Y, Chen L, Shang N (2009) Photocatalytic degradation of dimethyl phthalate in an aqueous solution with Pt-doped TiO<sub>2</sub>-coated magnetic PMMA microspheres. *J Hazard Mater* 172:20-29
- Choppin GR, Liljenzin JO, Rydberg J (2002) *Radiochemistry and Nuclear Chemistry*, Butterworth-Heinemann
- Cordero T, Duchamp C, Chovelon J, Ferronato C, Matos J (2007) Influence of L-type activated carbons on photocatalytic activity of TiO<sub>2</sub> in 4-chlorophenol photodegradation. *J Photochem Photobiol A* 191:122-131
- Coughlin RW, Ezra FS (1968) Role of Surface Acidity in the Adsorption of Organic Pollutants on the Surface of Carbon. *Environ Sci Technol* 2:291-297
- Criquet J, Leitner NKV (2009) Degradation of acetic acid with sulfate radical generated by persulfate ions photolysis. *Chemosphere* 77:194-200
- Fabish TJ, Schleifer DE (1984) Surface chemistry and the carbon black work function. *Carbon* 22:19-38
- Faisal M, Khan SB, Rahman MM, Jamal A, Akhtar K, Abdullah MM (2011) Role of ZnO-CeO<sub>2</sub> Nanostructures as a Photo-catalyst and Chemi-sensor. *J Mater Sci Technol* 27:594-600
- Ferradini C (1961) Kinetic Behavior of the Radiolysis Products of Water. In: *Advances in Inorganic Chemistry and Radiochemistry*. Academic Press, pp 171-205
- Ferro-García MA, Carrasco-Marín F, Rivera-Utrilla J, Utrera-Hidalgo E, Moreno-Castilla C (1990a) The use of activated carbon columns for the removal of ortho-phosphate ions from aqueous solutions. *Carbon* 28:91-95
- Ferro-García MA, Rivera-Utrilla J, Bautista-Toledo I, Mingorance MD (1990b) Removal of lead from water by activated carbons. *Carbon* 28:545-552
- Figueiredo JL, Pereira MFR, Freitas MMA, Órfão JJM (1999) Modification of the surface chemistry of activated carbons. *Carbon* 37:1379-1389

- Franz M, Arafat HA, Pinto NG (2000) Effect of chemical surface heterogeneity on the adsorption mechanism of dissolved aromatics on activated carbon. *Carbon* 38:1807-1819
- Gao J, Luan X, Wang J, Wang B, Li K, Li Y, Kang P, Han G (2011) Preparation of  $\text{Er}^{3+}:\text{YAlO}_3/\text{Fe}$ -doped  $\text{TiO}_2\text{-ZnO}$  and its application in photocatalytic degradation of dyes under solar light irradiation. *Desalination* 268:68-75
- Garten VA, Weiss DE (1957) Ion and Electron-Exchange Properties of Activated Carbon in Relation to its Behaviour as a Catalyst and Adsorbent. *Rev Pure Appl Chem* 7:69-122
- Getoff N (1996) Radiation-induced degradation of water pollutants-state of the art. *Radiat Phys Chem* 47:581-593
- Glaze WH, Kang J, Chapin DH (1987) Chemistry of Water Treatment Processes Involving Ozone, Hydrogen Peroxide and Ultraviolet Radiation. *Ozone-Sci Eng* 9:335-352
- Gregg SJ, Sing KSW (1982) Adsorption, Surface Area and Porosity. A Academic Press, London
- Hameed BH, Salman JM, Ahmad AL (2009) Adsorption isotherm and kinetic modeling of 2,4-D pesticide on activated carbon derived from date stones. *J Hazard Mater* 163:121-126
- Ito T, Morimoto S, Fujita S, Nishimoto S (2009) Radical intermediates generated in the reactions of l-arginine with hydroxyl radical and sulfate radical anion: A pulse radiolysis study. *Radiat Phys Chem* 78:256-260
- Kari FG, Hilger S, Canonica S (1995) Determination of the Reaction Quantum Yield for the Photochemical Degradation of Fe(III) - EDTA: Implications for the Environmental Fate of EDTA in Surface Waters. *Environ Sci Technol* 29:1008-1017

- Khataee AR, Mirzajani O (2010) UV/peroxydisulfate oxidation of C. I. Basic Blue 3: Modeling of key factors by artificial neural network. *Desalination* 251:64-69
- Kim SK, Chang H, Cho K, Kil DS, Cho SW, Jang HD, Choi J, Choi J (2011) Enhanced photocatalytic property of nanoporous TiO<sub>2</sub>/SiO<sub>2</sub> micro-particles prepared by aerosol assisted co-assembly of nanoparticles. *Mater Lett* 65:3330-3332
- Kurucz CN, Waite TD, Cooper WJ (1995) The Miami Electron Beam Research Facility: a large scale wastewater treatment application. *Radiat Phys Chem* 45:299-308
- Leon y leon CA, Radovic LR (2010) Interfacial Chemistry and Electrochemistry of Carbon Surfaces. *Chemistry and Physics of Carbon* 24:213-310
- Leon y Leon CA, Solar JM, Calemma V, Radovic LR (1992) Evidence for the protonation of basal plane sites on carbon. *Carbon* 30:797-811
- Leyva Ramos R, Bernal Jacome LA, Mendoza Barron J, Fuentes Rubio L, Guerrero Coronado RM (2002) Adsorption of zinc(II) from an aqueous solution onto activated carbon. *J Hazard Mater* 90:27-38
- Lim YN, Shaaban MG, Yin CY (2009) Treatment of landfill leachate using palm shell-activated carbon column: Axial dispersion modeling and treatment profile. *Chem Eng J* 146:86-89
- Liu G, Ma J, Li X, Qin Q (2009) Adsorption of bisphenol A from aqueous solution onto activated carbons with different modification treatments. *J Hazard Mater* 164:1275-1280
- Matos J, Laine J, Herrmann J (1998) Synergy effect in the photocatalytic degradation of phenol on a suspended mixture of titania and activated carbon. *Appl Catal B: Environ* 18:281-291
- Mattson JA, Mark Jr. HB, Malbin MD, Weber Jr. WJ, Crittenden JC (1969) Surface chemistry of active carbon: Specific adsorption of phenols. *J Colloid Interface Sci* 31:116-130

- Mezyk SP, Peller JR, Cole SK, Song W, Mincher BJ, Peake BM, Cooper WJ (2008) Studies in Radiation Chemistry: Application to Ozonation and Other Advanced Oxidation Processes. *Ozone-Sci Eng* 30:58-64
- Montes-Morán MA, Menéndez JA, Fuente E, Suárez D (1998) Contribution of the Basal Planes to Carbon Basicity: An Ab Initio Study of the  $\text{H}_3\text{O}^+$ - $\pi$  Interaction in Cluster Models. *J Phys Chem B* 102:5595-5601
- Mora VC, Rosso JA, Carrillo Le Roux G, Mártire DO, Gonzalez MC (2009) Thermally activated peroxydisulfate in the presence of additives: A clean method for the degradation of pollutants. *Chemosphere* 75:1405-1409
- Moreno-Castilla C, Rivera-Utrilla J, López-Ramón MV, Carrasco-Marín F (1995) Adsorption of some substituted phenols on activated carbons from a bituminous coal. *Carbon* 33:845-851
- Moreno-Castilla C (2004) Adsorption of organic molecules from aqueous solutions on carbon materials. *Carbon* 42:83-94
- Ohno T, Tanigawa F, Fujihara K, Izumi S, Matsumura M (1998) Photocatalytic oxidation of water on  $\text{TiO}_2$ -coated  $\text{WO}_3$  particles by visible light using Iron(III) ions as electron acceptor. *J Photochem Photobiol A* 118:41-44
- Papirer E, Li S, Donnet J (1987) Contribution to the study of basic surface groups on carbons. *Carbon* 25:243-247
- Radovic LR, Moreno-Castilla C, Rivera-Utrilla J (2001) Carbon materials as adsorbents in aqueous solutions. *Chem Phys Carbon* 27:227-405
- Radovic LR, Silva IF, Ume JI, Menéndez JA, Leon CALY, Scaroni AW (1997) An experimental and theoretical study of the adsorption of aromatics possessing electron-withdrawing and electron-donating functional groups by chemically modified activated carbons. *Carbon* 35:1339-1348

- Rodriguez-Reinoso F, Linares-Solano A (2011) A. Linares-Solano. Microporous Structure of Activated Carbons as Revealed by Adsorption Methods. *Chem Phys Carbon* 21:36-56
- Rivera-Utrilla J, Prados-Joya G, Sánchez-Polo M, Ferro-García MA, Bautista-Toledo I (2009) Removal of nitroimidazole antibiotics from aqueous solution by adsorption/bioadsorption on activated carbon. *J Hazard Mater* 170:298-305
- Salari D, Niaei A, Aber S, Rasoulifard MH (2012) The photooxidative destruction of C.I. Basic Yellow 2 using UV/S<sub>2</sub>O<sub>8</sub><sup>2-</sup> process in a rectangular continuous photoreactor. *J Hazard Mater* 166:61-66
- Stoeckli HF (1990) Microporous carbons and their characterization: The present state of the art. *Carbon* 28:1-6
- Sun W, Zhang S, Liu Z, Wang C, Mao Z (2008) Studies on the enhanced photocatalytic hydrogen evolution over Pt/PEG-modified TiO<sub>2</sub> photocatalysts. *Int J Hydrogen Energy* 33:1112-1117
- Voll M, Boehm HP (1971) Basische Oberflächenoxide auf Kohlenstoff—IV. Chemische Reaktionen zur Identifizierung der Oberflächengruppen. *Carbon* 9:481-488
- Woods RJ, Pikaev AK (1994) *Applied Radiation Chemistry: Radiation Processing*, Wiley, New York
- Wu C, Linden KG (2010) Phototransformation of selected organophosphorus pesticides: Roles of hydroxyl and carbonate radicals. *Water Res* 44:3585-3594
- Xu R, Wang Y, Tiwari D, Wang H (2009) Effect of ionic strength on adsorption of As(III) and As(V) on variable charge soils. *J Environ Sci* 21:927-932
- Xue G, Liu H, Chen Q, Hills C, Tyrer M, Innocent F (2011) Synergy between surface adsorption and photocatalysis during degradation of humic acid on TiO<sub>2</sub>/activated carbon composites. *J Hazard Mater* 186:765-772





### **3. OBJETIVOS DEL TRABAJO DESARROLLADO EN LA PRESENTE TESIS DOCTORAL**

A la vista de la revisión bibliográfica llevada a cabo acerca de la repercusión medioambiental de los contaminantes procedentes de los lixiviados en las aguas y de las tecnologías usadas para el tratamiento de las mismas, el objetivo general de esta Tesis Doctoral es estudiar la eliminación de estos contaminantes del agua mediante procesos de adsorción/bioadsorción en carbones activados comerciales, así como usando diferentes procesos avanzados de oxidación basados en el uso de radiación ultravioleta y radiación gamma. Los contaminantes seleccionados para este estudio son cinco: tres compuestos usados en la industria del plástico (ácido ftálico, bisfenol A y ácido difenólico) y dos usados como herbicidas (ácido 2,4-diclorofenoxiacético y ácido 4-cloro-2-metilfenoxiacético). Así, los objetivos específicos que se pretenden alcanzar son:

1. Estudiar los procesos de adsorción de los contaminantes mediante el uso de carbones activados.

Se analizará la viabilidad de los carbones activados como adsorbentes de los contaminantes seleccionados en aguas de diferente procedencia y composición química (ultrapura, superficial, subterránea y residual urbana). Para ello, los procesos de adsorción se llevarán a cabo tanto en régimen estático como en dinámico, determinando la capacidad de adsorción de los carbones. Se estudiará la influencia de las variables operacionales, cinética del proceso y mecanismos difusionales que controlan estos procesos de adsorción. Se analizarán los procesos de bioadsorción de los contaminantes, mediante el uso simultáneo de carbón activado y bacterias. Las bacterias que se van a utilizar en este estudio son las que se encuentran en los fangos activos procedentes del tratamiento secundario de una planta de depuración de aguas residuales. Al comparar los resultados obtenidos en la adsorción de los contaminantes sobre el carbón activado en presencia de bacterias con los correspondientes al proceso llevado a cabo en ausencia de bacterias, se podrá determinar el papel desempeñado por estas bacterias en la depuración del agua mediante estos sistemas.

2. Analizar los procesos de degradación de los contaminantes de las aguas por fotooxidación directa e indirecta utilizando lámparas de radiación UV de media y baja presión.

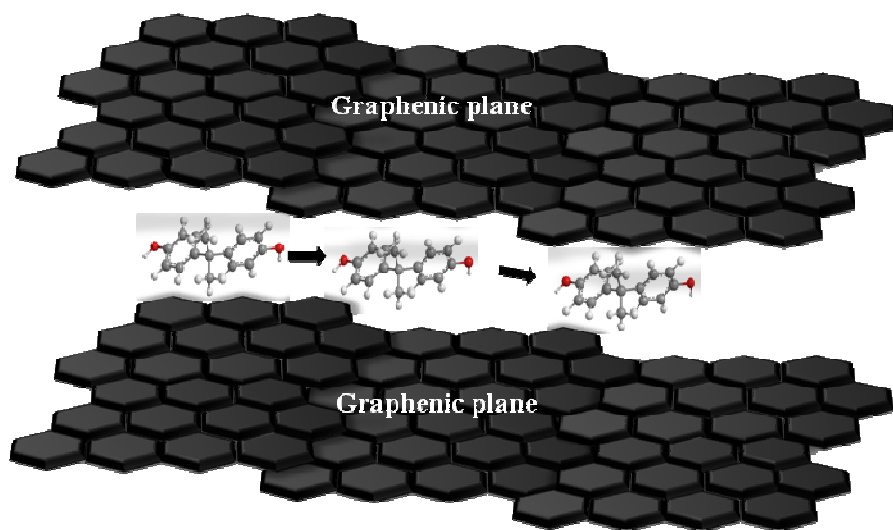
La fotooxidación de los contaminantes se estudiará usando radiación UV y evaluando la influencia de las variables operacionales, la cinética de los procesos y la influencia de la composición química del agua. Con objeto de incrementar la velocidad de degradación de los contaminantes, se analizará el efecto que produce la presencia de compuestos fotosensibles en el medio. Además, se comparará la eficiencia de los radicales  $\text{HO}^\bullet$ ,  $\text{SO}_4^{\bullet-}$  y  $\text{CO}_3^{\bullet-}/\text{HCO}_3^\bullet$  para eliminar los contaminantes de los sistemas acuosos. Un apartado muy importante lo constituirá el estudio de la eficacia del sistema integrado por radiación UV/ $\text{TiO}_2$ /carbón activado en la degradación de los contaminantes, donde se analizará el papel que juega el carbón y la influencia de sus características químicas y texturales en el rendimiento del proceso de fotodegradación.

3. Estudiar la radiólisis de las aguas contaminadas con los mencionados contaminantes usando radiación gamma y analizando los procesos de degradación de estos compuestos

Se analizarán las posibilidades que presenta este proceso avanzado de oxidación/reducción para eliminar dichos compuestos de aguas de diferente naturaleza. En este apartado se estudiarán: la cinética de descomposición de los contaminantes, la influencia de las distintas variables operacionales, los mecanismos de reacción, el efecto de la presencia de aniones inorgánicos en el medio y la aplicación de este sistema de tratamiento en aguas potables y residuales.

## CAPÍTULO 2

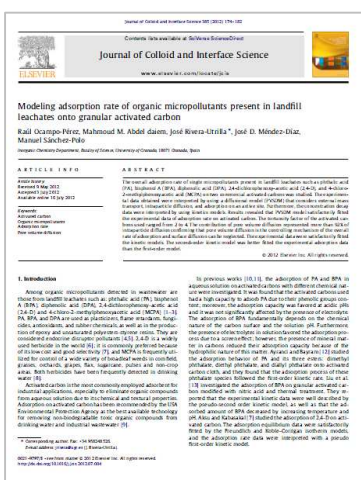
# MODELADO DE LA VELOCIDAD DE ADSORCIÓN DE MICROCONTAMINANTES ORGÁNICOS PRESENTES EN LOS LIXIVIADOS DE VERTEDEROS SOBRE CARBÓN ACTIVADO GRANULAR





# MODELING ADSORPTION RATE OF ORGANIC MICROPOLLUTANTS PRESENT IN LANDFILL LEACHATES ONTO GRANULAR ACTIVATED CARBON

Article published in Journal of Colloid and Interface Science 385, 174-182 (2012)



## Highlights

- The PVSDM model fitted the adsorption of pollutants from landfill leachates on activated carbon.
- The tortuosity factor of the activated carbons used ranged from 2 to 4.
- Pore volume diffusion is the controlling mechanism of the overall rate of adsorption
- Surface diffusion can be neglected.
- The external mass transport did not affect the overall adsorption rate.

## ABSTRACT

The overall adsorption rate of single micropollutants present in landfill leachates such as phthalic acid (PA), bisphenol A (BPA), diphenolic acid (DPA), 2, 4-dichlorophenoxy-acetic acid (2,4-D), and 4-chloro-2-methylphenoxyacetic acid (MCPA) on two commercial activated carbons was studied. The experimental data obtained were interpreted by using a diffusional model (PVSDM) that considers external mass transport, intraparticle diffusion, and adsorption on an active site. Furthermore, the concentration decay data were interpreted by using kinetics models. Results revealed that PVSDM model satisfactorily fitted the experimental data of adsorption rate on activated carbon. The tortuosity factor of the activated carbons used ranged from 2 to 4. The contribution of pore volume diffusion represented more than 92% of intraparticle diffusion confirming that pore volume diffusion is the controlling mechanism of the overall rate of adsorption and surface diffusion can be neglected. The experimental data were satisfactorily fitted the kinetic models. The second-order kinetic model was better fitted the experimental adsorption data than the first-order model.



**ABBREVIATIONS**

|                                  |  |
|----------------------------------|--|
| a                                | Prausnitz-Radke isotherm constant, L/g.  |
| b                                | Prausnitz-Radke isotherm constant, L <sup>β</sup> /mmol <sup>β</sup> .                           |
| C <sub>A</sub>                   | Concentration of adsorbate in aqueous solution, mg/L.  |
| C <sub>A0</sub>                  | Initial concentration of adsorbate in aqueous solution, mg/L.                                    |
| C <sub>Ar</sub>                  | Concentration of adsorbate within the particle at distance r, mg/L.                              |
| C <sub>Ar</sub>   <sub>r=R</sub> | Concentration of adsorbate at the external surface of the particle at r = R <sub>p</sub> , mg/L. |
| C <sub>Ae</sub>                  | Concentration of adsorbate at equilibrium, mg/L.   |
| D <sub>AB</sub>                  | Molecular diffusion coefficient at infinite dilution, cm <sup>2</sup> /s.                        |
| D <sub>ep</sub>                  | Effective pore volume diffusion coefficient, cm <sup>2</sup> /s.                                 |
| D <sub>s</sub>                   | Surface diffusion coefficient, cm <sup>2</sup> /s.   |
| k <sub>1</sub>                   | Rate constant of the first-order kinetic model, 1/h.   |
| k <sub>2</sub>                   | Rate constant of the second-order kinetic model, g/mg/h.   |
| k <sub>L, exp</sub>              | Experimental external mass transfer coefficient in liquid phase, cm/s.                           |
| m                                | Mass of adsorbent, g.  |
| M <sub>B</sub>                   | Molecular weight of water, g/mol.  |
| N <sub>AP</sub>                  | Mass transport due to pore volume diffusion, mg/cm <sup>2</sup> /s.                              |
| N <sub>AS</sub>                  | Mass transport due to surface diffusion, mg/cm <sup>2</sup> /s..                                 |
| q                                | Mass of adsorbate adsorbed, mg/g or mmol/g.  |
| q <sub>exp</sub>                 | Experimental mass of adsorbate adsorbed, mg/g or mmol/g.   |
| q <sub>pred,1</sub>              | Mass of adsorbate adsorbed predicted from the first-order kinetic model, mg/g.                   |
| q <sub>pred,2</sub>              | Mass of adsorbate adsorbed predicted from the second-order kinetic model, mg/g.                  |
| r                                | Distance in radial direction of the particle, cm.  |
| R <sub>p</sub>                   | Radius of the particle, cm.  |
| S                                | External surface area per mass of adsorbent, m <sup>2</sup> /g.                                  |
| T                                | Temperature, K.  |
| t                                | Time, min.   |
| V                                | Volume of the solution, mL.  |



## Greek symbols

|                      |   |
|----------------------|---|
| $\beta$              | Prausnitz-Radke isotherm constant.  |
| $\varepsilon_p$      | Void fraction of particles.   |
| $\eta_b$             | Viscosity of water, cp.   |
| $\rho_p$             | Density of adsorbent particles, g/mL.   |
| $\tau$               | Tortuosity factor.  |
| $\phi$               | Association parameter of water.   |
| $\phi_A$             | Dimensionless concentration of adsorbate in the solution.                                       |
| $\phi_{\text{exp}}$  | Experimental dimensionless concentration of adsorbate in the solution.                          |
| $\phi_{\text{pred}}$ | Dimensionless concentration of adsorbate in the solution predicted with the diffusional models. |

## 1. INTRODUCTION

Among organic micropollutants detected in wastewater are those from landfill leachates such as: phthalic acid (PA), bisphenol A (BPA), diphenolic acid (DPA), 2, 4-dichlorophenoxyacetic acid (2,4-D) and 4-chloro-2-methylphenoxyacetic acid (MCPA) [1-3]. PA, BPA, and DPA are used as plasticizers, flame retardants, fungicides, antioxidants, and rubber chemicals, as well as in the production of epoxy and unsaturated polyesters-styrene resins. They are considered endocrine disruptor pollutants [4,5]. 2,4-D is a widely used herbicide in the world [6]; it is commonly preferred because of its low cost and good selectivity [7], and MCPA is frequently utilized for control of a wide variety of broadleaf weeds in cornfield, grasses, orchards, grapes, flax, sugarcane, pulses and non-crop areas. Both herbicides have been frequently detected in drinking water [8].

Activated carbon is the most commonly employed adsorbent for industrial applications, especially to eliminate organic compounds from aqueous solution due to its chemical and textural properties. Adsorption on activated carbon has been recommended by the USA Environmental Protection Agency as the best available technology for removing non-biodegradable toxic organic compounds from drinking water and industrial wastewater [9].

In previous works [10,11], the adsorption of PA and BPA in aqueous solution on activated carbons with different chemical nature were investigated. It was found that the activated carbons used had a high capacity to adsorb PA due to their phenolic groups content; moreover, the adsorption capacity was favored at acidic pHs and it was not significantly affected by the presence of electrolyte. The adsorption of BPA fundamentally depends on the chemical nature of the carbon surface and the solution pH. Furthermore, the presence of electrolytes in solution favored the adsorption process due to a screen effect; however, the presence of mineral matter in carbons reduced their adsorption capacity because of the hydrophilic nature of this matter. Ayrançi and Bayram [12] studied the adsorption behavior of PA and its three esters: dimethyl phthalate, diethyl phthalate, and diallyl phthalate onto activated carbon cloth, and they

found that the adsorption process of these phthalate species followed the first-order kinetic rate. Liu et al. [13] investigated the adsorption of BPA on granular activated carbon modified with nitric acid and thermal treatment. They reported that the experimental kinetic data were well described by the pseudo-second order kinetic model, as well as that the adsorbed amount of BPA decreased by increasing temperature and pH. Aksu and Kabasakal [7] studied the adsorption of 2,4-D on activated carbon. The adsorption equilibrium data were satisfactorily fitted by the Freundlich and Koble-Corrigan isotherm models, and the adsorption rate data were interpreted with a pseudo first-order kinetic model.

One of the most important aspects of the adsorption processes from the point of view of treatment plant design is the adsorption kinetics. However, in general, the studies about the adsorption of the above pollutants on activated carbon have not been focused both on the overall adsorption rate and the mass transport mechanisms controlling these adsorption processes. Thus, the main objective of the present work was to study the overall adsorption rate of these single micropollutants (PA, BPA, DPA, 2,4-D, and MCPA) onto granular activated carbon by using diffusional and kinetic models. Moreover, the mechanism of mass transport controlling the overall rate of adsorption was also analyzed.

## **2. DIFFUSIONAL AND KINETIC MODELS**

### **2.1. Diffusional model**

It is well documented that the overall rate of adsorption on a porous solid includes the following three simultaneous steps: external mass transport, intraparticle diffusion, and adsorption on an active site; intraparticle diffusion may be due to pore volume diffusion, surface diffusion, or a combination of both mechanisms [14-16].

In this work, the diffusional model was derived by assuming the following: i) intraparticle diffusion occurs by pore volume diffusion (Fick diffusion) and surface diffusion, ii) the rate of adsorption on an active site is instantaneous, and iii) granular

activated carbon particles are spherical. Model equations and initial and boundary conditions are [14-16]:

$$V \frac{dC_A}{dt} = -mS k_{L,\text{exp}} (C_A - C_{Ar}|_{r=R_p}) \quad (1)$$

$$t = 0, \quad C_A = C_{A0} \quad (2)$$

$$\varepsilon_p \frac{\partial C_{Ar}}{\partial t} + \rho_p \frac{\partial q}{\partial t} = \frac{1}{r^2} \frac{\partial}{\partial r} \left[ r^2 \left( D_{ep} \frac{\partial C_{Ar}}{\partial r} + D_s \rho_p \frac{\partial q}{\partial r} \right) \right] \quad (3)$$

$$C_{Ar} = 0, \quad t = 0, \quad 0 \leq r \leq R_p \quad (4)$$

$$\left. \frac{\partial C_{Ar}}{\partial r} \right|_{r=0} = 0 \quad (5)$$

$$D_{ep} \left. \frac{\partial C_{Ar}}{\partial r} \right|_{r=R} + D_s \rho_p \left. \frac{\partial q}{\partial r} \right|_{r=R} = k_{L,\text{exp}} (C_A - C_{Ar}|_{r=R_p}) \quad (6)$$

The model represented by equations (1)-(6) is the general diffusional model (PVSDM). The parameters  $k_{L,\text{exp}}$ ,  $D_s$ , and  $D_{ep}$  correspond to experiment external transport coefficient, surface diffusion coefficient, and effective diffusion coefficient in the pore volume, respectively. The general model may be simplified in the pore volume diffusion model (PVDM) by assuming that the molecular diffusion in the pore volume is the only intraparticle diffusion mechanism ( $D_{ep} \neq 0$ ,  $D_s = 0$ ), or in the surface diffusion model (SDM) considering that the intraparticle diffusion is exclusively due to the surface diffusion ( $D_{ep} = 0$ ,  $D_s \neq 0$ ).

The coupled partial and ordinary differential equations of the three diffusional models were numerically solved using the program PDESOL v2, which is based on the numerical method of lines [17].

## 2.2. Kinetics models

Several kinetic models have been reported in the literature to interpret the overall adsorption rate of a pollutant on a porous solid adsorbent [18]. In the kinetic models, it is normally assumed that the overall rate of adsorption is exclusively controlled by the adsorption rate of the adsorbate on the surface of adsorbent, and both intraparticle

diffusion and external mass transport can be neglected. Moreover, it is considered that the adsorption rate of the adsorbate on the adsorbent surface can be represented in the same manner as the rate of chemical reactions. The adsorption kinetics is commonly modeled with the first- and second-order kinetic equations.

The first-order kinetic model can be represented by the following equation:

$$\frac{dq}{dt} = k_1 (q_{\text{pred},1} - q) \quad (7)$$

This equation can be integrated using the boundary conditions,  $t = 0$  to  $t$  and  $q = 0$  to  $q_{\text{pred},1}$  and the following equation is obtained:

$$q = q_{\text{pred},1} (1 - e^{-k_1 t}) \quad (8)$$

The second-order kinetic model can be represented by the following equation:

$$\frac{dq}{dt} = k_2 (q_{\text{pred},2} - q)^2 \quad (9)$$

The integration of equation (9), and using the initial conditions,  $t = 0$  to  $t$  and  $q = 0$  to  $q_{\text{pred},2}$ , one can obtain the following equation:

$$q = \frac{q_{\text{pred},2}^2 k_2 t}{1 + q_{\text{pred},2} k_2 t} \quad (10)$$

### 3. EXPERIMENTAL

#### 3.1. Reagents

All chemical reagents used in this study (phthalic acid, bisphenol A, diphenolic acid, 2,4- dichlorophenoxy-acetic acid, and 4-chloro-2-methylphenoxyacetic acid) were high-

purity analytical grade reagents supplied by Sigma-Aldrich. All solutions were prepared with ultrapure water obtained from Milli-Q<sup>®</sup> equipment (Millipore).

Table 1 shows the chemical structure of the pollutants studied, their dimensions (determined by using Chemoffice software, Chem3D Ultra 9.0), and other physicochemical characteristics which were obtained from the ChemIDplus Advanced database.

### 3.2. Activated carbons

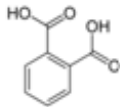
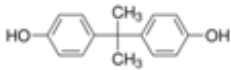
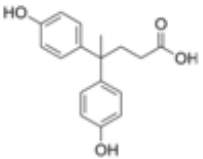
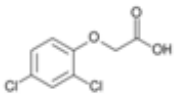
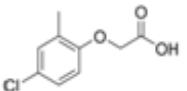
Two commercial activated carbons, Sorbo Norit (S) and Ceca AC40 (C), were used as adsorbents. The activated carbon particle size was 0.45-1.00 mm. These carbon samples were chemically and texturally characterized, determining their surface area, pore volume accessible to water, pore size distribution, elemental analysis, ash content, oxygen surface groups, and pH of the point of zero charge. Detailed descriptions of the techniques and methods used for this characterization were previously reported [19-21].

The hydrophobicity of the activated carbons was determined by measuring immersion enthalpies in benzene,  $\Delta H_i(\text{C}_6\text{H}_6)$ , and water,  $\Delta H_i(\text{H}_2\text{O})$ , using a SETARAM C80 calorimeter. For this purpose, 0.10 g of activated carbon was degasified in a glass capsule at a pressure of  $10^{-5}$  mbar and temperature of 383 K for 12 h. The sample was then left to stabilize in the calorimeter for 3 h at 303 K before the experiment.

### 3.3. Adsorption isotherms

In order to apply the diffusional model, the corresponding adsorption isotherms were obtained. Solutions containing different concentrations (50, 100, 200, 300, 400, and 500 mg/L) of PA, BPA, DPA, 2,4-D or MCPA and 0.1 g of activated carbon samples (S or C) were introduced into a 100 mL Erlenmeyer flask. The flasks were capped with a rubber stopper to avoid evaporation. Subsequently, the flasks were partially submerged into a constant temperature water bath (298 K) and continuously stirred with a mixing shaking. Adsorption equilibrium was attained when the concentration of two consecutive samples did not change. The amount of contaminant adsorbed was calculated performing a mass balance.

**Table 1.** Physico-chemical properties of the contaminants used.

| Pollutant | Molecular Weight (g/mol) | Molecular Size (x, y, z) (nm) | Molecular formula  | $V_A^a)$ (cm <sup>3</sup> /mol) | Solubility in water (g/L) | log $K_{ow}^b)$ | $pK_{a1}^c)$ | $pK_{a2}^d)$ | $pK_{a3}^e)$ |
|-----------|--------------------------|-------------------------------|--|---------------------------------|---------------------------|-----------------|--------------|--------------|--------------|
| PA        | 166.13                   | 0.89 × 0.89 × 0.34            |    | 114                             | 12.50                     | 1.15            | 2.90         | 5.40         | --           |
| BPA       | 228.29                   | 1.27 × 0.86 × 0.68            |    | 294                             | 0.09                      | 4.15            | 9.59         | 11.30        | --           |
| DPA       | 286.33                   | 1.27 × 1.23 × 0.96            |    | 315                             | 0.40                      | 3.58            | 4.66         | 9.70         | 10.45        |
| 2,4-D     | 221.00                   | 1.29 × 0.73 × 0.42            |   | 182                             | 2.16                      | 2.69            | 2.98         | --           | --           |
| MCPA      | 200.62                   | 1.24 × 0.84 × 0.42            |  | 185                             | 1.38                      | 2.22            | 3.14         | --           | --           |

a) Liquid molar volume at the normal boiling point.

b) Log octanol-water partition coefficient.

c, d, e) pKa corresponding to the successive deprotonations.

The concentrations of PA, BPA, DPA, 2,4-D or MCPA in aqueous solution were determined by UV-visible spectrophotometer, Genesys 5, at a wavelengths of  $\lambda_{\text{PA}}=231\text{nm}$ ,  $\lambda_{\text{BPA}}=276\text{ nm}$ ,  $\lambda_{\text{DPA}}=276\text{ nm}$ ,  $\lambda_{2,4\text{-D}}=284\text{ nm}$ ,  $\lambda_{\text{MCPA}}=279\text{ nm}$  and at a solution pH of 7.

### 3.4. Adsorption kinetics

The concentration decay data for the adsorption of these pollutants on the activated carbon samples (S and C) were obtained by placing 25, 50, or 100 mg of activated carbon in 100 mL Erlenmeyer flasks containing around 100 mg/L of the target pollutant. These flasks were kept in a thermostatic mechanical shaker batch operating at a constant agitation speed (135 rpm), temperature of 298 K, and a solution pH of 3 (PA), 5 (BPA), 5 (DPA), 3 (2,4-D), and 3 (MCPA) (no solution buffer added). At different periods of time, samples were taken to determine the pollutant concentration. Kinetics experiments showed that the required period of time to reach the equilibrium was 7 days for PA, BPA, and DPA and 5 days for 2,4-D and MCPA.

## 4. RESULTS AND DISCUSSION

### 4.1. Characterization of activated carbons

Table 2 shows the textural characteristics of the two activated carbons used in this study. Both had a large surface area ( $>1200\text{ m}^2/\text{g}$ ) and a highly developed porosity, with a very large volume of pores accessible to water ( $>0.80\text{ cm}^3/\text{g}$ ). Pore size distribution of carbons is important for adsorption of a given compound in aqueous solution, because pores that are not accessible to water will not be effective in the adsorption process. The external surface area (corresponding to pores with diameter  $> 6.6\text{ nm}$ ) was larger for carbon S ( $46.90\text{ m}^2/\text{g}$ ) than for carbon C ( $21.30\text{ m}^2/\text{g}$ ).

Micropore volumes ( $W_0$ ) obtained by  $\text{N}_2$  adsorption were  $0.391\text{ cm}^3/\text{g}$  (carbon S), and  $0.406\text{ cm}^3/\text{g}$  (carbon C), both were considerably higher than those determined by  $\text{CO}_2$  adsorption (Table 2). The  $W_0(\text{N}_2)/W_0(\text{CO}_2)$  ratio was higher for carbon C (1.60) than for carbon S (1.40), with both values indicating a very heterogeneous micropore distribution, because  $\text{CO}_2$  is only adsorbed in smaller micropores (ultramicropores),



whereas  $N_2$  is adsorbed on the surface of all micropores [22,23]; therefore,  $N_2$  adsorption data give the total micropore volume,  $W_o(N_2)$ ; thus, the mean micropore size ( $L_o$ ) was higher when determined by  $N_2$  adsorption (Table 2).

Table 3 lists the chemical characteristics of the activated carbons. The pH of point of zero charge was 9.0 for carbon S and 6.0 for carbon C, which means that carbon C has a chemical nature more acidic than carbon S, which is due to the higher concentration of carboxyl, lactone and phenol groups of carbon C. The ash content was lower than 8.5% in both activated carbons.

Table 4 shows the water and benzene immersion calorimetry results for the activated carbon samples. Adsorption enthalpy values determined by immersion calorimetry of an activated carbon in water depend on: the interactions with polar sites (acidic or basic), the micropore filling, and the external surface wetting. Hence, the first of these three processes is specific and corresponds to relatively high energies, whereas the other two are due to lower energy non-specific interactions [24,25]. Because of this specific interaction, a relationship can be established between the water immersion enthalpy and surface oxygen content of different carbons [26,27]. Thus, carbon C, with its higher oxygen and ash contents, shows a greater water immersion enthalpy when water adsorption heat is expressed per gram of carbon (Table 4). Furthermore, the adsorption enthalpy of the non-polar benzene molecule,  $\Delta H_i(C_6H_6)$ , is less dependent on the chemical nature of carbon surface than on the distribution of its porosity [24,25]. Thus, in the present study, the data obtained from calorimetry with benzene showed an inverse relationship with mean  $L_o(N_2)$  and  $L_o(CO_2)$  micropore size (Table 2).

Given the polar nature of the water molecule and non-polar nature of benzene, the relative hydrophobicity of carbon can be determined by means of the hydrophobicity coefficient (HC) given by Equation (11).

**Table 2.** Textural characteristics of activated carbons.

| Activated Carbon | $S_{N_2}^a)$<br>( $m^2/g$ ) | $S_{ext}^b)$<br>( $m^2/g$ ) | $V_2^c)$<br>( $cm^3/g$ ) | $V_3^d)$<br>( $cm^3/g$ ) | $V_{H_2O}^e)$<br>( $cm^3/g$ ) | $W_o(N_2)^f)$<br>( $cm^3/g$ ) | $W_o(CO_2)^g)$<br>( $cm^3/g$ ) | $L_o(N_2)^h)$<br>(nm) | $L_o(CO_2)^i)$<br>(nm) | $W_o(N_2) / W_o(CO_2)$ |
|------------------|-----------------------------|-----------------------------|--------------------------|--------------------------|-------------------------------|-------------------------------|--------------------------------|-----------------------|------------------------|------------------------|
| S                | 1225                        | 46.90                       | 0.044                    | 0.481                    | 0.983                         | 0.391                         | 0.279                          | 1.02                  | 0.65                   | 1.40                   |
| C                | 1201                        | 21.30                       | 0.046                    | 0.409                    | 0.835                         | 0.406                         | 0.253                          | 1.30                  | 0.71                   | 1.60                   |

- a) Surface area determined from  $N_2$  adsorption isotherms at 77 K.
- b) External surface area determined by mercury porosimetry.
- c) Volume of pores with diameter of 6.6-50 nm determined by mercury porosimetry.
- d) Volume of pores with diameter >50 nm determined by mercury porosimetry.
- e) Volume of pores accessible to water determined by pycnometric densities.
- f, g) Volumes of micropores determined by  $N_2$  and  $CO_2$  adsorption, respectively.
- h, i) Mean widths of micropores determined with the Dubinin equation [35].

**Table 3.** Chemical characteristics of activated carbons.

| Activated Carbon | Carboxyl Groups <sup>a)</sup><br>( $\mu eq/g$ ) | Lactone Groups <sup>b)</sup><br>( $\mu eq/g$ ) | Phenol Groups <sup>c)</sup><br>( $\mu eq/g$ ) | Carbonyl Groups <sup>d)</sup><br>( $\mu eq/g$ ) | Total Acidic Groups <sup>e)</sup><br>( $\mu eq/g$ ) | Total Basic Groups <sup>f)</sup><br>( $\mu eq/g$ ) | $pH_{pzc}^g)$ | Oxygen (% wt) | Ashes (%) |
|------------------|---|--|---|---|---|--|---------------|---------------|-----------|
| S                | 0.0   | 56.0   | 244.0   | 146.7   | 446.7   | 1080.0   | 9.0           | 9.8           | 6.07      |
| C                | 44.6  | 156.1  | 557.6   | 149.4   | 907.7   | 96.0   | 6.0           | 10.0          | 8.30      |

- a) Concentration of carboxyl groups determined by titration with  $NaHCO_3$  (0.02 N).
- b) Concentration of lactone groups determined by titration with  $Na_2CO_3$  (0.02 N) -  $NaHCO_3$  (0.02 N).
- c) Concentration of phenol groups determined by titration with  $NaOH$  (0.02 N) -  $Na_2CO_3$  (0.02 N).
- d) Concentration of carbonyl groups determined by titration with  $NaOH$  (0.1 N) -  $NaOH$  (0.02 N).
- e) Concentration of acidic groups determined by titration with  $NaOH$  (0.1 N).
- f) Concentration of basic groups determined by titration with  $HCl$  (0.1 N).
- g) pH of the point of zero charge.

$$HC = 1 - \left( \frac{\Delta H_i(H_2O)}{\Delta H_i(C_6H_6)} \right) \quad (11)$$

Table 4 shows the relative hydrophobicity coefficients for both activated carbons. The hydrophobicity of a carbon is a key factor in its effectiveness as an adsorbent in aqueous phase and was higher for carbon S than for carbon C, attributable to the lower oxygen and ash contents of the former.

**Table 4.** Results obtained from immersion calorimetry of activated carbon in water and benzene.

| Activated carbon | $-\Delta H_i(C_6H_6)^a$ |                      | $-\Delta H_i(H_2O)^b$ |                      | HC <sup>c</sup> |
|------------------|-------------------------|----------------------|-----------------------|----------------------|-----------------|
|                  | (J/g)                   | (mJ/m <sup>2</sup> ) | (J/g)                 | (mJ/m <sup>2</sup> ) |                 |
| S                | 136.7                   | 111.6                | 48.4                  | 39.5                 | 0.65            |
| C                | 112.2                   | 93.4                 | 52.8                  | 44.0                 | 0.53            |

a) Benzene adsorption enthalpy.

b) Water adsorption enthalpy.

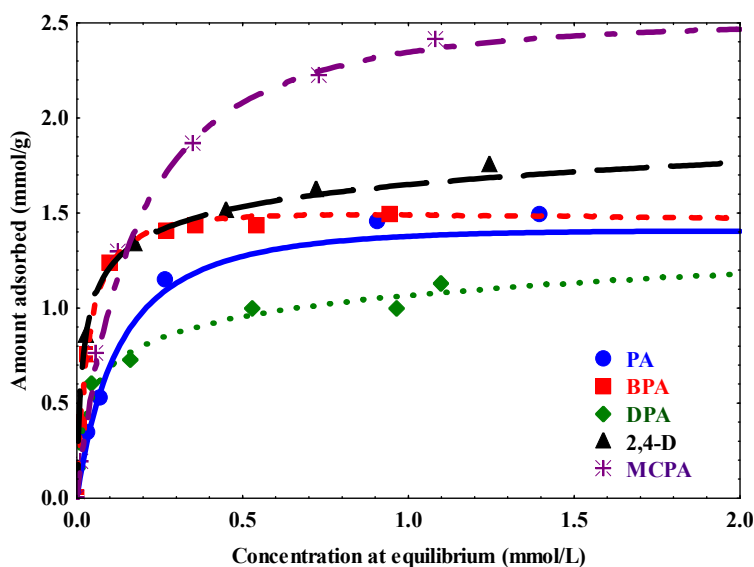
c) Relative hydrophobicity coefficient.

#### 4.2. Adsorption isotherm of micropollutants on activated carbon

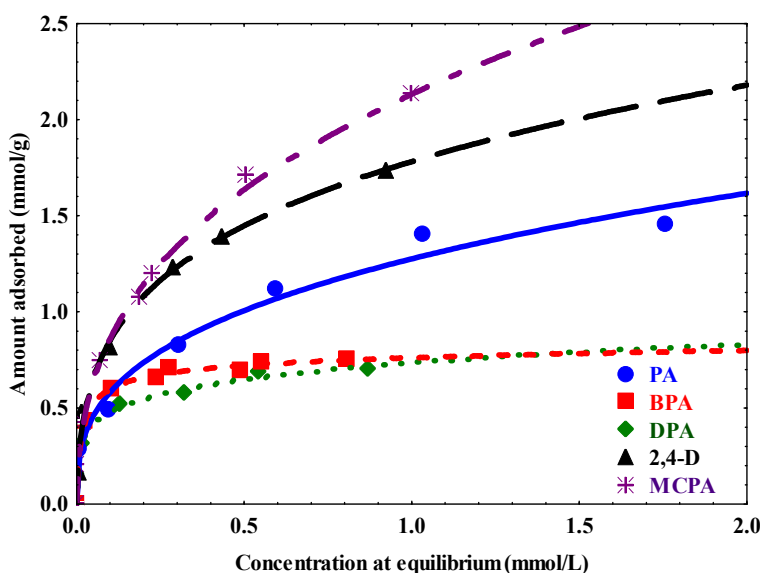
In order to apply the diffusional model, it is needed to obtain the adsorption isotherms of all systems. Figure 1a)-1b) depicts the adsorption isotherms of PA, BPA, DPA, 2,4-D and MCPA at T=298 K and pH (3-5) on the two activated carbon samples C and S. All isotherms showed the L type of Giles classification [27,28], indicating both that the aromatic rings of these contaminant molecules were adsorbed parallel to the carbon surface and there is no major competition between contaminant molecules and water molecules for the active adsorption centres on the carbon surface.

The adsorption equilibrium data of these compounds on the activated carbon samples shown in Figure 1a)-1b) were interpreted with the Prausnitz-Radke adsorption isotherm model. This model can be mathematically represented by the following equation:

$$q = \frac{aC_A}{1+bC_A^\beta} \quad (12)$$



a)



b)

**Figure 1.** Adsorption isotherms of the pollutants studied on activated carbon. a) Carbon C, and b) Carbon S. T= 298 K. The lines represent the Prausnitz-Radke isotherm.

The adsorption constants were evaluated by using a non-linear estimation method with *Statistica* software. The values of the isotherm constants, as well as the average absolute deviation percentages are given in Table 5. The deviation percentages were calculated with the following equation:

$$\%D = \frac{1}{N} \sum_{i=1}^N \left| \frac{q_{\text{exp}} - q_{\text{pred}}}{q_{\text{exp}}} \right| \times 100\% \quad (13)$$

Prausnitz-Radke isotherm model fitted reasonably well the experimental data of adsorption equilibrium since the average deviation percentages were less than 10% for all adsorption systems.

**Table 5.** Constants of the Prausnitz-Radke isotherm at 298 K.

| Pollutant | Carbon | a      | b  | $\beta$ | %D   |
|-----------|--------|--------|--|---------|------|
|           |        | (L/g)  | (L <sup><math>\beta</math></sup> /mmol <sup><math>\beta</math></sup> ) |         |      |
| PA        | C      | 11.20  | 7.13   | 1.07    | 3.72 |
|           | S      | 19.35  | 37.75  | 0.91    | 7.12 |
| BPA       | C      | 43.73  | 28.37  | 1.04    | 3.69 |
|           | S      | 54.97  | 70.87  | 0.94    | 1.86 |
| DPA       | C      | 44.95  | 41.17  | 0.87    | 9.93 |
|           | S      | 227.35 | 306.14   | 0.82    | 2.86 |
| 2,4-D     | C      | 102.42 | 61.08  | 0.91    | 0.10 |
|           | S      | 70.47  | 38.02  | 0.72    | 4.12 |
| MCPA      | C      | 19.28  | 619.16   | 1.04    | 3.98 |
|           | S      | 103.28 | 47.44  | 0.63    | 6.10 |

### 4.3. Calculation of mass transport parameters

Prior to apply the diffusional model to the adsorption kinetic data, the mass transport parameters should be determined. The molecular diffusion coefficient of pollutants in aqueous solution was assessed employing the Wilke-Chang correlation [29]. This correlation can be mathematically represented as follows:

$$D_{AB} = \frac{7.4 \times 10^{-8} (\phi M_B)^{1/2} T}{\eta_b V_A^{0.6}} \quad (14)$$

Where  $\phi = 2.60$ ,  $M_B = 18$  g/mol,  $\eta_b = 0.89$  cp, and  $V_A$  values of PA, BPA, DPA, 2,4-D and MCPA were estimated by using the Le Bas method [30], and they are given in Table 1. The molecular diffusion coefficient determined were  $8.74 \times 10^{-6}$ ,  $5.60 \times 10^{-6}$ ,  $5.37 \times 10^{-6}$ ,  $7.46 \times 10^{-6}$  and  $7.38 \times 10^{-6}$  cm<sup>2</sup>/s for PA, BPA, DPA, 2,4-D, and MCPA, respectively.

The experimental external mass transfer coefficient was assessed by the procedure proposed by Furusawa and Smith [31], based on the fact that when  $t \rightarrow 0$ ,  $C_{Ar} \rightarrow 0$  and  $C_A \rightarrow C_{A0}$ . Substituting these conditions in equation (1), the following equation can be derived:

$$\left[ \frac{d\left(\frac{C_A}{C_{A0}}\right)}{dt} \right]_{t=0} = \frac{-mSk_{L,\text{exp}}}{V} \quad (15)$$

The term in the right part of equation (15) is the slope of the concentration decay at  $t = 0$ , and it was estimated by using the first two data points of the concentration decay curve, at  $t = 0$  and  $t = 15$  min.

The experimental values of  $k_{L,\text{exp}}$  obtained are listed in Table 6, and they vary between  $0.57 \times 10^{-3}$  and  $2.10 \times 10^{-3}$  cm/s for PA, between  $1.08 \times 10^{-3}$  and  $5.67 \times 10^{-3}$  cm/s for BPA, between  $2.35 \times 10^{-3}$  and  $9.25 \times 10^{-3}$  cm/s for DPA, between  $0.23 \times 10^{-3}$  and  $0.73 \times 10^{-3}$  cm/s for 2,4-D, and between  $0.07 \times 10^{-3}$  and  $0.85 \times 10^{-3}$  cm/s for MCPA.

#### 4.4. Pore volume diffusion model (PVDM)

In a porous system, the presence of solid particles causes the diffusion paths of molecules to deviate from straight lines. Thus, to represent the role of porosity on diffusion, the diffusion coefficient must be scaled with tortuosity, which is defined as the ratio of an effective path length to the shortest path length in the microporosity. The relationship between the effective diffusion coefficient,  $D_{\text{ep}}$ , in a porous material and the molecular diffusivity,  $D_{AB}$ , can be described by various models. The simplest and

commonly used model is based on the tortuosity factor,  $\tau$ . In this model  $D_{ep}$  can be estimated from the following equation [18,32,33]:

$$D_{ep} = \frac{D_{AB}\epsilon_p}{\tau} \quad (16)$$

**Table 6.** Experimental conditions for calculation of mass transfer coefficient, effective diffusion coefficient and tortuosity factor.

| Exp. No. | Pollutant | Carbon | Mass of carbon (mg) | $C_{A0}$ (mg/L) | $C_{Ae}$ (mg/L) | $q_e$ (mg/g) | $k_{L,exp} \times 10^3$ (cm/s) | $D_{ep} \times 10^7$ (cm <sup>2</sup> /s) | $\tau$ |
|----------|-----------|--------|---------------------|-----------------|-----------------|--------------|--------------------------------|---|--------|
| 1        | PA        | C      | 25                  | 98.9            | 54.95           | 175.7        | 2.01                           | 9.61                                      | 3.42   |
| 2        |           | C      | 50                  | 98.9            | 32.66           | 132.4        | 0.57                           | 10.50                                     | 3.13   |
| 3        |           | C      | 100                 | 98.9            | 11.48           | 87.4         | 1.23                           | 11.36                                     | 2.84   |
| 4        |           | S      | 50                  | 98.9            | 36.45           | 124.9        | 2.10                           | 13.10                                     | 2.51   |
| 5        | BPA       | C      | 25                  | 93.5            | 29.33           | 256.5        | 5.10                           | 12.32                                     | 1.71   |
| 6        |           | C      | 50                  | 93.5            | 12.01           | 162.9        | 2.69                           | 5.60                                      | 3.76   |
| 7        |           | C      | 100                 | 93.5            | 2.46            | 91.1         | 1.08                           | 6.16                                      | 3.42   |
| 8        |           | S      | 25                  | 93.5            | 54.98           | 153.9        | 5.67                           | 10.60                                     | 2.08   |
| 9        |           | S      | 50                  | 93.5            | 29.27           | 128.4        | 2.83                           | 6.16                                      | 3.58   |
| 10       |           | S      | 100                 | 93.5            | 10.92           | 82.5         | 1.38                           | 3.36                                      | 6.57   |
| 11       | DPA       | C      | 100                 | 99.7            | 2.30            | 97.5         | 2.99                           | 10.70                                     | 1.89   |
| 12       |           | S      | 25                  | 99.7            | 48.95           | 203.3        | 9.25                           | 8.06                                      | 2.63   |
| 13       |           | S      | 100                 | 99.7            | 2.98            | 96.7         | 2.35                           | 6.98                                      | 3.03   |
| 14       | 2,4-D     | C      | 25                  | 100.7           | 20.66           | 320.0        | 0.73                           | 4.48                                      | 6.26   |
| 15       |           | C      | 100                 | 100.7           | 3.50            | 97.2         | 0.43                           | 7.46                                      | 3.76   |
| 16       |           | S      | 50                  | 100.7           | 6.89            | 187.5        | 0.40                           | 18.70                                     | 1.57   |
| 17       |           | S      | 100                 | 100.7           | 0.00            | 100.7        | 0.23                           | 22.40                                     | 1.31   |
| 18       | MCPA      | C      | 50                  | 100.0           | 12.84           | 174.2        | 0.07                           | 14.80                                     | 1.87   |
| 19       |           | C      | 100                 | 100.0           | 5.88            | 94.1         | 0.49                           | 6.64                                      | 4.18   |
| 20       |           | S      | 50                  | 100.0           | 14.76           | 170.4        | 0.85                           | 11.10                                     | 2.62   |
| 21       |           | S      | 100                 | 100.0           | 5.64            | 94.3         | 0.45                           | 5.17                                      | 5.62   |

Leyva-Ramos and Geankoplis [15] studied the intraparticle diffusion of several organic compounds in granular activated carbon and found that  $\tau$  varied between 3.0 and 4.6 and they recommended to use  $\tau = 3.5$  for activated carbon. Recently, Leyva-Ramos et al. [34] studied the rate of adsorption of 1-naphthalenesulfonic, 1,5-naphthalenedisulfonic and 1,3,6-naphthalenetrisulfonic acids on activated carbon and found that the totuosity factors ranged from 3.70 to 5.50

The experimental concentration decay curves of all our adsorption systems were interpreted with the PVDM model. The mass transport parameters required to solve this model were  $D_{ep}$  and  $k_{L,exp}$ .  $D_{ep}$  was determined with equation (16) using  $\tau = 3.5$  as a first approximation and  $k_{L,exp}$  was calculated using equation (15), and its values are listed in Table 6.

Figure 2 depicts the experimental concentration decay data for Exp. Nos. 3 and 9, as an example, and the corresponding concentration decay curves predicted with the PVDM model using  $\tau = 3.5$ . It can notice that the PVDM model interprets the experimental data very satisfactorily; however, a better value of  $D_{ep}$  can be obtained by fitting the numerical solution of the PVDM model with the experimental concentration decay data minimizing the following objective function:

$$\text{Minimum} = \sum_1^N (\phi_{exp} - \phi_{pred})^2 \quad (17)$$

The best values of  $D_{ep}$  were  $11.36 \times 10^{-7}$  and  $6.16 \times 10^{-7}$  cm<sup>2</sup>/s. From these optimal values of  $D_{ep}$  the corresponding  $\tau$  values were recalculated by using equation (16), being 2.84 and 3.58 for PA and BPA, respectively. Evidently, the prediction of PVDM model with the optimal  $D_{ep}$  values fitted slightly better the experimental data than the prediction of PVDM by using the former  $D_{ep}$  values. These results indicate that, for the studied systems, both methods of interpreting the experimental data are correct.



The optimal  $D_{ep}$  and  $\tau$  values obtained for all adsorption systems are given in Table 6. It is important to note that the tortuosity factor values obtained are between 1.31 and 6.57; however, most of these values are in the range from 2 to 4. The knowledge of these  $\tau$  values is worthy since it allows to predict the behavior of these types of adsorption systems in the experimental conditions range studied in the present work.

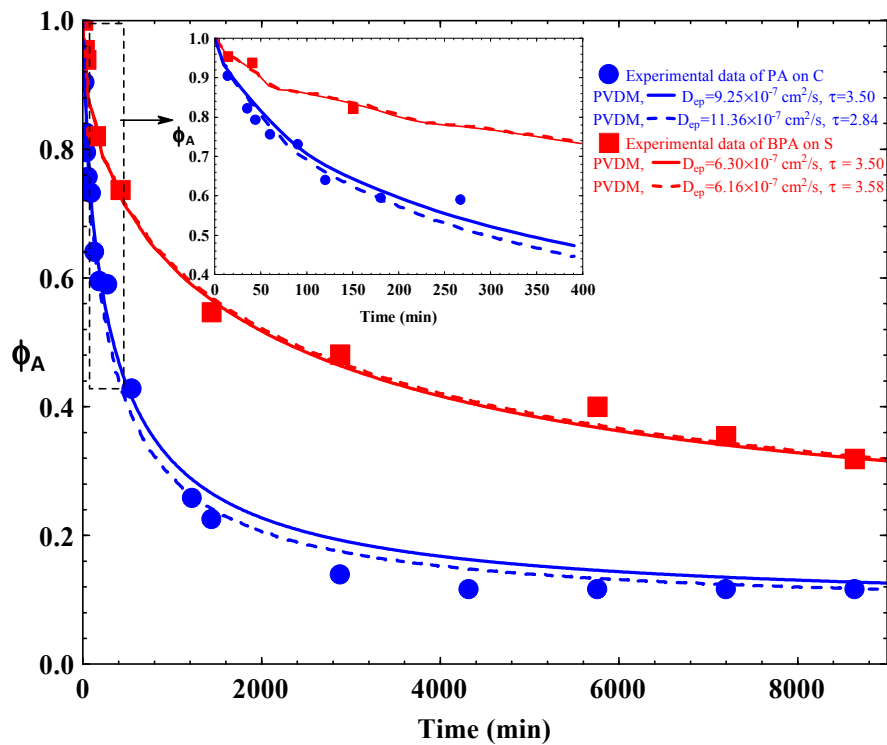


**Figure 2.** Concentration decay curves for PA and BPA adsorption on carbons C and S, respectively. The lines represent the PVDM model prediction. Exp. Nos. 3 and 9.

#### 4.5. Pore volume and surface diffusion model (PVSDM)

The PVSDM model considers that intraparticle diffusion is due to both pore volume and surface diffusion mechanisms. In order to solve the PVSDM model,  $k_{L,exp}$  was calculated from equation (15) and  $D_{ep}$  was evaluated with equation (16) assuming that  $\tau = 3.5$ . Hence, the surface diffusion coefficient,  $D_s$ , was the only unknown parameter and it was evaluated by fitting the numerical solution of the PVSDM model to the concentration decay data. The optimal value of  $D_s$  was obtained by minimizing equation (17). Figure 3 depicts, as an example, the experimental concentration decay data for Exp. Nos. 3 and 9, and the concentration decay curve predicted with the PVSDM model

using the optimal value of  $D_s= 8.74 \times 10^{-11}$  and  $D_s= 2.80 \times 10^{-11}$  cm<sup>2</sup>/s, respectively, showing that this model fitted the experimental adsorption data very satisfactorily.

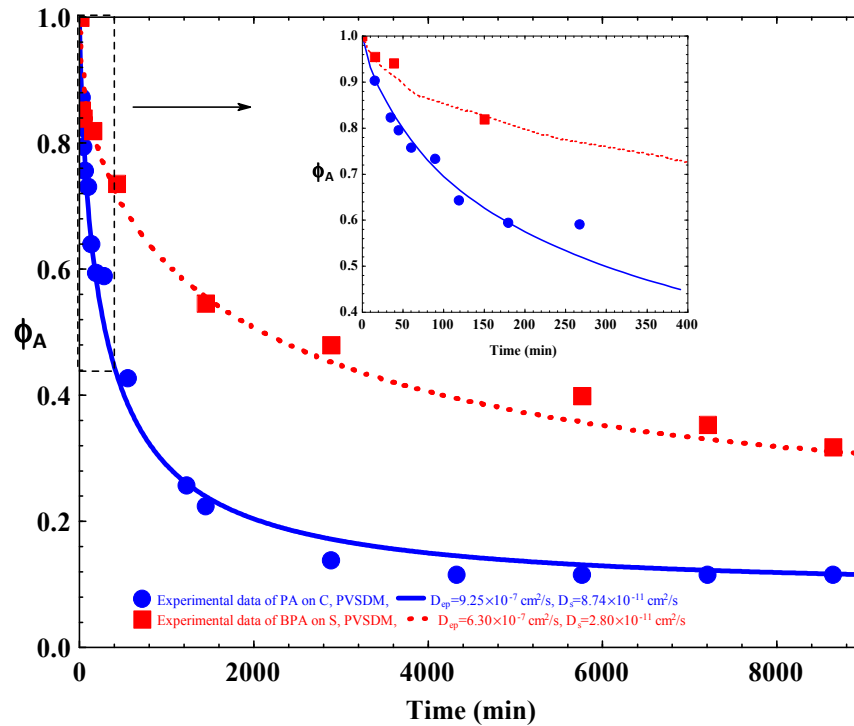


**Figure 3.** Concentration decay curve for PA and BPA adsorption on carbons C and S, respectively. The lines represent the PVSDM model prediction. Exp. Nos. 3 and 9.

In order to evaluate the relative contribution of each diffusion mechanism to the overall intraparticle diffusion of the different pollutants studied, the mass transport due to pore volume diffusion,  $N_{AP}$ , and surface diffusion,  $N_{AS}$ , were estimated by the following equations:

$$N_{AP} = -D_{ep} \frac{\partial C_{Ar}}{\partial r} \tag{18}$$

$$N_{AS} = -D_s \rho_p \frac{\partial q}{\partial r} \tag{19}$$

The relative contribution of pore volume diffusion to the overall intraparticle diffusion was estimated using the following equation:

$$\frac{N_{AP}}{N_{AS}+N_{AP}} = \frac{D_{ep} \frac{\partial C_{Ar}}{\partial r}}{D_s \rho_p \frac{\partial q}{\partial r} + D_{ep} \frac{\partial C_{Ar}}{\partial r}} \quad (20)$$

The relative contribution of pore volume diffusion with respect to time at different dimensionless radial positions  $\xi(r/R)$  is plotted, as an example, in Figures 4a) and 4b) for PA adsorption on carbon C and BPA adsorption on carbon S, respectively. The results revealed that the contribution of pore volume diffusion represented over 92 % of the overall intraparticle diffusion for both adsorption systems regardless of the radial position and time. Similar results (not shown) were founded for all systems studied. Hence, the intraparticle diffusion of these micropollutants during adsorption on activated carbon samples S and C was predominantly due to pore volume diffusion. Therefore, the PVDM model was used to interpret the experimental adsorption data in the following sections.

#### 4.6. Effect of the mass external transport on overall adsorption rate

The study of the influence of mass external transport on the overall adsorption rate of these micropollutants on granular activated carbon was carried out by comparing the concentration decay curves predicted with PVDM model, obtained by using the optimal value of  $D_{ep}$  and for different values of the external mass transfer coefficient,  $k_{L,exp}$ . The  $k_{L,exp}$  values of  $1.23 \times 10^{-3}$  and  $2.83 \times 10^{-3}$  cm/s for PA and BPA, respectively, obtained with equation (15) were increased and diminished 10 times. Figure 5 depicts the results obtained for experiments Nos. 3 and 9 as an example. The PVDM model fitted the experimental adsorption kinetic data independently of the  $k_{L,exp}$  value used.. Similar results (not shown) were obtained for all adsorption systems studied. These results confirm that the adsorption experiments were carried out under experimental conditions where the mass external transport did not affect to the overall rate of adsorption.

#### 4.7. Effect of the adsorbed pollutant mass on the effective diffusion coefficient

The mass of PA, BPA, DPA, 2,4-D, and MCPA adsorbed on activated carbon can affect the diffusion of these pollutant molecules inside the pores since they could reduce the pore volume accessible to adsorbate by partially blocking the pores. The effect of the

mass of pollutants adsorbed at equilibrium,  $q_{exp}$ , on  $D_{ep}$  was studied by carrying out experiments at the same experimental conditions but different mass of activated carbon (Table 6).

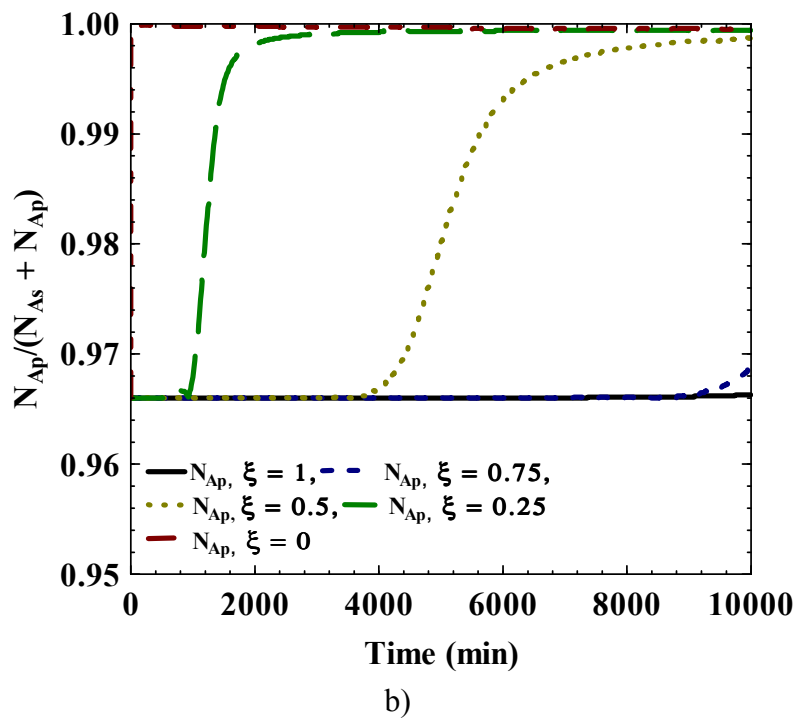
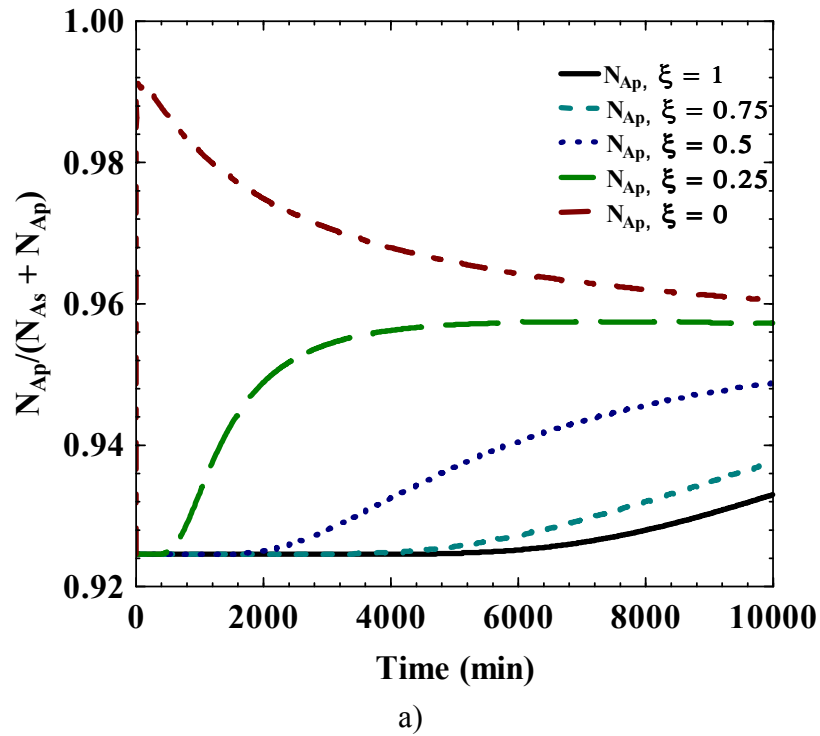


**Figure 4.** Contribution of pore volume diffusion to intraparticle diffusion at different radial positions, a) PA on carbon C; b) BPA on carbon S. Exp. Nos. 3 and 9.

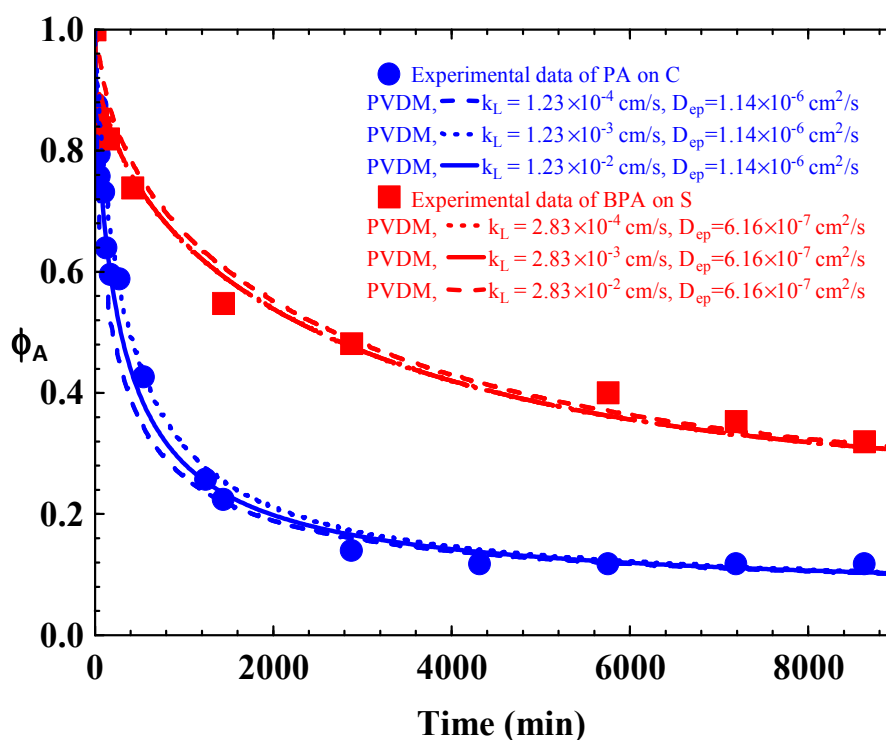
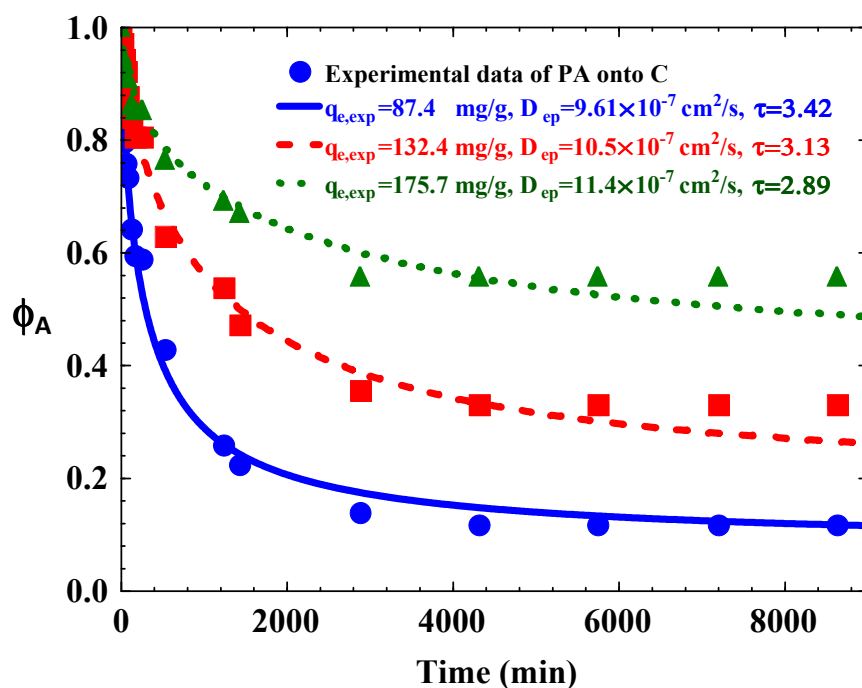


**Figure 5.** Effect of external mass transfer on the overall rate of adsorption of PA and BPA on carbons C and S, respectively. Exp. Nos. 3 and 9.

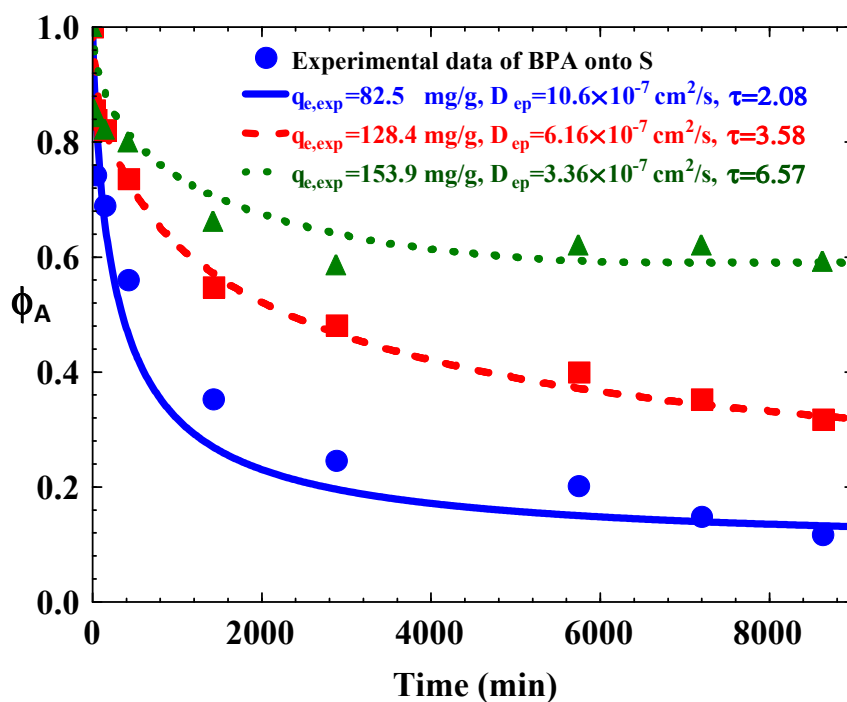
Figure 6a) and 6b) depicts, as an example, the concentration decay curves for PA and BPA, at initial concentration of 98.7 and 93.5 mg/L, respectively, and with 25, 50, and 100 mg of carbon (Exp. Nos. 1-3, 8-10). The corresponding  $q_{e,exp}$  values were 175.7, 132.4, 87.4, 153.9, 128.4, and 82.5 mg/g, respectively. It was noticed that the value of  $q_{e,exp}$  dropped as the mass of activated carbon increased. The PVDM model interpreted the experimental data reasonably well; however, while for PA, the effective pore volume diffusion coefficient,  $D_{ep}$ , increased with the amount adsorbed (Figure 6a)), for BPA the trend was the opposite (Figure 6b)).

For the rest of pollutants, 2,4-D followed a similar trend to PA, whereas the behavior of DPA and MCPA was similar to that of BPA. These trends were the same for both activated carbons. From these results it is not possible to establish a general tendency for both adsorbed pollutant mass and effective diffusion coefficients of these adsorption systems, which is attributed to the differences in: molecular size and shape of these

pollutant compounds, species distribution of adsorbates, and shape and distribution of carbon pores.



a)



b)

**Figure 6.** Concentration decay at different experimental conditions. a) PA on carbon C; b) BPA on carbon S. The lines represent the PVDM model predictions. Exp. Nos. 1-3 and 8-10.

#### 4.8. Interpretation of the adsorption rate data with the kinetic models

The experimental concentration decay data (Exp. Nos. 1-21) were interpreted with the first-order and second-order kinetic models Eqs. (8) and (10), respectively. The adsorption rate constants ( $k_1$  and  $k_2$ ) were estimated by fitting the kinetic models to the experimental concentration decay curves, and the best values of these kinetic constants were calculated by employing a least squares method based on an optimization algorithm.

The kinetic constants of each model and the values of the correlation coefficient,  $R^2$ , are given in Table 7. All  $R^2$  values for both first-order and second-order kinetic models were higher than 0.90 except for  $k_1$  in runs 8 and 11. Thus, the two kinetic models fitted the experimental data reasonably well. Nevertheless, the second-order kinetic model had the  $R^2$  values greater than those of the first-order kinetic model. Moreover,  $q_{\text{pred},2}$  values were more similar to  $q_{\text{exp}}$  ones than  $q_{\text{pred},1}$ ; therefore, the second order kinetic model interpreted much better our experimental adsorption data than first order one.

$k_2$  values for carbon C, at the same concentration of pollutants, increased in the following order:  $\text{DPA} < \text{MCPA} < 2,4\text{-D} < \text{BPA} < \text{PA}$ , and for carbon S the order was:  $\text{BPA} \leq 2,4\text{-D} \leq \text{MCPA} < \text{DPA}$ ; moreover,  $k_2$  values were higher for carbon S than for carbon C when using PA, BPA and DPA, and viceversa when the adsorbates were 2,4-D and MCPA. We have not found a clear relationship between the above trends and both pollutant molecular size and pore size of activated carbons; therefore, other parameters such as molecular shape, pollutant deprotonated species, surface groups of activated carbons should play an important role on the adsorption kinetics.

The effect of the adsorbed pollutant mass,  $q_{\text{exp}}$ , on  $k_1$  and  $k_2$  is shown in Table 7. In general,  $k_1$  and  $k_2$  decreased when  $q_{\text{exp}}$  was increased for both activated carbons. This behavior can be argued considering that the adsorption rate depends on the numbers of unoccupied adsorption sites, and this number diminished with the adsorption progress.

**Table 7.** Results obtained by applying first and second-order models to the PA, BPA, DPA, 2,4-D and MCPA adsorption kinetic data.

| Exp. No. | $q_{\text{exp}}$ (mg/g) | Pseudo 1 <sup>er</sup> order |             |       | Pseudo 2 <sup>nd</sup> order |                            |       |
|----------|-------------------------|------------------------------|-------------|-------|------------------------------|----------------------------|-------|
|          |                         | $q_{\text{pred},1}$ (mg/g)   | $k_1$ (1/h) | $R^2$ | $q_{\text{pred},2}$ (mg/g)   | $k_2 \times 10^3$ (g/mg/h) | $R^2$ |
| 1        | 175.7                   | 159.10                       | 0.103       | 0.973 | 173.50                       | 0.840                      | 0.987 |
| 2        | 132.4                   | 121.10                       | 0.090       | 0.991 | 134.11                       | 0.890                      | 0.996 |
| 3        | 87.4                    | 76.80                        | 0.220       | 0.972 | 82.28                        | 3.680                      | 0.990 |
| 4        | 124.9                   | 113.47                       | 0.180       | 0.985 | 122.28                       | 1.990                      | 0.995 |
| 5        | 256.5                   | 211.10                       | 0.066       | 0.954 | 228.16                       | 0.474                      | 0.970 |
| 6        | 162.9                   | 134.38                       | 0.056       | 0.967 | 146.53                       | 0.610                      | 0.979 |
| 7        | 91.1                    | 76.85                        | 0.150       | 0.990 | 80.79                        | 2.870                      | 0.993 |
| 8        | 153.9                   | 125.38                       | 0.241       | 0.867 | 125.54                       | 5.653                      | 0.913 |
| 9        | 128.4                   | 100.76                       | 0.090       | 0.944 | 108.62                       | 1.257                      | 0.963 |
| 10       | 82.5                    | 66.99                        | 0.071       | 0.969 | 72.66                        | 1.508                      | 0.982 |
| 11       | 97.5                    | 140.00                       | 0.161       | 0.897 | 149.34                       | 1.693                      | 0.930 |
| 12       | 203.3                   | 162.88                       | 0.388       | 0.985 | 165.23                       | 4.446                      | 0.993 |
| 13       | 96.7                    | 77.06                        | 0.113       | 0.911 | 81.12                        | 2.400                      | 0.939 |
| 14       | 320.0                   | 265.22                       | 0.050       | 0.996 | 297.17                       | 0.236                      | 0.998 |
| 15       | 97.2                    | 82.67                        | 0.160       | 0.996 | 86.88                        | 2.796                      | 0.992 |
| 16       | 187.5                   | 155.83                       | 0.059       | 0.996 | 171.85                       | 0.484                      | 0.997 |
| 17       | 100.7                   | 86.45                        | 0.098       | 0.998 | 92.82                        | 1.516                      | 0.992 |
| 18       | 174.2                   | 144.17                       | 0.128       | 0.994 | 152.89                       | 1.232                      | 0.995 |
| 19       | 94.1                    | 74.98                        | 0.110       | 0.990 | 79.73                        | 2.101                      | 0.993 |
| 20       | 170.4                   | 135.30                       | 0.072       | 0.987 | 146.78                       | 0.745                      | 0.994 |
| 21       | 94.3                    | 76.69                        | 0.086       | 0.992 | 82.57                        | 1.559                      | 0.995 |

## 5. CONCLUSIONS

The PVSDM model satisfactorily fitted the experimental data of single adsorption of micropollutants present in landfill leachates on activated carbon. The tortuosity factor of the activated carbons used in this study ranged from 2 to 4.



The contribution of pore volume diffusion represented more than 92% of intraparticle diffusion. This finding confirmed that pore volume diffusion is the controlling mechanism of the overall rate of adsorption and surface diffusion can be neglected.

The external mass transport did not affect the overall adsorption rate of these pollutants on the activated carbon samples.

The adsorption experimental data were satisfactorily fitted with kinetic models. The second-order kinetic model was better fitted these data than the first-order one.

Although both diffusional models and kinetic models successfully fitted the adsorption rate experimental data, we recommend the use of diffusional models, with a  $\tau$  range of 2-4, since their assumptions are nearer to the real adsorption process, than those of kinetic models.

## 6. REFERENCES

- [1] C. Fang, Y. Long, Y. Lu, D. Shen, *Int. Biodeterior. Biodegrad.* 63(6) (2009) 732.
- [2] S.K. Marttinen, R.H. Kettunen, J.A. Rintala, *Sci. Total Environ.* 301(1-3) (2003) 1.
- [3] A. Yasuhara, H. Shiraishi, M. Nishikawa, T. Yamamoto, T. Uehiro, O. Nakasugi, T. Okumura, K. Kenmotsu, H. Fukui, M. Nagase, Y. Ono, Y. Kawagoshi, K. Baba, Y. Noma, *J. Chromatogr. A*, 774(1-2) (1997) 321.
- [4] I. Gültekin, N.H. Ince, *J. Environ. Manage.* 85(4) (2007) 816.
- [5] S. Tanaka, Y. Nakata, T. Kimura, Yustiawati, M. Kawasaki, H. Kuramitz, *J. Appl. Electrochem.* 32(2) (2001) 197.
- [6] D. Han, W. Jia, H. Liang, *J. Environ. Sci.* 22(1-3) (2010) 237.
- [7] Z. Aksu, E. Kabasakal, *Separ. Purif. Technol.* 35(3) (2004) 223.
- [8] F.P. Peixoto, M.L. Lopes, V.M.C. Madeira, J.A.F. Vicente, *Acta Physiol. Plant*, 31(1) (2009) 103.
- [9] Granular Activated Carbon Treatment; Report EPA-540/2-91/024; U.S. Environmental Protection Agency, U.S. Government Printing Office: Washington, DC, 1991.
- [10] J.D. Méndez-Díaz, M.M. Abdel daiem, J. Rivera-Utrilla, M. Sánchez-Polo, I. Bautista-Toledo, *J. Colloid Interface Sci.* 369(1) (2012) 358.
- [11] I. Bautista-Toledo, M.A. Ferro-García, J. Rivera-Utrilla, C. Moreno-Castilla, F.J. Vegas Fernández, *Environ. Sci. Technol.* 39(16) (2005) 6246.
- [12] E. Ayranci, E. Bayram, *J. Hazard. Mater.* 122(1-2) (2005) 147.
- [13] G. Liu, J. Ma, X. Li, Q. Qin, *J. Hazard. Mater.* 164(2-3) (2009) 1275.
- [14] R. Leyva-Ramos, G.J. Geankoplis, *Chem. Eng. Sci.* 40(5) (1985) 799.

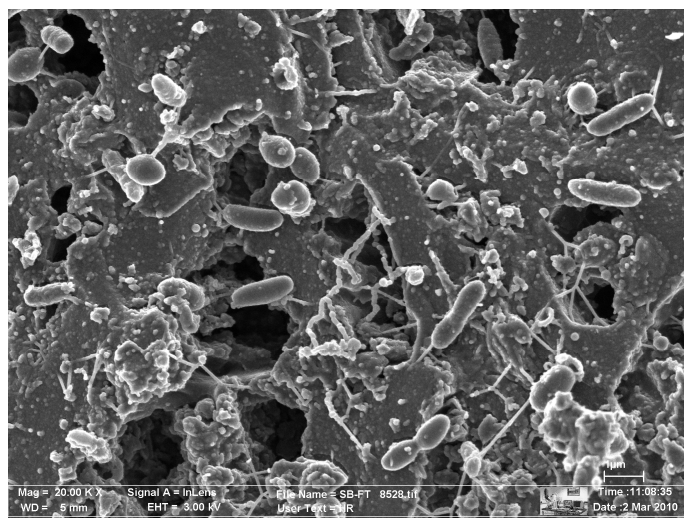
- 
- [15] R. Leyva-Ramos, C.J. Geankoplis, *Can. J. Chem. Eng.* 72(2) (1994) 262.
- [16] T.S.Y. Choong, T.N. Wong, T.G. Chuah, A. Idris, *J. Colloid Interface Sci.* 301 (2) (2006) 436.
- [17] W.E. Schiesser, C.A. Silebi, *Numerical Methods for the solution of Transport Problems*; Cambridge University Press: Cambridge, U.K., 1997.
- [18] D.M. Ruthven, *Principles of adsorption and adsorption processes*; New Brunswick University Press: Fredericton, Canada, 1984.
- [19] M.I. Bautista-Toledo, J.D. Méndez-Díaz, M. Sánchez-Polo, J. Rivera-Utrilla, M.A. Ferro-García, *J. Colloid Interface Sci.* 317(1) (2008) 11.
- [20] M. Sánchez-Polo, J. Rivera-Utrilla, *Carbon* 41(2) (2003) 303.
- [21] J. Rivera-Utrilla, M. Sánchez-Polo, *Langmuir* 20 (2004) 9217.
- [22] J. Garrido, A. Linares-Solano, J.M. Martín-Martínez, M. Molina-Sabio, F. Rodríguez-Reinoso, R. Torregrosa, *Langmuir* 3 (1987) 76.
- [23] F. Rodríguez-Reinoso, A. Linares-Solano, *Microporous Structure of Activated Carbons as Revealed by Adsorption Methods, in chemistry and physics of carbon.* New York, 1988.
- [24] M.V. Lopez-Ramon, F. Stoeckli, C. Moreno-Castilla, F. Carrasco-Marin, *Carbon* 37(8) (1999) 1215.
- [25] M.V. Lopez-Ramon, F. Stoeckli, C. Moreno-Castilla, F. Carrasco-Marin, *Carbon* 38(6) (2000) 825.
- [26] R.H. Bradley, I. Sutherland, E. Sheng, *J. Chem. Soc., Faraday Trans.* 91 (18) (1995) 3201.
- [27] S.S. Barton, M.J.B. Evans, J.A.F. MacDonald, *Langmuir* 10(11) (1994) 4250.
- [28] C.H. Giles, D. Smith, A. Huitson, *J. Colloid Interface Sci.* 47(3) (1974) 755.

- 
- [29] K.E. Noll, V. Gounaris, W.S. Hou, Adsorption Technology for Air and Water Pollution Control; Lewis Publishers: Michigan, U.S.A., 1992
- [30] M. Prausnitz, P. John, O'Connell. The Properties of Gases and Liquids; McGraw-Hill Companies, 2004.
- [31] Y. Furusawa, J.M. Smith, J.M. Ind. Eng. Chem. Fundamen. 12 (2) (1973) 197.
- [32] D.D. Do, Adsorption analysis: Equilibria and kinetics; Queensland University Press: Queensland, Australia, 1998.
- [33] M. Suzuki, Adsorption Engineering; Tokyo University Press: Tokyo, Japan, 1990.
- [34] R. Leyva-Ramos, J. Rivera-Utrilla, N.A. Medellín-Castillo, M. Sánchez-Polo, Adsorpt. Sci. Technol. 27 (4) (2009) 395.
- [35] M.M. Dubinin, Carbon 23 (1985) 373.



## CAPÍTULO 3

# ADSORCIÓN/BIOADSORCIÓN DE ÁCIDO FTÁLICO, UN MICROCONTAMINANTE ORGÁNICO PRESENTE EN LOS LIXIVIADOS DE VERTEDEROS, SOBRE CARBONES ACTIVADOS





# ADSORPTION/BIOADSORPTION OF PHTHALIC ACID, AN ORGANIC MICROPOLLUTANT PRESENT IN LANDFILL LEACHATES, ON ACTIVATED CARBONS

Article published in Journal of Colloid and Interface Science 369, 358-365 (2012)



## Highlights

- Phthalic acid adsorption is governed by dispersion and electrostatic interactions.
- The phthalic acid adsorption process is highly dependent on the solution pH.
- The presence of microorganisms during adsorption increases the adsorption yield.
- Phthalic acid removal varies as a function of the natural water type

## ABSTRACT

This study investigated the adsorption of phthalic acid (PA) in aqueous phase on two activated carbons with different chemical natures, analyzing the influence of: solution pH, ionic strength, water matrix (ultrapure water, ground water, surface water, and wastewater), the presence of microorganisms in the medium, and the type of regime (static and dynamic). The activated carbons used had a high adsorption capacity (242.9 mg/g and 274.5 mg/g) which is enhanced with their phenolic groups content. The solution pH had a major effect on PA adsorption on activated carbon; this process is favoured at acidic pHs. PA adsorption was not affected by the presence of electrolytes (ionic strength) in solution but was enhanced by the presence of microorganisms (bacteria) due to their adsorption on the carbon which led up to an increase in the activated carbon surface hydrophobicity. PA removal varies as a function of the water type, increasing in the order: ground water < surface water ≈ ultrapure water < wastewater. The effectiveness of PA adsorption was lower in dynamic than in static regime due to the shorter adsorbent-adsorbate contact time in dynamic regime.





## 1. INTRODUCTION

Industrial activity has led to the release of a large number of synthetic organic chemicals into the environment [1], including plasticizers and organic esters, which are added to polymers to facilitate their processing and increase the flexibility and toughness of the final product by internal modification of the polymer molecules [2, 3].

The extensive use of plasticizers worldwide has resulted in the presence of phthalates in multiple environments, with evidence of phthalic acid esters (PAEs) in soils, natural water and wastewater [4]. Due to their very large production and wide distribution, PAEs have become ubiquitous environmental pollutants [5], and some of them are suspected to be mutagens [6] or carcinogens [7]. They are also considered to be endocrine disruptors, a group of contaminants causing special concern [8].

Large amounts of PAEs are leached from plastics dumped at municipal landfills [9]. PAE concentrations in wastewater from chemical plants and nearby rivers ranged from 10 to 300  $\mu\text{g/L}$ , reaching 30  $\text{mg/L}$  in wastewater near plasticiser-producing factories [10].

Adsorption on activated carbon has proven the most effective and reliable physicochemical non-destructive technique for landfill leachate treatment, achieving a higher reduction in dissolved organic carbon in comparison to chemical methods [11-13]. In fact, the USA Environmental Protection Agency has acknowledged that adsorption on activated carbon, one of the oldest water treatments, is one of the best methods available to remove organic and inorganic pollutants from water intended for human consumption [14].

Despite its high effectiveness to remove lixivate-derived contaminants, few data have been published on the use of adsorption on activated carbon to eliminate PAEs from waters [13, 15]. Furthermore, there have been no studies on the effect of the aqueous medium (i.e., natural waters) or of the presence of bacteria on this process, which are highly relevant issues in the real-life treatment of waters polluted with PAEs.

With this background, the objective of this study was to examine the adsorption of phthalic acid (PA), used as model PAE compound, on two activated carbons with different chemical characteristics, analyzing the influence of the medium pH and ionic strength on the adsorption yield. The influence of water type was studied by means of experiments in ultrapure, superficial, subterranean and waste waters. The effect on PA adsorption of the presence of bacteria in the medium was also investigated.

## **2. EXPERIMENTAL**

### **2.1. Reagents**

All chemical reagents used in this study (phthalic acid, potassium phosphates, hydrochloric acid, and sodium chloride) were high-purity analytical grade reagents supplied by Sigma-Aldrich. All solutions were prepared with ultrapure water obtained from Milli-Q<sup>®</sup> equipment (Millipore).

Figure 1 depicts the chemical structure of PA. The dimensions of this pollutant molecule were determined by using Advanced Chemistry Development software version 8.14 (ACD/Labs). Other physiochemical characteristics of PA were obtained from the ChemIDplus Advanced database (see Table 1). The concentration of PA in aqueous solution was determined with a UV-visible spectrophotometer Genesys 5 at a wavelength of 231 nm.

### **2.2. Activated carbon**

Two commercial activated carbons, Sorbo Norit (S) and Ceca AC40 (C), were used as adsorbents. The activated carbon particle size was 0.45-1.00 mm. These carbon samples were chemically and texturally characterized, recording the surface area, pore volume accessible to water, pore size distribution, elemental analysis, ash content, oxygen surface groups, and pH of the point of zero charge. Detailed descriptions of the techniques and methods used for this characterization were previously reported [16 - 18].

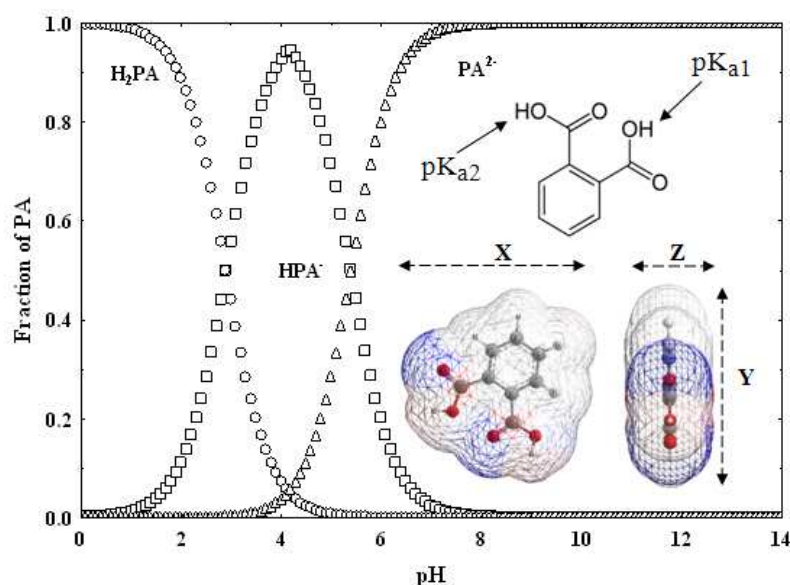


**Figure 1.** Species distribution of phthalic acid as a function of solution pH.

**Table 1.** Properties of phthalic acid.

| Molecular Weight (g/mol) | Molecular Size <sup>a)</sup> (x, y, z) (Å) | Volume <sup>b)</sup> (cm <sup>3</sup> /mol) | Solubility in water (g/L) | log <sub>ow</sub> <sup>c)</sup> | p <sub>k</sub> <sub>a1</sub> <sup>d)</sup> | p <sub>k</sub> <sub>a2</sub> <sup>e)</sup> |
|--------------------------|--|---|---------------------------|---------------------------------|--|--|
| 166.13                   | 8.90 x 8.90 x 3.40                         | 114   | 12.50                     | 1.15                            | 2.90                                       | 5.40                                       |

a) Dimensions of phthalic acid molecule shown in Figure 1.

b) Volume at boiling point.

c) Log octanol-water partition coefficient.

d, e) p<sub>k</sub><sub>a</sub> depicted in Figure 1.

The hydrophobicity of the activated carbons was determined by measuring immersion enthalpies in benzene  $\Delta H_i(\text{C}_6\text{H}_6)$  and water  $\Delta H_i(\text{H}_2\text{O})$ , using a SETARAM C80 calorimeter. For this purpose, 0.10 g of activated carbon was degasified in a glass capsule at a pressure of  $10^{-5}$  mbar and temperature of 383 K for 12 h. The sample was then left to stabilize in the calorimeter for 3 h at 303 K before the experiment.

### 2.3. PA adsorption on activated carbon

PA adsorption isotherms on the activated carbon samples (S and C) were obtained by placing 0.10 g of activated carbon in flasks, adding 100 mL of PA aqueous solution at increasing concentrations (50-500 mg/L), and determining the PA concentration after

equilibrium was reached (7 days). Adsorption isotherms were obtained at a temperature of 298 K, the solution pH was around 4, and solutions were stirred on a thermostatic mechanical shaker operating at constant agitation speed (135 rpm).

The influence of the solution pH on PA adsorption was studied by adding 0.1 g of activated carbon to Erlenmeyer flasks containing 100 mL of PA solution (500 mg/L) at different pH value for each flask, ranging from 3 to 10. The working pH was obtained by adding the appropriate volume of  $\text{KH}_2\text{PO}_4$  (50 mM) and  $\text{K}_2\text{HPO}_4$  (50 mM) to the solution. A CRISON micropH2002 meter was used to measure the final solution pH.

The effect of the presence of electrolytes on PA adsorption was analysed by placing 100 mL of PA solution (500 mg/L) with increasing concentrations of NaCl (0.0-0.01 M) in contact with 0.10 g of activated carbon. The ionic strengths of these solutions are similar to that of many types of natural water.

PA adsorption isotherms were obtained in the presence of bacteria (bioadsorption), seeding the microorganisms from unfiltered effluent water samples taken at the outlet of a bioreactor in our laboratory. Briefly, 1 mL of unfiltered sample was cultivated in Tryptone Soy Broth (dehydrated culture medium) (Difco Lab) with 50 mL distilled water at 37°C for three days with slight agitation (45 rpm). Next, the sample was centrifuged for 15 min at 4000 rpm to recover the cells, washing the sediment three times with sterile distilled water and finally resuspending the cells in 50 mL of sterile distilled water, thereby obtaining a suspension with a high concentration of bacteria [19]. Adsorption isotherms were obtained as described above, adding 5 mL of bacteria suspension, with absorbance (0.08-0.118) at a wavelength of 520 nm and (0.07-0.105) at a wavelength of 600 nm, to each flask containing both activated carbon and PA. These experiments were repeated in the absence of activated carbon in order to determine the biodegradability of PA.

In PA bioadsorption experiments, some of the bacteria are adsorbed on the activated carbon. In order to confirm this adsorption, scanning electron microscopy (SEM) images of the carbon samples were taken before and after of PA bioadsorption, using a LEO GEMINI-1530 high resolution electron microscope (Carl Zeiss).

All the above adsorption experiments were run in triplicate in order to determine the mean values and their standard deviation.

PA adsorption was also studied in dynamic regime, passing a solution of PA (100 mg/L) through a glass column (6.6-cm high, 1-cm diameter) well packed with approximately 2 g of activated carbon. Distilled water was passed through the bed overnight before each experiment. A peristaltic pump was used to pass the PA solution through the active carbon beds at a flow of 1.6 mL/min. As in the isotherm determination, solutions with no pH buffer were used. Samples of solution were taken periodically at the column outlet until saturation was reached. Carbon column breakthrough curves and column characteristics were obtained from these experiments [20-23].

Natural water samples (ground water, and surface water) from a drinking water treatment plant and wastewater samples from a wastewater treatment plant were supplied by *Agua y Servicios de la Costa Tropical de Granada* in Motril (Granada). Standard methods [24] were used to determine their characteristics, which are listed in Table 2. After their characterisation, samples were filtered and stored in cold until their use as medium to carry out PA adsorption experiments.

### **3. RESULTS AND DISCUSSION**

#### **3.1. Characteristics of activated carbon**

Table 3 shows the textural characteristics of the two activated carbons used in this study. Both had a large surface area ( $>1200 \text{ m}^2/\text{g}$ ) and a highly developed porosity, with a very large volume ( $>0.80 \text{ cm}^3/\text{g}$ ) of pores accessible to water. The pore size distribution of the carbon is important for the adsorption of a compound in aqueous

solution, because pores that are not accessible to water will not be effective in the adsorption process. The external surface area (corresponding to pores with diameter > 6.6 nm) was larger for carbon S (46.90 m<sup>2</sup>/g) than for carbon C (21.30 m<sup>2</sup>/g).

Micropore volumes ( $W_0$ ) obtained by N<sub>2</sub> adsorption were 0.391 cm<sup>3</sup>/g (carbon S), and 0.406 cm<sup>3</sup>/g (carbon C), which were both considerably higher than those determined by CO<sub>2</sub> adsorption (see Table 3). The  $W_0(\text{N}_2)/W_0(\text{CO}_2)$  ratio was higher for carbon C (1.60) than for carbon S (1.40), with both values indicating a very heterogeneous micropore distribution.

CO<sub>2</sub> is only adsorbed in smaller micropores (ultramicropores), whereas N<sub>2</sub> is adsorbed on the surface of all micropores [25, 26]; therefore, N<sub>2</sub> adsorption data give the total micropore volume,  $W_0(\text{N}_2)$ ; thus the mean micropore size ( $L_0$ ) was higher when determined by N<sub>2</sub> adsorption (Table 3).

Table 4 lists the chemical characteristics of the activated carbons. The pH of point of zero charge was 9.0 for carbon S and 6.0 for carbon C, which means that carbon C has a chemical nature more acidic than carbon S, which is due to the higher concentration of carboxyl, lactone and phenolic groups of carbon C. The ash content was < 8.5% in both activated carbons.

Table 5 shows the water and benzene immersion calorimetry results for these activated carbons. Adsorption enthalpy values determined by immersion calorimetry of an activated carbon in water depend on: the interactions with polar sites (acidic or basic), the micropore filling, and the external surface wetting. Hence, the first of these three processes is specific and corresponds to relatively high energies, whereas the other two are due to lower energy non-specific interactions [27, 28]. Because of this specific interaction, a relationship can be established between the water immersion enthalpy and surface oxygen content of different carbons [29, 30].

Carbon C, with its higher oxygen and ash contents, shows a greater water immersion enthalpy when water adsorption heat is expressed per gram of carbon (Table 5).

**Table 2.** Chemical characteristics of the four types of water used.

| <b>Water</b>           | <b>pH</b> | <b>TOC<br/>(mg/L)</b> | <b>[HCO<sub>3</sub><sup>-</sup>]<br/>(meq/L)</b> | <b>[Ca<sup>2+</sup>]<br/>(mmol/L)</b> | <b>[Mg<sup>2+</sup>]<br/>(mmol/L)</b> | <b>Total hardness<br/>CaCO<sub>3</sub> (mg/L)</b> | <b>Conductivity<sup>a)</sup><br/>(μS/cm)</b> |
|------------------------|-----------|-----------------------|--|---------------------------------------|---------------------------------------|---|--|
| <b>Ultrapure water</b> | 6.80      | 0.0                   | 0.0  | 0.00                                  | 0.00                                  | 0.00  | 0.055  |
| <b>Surface water</b>   | 8.30      | 14.9                  | 6.4  | 1.55                                  | 1.11                                  | 266   | 688  |
| <b>Ground water</b>    | 7.45      | 29.7                  | 8.8  | 2.53                                  | 2.18                                  | 471   | 1623   |
| <b>Wastewater</b>      | 7.77      | 88.9                  | 7.2  | 2.12                                  | 1.53                                  | 365   | 1578   |

a) Conductivity in μSiemens/cm at 298K.

**Table 3.** Textural characterization of the activated carbons used.

| <b>Activated<br/>Carbon</b> | <b>S<sub>N<sub>2</sub></sub><sup>a)</sup><br/>(m<sup>2</sup>/g)</b> | <b>S<sub>ext</sub><sup>b)</sup><br/>(m<sup>2</sup>/g)</b> | <b>V<sub>2</sub><sup>c)</sup><br/>(cm<sup>3</sup>/g)</b> | <b>V<sub>3</sub><sup>d)</sup><br/>(cm<sup>3</sup>/g)</b> | <b>V<sub>H<sub>2</sub>O</sub><sup>e)</sup><br/>(cm<sup>3</sup>/g)</b> | <b>W<sub>o</sub><br/>(N<sub>2</sub>)<sup>f)</sup><br/>(cm<sup>3</sup>/g)</b> | <b>W<sub>o</sub><br/>(CO<sub>2</sub>)<sup>g)</sup><br/>(cm<sup>3</sup>/g)</b> | <b>L<sub>o</sub><br/>(N<sub>2</sub>)<sup>h)</sup><br/>(nm)</b> | <b>L<sub>o</sub><br/>(CO<sub>2</sub>)<sup>i)</sup><br/>(nm)</b> | <b>W<sub>o</sub> (N<sub>2</sub>)<br/>/ W<sub>o</sub><br/>(CO<sub>2</sub>)</b> |
|-----------------------------|---|---|--|--|---|--|---|--|---|---|
| <b>S</b>                    | 1225  | 46.90   | 0.044  | 0.481  | 0.983   | 0.391  | 0.279   | 1.02   | 0.65  | 1.40  |
| <b>C</b>                    | 1201  | 21.30   | 0.046  | 0.409  | 0.835   | 0.406  | 0.253   | 1.30   | 0.71  | 1.60  |

f) Surface area determined from N<sub>2</sub> adsorption isotherms at 77 K.

g) External surface area determined by mercury porosimetry.

h) Volume of pores with diameter of 6.6-50 nm determined by mercury porosimetry.

i) Volume of pores with diameter >50 nm determined by mercury porosimetry.

j) Volume of pores accessible to water determined by pycnometric densities.

f,g) Volumes of micropores determined by N<sub>2</sub> and CO<sub>2</sub> adsorption, respectively.

h, i) Mean widths of micropores determined with the Dubinin equation [46].



**Table 4.** Chemical characteristics of the activated carbons

| Activated Carbon | Carboxyl Groups <sup>a)</sup> | Lactone Groups <sup>b)</sup> | Phenol Groups <sup>c)</sup> | Carbonyl Groups <sup>d)</sup> | Total Acidic Groups <sup>e)</sup> | Total Basic Groups <sup>f)</sup> | pH <sub>pzc</sub> <sup>g)</sup> | Oxygen (% wt) | Ashes (%) |
|------------------|-------------------------------|------------------------------|-----------------------------|-------------------------------|-----------------------------------|----------------------------------|---------------------------------|---------------|-----------|
|                  | ( $\mu\text{eq/g}$ )          | ( $\mu\text{eq/g}$ )         | ( $\mu\text{eq/g}$ )        | ( $\mu\text{eq/g}$ )          | ( $\mu\text{eq/g}$ )              | ( $\mu\text{eq/g}$ )             |                                 |               |           |
| S                | 0.00                          | 56.00                        | 244.0                       | 146.7                         | 446.7                             | 1080.0                           | 9.0                             | 9.80          | 6.07      |
| C                | 44.60                         | 156.10                       | 557.6                       | 149.4                         | 907.7                             | 96.0                             | 6.0                             | 10.00         | 8.30      |

h) Concentration of carboxyl groups determined by titration with  $\text{NaHCO}_3$  (0.02 N).

i) Concentration of lactone groups determined by titration with  $\text{Na}_2\text{CO}_3$  (0.02 N) -  $\text{NaHCO}_3$  (0.02 N).

j) Concentration of phenol groups determined by titration with  $\text{NaOH}$  (0.02 N) -  $\text{Na}_2\text{CO}_3$  (0.02 N).

k) Concentration of carbonyl groups determined by titration with  $\text{NaOH}$  (0.1 N) -  $\text{NaOH}$  (0.02 N).

l) Concentration of acidic groups determined by titration with  $\text{NaOH}$  (0.1 N).

m) Concentration of basic groups determined by titration with  $\text{HCl}$  (0.1 N).

n) pH of the point of zero charge.

**Table 5.** Results obtained from immersion calorimetry of activated carbon in water and benzene.

| Activated carbon | $-\Delta H_i(\text{C}_6\text{H}_6)^{\text{a)}$ |                                   | $-\Delta H_i(\text{H}_2\text{O})^{\text{b)}$ |                                   | HC <sup>c)</sup> |
|------------------|--|-----------------------------------|--|-----------------------------------|------------------|
|                  | ( $\text{J}\cdot\text{g}^{-1}$ )               | ( $\text{mJ}\cdot\text{m}^{-2}$ ) | ( $\text{J}\cdot\text{g}^{-1}$ )             | ( $\text{mJ}\cdot\text{m}^{-2}$ ) |                  |
| S                | 136.7  | 111.6                             | 48.4   | 39.5                              | 0.65             |
| C                | 112.2  | 93.4                              | 52.8   | 44.0                              | 0.53             |

a) Benzene adsorption enthalpy.

b) Water adsorption enthalpy.

c) Relative hydrophobicity coefficient.

Furthermore, the adsorption enthalpy of the non-polar benzene molecule,  $\Delta H_i(\text{C}_6\text{H}_6)$ , is less dependent on the chemical nature of carbon surface than on the distribution of its porosity [27, 28]. In the present study, the data obtained from calorimetry with benzene showed an inverse relationship with mean  $L_o$  ( $\text{N}_2$ ) and  $L_o$  ( $\text{CO}_2$ ) micropore size (Table 3).

Given the polar nature of the water molecule and non-polar nature of benzene, the relative hydrophobicity of carbon can be determined by means of the hydrophobicity coefficient given in Equation (1).

$$\text{HC} = 1 - \left( \frac{\Delta H_i(\text{H}_2\text{O})}{\Delta H_i(\text{C}_6\text{H}_6)} \right) \quad (1)$$

Table 5 shows the relative hydrophobicity coefficients for activated carbon. The hydrophobicity of a carbon is a key factor in its effectiveness as an adsorbent in aqueous phase and was higher for carbon S than for carbon C, attributable to the lower oxygen and ash contents of the former.

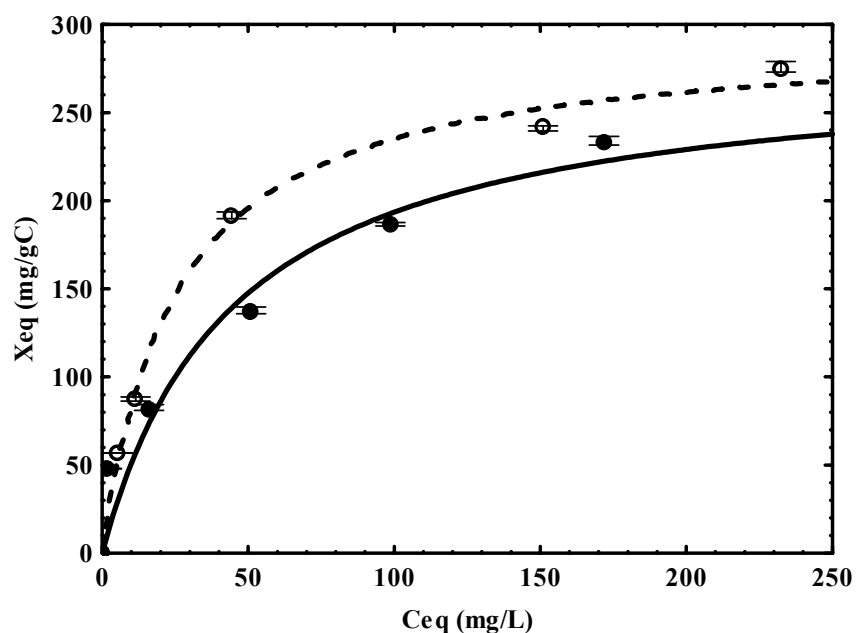
### 3.2. Phthalic acid adsorption process

Figure 2 depicts the PA adsorption isotherms for the two activated carbon samples. They both showed the L form in the classification of Giles et al. [31, 32], indicating that the aromatic ring of the PA molecule is adsorbed parallel to the carbon surface and there is no major competition between PA and water molecules for active adsorption centres on the carbon.

The Langmuir isotherm model was applied to the experimental adsorption isotherm data. It is the most widely used model for this type of process and is represented mathematically as:

$$\frac{C_{\text{eq}}}{X_{\text{eq}}} = \frac{C_{\text{eq}}}{X_m} + \frac{1}{BX_m} \quad (2)$$

where  $C_{eq}$  is the equilibrium concentration (mg/L),  $X_{eq}$  is the amount of adsorbate adsorbed at the equilibrium (mg/g),  $X_m$  is the adsorption capacity (mg/g), and  $B$  is a constant related to the adsorption energy. Langmuir model assumes the presence of a finite number of binding sites, homogeneously distributed over the adsorbent surface, presenting the same affinity for sorption of a single layer, and with no interaction between adsorbent species.



**Figure 2.** Adsorption isotherms of PA on activated carbons S (●) and C (○). pH 4, T 298 K.

Results obtained are shown in Table 6. The adsorption capacity ( $X_m$ ) of the carbon samples was high: 274.5 mg/g for carbon C and 242.9 mg/g for carbon S. Langmuir constant ( $B$ ) values, related to the adsorption energy, and relative affinity ( $BX_m$ ) values were lower than those reported for the adsorption of aromatic compounds on activated carbon [33, 34].

The PA adsorption capacity of the activated carbons was expressed per unit of carbon surface area,  $X'_m$ , to permit comparisons (Table 6). PA adsorption capacity was higher for carbon C than for carbon S, despite the former's lower surface area, external surface

area, water-accessible pore volume, and hydrophobicity. Therefore, the higher adsorption capacity of carbon C may be related to its greater content of phenolic groups (Table 4), which are electronic activators of the aromatic rings of carbon graphene planes, favouring the adsorption of aromatic compounds like PA, which can be adsorbed by dispersion interactions between  $\pi$  electrons of its aromatic ring with  $\pi$  electrons of the carbon graphene planes [35]. Hence, the presence of two electron-withdrawing carboxylic groups in the aromatic ring of PA reduces its electronic density and, therefore, the adsorbent-adsorbate interactions, which may explain the low B values obtained (Table 6).

**Table 6.** Parameters obtained by applying the Langmuir equation to PA adsorption isotherms on activated carbon samples.

| Carbon | $X_m^a$ (mg/g) | $X'_m$ (mg/m <sup>2</sup> ) | $B^b$ (L/mg) | $BX_m^c$ (L·g <sup>-1</sup> ) |
|--------|----------------|-----------------------------|--------------|-------------------------------|
| S      | 242.9 ± 1.6    | 0.20                        | 0.15         | 36.4                          |
| C      | 274.5 ± 1.3    | 0.23                        | 0.08         | 21.6                          |

a)  $X_m$ : Adsorption capacity

b) B: Langmuir constant

c)  $BX_m$ : Adsorbent-adsorbate relative affinity

Because the solution pH during the PA adsorption process was around 4, the charge density of both activated carbon samples was positive ( $pH_{PZC}$  of both activated carbons >4), while the PA molecules were deprotonated and therefore had a negative charge (Figure 1). Under these experimental conditions, attractive electrostatic interactions between adsorbent and adsorbate would be established.

According to the above observations, we conclude that PA adsorption on these activated carbons was largely determined by dispersion and by electrostatic adsorbent-adsorbate interactions.

### 3.3. Influence of both medium pH and solution ionic strength on PA adsorption

Figure 3 shows the influence of solution pH on PA adsorption on both activated carbon samples. The adsorption process was highly dependent on the solution pH, finding that

the adsorption capacity was elevated at acidic pH, markedly decreased with higher pH up to pH 6, and then remained virtually constant at higher pH values.

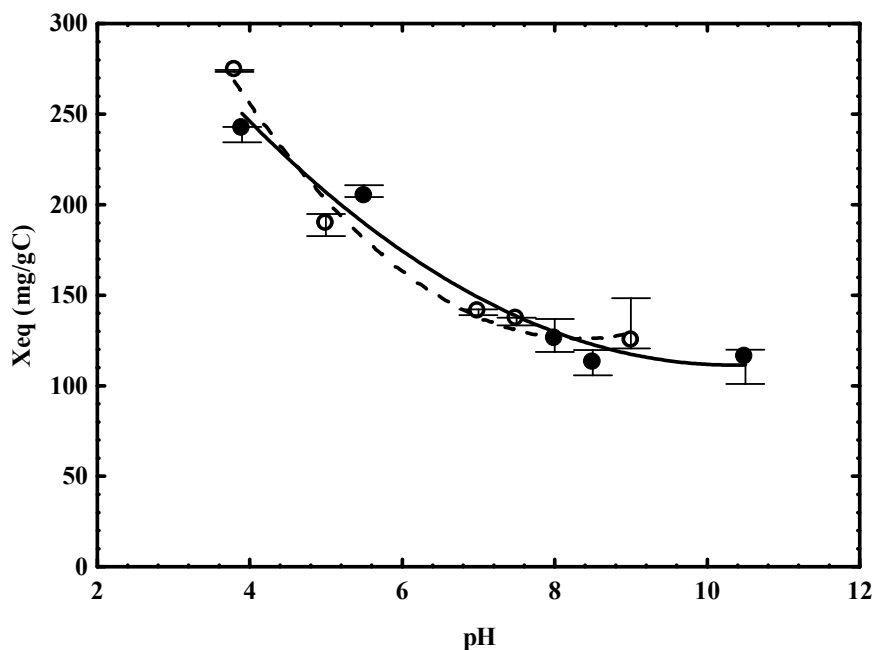


**Figure 3.** PA adsorption capacity of activated carbons S (●) and C (○) as a function of the final solution pH, T 298 K.

Adsorption on activated carbons in aqueous phase is governed by electrostatic and non-electrostatic interactions [33]. The electrostatic interactions mainly derive from the surface charges generated on carbon after water immersion and from the ions in solution [33]. Non-electrostatic interactions are largely of the Van der Waals type [33, 36]. Results in Figure 3 demonstrate that adsorbent-adsorbate electrostatic interactions play a major role in this adsorption process and are affected by the solution pH, which is attributable to two factors: i) the  $\text{pH}_{\text{pzc}}$  of the carbon samples (Table 4), and ii) the species distribution of PA as a function of solution pH (Figure 1). Thus, both activated carbons have a positive charge density at pH values lower than their  $\text{pH}_{\text{pzc}}$  and a negative charge density at higher pH values. PA is deprotonated at  $\text{pH} > 2.90$ ; therefore, PA molecules show a negative charge density at  $\text{pH} > 3$ .

According to the above data, the behavior shown in Figure 3 is due to electrostatic interactions between carbon surface and PA molecules with increased solution pH.

Oxygenated acidic groups on the carbon surface are progressively ionized with higher solution pH, increasing the negative surface charge of the carbon, enhancing repulsive electrostatic carbon-PA interactions, and consequently reducing PA adsorption.

The solution ionic strength can influence the adsorption yield of electrolytes [33, 37]. Figure 4 depicts the results of PA adsorption on the activated carbon samples in the presence of an increasing NaCl concentration at a solution pH of around 4 (no reagents were added to control this pH). As shown, the presence of ionic strength in solution did not have a major influence on PA adsorption. The slight decrease in PA adsorption observed with the presence of NaCl in solution may be due to a screening effect [37] between the positively charged activated carbon surface and the PA molecule, which is negatively charged at the working pH.

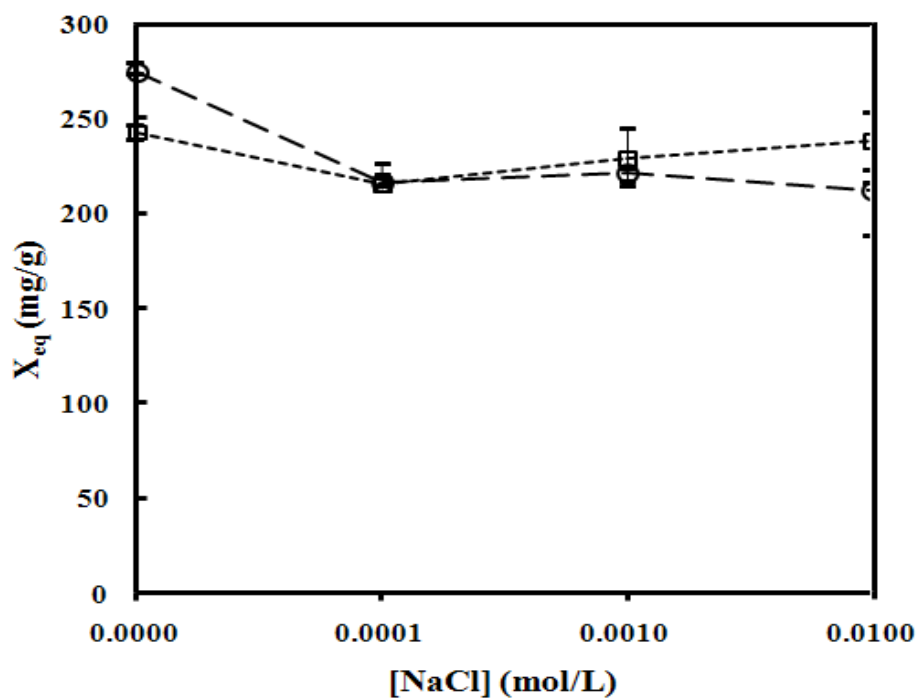


**Figure 4.** PA adsorption capacity of activated carbons S (□) and C (○) as a function of ionic strength. pH 4, T 298 K.

### 3.4. Influence of the presence of microorganisms on PA adsorption (bioadsorption)

The presence of microorganisms has a major influence on the effectiveness of activated carbon in water treatments because they can be adsorbed on the carbon and form

bacteria colonies on its surface (biological activated carbon) [38, 39]. Their presence on the carbon surface can have beneficial effects, including: 1) prolongation of carbon bed life by transforming organic biodegradable matter into biomass, carbon dioxide, and waste products, thereby avoiding carbon saturation [39]; and 2) formation by the adsorbed microorganisms of a biofilm that changes the texture of the carbon and its surface charge, which can improve the adsorption of some cation/metal contaminants [38]. Bacteria range in size from 0.3 to 30  $\mu\text{m}$  [40, 41], therefore their adsorption on the carbon has a direct effect on the largest micropores, although they also exert an indirect effect by blocking the entrance of smaller pores.

Figure 5 depicts the adsorption/bioadsorption isotherms of PA on carbon S in the presence and absence of microorganisms. Application of the Langmuir equation to these isotherms (Table 7) showed that the presence of microorganisms during PA adsorption increased the adsorption capacity of carbon S by 15% and slightly enhanced the adsorbate-adsorbent relative affinity value ( $BX_m$ ) by around 3%. PA biodegradation kinetics with the bacteria under study were investigated before obtaining the bioadsorption isotherms, observing a slight biodegradation (around 5 mg of PA per mL of bacteria solution) of this compound under the present experimental conditions.

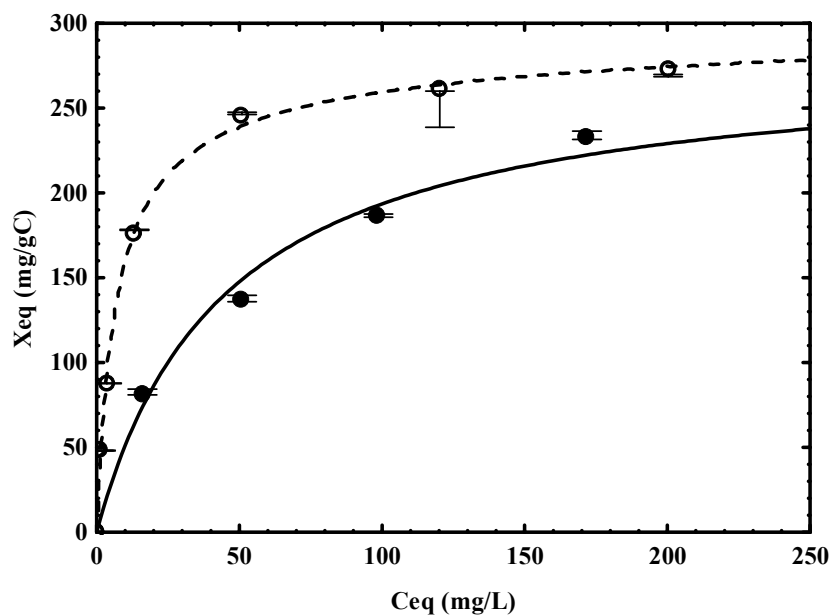


**Figure 5.** Adsorption isotherms of PA on carbon S in the presence (○) and absence (●) of microorganisms. pH 4, T 298 K.

**Table 7.** Results obtained by applying the Langmuir equation to PA adsorption isotherms on carbon S in the presence and absence of microorganisms.

| Activated<br>carbon | Without Bacteria |                 | With bacteria   |                 |
|---------------------|------------------|-----------------|-----------------|-----------------|
|                     | $X_m$<br>(mg/g)  | $BX_m$<br>(L/g) | $X_m$<br>(mg/g) | $BX_m$<br>(L/g) |
| S                   | 242.9±1.6        | 36.4            | 279.5±2.5       | 37.5            |

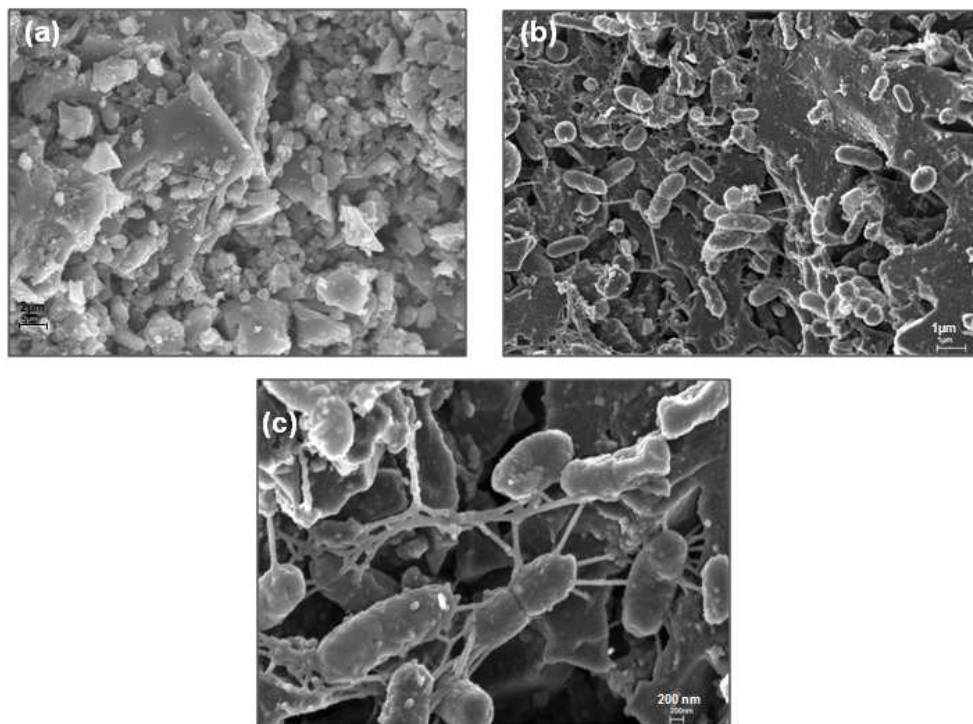
According to previous reports [38, 39], the effects of microorganism adsorption on the chemical and textural properties of activated carbon S include: i) a decreased external surface area, due to pore blocking; and ii) a reduced  $pH_{PZC}$  value, increasing the negative charge density on the activated carbon surface. Moreover, because the external walls of bacteria are formed by phospholipids [42, 43], their adsorption on activated carbon (Figure 6) increases the hydrophobicity of the carbon surface. The results depicted in Figure 5 and Table 7 may be explained by this increased hydrophobicity of the activated carbon surface, known to considerably favour the adsorption of pollutants in aqueous phase. Moreover, bacteria on activated carbon produced extracellular polymeric substances (Figure 6, b and c) that could be involved in PA adsorption.

### 3.5. Influence of the chemical characteristics of the water matrix on PA adsorption

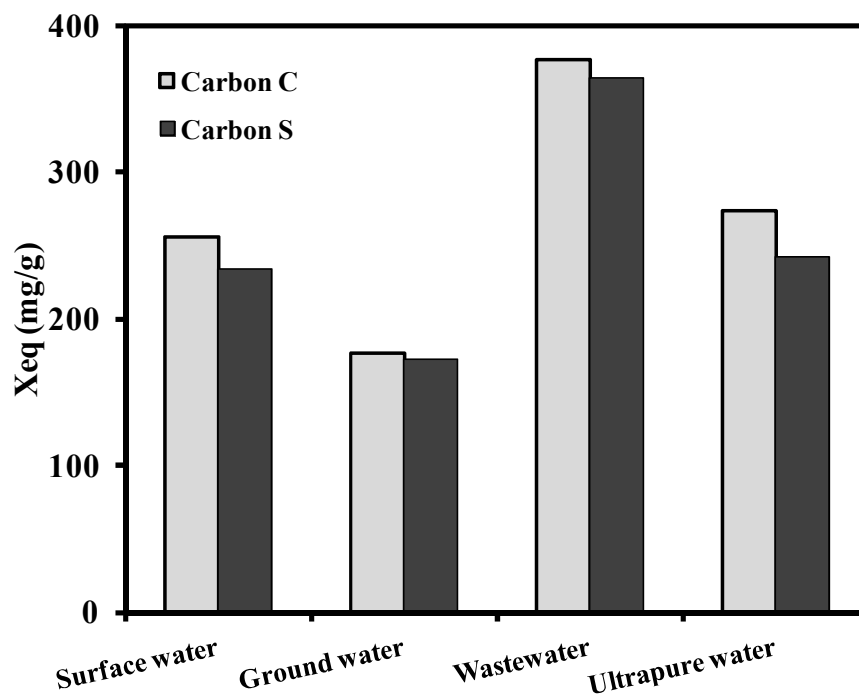
Table 2 lists the chemical characteristics of the four types of water (ultrapure water, surface water, ground water, and wastewater) used to determine their influence on PA adsorption on activated carbon. The wastewater contained a large amount of organic matter (high TOC concentration), while the surface, ground, and waste waters had high concentrations of calcium and magnesium ions and the ground water showed a high degree of mineralization, with elevated electric conductivity and hardness values.

Figure 7 depicts the capacity of the two activated carbons to adsorb PA as a function of the type of water. The adsorption capacity of carbon C was higher than that of S in all four water types and varied as a function of water type in the order: ground water < surface water  $\approx$  ultrapure water < wastewater.





**Figure 6.** SEM images of carbon S before and after PA bioadsorption. a) Carbon S; b) and c) Carbon S + bacteria + PA.



**Figure 7.** Adsorption capacity of PA on activated carbons S and C in difference water types.

The elevated PA removal from the wastewater can be attributed to the formation of organic phthalates with a low water solubility [44], which is increased by the presence of a high concentration of organic matter (Table 2). PA removal may also be enhanced by the formation of complex species [45] from reactions of phthalate anions and metal cations present in wastewater.

### 3.6. PA adsorption on activated carbon in dynamic regime

Figure 8 depicts the breakthrough curves for PA adsorption on columns of activated carbons S and C. These curves were used [20-23] to determine the characteristics of the columns, which are exhibited in Table 8. In both activated carbon samples, the amount of PA adsorbed at the breakthrough point of the column ( $X_{0.02}$ ) was much lower than that obtained from the isotherms in static regime (Table 6). This less effective adsorption in dynamic versus static regime can be attributed to problems of PA diffusion to the interior of carbon pores and the shorter adsorbent-adsorbate contact time in dynamic regime.

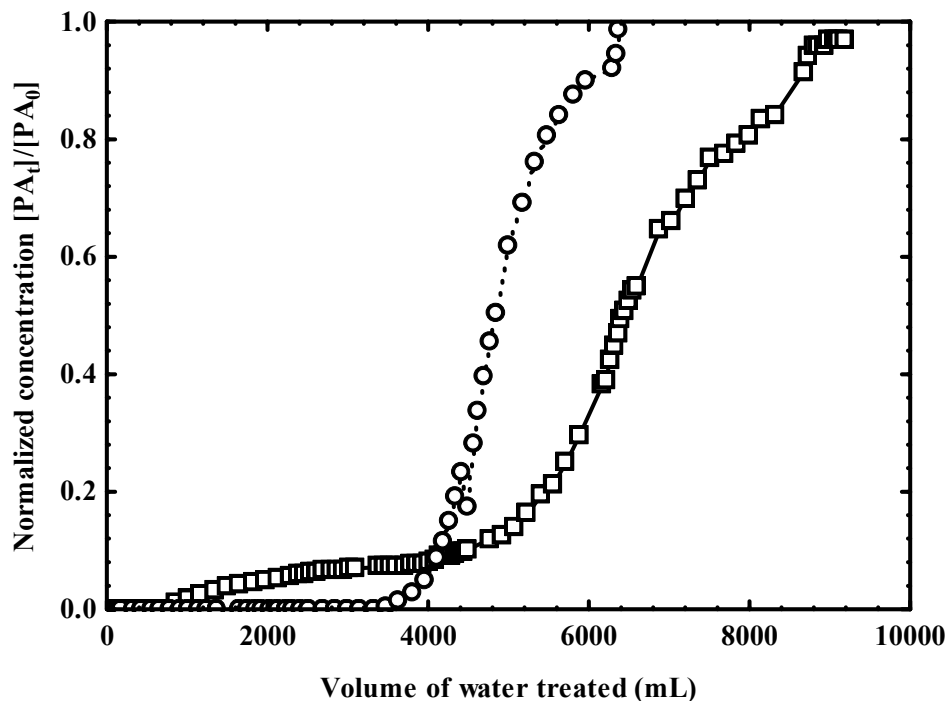


**Figure 8.** Breakthrough curves for PA adsorption on activated carbons S (□) and C (○) in ultrapure water. T 298 K, pH 4.

Comparison between the characteristics of the columns (Table 8) reveals that the volume treated at the breakthrough point of the column ( $V_{0.02}$ ), i.e., the amount of PA adsorbed at this point ( $X_{0.02}$ ), was much higher for carbon C than for carbon S: this confirms the finding in static regime of a much higher adsorption capacity for carbon C than for carbon S. In addition, the height of the mass transference zone of the bed was lower for carbon C than for carbon S, indicating that the water treatment was more effective with carbon C than with carbon S, as confirmed by the higher degree of utility of carbon C bed (81.5%) than of carbon S bed (17.6%). These are highly relevant findings from an application standpoint, indicating that carbon C can be used as column bed for the effective removal of PA from aqueous solution.

**Table 8.** PA adsorption characteristics of the activated carbon columns.

| Carbon | $X_{0.02}$ <sup>a)</sup><br>(mg/g) | $V_{0.02}$ <sup>b)</sup><br>(mL) | $\Phi$ <sup>c)</sup> | $H_{MTZ}$ <sup>d)</sup><br>(cm) | $R_{MTZ} \times 10^2$ <sup>e)</sup><br>(cm/min) | $Du$ <sup>f)</sup><br>(%) |
|--------|------------------------------------|----------------------------------|----------------------|---------------------------------|---|---------------------------|
| S      | 50.3                               | 1016.0                           | 0.75                 | 7.37                            | 0.17  | 17.6                      |
| C      | 176.2                              | 3801.6                           | 0.62                 | 2.33                            | 0.22  | 81.5                      |

a)  $X_{0.02}$ : Amount of PA adsorbed at the breakthrough point of the column.

b)  $V_{0.02}$ : Volume treated at the breakthrough point of the column.

c)  $\Phi$ : Fractional capacity of the mass transference zone.

d)  $H_{MTZ}$ : Height of the mass transference zone.

e)  $R_{MTZ}$ : Rate of movement of the mass transfer zone.

f)  $Du$ : Degree of utility.

#### 4. CONCLUSIONS

The high PA adsorption capacity of the activated carbon samples used in this study is largely attributable to dispersion and electrostatic adsorbent-adsorbate interactions. The PA adsorption process is highly dependent on the solution pH, with an elevated capacity at acidic pH that markedly reduces with increased pH up to pH 6 and then remains practically constant at higher pH values. This behavior is explained by the electrostatic interactions between carbon surface and PA molecules with increased solution pH. The presence of ionic strength in solution does not have a major influence on PA adsorption; a slight decrease observed when NaCl is present in solution may be due to a screening

effect between the positively charged activated carbon surface and the PA molecule, which is negatively charged at the working pH.

The presence of microorganisms during PA adsorption increases the adsorption/bioadsorption capacity of activated carbon by around 15% and slightly enhances the adsorbate-adsorbent relative affinity values (by ~ 3%.) These results can be explained by an increase in carbon surface hydrophobicity produced by adsorption of the bacteria. PA removal varies as a function of the water type, increasing in the order: ground water < surface water  $\simeq$  ultrapure water < wastewater. The high removal of PA from wastewater would be due to the formation of organic phthalates and complex species. The adsorption yield is much lower in dynamic versus static regime, attributable to difficulties of PA diffusion into the carbon pores and the shorter adsorbent-adsorbate contact time in dynamic regime.

From all these results we can conclude that the system based on the use of activated carbons is appropriate to treat natural water and wastewater contaminated with phthalic acid which is extensively adsorbed on these carbons. Our recommendation is to use activated carbons with both a high content of phenolic groups and a negative charge density at the working experimental conditions, as well as to carry out this treatment at acidic pH.

## 5. REFERENCES

- [1] M. Castillo D. Barceló, *Anal. Chim. Acta.* 426 (2001) 253.
- [2] I.D. Nascimento Filho, C. von Mühlen, P. Schossler, E. Bastos Caramão, *Chemosphere* 50 (2003) 657.
- [3] M.J. Bauer, R. Herrmann, *Sci. Total Environ.* 208 (1997) 49.
- [4] D. Wu, B. Hu, P. Zheng, M. Qaisar, *J. Environ. Sci. (China)*. 19 (2007) 1252.
- [5] W. Jianlong, C. Lujun, S. Hanchang, Q. Yi, *Chemosphere* 41 (2000) 1245.
- [6] W.J. Kozumbo, R. Kroll, R.J. Rubin, *Environ. Health Perspect.* 45 (1982) 103.
- [7] J.E. Huff, W.M. Kluwe, *Prog. Clin. Biol. Res.* 141 (1984) 137.
- [8] Z. Zheng, H. Zhang, P. He, L. Shao, Y. Chen, L. Pang, *Chemosphere* 75 (2009) 180.
- [9] M.J. Bauer, R. Herrmann, A. Martin, H. Zellmann, *Water Sci. Technol.* 38 (1998) 185.
- [10] G. Mailhot, M. Sarakha, B. Lavedrine, J. Cáceres, S. Malato, *Chemosphere* 49 (2002) 525.
- [11] A. Imai, K. Onuma, Y. Inamori, R. Sudo, *Environ. Technol.* 19 (1998) 213.
- [12] F. Kargi, M. Yunus Pamukoglu, *Process Biochem.* 38 (2003) 1413.
- [13] S. Venkata Mohan, S. Shailaja, M. Rama Krishan, P.N. Sarma, *J. Hazard. Mater.* 122 (2007) 278.
- [14] C. Zhang, Y. Wang, *Waste Manage.* 29 (2009) 110.
- [15] E. Ayrançi, E. Bayram, *J. Hazard. Mater.* 122 (2005) 147.
- [16] M. Sánchez-Polo, J. Rivera-Utrilla, *Carbon* 41 (2003) 303.

- [17] J. Rivera-Utrilla, M. Sánchez-Polo, *Langmuir* 20 (2004) 9217.
- [18] M.I. Bautista-Toledo, J.D. Mendez-Díaz, M. Sánchez-Polo, J. Rivera-Utrilla, M.A. Ferro-García, *J. Colloid Interface Sci.* 317 (2008) 11.
- [19] D.J. Brenner, N.R. Krieg, J.T. Staley, G.M. Garrity, *Bergey's Manual of Systematic Bacteriology*, Springer, New York, 2005.
- [20] J. S. Zogorski, S. D. Faust, in: P. H. Cheremisinoff, E. Ellerbusch (Eds.), *Carbon Adsorption Handbook*, Ann Arbor Science, Michigan, 1978, p. 753.
- [21] M.A. Ferro-García, F. Carrasco-Marín, J. Rivera-Utrilla, E. Utrera-Hidalgo, C. Moreno-Castilla, *Carbon* 28 (1990) 91.
- [22] M.A. Ferro-García, J. Rivera-Utrilla, M.I. Bautista-Toledo, M.D. Mingorance, *Carbon* 28 (1990) 545.
- [23] J. Rivera-Utrilla, G. Prados-Joya, M. Sánchez-Polo, M.A. Ferro-García, M.I. Bautista-Toledo, *J. Hazard. Mater.* 170 (2009) 298.
- [24] APHA, AWWA, WPCF. American water works Association; and Water Pollution Control Federation, Washington DC, 1998.
- [25] J. Garrido, A. Linares-Solano, J.M. Martín-Martínez, M. Molina-Sabio, F. Rodríguez-Reinoso, R. Torregrosa, *Langmuir* 3 (1987) 76.
- [26] F. Rodríguez-Reinoso, A. Linares-Solano, in: P.A. Thrower (Ed.), *Microporous Structure of Activated Carbons as Revealed by Adsorption Methods*, Marcel Dekker, New York, 1988, p. 18.
- [27] M.V. López-Ramón, F. Stoeckli, C. Moreno-Castilla, F. Carrasco-Marín, *Carbon* 37 (1999) 1215.
- [28] M.V. López-Ramón, F. Stoeckli, C. Moreno-Castilla, F. Carrasco-Marín, *Carbon* 38 (2000) 825.

- [29] R.H. Bradley, I. Sutherland, E. Sheng, *J. Chem. Soc., Faraday Trans.* 91 (1995) 3201.
- [30] S.S. Barton, M.J.B. Evans, J.A.F. MacDonald, *Langmuir* 10 (1994) 4250.
- [31] C.H. Giles, D. Smith, A. Huitson, *J. Colloid Interface Sci.* 47 (1974) 755.
- [32] C.H. Giles, D. Smith, A. Huitson, *J. Colloid Interface Sci.* 47 (1974) 766.
- [33] L.R. Radovic, C. Moreno-Castilla, J. Rivera-Utrilla, in: L.R. Radovic (Ed.), *Chemistry and physics of carbon*, Marcel Dekker, New York, 2001, p. 227.
- [34] R. Xu, Y. Wang, D. Tiwari, H. Wang, *J. Environ. Sci.* 21 (2009) 927.
- [35] R. W. Coughlin, F. S. Ezra, *Environ. Sci. Technol.* 2 (1968) 291.
- [36] J. Lyklema, *Solid-liquid interfaces: Fundamentals of interface and colloid science*, Academic press, New York, 1995.
- [37] M.V. López-Ramón, C. Moreno-Castilla, J. Rivera-Utrilla, R.L. Radovic, *Carbon* 41 (2002) 2009.
- [38] J. Rivera-Utrilla, M.I. Bautista-Toledo, M.A. Ferro-Garcia, C. Moreno-Castilla, *Carbon* 41 (2003) 323.
- [39] J. Rivera-Utrilla, M.I. Bautista-Toledo, M.A. Ferro-García, C. Moreno-Castilla, *J. Chem. Technol. Biotechnol.* 76 (2001) 1209.
- [40] D.P. Wilcox, R. Chang, K.L. Dickson, K.R. Johansson, *Appl. Environ. Microbiol.* 46 (1983) 406.
- [41] T.J. Beveridge, R.J. Doyle, *Metal Ions and Bacteria*, John Wiley & Sons, New York, 1989.
- [42] M.N. Hughes, R.K. Poole, *J. Gen. Microbiol.* 137 (1991) 725.

- 
- [43] H. Mikaido, H. Vaara, in: F.C. Neidhardt (Ed.), *Cellular and Molecular Biology*, American Society for Microbiology, Washington D.C, 1987, p 3.
- [44] J. Ejlertsson, M. Alnervik, S. Jonsson, B. H. Svensson, *Environ. Sci. Technol.* 31 (1997) 2761.
- [45] R. Ghosh, V.S.K. Nair, *J. Inorg. Nucl. Chem.* 32 (1970) 3033.
- [46] M. M. Dubinin, *Carbon* 23 (1985) 373.





## CAPÍTULO 4

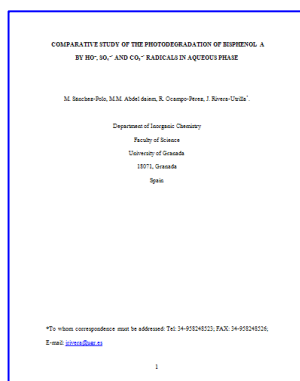
# ESTUDIO COMPARATIVO DE LA FOTODEGRADACIÓN DEL BISFENOL A CON RADICALES $\text{HO}^\bullet$ , $\text{SO}_4^{\bullet-}$ , Y $\text{CO}_3^{\bullet-}/\text{HCO}_3^\bullet$ EN FASE ACUOSA





# COMPARATIVE STUDY OF THE PHOTO-DEGRADATION OF BISPHENOL A BY HO<sup>•</sup>, SO<sub>4</sub><sup>•-</sup> AND CO<sub>3</sub><sup>•-</sup>/HCO<sub>3</sub><sup>•</sup> RADICALS IN AQUEOUS PHASE

Manuscript submitted for publication



## Highlights

- Removal of Bisphenol A (BPA) using UV, UV/H<sub>2</sub>O<sub>2</sub>, UV/K<sub>2</sub>S<sub>2</sub>O<sub>8</sub>, or UV/Na<sub>2</sub>CO<sub>3</sub> was studied.
- The reaction rate constants between BPA and HO<sup>•</sup>, SO<sub>4</sub><sup>•-</sup>, and CO<sub>3</sub><sup>•-</sup>/HCO<sub>3</sub><sup>•</sup> were obtained.
- Both the solution pH and temperature had a major effect on BPA photodegradation.
- The UV/K<sub>2</sub>S<sub>2</sub>O<sub>8</sub> system was the most efficient to remove and mineralize BPA.
- The three oxidation systems showed 100% effectiveness to remove BPA from wastewater.

## ABSTRACT

The aim of this study was to determine the effectiveness of oxidation processes based on UV radiation (UV, UV/H<sub>2</sub>O<sub>2</sub>, UV/K<sub>2</sub>S<sub>2</sub>O<sub>8</sub>, and UV/Na<sub>2</sub>CO<sub>3</sub>) to remove Bisphenol A (BPA) from aqueous solution. Results showed that UV radiation was not effective to remove BPA from the medium, due to its low quantum yield ( $\Phi_{\lambda} = 2.37 \times 10^{-6}$  mol/Einstein). The addition of radical promoters such as H<sub>2</sub>O<sub>2</sub>, K<sub>2</sub>S<sub>2</sub>O<sub>8</sub>, or Na<sub>2</sub>CO<sub>3</sub> markedly increased the effectiveness of UV radiation through the generation of HO<sup>•</sup>, SO<sub>4</sub><sup>•-</sup>, or CO<sub>3</sub><sup>•-</sup>/HCO<sub>3</sub><sup>•</sup> radicals, respectively. The reaction rate constants between BPA and HO<sup>•</sup>, SO<sub>4</sub><sup>•-</sup>, and CO<sub>3</sub><sup>•-</sup>/HCO<sub>3</sub><sup>•</sup> radicals were  $k_{\text{HO}^{\bullet}\text{BPA}} = 1.70 \pm 0.21 \times 10^{10} \text{ M}^{-1} \text{ s}^{-1}$ ,  $k_{\text{SO}_4^{\bullet-}\text{BPA}} = 1.37 \pm 0.15 \times 10^9 \text{ M}^{-1} \text{ s}^{-1}$ , and  $k_{\text{CO}_3^{\bullet-}/\text{HCO}_3^{\bullet}\text{BPA}} = 3.89 \pm 0.09 \times 10^6 \text{ M}^{-1} \text{ s}^{-1}$ , respectively. Regardless of the system considered, the results obtained showed that the BPA degradation rate was higher with lower BPA concentrations. The solution pH had a major effect on BPA degradation with the UV/H<sub>2</sub>O<sub>2</sub>, UV/K<sub>2</sub>S<sub>2</sub>O<sub>8</sub>, and UV/Na<sub>2</sub>CO<sub>3</sub> systems. The BPA photooxidation was enhanced at higher temperatures with UV/K<sub>2</sub>S<sub>2</sub>O<sub>8</sub> systems but decreased with UV/H<sub>2</sub>O<sub>2</sub> and UV/Na<sub>2</sub>CO<sub>3</sub> systems. All oxidation systems in this study showed 100% effectiveness to remove BPA from wastewater, due to its large content of natural organic matter (NOM), which can absorb UV radiation and generate excited triplet states (<sup>3</sup>NOM\*) and various reactive oxygen species. The lowest BPA degradation was detected in ground water, due to its higher content of metal species and bicarbonate ions, which act as radical scavengers. With all three systems, the total organic carbon in the medium was markedly decreased after five minutes of treatment. The toxicity of byproducts was higher than that of BPA when using UV/H<sub>2</sub>O<sub>2</sub>, similar to that of BPA with the UV/Na<sub>2</sub>CO<sub>3</sub> system, and lower than that of BPA after 40 min of treatment with the UV/K<sub>2</sub>S<sub>2</sub>O<sub>8</sub> system.



## 1. INTRODUCTION

Endocrine-disrupting chemicals (EDCs) have attracted considerable attention due to their adverse health and ecological effects. EDCs mimic hormonal activity and interfere with endocrine system functions [1]. EDCs are associated with various adverse effects, including spontaneous abortion, neural behavioral disorders, impaired immune function, and some cancers [1].

Bisphenol A (BPA), considered representative of EDCs, causes reproductive damage to aquatic organisms and is widely used as a raw material in the production of polycarbonate plastics and epoxy resins. Because of its wide applications, there is increasing interest in effective remediation technologies to remove BPA from contaminated waters [2]. It has been detected in all types of environmental waters, in concentrations up to 17.2 mg/L in hazardous waste landfill leachate [3], 12 µg/L in stream water [4], and 0.1 µg/L in drinking water [5].

Various techniques have been examined for the removal of BPA from aqueous solution by physical, chemical, and biological processes [3, 6, 7]. Biological treatment is effective to eliminate only very low concentrations of BPA from aqueous solution and requires a long treatment time [8-10].

Technologies based on advanced oxidation processes (AOPs) have proven highly effective to degrade organic compounds in aqueous solution. AOPs generate species with high oxidizing power (e.g., HO• radicals) that interact with the pollutant and degrade it into byproducts with lower molecular weight, and they can even achieve its complete mineralization.

Hydroxyl radicals have been used to eliminate BPA from aqueous phase in various studies. Rosenfeldt et al. [11] used ultraviolet radiation (UV) combined with H<sub>2</sub>O<sub>2</sub> and reported that BPA degradation was more effective with the UV/H<sub>2</sub>O<sub>2</sub> system than with direct photolysis, obtaining a reaction rate constant of hydroxyl radical (HO•) with BPA of  $1.02 \pm 0.23 \times 10^{10} \text{ M}^{-1}\text{s}^{-1}$ . Rivas et al. [12] studied both the elimination and

mineralization of BPA with multiple technologies, i.e., UV, O<sub>3</sub>, UV/O<sub>3</sub>, UV/O<sub>3</sub>/carbon, UV/O<sub>3</sub>/TiO<sub>2</sub>, and UV/O<sub>3</sub>/TiO<sub>2</sub>/carbon. They found that ozonation or photooxidation effectively remove BPA from water but that the mineralization levels are rather low, whereas the combination of O<sub>3</sub>/UV/carbon completely mineralized the organic matter. Katsumata et al. [13] studied the photodegradation of BPA in the presence of the Fenton reagent and found the degradation rate to be strongly influenced by the solution pH and the initial H<sub>2</sub>O<sub>2</sub> and Fe (II) concentrations. Total BPA degradation was achieved after 9 min of treatment under optimal conditions, and the formation of CO<sub>2</sub> due to BPA mineralization was observed during the photo-Fenton process, with >90% conversion of BPA to CO<sub>2</sub> after 36 h of treatment.

Unlike the hydroxyl radical, the sulfate and carbonate radicals are selective transient species against organic compounds with a high oxidization potential ( $E^0 = 2.6 \text{ V}$  and  $E^0 = 1.78 \text{ V}$ , respectively). The most frequent methods to generate sulfate radicals,  $\text{SO}_4^{\bullet-}$ , are by the photochemical, thermal, or chemical decomposition of  $\text{S}_2\text{O}_8^{2-}$ . The  $\text{CO}_3^{\bullet-}/\text{HCO}_3^{\bullet}$  radical is usually formed *via* a reaction between bi/carbonate ions and hydroxyl radicals or by quenching the aromatic ketone triplet excited state [14, 15].

Various studies have found the UV/K<sub>2</sub>S<sub>2</sub>O<sub>8</sub> system to be more effective than the UV/H<sub>2</sub>O<sub>2</sub> system to treat organic compounds in aqueous solution, offering a higher percentage degradation within a shorter treatment time and reducing the medium toxicity to a greater extent [16, 17]. For its part, the carbonate radical is one of the most extensively studied inorganic radicals, due to its ubiquitous nature in the environment and relatively long lifetime. However, there has been little research on the use of this radical species to degrade organic compounds [18].

With this background, the main aim of this study was to investigate the effectiveness of  $\text{HO}^{\bullet}$ ,  $\text{SO}_4^{\bullet-}$ , and  $\text{CO}_3^{\bullet-}/\text{HCO}_3^{\bullet}$  radicals in the photodegradation of BPA in aqueous solution, studying the influence of some operational parameters, i.e., initial concentration of BPA, initial concentration of H<sub>2</sub>O<sub>2</sub>, K<sub>2</sub>S<sub>2</sub>O<sub>8</sub> or Na<sub>2</sub>CO<sub>3</sub>, solution pH, temperature, and chemical composition of the water. A further aim was to determine the

variation in the total organic carbon and in the toxicity of BPA photodegradation byproducts during these treatments.

## 2. MATERIALS AND METHODS

### 2.1. Reagents

All reagents used in the present study (atrazine, hydrogen peroxide ( $\text{H}_2\text{O}_2$ ), potassium peroxydisulfate ( $\text{K}_2\text{S}_2\text{O}_8$ ), sodium carbonate ( $\text{Na}_2\text{CO}_3$ ), sodium dihydrogen phosphate ( $\text{NaH}_2\text{PO}_4$ ), disodium hydrogen phosphate ( $\text{Na}_2\text{HPO}_4$ ), bisphenol A, phosphoric acid, and methanol) were high-purity analytical grade reagents supplied by Sigma-Aldrich. All solutions were prepared with ultrapure water obtained from Milli-Q<sup>®</sup> equipment (Millipore). Figure 1 depicts the molecular structure and species distribution diagram of BPA as a function of solution pH.

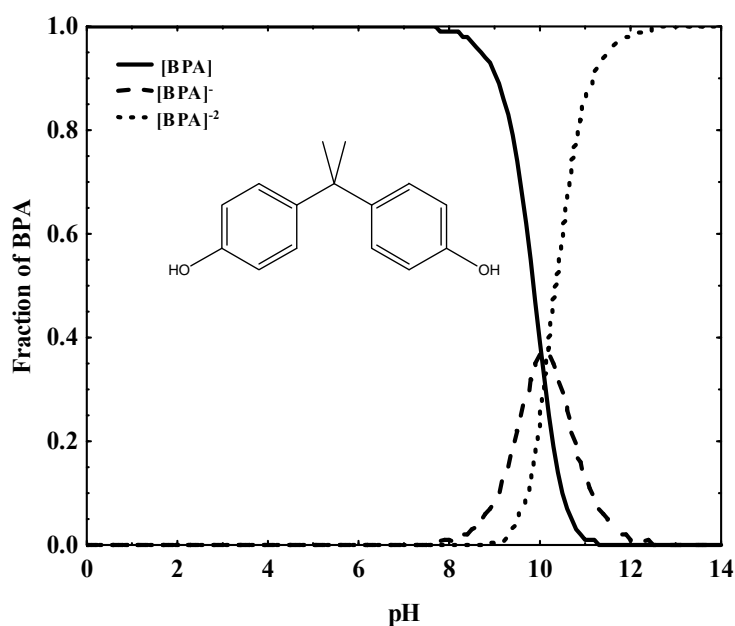


**Figure 1.** Molecular structure and species distribution of BPA as a function of solution pH.

### 2.2. Experimental methodology

BPA degradation experiments were conducted in a photoreactor formed of concentric tubes: a stainless steel outer tube (inner diameter [i.d.] of 13 cm x height of 18 cm) and



quartz inner tube (i.d. of 5.5 cm x height of 23 cm). The inner tube is equipped with a medium pressure mercury lamp (Heraeus Noblelight TQ718-700W) emitting in a range from 238 to 334 nm. The irradiating intensity of the lamp ( $I_0 = 3.75 \times 10^{-7}$  Einstein  $s^{-1}$ ) was measured by using atrazine as the actinometer according to the procedures reported by Canonical et al. [19]. In the annular space of the photoreactor there is a sample holder with a capacity for six quartz reaction tubes (i.d. of 1.6 cm  $\times$  height of 20 cm, with capacity  $\approx$  40 mL). Solutions in reaction tubes were maintained at constant temperature by using a Frigiterm ultrathermostat, and they were kept in agitation by means of a magnetic agitation system.

### 2.3. Bisphenol A degradation by UV, UV/H<sub>2</sub>O<sub>2</sub>, UV/K<sub>2</sub>S<sub>2</sub>O<sub>8</sub>, and UV/Na<sub>2</sub>CO<sub>3</sub> systems

BPA photodegradation experimental data were obtained as follows: a concentrated (100 mg/L) BPA solution was prepared by adding 0.1 g of BPA to a 1 L flask and filling with ultrapure water. An aliquot (15.0 to 29.4 mL) of ultrapure water was placed in the reaction tubes, and an aliquot (15.0 to 0.6 mL) of concentrated BPA solution was added to obtain a total volume of 30 mL at the desired initial concentration. Several samples were drawn from the reactor at regular time intervals to measure the BPA concentration, total organic carbon (TOC), and toxicity of photodegradation byproducts as a function of treatment time.

Reaction rate constants of BPA with HO $\bullet$ , SO<sub>4</sub> $\bullet^-$ , and CO<sub>3</sub> $\bullet^-$ /HCO<sub>3</sub> $\bullet^-$  radicals were determined by competitive kinetic experiments using atrazine (Atr) as reference compound ( $k_{HO\bullet atr} = 1.80 \times 10^{10}$  M<sup>-1</sup> s<sup>-1</sup>,  $k_{SO_4\bullet^- atr} = 1.4 \times 10^9$  M<sup>-1</sup> s<sup>-1</sup>, and  $k_{CO_3\bullet^-/HCO_3\bullet^- atr} = 1.60 \times 10^7$  M<sup>-1</sup> s<sup>-1</sup>) [18, 20, 21]. For these experiments, 2.5, 5.0 or 10.0 mg/L BPA was photooxidized in the presence of 5.0 mg/L of Atr and 1000  $\mu$ M of H<sub>2</sub>O<sub>2</sub>, K<sub>2</sub>S<sub>2</sub>O<sub>8</sub>, or Na<sub>2</sub>CO<sub>3</sub>. Then, the concentrations of BPA and Atr were obtained at different treatment time intervals and the rate constants  $k_{HO\bullet BPA}$ ,  $k_{SO_4\bullet^- BPA}$ , and  $k_{CO_3\bullet^-/HCO_3\bullet^- BPA}$  were calculated using the following equation:

$$k_{\text{rad BPA}} = k_{\text{radAtr}} \times \left[ \frac{\text{Ln} \left( \frac{[\text{BPA}]_t}{[\text{BPA}]_0} \right)}{\text{Ln} \left( \frac{[\text{Atr}]_t}{[\text{Atr}]_0} \right)} \right] \quad (1)$$

Natural water samples (ground and surface waters) from a drinking water treatment plant and wastewater samples from a wastewater treatment plant were supplied by *Aguas y Servicios de la Costa Tropical de Granada* in Motril (Granada). Standard methods [22] were used to determine their characteristics, which are listed in Table 1. After their characterization, samples were filtered and stored in cold until their use as media for the BPA photodegradation experiments.

**Table 1.** Chemical characteristics of different water types.

| <b>Water</b>           | <b>pH</b> | <b>TOC<br/>(mg/L)</b> | <b>[Ca<sup>2+</sup>]<br/>(meq/L)</b> | <b>[Mg<sup>2+</sup>]<br/>(meq/L)</b> | <b>[HCO<sub>3</sub><sup>-</sup>]<br/>(meq/L)</b> | <b>T %<sup>a)</sup></b> |
|------------------------|-----------|-----------------------|--------------------------------------|--------------------------------------|--|-------------------------|
| <b>Ultrapure water</b> | 6.8       | 0.0                   | 0.0                                  | 0.0                                  | 0.0  | 100                     |
| <b>Surface water</b>   | 8.3       | 14.9                  | 1.6                                  | 1.1                                  | 6.4  | 97                      |
| <b>Ground water</b>    | 7.6       | 29.7                  | 2.5                                  | 2.2                                  | 8.8  | 99                      |
| <b>Wastewater</b>      | 7.8       | 88.9                  | 2.1                                  | 1.5                                  | 7.2  | 64                      |

<sup>a)</sup> Transmittance % at 271 nm

#### 2.4. Analytical methods

The solution pH was adjusted to the desired value by addition of phosphoric acid, sodium dihydrogen phosphate, and/or disodium hydrogen phosphate. The pH was measured with a pH meter (CRISON micropH 2002).

BPA and Atr concentrations were determined using a high performance liquid chromatography (HPLC) (Thermo-Fisher) equipped with a UV-detector and autosampler with capacity for 120 vials. The column used was Nova-Pak® C<sub>18</sub> (4 μm particular size and 3.9×150 mm). Five-point linear standard calibration curves were measured before and periodically during the period of analyses to verify the stability of

the system. Triplicate samples were prepared and analyzed for each experimental condition.

The mobile phase for BPA was 50% of 0.4% phosphoric acid solution v/v and 50% methanol in isocratic mode at flow of 1.5 mL/min, detector wavelength was set at 270 nm, and injection volume of BPA was 100  $\mu$ L. For atrazine, it was 50% 1 mM ammonium acetate solution and 50% acetonitrile in isocratic mode at flow of 1 mL/min, with detector wavelength set at 226 nm and injection volume at 20  $\mu$ L.

Total organic carbon (TOC) present in the medium was determined by using a Shimadzu V-CSH analyzer with ASI-V autosampler, calculating the TOC in the water samples by subtracting the inorganic carbon (IC) value from the total carbon (TC) value. The TC value was determined by injecting the water sample (1.20 mL) into a reaction chamber (at 680°C) filled with oxidant catalyst; under these conditions, the organic carbon and IC are both transformed into CO<sub>2</sub>, which was measured with a non-dispersive infrared detector. The IC was determined by injecting the water sample (1.20 mL) into another reaction chamber under acid conditions; in this situation, IC alone is transformed into CO<sub>2</sub>, which was measured with an infrared detector. Analyses of TC and IC were performed in triplicate to ensure the correct TOC value was obtained.

Degradation byproducts were determined after 60 min of treatment with the UV/H<sub>2</sub>O<sub>2</sub>, UV/K<sub>2</sub>S<sub>2</sub>O<sub>8</sub>, or UV/Na<sub>2</sub>CO<sub>3</sub> systems with an initial BPA concentration of 50 mg/L at 25 °C and pH = 7. BPA degradation by-products were separated from the water by using an UPLC (Waters, USA) equipped with a C<sub>18</sub> analytical column (2.1×100 mm, 1.7  $\mu$ m) and coupled to a mass spectrometer (Waters, USA). The mobile phase was 50 % water and 50% methanol in isocratic mode; the column temperature was kept at 25°C and the injection volume was 50  $\mu$ L.

Assessment of the toxicity of degradation byproducts was based on the normalized biotest (UNE/EN/ISO 11348-2) [23, 24] of luminescent inhibition of *Vibrio Fischeri* bacteria (NRRL B-11177, using the LUMISTox 300 system (Dr. Lange GmbH) with a

LUMIStherm incubator. Toxicity is expressed as percentage inhibition at 15 min of exposure with reference to a stock saline solution (control).

### 3. RESULTS AND DISCUSSION

#### 3.1. Photolysis of BPA

Results for the direct photodegradation of BPA showed that only 15.11 % of the initial BPA was degraded after 180 min of treatment (Exp. No. 1, Table 2). The BPA absorption spectrum shows a maximum absorption peak at a wavelength of 275 nm ( $\epsilon = 329 \text{ m}^2/\text{mol}$ ), and only 1.48 % of the total energy emitted by the lamp corresponded to this wavelength, implying that the amount of radiation absorbed at 275 nm was inadequate to induce electron state transitions capable of transforming BPA, explaining the low degradation rate. Previous studies using low pressure lamps for BPA photolysis reported similar results [11, 12].

The effectiveness of UV light to degrade a given compound is directly related to its quantum yield, i.e., the number of degraded moles of the compound divided by the number of photons absorbed by the system. The quantum yield of BPA was assessed by using the following equation:

$$\Phi_{(239 \text{ to } 334 \text{ nm})} = \frac{k_t}{2.303 \times \sum_{239}^{334} E \times \epsilon} \quad (2)$$

where  $\Phi_{(239 \text{ to } 334 \text{ nm})}$  is the quantum yield of BPA depletion ( $\text{mol Einstein}^{-1}$ ),  $k_t$  is the pseudo-first-order rate constant of BPA photodegradation ( $\text{min}^{-1}$ ),  $E$  is the photon fluence rate in the wavelength interval of 239 to 334 nm ( $\text{Einstein}/\text{m}^2/\text{min}$ ),  $\epsilon$  is the molar absorption coefficient of BPA at the wavelength interval of 239 to 334 nm ( $\text{m}^2/\text{mol}$ ).

The experimental BPA photolysis data were fitted to a first order kinetic model, yielding a reaction rate constant value  $k_t = 9.09 \pm 0.23 \times 10^{-4} \text{ min}^{-1}$ . The quantum yield obtained was  $\Phi = 2.37 \times 10^{-6} \text{ mol/Einstein}$ , demonstrating the low effectiveness of direct BPA photodegradation.

**Table 2.** Photodegradation of bisphenol A under different experimental conditions for a treatment time of 180 min.

| Exp. No. | [BPA] (mg/L) | [H <sub>2</sub> O <sub>2</sub> ] (μM) | [K <sub>2</sub> S <sub>2</sub> O <sub>8</sub> ] (μM) | [Na <sub>2</sub> CO <sub>3</sub> ] (μM) | T (°C) | pH  | $1 - \left(\frac{C_e}{C_0}\right) \times 100$ (%) | $k_t \times 10^3$ (min <sup>-1</sup> ) | %D   |
|----------|--------------|---------------------------------------|--|---|--------|-----|---|--|------|
| 1        | 10           | 0                                     | --   | --                                      | 25     | 7.0 | 15.11   | 0.91±0.23                              | 1.79 |
| 2        | 10           | 100                                   | --   | --                                      | 25     | 7.0 | 26.63   | 1.72±0.00                              | 0.01 |
| 3        | 10           | 200                                   | --   | --                                      | 25     | 7.0 | 56.15   | 4.58±0.03                              | 0.01 |
| 4        | 10           | 300                                   | --   | --                                      | 25     | 7.0 | 61.48   | 5.30±0.71                              | 0.01 |
| 5        | 10           | 400                                   | --   | --                                      | 25     | 7.0 | 66.16   | 6.02±0.02                              | 0.01 |
| 6        | 10           | 500                                   | --   | --                                      | 25     | 7.0 | 67.53   | 6.25±0.00                              | 0.00 |
| 7        | 10           | 1000                                  | --   | --                                      | 25     | 7.0 | 91.73   | 13.85±0.03                             | 0.09 |
| 8        | 2            | 1000                                  | --   | --                                      | 25     | 7.0 | 100.00  | 61.16±1.54                             | 1.40 |
| 9        | 5            | 1000                                  | --   | --                                      | 25     | 7.0 | 99.98   | 48.08±2.08                             | 6.45 |
| 10       | 25           | 1000                                  | --   | --                                      | 25     | 7.0 | 71.84   | 7.04±0.15                              | 1.75 |
| 11       | 50           | 1000                                  | --   | --                                      | 25     | 7.0 | 39.91   | 2.83±0.06                              | 0.72 |
| 12       | 10           | 1000                                  | --   | --                                      | 25     | 2.0 | 33.18   | 2.24±0.32                              | 6.32 |
| 13       | 10           | 1000                                  | --   | --                                      | 25     | 4.0 | 29.98   | 1.98±0.11                              | 1.93 |
| 14       | 10           | 1000                                  | --   | --                                      | 25     | 9.0 | 28.32   | 1.85±0.50                              | 4.09 |
| 15       | 10           | 1000                                  | --   | --                                      | 35     | 7.0 | 90.99   | 13.37±0.17                             | 8.28 |
| 16       | 10           | 1000                                  | --   | --                                      | 45     | 7.0 | 90.28   | 12.95±0.25                             | 2.22 |
| 17       | 10           | --                                    | 100  | --                                      | 25     | 7.0 | 30.98   | 2.06±0.17                              | 0.85 |
| 18       | 10           | --                                    | 200  | --                                      | 25     | 7.0 | 49.18   | 3.76±0.27                              | 1.48 |
| 19       | 10           | --                                    | 300  | --                                      | 25     | 7.0 | 69.02   | 6.51±0.34                              | 1.78 |
| 20       | 10           | --                                    | 400  | --                                      | 25     | 7.0 | 81.11   | 9.26±0.49                              | 2.71 |
| 21       | 10           | --                                    | 500  | --                                      | 25     | 7.0 | 89.80   | 12.68±0.88                             | 3.86 |
| 22       | 10           | --                                    | 1000   | --                                      | 25     | 7.0 | 91.46   | 13.67±0.64                             | 2.77 |
| 23       | 2            | --                                    | 1000   | --                                      | 25     | 7.0 | 100.00  | 199.59±11.60                           | 9.62 |
| 24       | 5            | --                                    | 1000   | --                                      | 25     | 7.0 | 100.00  | 125.12±35.72                           | 4.21 |
| 25       | 25           | --                                    | 1000   | --                                      | 25     | 7.0 | 78.73   | 8.60±0.21                              | 3.02 |
| 26       | 50           | --                                    | 1000   | --                                      | 25     | 7.0 | 59.92   | 5.08±0.19                              | 2.55 |

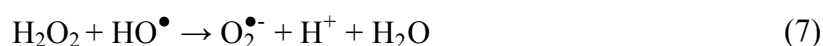
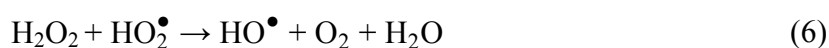
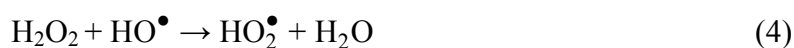
**Table 2.** Degradation of bisphenol A under different experimental conditions at treatment time of 180 min (continued).

| Exp. No. | [BPA] (mg/L) | [H <sub>2</sub> O <sub>2</sub> ] (μM) | [K <sub>2</sub> S <sub>2</sub> O <sub>8</sub> ] (μM) | [Na <sub>2</sub> CO <sub>3</sub> ] (μM) | T (°C) | pH   | $1 - \left(\frac{C_e}{C_0}\right) \times 100$ (%) | $k_t \times 10^3$ (min <sup>-1</sup> ) | %D    |
|----------|--------------|---------------------------------------|--|---|--------|------|---|--|-------|
| 27       | 10           | --                                    | 1000   | --                                      | 25     | 2.0  | 99.04   | 25.80±2.22                             | 15.76 |
| 28       | 10           | --                                    | 1000   | --                                      | 25     | 4.0  | 97.25   | 19.97±0.85                             | 6.22  |
| 29       | 10           | --                                    | 1000   | --                                      | 25     | 9.0  | 65.92   | 5.98±0.68                              | 10.64 |
| 30       | 10           | --                                    | 1000   | --                                      | 35     | 7.0  | 100.00  | 61.80±0.00                             | 7.46  |
| 31       | 10           | --                                    | 1000   | --                                      | 45     | 7.0  | 100.00  | 66.89±0.00                             | 14.21 |
| 32       | 10           | --                                    | --   | 100                                     | 25     | 9.4  | 24.89   | 1.59±0.15                              | 0.48  |
| 33       | 10           | --                                    | --   | 200                                     | 25     | 9.5  | 44.89   | 3.31±0.12                              | 0.46  |
| 34       | 10           | --                                    | --   | 300                                     | 25     | 9.7  | 54.05   | 4.32±0.11                              | 0.65  |
| 35       | 10           | --                                    | --   | 400                                     | 25     | 10.0 | 61.69   | 5.33±0.48                              | 2.34  |
| 36       | 10           | --                                    | --   | 500                                     | 25     | 10.1 | 66.16   | 6.16±0.22                              | 1.23  |
| 37       | 10           | --                                    | --   | 1000                                    | 25     | 10.3 | 68.23   | 6.37±0.12                              | 0.68  |
| 38       | 2            | --                                    | --   | 1000                                    | 25     | 10.3 | 98.20   | 22.32±2.03                             | 18.34 |
| 39       | 5            | --                                    | --   | 1000                                    | 25     | 10.3 | 88.47   | 12.00±1.39                             | 11.90 |
| 40       | 25           | --                                    | --   | 1000                                    | 25     | 10.3 | 50.53   | 3.91±0.16                              | 2.35  |
| 41       | 50           | --                                    | --   | 1000                                    | 25     | 10.3 | 40.88   | 2.92±0.02                              | 0.92  |
| 42       | 10           | --                                    | --   | 1000                                    | 25     | 2.0  | 25.43   | 1.63±0.21                              | 3.65  |
| 43       | 10           | --                                    | --   | 1000                                    | 25     | 4.0  | 26.23   | 1.69±0.01                              | 1.53  |
| 44       | 10           | --                                    | --   | 1000                                    | 25     | 7.0  | 67.65   | 6.27±0.25                              | 0.37  |
| 45       | 10           | --                                    | --   | 1000                                    | 35     | 10.3 | 50.44   | 4.14±0.00                              | 1.02  |
| 46       | 10           | --                                    | --   | 1000                                    | 45     | 10.3 | 51.50   | 3.67±0.00                              | 2.54  |

### 3.2. Indirect photodegradation of BPA

#### 3.2.1. BPA degradation by the UV/H<sub>2</sub>O<sub>2</sub> system

The UV/H<sub>2</sub>O<sub>2</sub> system generates HO• radicals following reactions (3-8) [25].



Determination of the reaction rate constant of the radical with the pollutant is critically important for the good design of a treatment system. The value of the HO• radical reaction rate constant determined by equation (1) was  $k_{\text{HO}^\bullet\text{BPA}} = 1.70 \pm 0.21 \times 10^{10} \text{ M}^{-1}\text{s}^{-1}$ , slightly higher than the value of  $1.02 \pm 0.23 \times 10^{10} \text{ M}^{-1}\text{s}^{-1}$  reported by Rosenfeldt et al. [11]. This difference may be due to the difference in reference compound for the competitive kinetics, which was isopropyl alcohol in the study by Rosenfeldt et al. and atrazine in the present experiments.

The effectiveness of the UV/H<sub>2</sub>O<sub>2</sub> system was assessed by studying the influence of some operational parameters (initial concentration of BPA, initial concentration of H<sub>2</sub>O<sub>2</sub>, pH, temperature, and water chemical composition) on BPA degradation kinetics. Table 2 shows the experimental conditions for each study parameter. BPA degradation kinetics were interpreted by using a pseudo first-order kinetic model, represented by the following equation:

$$\frac{d[\text{C}_{\text{BPA}_t}/\text{C}_{\text{BPA}_0}]}{dt} = -k_t[\text{C}_{\text{BPA}_t}/\text{C}_{\text{BPA}_0}] \quad (9)$$

Percentage deviation values were calculated by using equation (10) and are given in Table 2.

$$\%D = \frac{1}{N} \sum_{i=1}^N \left| \frac{[C_{\text{BPA exp}}] - [C_{\text{BPA pred}}]}{[C_{\text{BPA exp}}]} \right| \times 100 \quad (10)$$

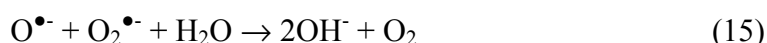
The results in Table 2 (Exp. Nos. 1-7) demonstrate that BPA degradation was enhanced by the presence of H<sub>2</sub>O<sub>2</sub>. For example, the addition of 1000 μM of H<sub>2</sub>O<sub>2</sub> produced around a 15-fold increase in the reaction rate constant,  $k_t$ , from  $0.91 \pm 0.23 \times 10^{-3}$  to  $13.85 \pm 0.03 \times 10^{-3} \text{ min}^{-1}$ , producing an increase in BPA degradation from 15.11% to 91.73%. Moreover, there was a linear increase in percentage degradation (from 26.63 to 91.73 %) with a rise in the initial H<sub>2</sub>O<sub>2</sub> concentration from 100 to 1000 μM. This is because a higher dose of H<sub>2</sub>O<sub>2</sub> increases the HO• generation rate, enhancing BPA oxidation.

The effect of BPA concentration on the BPA degradation rate was investigated by varying the initial BPA concentration from 2 to 50 mg/L while keeping the H<sub>2</sub>O<sub>2</sub> concentration constant (1000 μM). Table 2 exhibits the  $k_t$  values and percentage degradation values obtained (Exp. Nos. 7-11), showing that 100 % degradation was achieved at low BPA concentrations. The main reason for the rise in reaction rate constant at lower initial BPA initial concentrations is the increase in the  $[\text{HO}^\bullet]/[\text{C}_{\text{BPA}}]_0$  ratio.

The influence of solution pH on BPA degradation was studied in the pH range from 2 to 9 (Exp. Nos. 7, 12-14, Table 2). The highest  $k_t$  value was observed at pH 7. The BPA degradation rate was markedly reduced at acidic and basic pH values, because the PO<sub>4</sub><sup>3-</sup>, HPO<sub>4</sub><sup>2-</sup>, and H<sub>2</sub>PO<sub>4</sub><sup>-</sup> ions in the system under these conditions act as scavengers of HO• radicals, with rate constants of  $k = 1.0 \times 10^7 \text{ M}^{-1} \text{ s}^{-1}$ ,  $k = 1.5 \times 10^5 \text{ M}^{-1} \text{ s}^{-1}$ , and  $k = 2.0 \times 10^4 \text{ M}^{-1} \text{ s}^{-1}$ , respectively [26]. HO• radicals can also be recombined at acidic pH to form H<sub>2</sub>O<sub>2</sub>, reducing their effectiveness in BPA oxidation. Furthermore, most of the oxidation reactions of organic compounds with HO• in aqueous phase are reduced at acidic pH due to the presence of H<sup>+</sup>, because H<sup>+</sup> ions act as HO• radical scavengers with a rate constant of  $k = 7 \times 10^9 \text{ M}^{-1} \text{ s}^{-1}$  [26]. A solution at basic pH favors the decomposition of H<sub>2</sub>O<sub>2</sub> to form water and oxygen instead of HO• radicals, and, moreover, the



conjugate base of  $\text{H}_2\text{O}_2$  ( $\text{HO}_2^-$ ) acts as an  $\text{HO}^\bullet$  radical scavenger by the following reactions [26]:



The effect of reaction temperature on BPA photodegradation with the UV/ $\text{H}_2\text{O}_2$  system was investigated in experiments conducted at 25, 35, and 45° C. The results in Table 2 (Exp. Nos. 7, 15, 16) show that  $k_t$  values were very similar at the three temperatures, indicating that the temperature had no substantial effect on the BPA degradation rate.

The Arrhenius equation was applied to the experimental data to estimate the activation energy ( $E_a$ ) by using the following equation (16):

$$k_t = A e^{\left(\frac{E_a}{RT}\right)} \quad (16)$$

where  $k_t$  is the degradation rate constant,  $A$  is the pre-exponential factor,  $E_a$  (J/mol) is the activation energy,  $R$  is the gas constant (8.3145 J/mol/K), and  $T$  is the temperature (K).  $E_a$  values are listed in Table 3.

The thermodynamic parameters for BPA photooxidation by UV/ $\text{H}_2\text{O}_2$  (Gibbs free energy change [ $\Delta G^\circ$ ], enthalpy change [ $\Delta H^\circ$ ], and entropy change [ $\Delta S^\circ$ ]) were calculated by using the thermodynamic relation (17-19) [27]; the results are given in Table 3. According to the positive free energy change values, the reaction was non-spontaneous. Moreover, the negative value of  $\Delta H^\circ$  indicates that the process was exothermic, and the negative value of  $\Delta S^\circ$  demonstrates a decrease in entropy.

$$\Delta G^\circ = \Delta H^\circ - T \times \Delta S^\circ \quad (17)$$

$$\Delta H^\circ = \frac{-R(T_2 \times T_1)}{(T_2 - T_1)} \times \ln\left(\frac{k_1}{k_2}\right) \quad (18)$$

$$\Delta S^\circ = \frac{\Delta H^\circ - \Delta G^\circ}{T} \quad (19)$$

**Table 3.** Thermodynamic parameters for the photooxidation of BPA.

| Oxidants<br>(1000 $\mu$ M)                   | Temperature<br>(K) | E <sub>a</sub><br>(kJ/mol) | $\Delta G^\circ$<br>(kJ/mol) | $\Delta H^\circ$<br>(kJ/mol) | $\Delta S^\circ$<br>(J/mol/K) |
|--|--------------------|----------------------------|------------------------------|------------------------------|-------------------------------|
| H <sub>2</sub> O <sub>2</sub>                | 298                |                            | +20.75                       |                              | -78.51                        |
|  | 308                | 2.65                       | +21.53                       | -2.65                        | -78.51                        |
|  | 318                |                            | +22.32                       |                              | -78.51                        |
| K <sub>2</sub> S <sub>2</sub> O <sub>8</sub> | 298                |                            | +20.78                       |                              | +124.53                       |
|  | 308                | 58.62                      | +17.34                       | +57.89                       | +131.66                       |
|  | 318                |                            | +18.29                       |                              | +124.53                       |
| Na <sub>2</sub> CO <sub>3</sub>              | 298                |                            | +22.67                       |                              | -136.94                       |
|  | 308                | 18.35                      | +24.69                       | -18.13                       | -139.04                       |
|  | 318                |                            | +25.41                       |                              | -136.94                       |

In order to analyze the applicability of the UV/H<sub>2</sub>O<sub>2</sub> system in the treatment of BPA-contaminated water, experiments were conducted with surface water, groundwater, and wastewater; their chemical characteristics are listed in Table 1. The wastewater contained a large amount of organic matter and had a high TOC concentration, while the ground water had the highest transmittance value. Table 4 exhibits the reaction rate constants for BPA photodegradation in these three types of water and in ultrapure water and gives the percentage degradation values after 180 min of treatment. In general, reaction rate constants decreased in the following order: wastewater > surface water > ultrapure water > groundwater. The k<sub>t</sub> value was almost four-fold higher for wastewater than for ultrapure water.

**Table 4.** Reaction rate constants for the photodegradation of BPA, radical inhibition rates, and percentage degradation for a treatment time of 180 min in different water types.

| Water type             | Oxidants<br>(500 $\mu$ M)                    | $k_t \times 10^3$<br>( $\text{min}^{-1}$ ) | $1 - \left(\frac{C_e}{C_0}\right) \times 100$ (%) | $r^\bullet$<br>( $\text{s}^{-1}$ ) | %D    |
|------------------------|--|--|---|------------------------------------|-------|
| <b>Ultrapure water</b> | H <sub>2</sub> O <sub>2</sub>                | 6.25 $\pm$ 0.00                            | 67.53   | 1.11 $\times 10^3$                 | 0.00  |
|                        | K <sub>2</sub> S <sub>2</sub> O <sub>8</sub> | 12.68 $\pm$ 0.88                           | 89.80   | ---                                | 3.86  |
|                        | Na <sub>2</sub> CO <sub>3</sub>              | 6.16 $\pm$ 0.22                            | 66.16   | ---                                | 1.23  |
| <b>Surface water</b>   | H <sub>2</sub> O <sub>2</sub>                | 12.91 $\pm$ 0.97                           | 90.21   | 3.03 $\times 10^8$                 | 11.95 |
|                        | K <sub>2</sub> S <sub>2</sub> O <sub>8</sub> | 36.36 $\pm$ 0.21                           | 99.86   | 1.25 $\times 10^{10}$              | 0.56  |
|                        | Na <sub>2</sub> CO <sub>3</sub>              | 1.34 $\pm$ 0.00                            | 21.43   | 1.29 $\times 10^9$                 | 1.30  |
| <b>Ground water</b>    | H <sub>2</sub> O <sub>2</sub>                | 0.28 $\pm$ 0.02                            | 4.92  | 5.70 $\times 10^8$                 | 2.68  |
|                        | K <sub>2</sub> S <sub>2</sub> O <sub>8</sub> | 0.29 $\pm$ 0.02                            | 5.09  | 1.72 $\times 10^{10}$              | 2.68  |
|                        | Na <sub>2</sub> CO <sub>3</sub>              | 1.86 $\pm$ 0.12                            | 28.45   | 2.54 $\times 10^9$                 | 1.86  |
| <b>Wastewater</b>      | H <sub>2</sub> O <sub>2</sub>                | 67.10 $\pm$ 0.02                           | 100.00  | 1.54 $\times 10^9$                 | 3.22  |
|                        | K <sub>2</sub> S <sub>2</sub> O <sub>8</sub> | 98.27 $\pm$ 4.44                           | 100.00  | 1.41 $\times 10^{10}$              | 1.58  |
|                        | Na <sub>2</sub> CO <sub>3</sub>              | 77.16 $\pm$ 0.93                           | 100.00  | 7.64 $\times 10^9$                 | 1.10  |

In order to explain these results, the inhibition rates of HO $\bullet$  radicals by the species present in each water matrix were calculated using Eq. (20).

$$r^\bullet = k_{\text{H}^+}[\text{H}^+] + k_{\text{TOC}}[\text{TOC}] + k_{\text{HCO}_3^-}[\text{HCO}_3^-] \quad (20)$$

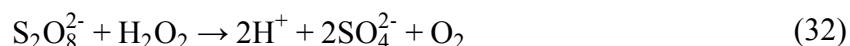
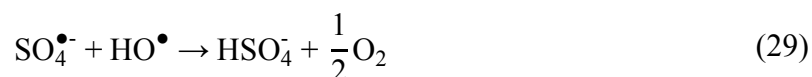
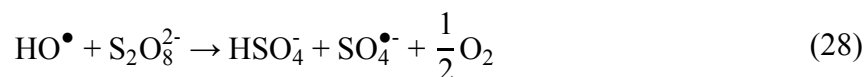
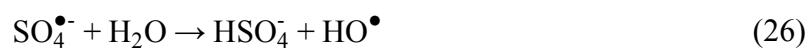
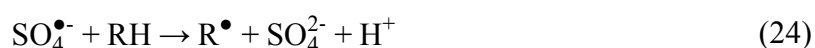
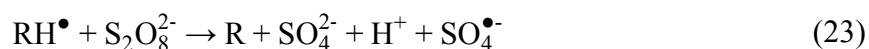
where  $r^\bullet$  is the inhibition rate of HO $\bullet$  radicals due to the presence of H $^+$ , TOC, and HCO $_3^-$ ; the kinetic rate constants of HO $\bullet$  for H $^+$ , TOC, and HCO $_3^-$  are  $k_{\text{H}^+} = 7 \times 10^9 \text{ M}^{-1} \text{ s}^{-1}$ ,  $k_{\text{TOC}} = 2 \times 10^8 \text{ M}_c^{-1} \text{ s}^{-1}$ , and  $k_{\text{HCO}_3^-} = 8.5 \times 10^6 \text{ M}^{-1} \text{ s}^{-1}$  [26, 28-30]; and [H $^+$ ], [TOC], and [HCO $_3^-$ ] are the initial concentrations of each species in the water.  $\text{M}_c$  is the molarity of natural organic matter, based on the moles of carbon and was

assumed to be  $12 \text{ g mol}^{-1}$ . Table 4 lists the inhibition rate of  $\text{HO}^\bullet$  radicals for the different water types, showing that wastewater had the highest  $\text{HO}^\bullet$  radical inhibition rate, reducing the concentration of  $\text{HO}^\bullet$  radicals in the medium. These results suggest, therefore, that the high degradation of BPA in wastewater may be related to its considerable content of NOM, which can absorb UV radiation and generate excited triplet states ( $^3\text{NOM}^*$ ) and various reactive oxygen species, including additional  $\text{HO}^\bullet$  radicals, singlet oxygen ( $^1\text{O}_2$ ) and  $\text{H}_2\text{O}_2$  [31-33], which enhance BPA degradation. The lowest  $k_t$  and BPA percentage degradation values were observed for groundwater, which may be attributable to its elevated content of ionic metal species and bicarbonate ions, which act as radical scavengers of  $\text{HO}^\bullet$  radicals [26].

The BPA degradation by-products detected with the UV/ $\text{H}_2\text{O}_2$  system were monohydroxylated bisphenol A and quinone of monohydroxylated bisphenol A.

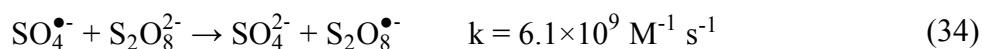
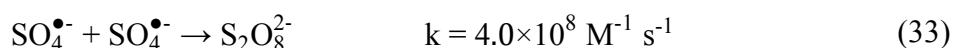
### 3.2.2. BPA degradation by the UV/ $\text{K}_2\text{S}_2\text{O}_8$ system

The UV/ $\text{K}_2\text{S}_2\text{O}_8$  system generates  $\text{SO}_4^{\bullet-}$  radicals through reactions (21-32) [34, 35].



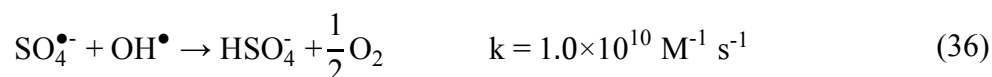
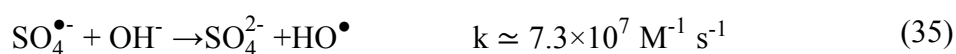
The rate constant for the reaction of BPA with  $\text{SO}_4^{\bullet-}$  radicals was determined by using Eq. (1), which yielded a value of  $k_{\text{SO}_4^{\bullet-}\text{BPA}} = 1.37 \pm 0.15 \times 10^9 \text{ M}^{-1}\text{s}^{-1}$ ; this value is in the range of values reported for the degradation of aromatic compounds with  $\text{SO}_4^{\bullet-}$  radicals [17, 36]. Moreover, the rate constant is lower for the UV/ $\text{K}_2\text{S}_2\text{O}_8$  system than for the UV/ $\text{H}_2\text{O}_2$  system, indicating that the reaction is faster between BPA and  $\text{HO}^{\bullet}$  radicals than between BPA and  $\text{SO}_4^{\bullet-}$  radicals.

The effect of the initial  $\text{K}_2\text{S}_2\text{O}_8$  concentration was assessed by carrying out experiments at an initial BPA concentration of 10 mg/L (44  $\mu\text{M}$ ) and  $\text{K}_2\text{S}_2\text{O}_8$  concentrations of 100, 200, 300 400, 500, and 1000  $\mu\text{M}$  (Table 2, Exp. Nos. 17-22). In most cases, the addition of  $\text{K}_2\text{S}_2\text{O}_8$  to the system produced a slight increase in the BPA degradation rate in comparison to the rate obtained for the same concentration of  $\text{H}_2\text{O}_2$  in the UV/ $\text{H}_2\text{O}_2$  system. Thus, under the same conditions, the percentage BPA degradation was 1.3-fold higher with UV/ $\text{K}_2\text{S}_2\text{O}_8$  than with UV/ $\text{H}_2\text{O}_2$  (Table 2, Exp. 6, 21), attributed to the generation of both  $\text{HO}^{\bullet}$  and  $\text{SO}_4^{\bullet-}$  radicals in the UV/ $\text{K}_2\text{S}_2\text{O}_8$  system, (reactions 21 and 26). The results in Table 2 also show that the addition of elevated concentrations of  $\text{K}_2\text{S}_2\text{O}_8$  (e.g., 1000  $\mu\text{M}$ ) did not substantially increase the BPA degradation rate due to an excessive generation of  $\text{SO}_4^{\bullet-}$  radicals, which can recombine according to the following equations [26].



The influence of the initial BPA concentration was studied by performing experiments at different initial BPA concentrations (2, 5, 10, 25 and 50 mg/L) with the same initial  $\text{K}_2\text{S}_2\text{O}_8$  concentration (1000  $\mu\text{M}$ ) (Table 2, Exp. Nos. 22-26). The  $k_t$  values obtained, as in the UV/ $\text{H}_2\text{O}_2$  system, show that the degradation kinetics became much faster with a decrease in the BPA concentration. However, at both low and high BPA concentrations, the UV/ $\text{K}_2\text{S}_2\text{O}_8$  system was considerably more effective than the UV/ $\text{H}_2\text{O}_2$  system.

The effect of the solution pH on BPA degradation by the UV/K<sub>2</sub>S<sub>2</sub>O<sub>8</sub> system was also studied. Results obtained (Table 2, Exp. Nos. 22, 27-29) show that the percentage BPA degradation with a treatment time of 180 min remained constant from pH = 2 to 7, with values higher than 90 %. At basic pH (9) however, the degradation rate was reduced by up to 25%. These results can be attributed to an excessive generation of HO<sup>•</sup> and SO<sub>4</sub><sup>•-</sup> radicals, which can recombine via reactions (35) and (36) [26], thereby reducing their effectiveness to eliminate BPA.



The working temperature is an important factor that influences the decomposition of persulfate to generate SO<sub>4</sub><sup>•-</sup> radicals [37]; therefore, the influence of temperature on BPA degradation was examined. The results (Table 2, Exp. Nos. 22, 30, 31) show an increase in BPA degradation rates with a rise in temperature from 25 to 45 °C.

The positive free energy values obtained for the UV/K<sub>2</sub>S<sub>2</sub>O<sub>8</sub> system (Table 3) indicate that the BPA degradation was non-spontaneous, and the positive ΔH° value indicates that it was endothermic, i.e., in contrast to UV/H<sub>2</sub>O<sub>2</sub>, increased temperature favors this process, as experimentally demonstrated (see above).

SO<sub>4</sub><sup>•-</sup> radical inhibition rates for the species in each water matrix were calculated, Eq. (20), by using the kinetics rate constants of SO<sub>4</sub><sup>•-</sup> radicals with TOC and HCO<sub>3</sub><sup>-</sup> (k<sub>TOC</sub> = 1.60 × 10<sup>6</sup> M<sub>c</sub><sup>-1</sup> s<sup>-1</sup> and k<sub>HCO<sub>3</sub><sup>-</sup></sub> = 1.95 × 10<sup>9</sup> M<sup>-1</sup> s<sup>-1</sup>) [38, 39]. Table 4 lists the results obtained for the photodegradation of BPA in ultrapure water, surface water, ground water, and wastewater. The fastest BPA degradation was obtained in wastewater, followed by surface water, ultrapure water, and groundwater. These results confirm that BPA photodegradation in wastewater is mainly by photosensitized degradation due to the photolysis of organic matter. The lowest percentage BPA degradation was in ground water. These results are similar to those obtained from the UV/H<sub>2</sub>O<sub>2</sub> system.

The BPA degradation by-products with the UV/K<sub>2</sub>O<sub>8</sub>S<sub>2</sub> system were 4-isopropenylphenol and monohydroxylated 4-isopropenylphenol.

### 3.2.3. Bisphenol A degradation by the UV/Na<sub>2</sub>CO<sub>3</sub> system

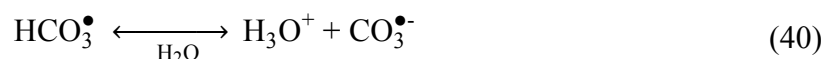
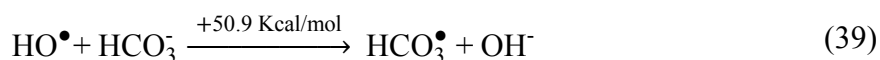
Several chemical reactions have been employed to generate CO<sub>3</sub><sup>•-</sup> radicals in aqueous solutions. These include one-electron oxidation of bicarbonate or carbonate by hydroxyl radical [14], the sulfate radical anion [15], or the quenching of the excited triplet state of a sensitizer such as an *anthraquinone* sulfonate or duroquinone [15]. Photolysis of the cobalt (III)-tetraaminocarbonate ion has also been used to generate CO<sub>3</sub><sup>•-</sup> radicals [40]. However, no data are available on the generation of CO<sub>3</sub><sup>•-</sup> or HCO<sub>3</sub><sup>•</sup> radicals by UV radiation in the presence of CO<sub>3</sub><sup>2-</sup> or HCO<sub>3</sub><sup>-</sup>.

Figure 2 depicts the BPA photodegradation kinetics in the presence of different doses of Na<sub>2</sub>CO<sub>3</sub>. It shows that the addition of Na<sub>2</sub>CO<sub>3</sub> produced an increase in the BPA degradation rate, which rose from 24.89% to 68.23% with an increase in initial Na<sub>2</sub>CO<sub>3</sub> dose from 100 to 1000 μM. The initial solution pH of the above experiments ranged from 9.4 to 10.3. Under these experimental conditions, carbonate anions are in equilibrium with hydrogen carbonate anions according to the following reaction [41]:



Hence, the solution contains 85 % of bicarbonate at a solution pH of 9.4, which reduces to 45 % at a pH of 10.3.

Experiments were conducted under the same experimental conditions as above but in the absence of UV radiation to investigate the possibility of CO<sub>3</sub><sup>•-</sup>/HCO<sub>3</sub><sup>•</sup> radicals generation in the UV/Na<sub>2</sub>CO<sub>3</sub> system due to the formation of complexes between BPA and Na<sup>+</sup>, CO<sub>3</sub><sup>2-</sup> and/or HCO<sub>3</sub><sup>-</sup> anions. Results obtained showed that the absorbance of BPA solutions remained constant over time, indicating that these complexes are not formed. Therefore, the explanation for the results in Figure 2 is the formation of carbonate radicals CO<sub>3</sub><sup>•-</sup> and bicarbonate radicals HCO<sub>3</sub><sup>•</sup> *via* the following reactions:



This mechanism was corroborated by means of the program Gaussian09 (CCSD/aug-cc-pVTZ) obtaining the corresponding reaction enthalpies. Thus, the energy of our UV system was enough to carry out the above reactions.

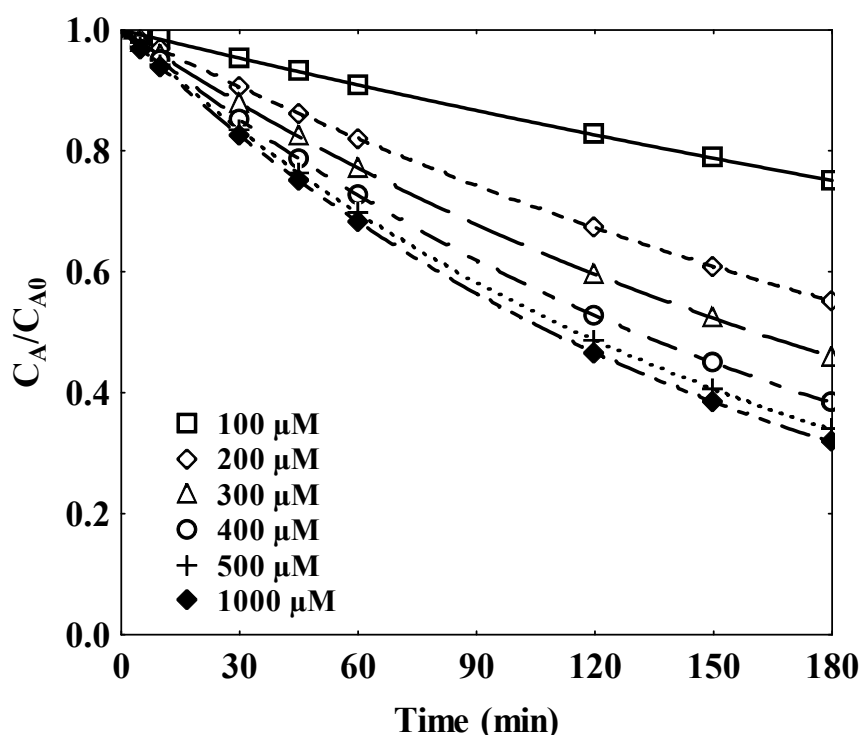


**Figure 2.** Effect of initial concentration of  $\text{Na}_2\text{CO}_3$  on BPA degradation with the UV/ $\text{Na}_2\text{CO}_3$  system.  $[\text{BPA}]_0 = 10 \text{ mg/L}$ ,  $T = 25^\circ\text{C}$ .

$k_t$  values obtained at different initial concentrations of  $\text{Na}_2\text{CO}_3$  are given in Table 2. These values were lower than those obtained for the UV/ $\text{H}_2\text{O}_2$  and UV/ $\text{K}_2\text{S}_2\text{O}_8$  systems, which may be due to the lesser reactivity of  $\text{CO}_3^{\bullet-}/\text{HCO}_3^\bullet$  radicals in comparison to  $\text{HO}^\bullet$  and  $\text{SO}_4^{\bullet-}$  radicals. To test this hypothesis, the value of the radical reaction rate constant ( $k_{\text{CO}_3^{\bullet-}/\text{HCO}_3^\bullet\text{BPA}}$ ) was determined by using Eq. (1), which yielded a value of

$k_{\text{CO}_3^{\bullet-}/\text{HCO}_3^\bullet\text{BPA}} = 3.89 \pm 0.09 \times 10^6 \text{ M}^{-1} \text{ s}^{-1}$ . This value is within the range of values



reported for the degradation of aromatic compounds with  $\text{CO}_3^{\bullet-}$  radicals [14]. The reaction rate constant was lowest between BPA and  $\text{CO}_3^{\bullet-}/\text{HCO}_3^{\bullet}$  radicals, followed by  $\text{SO}_4^{\bullet-}$  radicals and  $\text{HO}^{\bullet}$  radicals; i.e., the capacity to attack BPA was lower for  $\text{CO}_3^{\bullet-}/\text{HCO}_3^{\bullet}$  radicals than for  $\text{SO}_4^{\bullet-}$  and  $\text{HO}^{\bullet}$  radicals.

The influence of the initial BPA concentration on its photodegradation with the UV/ $\text{Na}_2\text{CO}_3$  system was investigated (Figure 3 and Table 2, Exp. Nos. 37-41). The BPA degradation rate constant was lower at higher initial concentrations of BPA. Thus, it was  $22.32 \pm 2.03 \times 10^{-3} \text{ min}^{-1}$  for a concentration of 2 mg/L and  $2.92 \pm 0.02 \times 10^{-3} \text{ min}^{-1}$  for one of 50 mg/L, respectively. Once again, BPA degradation rates were lower with this system than with the UV/ $\text{H}_2\text{O}_2$  or UV/ $\text{K}_2\text{S}_2\text{O}_8$  systems.

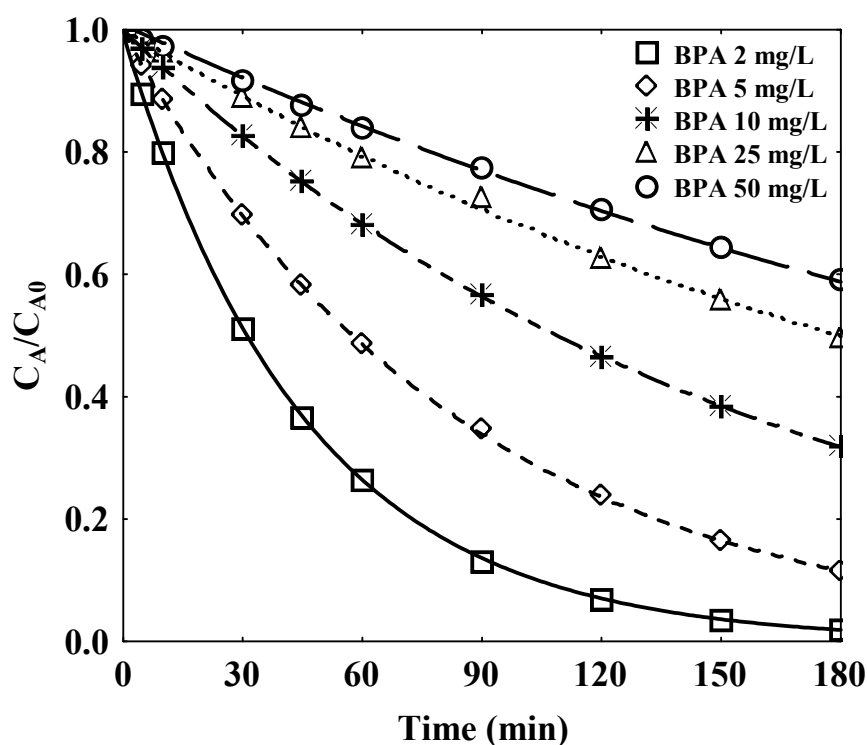


**Figure 3.** Effect of initial concentration of BPA on its degradation with the UV/ $\text{Na}_2\text{CO}_3$  system in ultrapure water.  $[\text{Na}_2\text{CO}_3]_0 = 1000 \mu\text{M}$ ,  $T = 25^\circ\text{C}$ ,  $\text{pH} = 10.3$ .

The effect of temperature on BPA photodegradation with the UV/ $\text{Na}_2\text{CO}_3$  system was investigated. As shown in Table 2 (Exp. Nos. 37, 45, 46), the BPA degradation rate decreased with higher temperatures, indicating that, like the UV/ $\text{H}_2\text{O}_2$  system, this

process is exothermic, as corroborated by the  $\Delta H^\circ$  value (Table 3). The activation energy and thermodynamic parameters were calculated by using equations (16-19) and are shown in Table 3. The activation energy with UV/ $\text{Na}_2\text{CO}_3$  was around 7-fold higher than with UV/ $\text{H}_2\text{O}_2$  and around 3-fold lower than that obtained with UV/ $\text{K}_2\text{S}_2\text{O}_8$ .

$\text{CO}_3^{\bullet-}$  radical inhibition rates by the species in each water matrix were calculated by Eq. (20), using the kinetic rate constants of  $\text{CO}_3^{\bullet-}$  radicals with TOC and  $\text{HCO}_3^-$  ( $k_{\text{TOC}} = 1.0 \times 10^9 \text{ M}_c^{-1} \text{ s}^{-1}$  and  $k_{\text{HCO}_3^-} = 7.50 \times 10^6 \text{ M}^{-1} \text{ s}^{-1}$ ) [15, 41]. Table 4 exhibits the BPA photodegradation parameters with the UV/ $\text{Na}_2\text{CO}_3$  system in the different water types (ultrapure water, surface water, ground water, and wastewater). The BPA degradation rate was highest in wastewater, followed by ultrapure water, groundwater, and surface water. As in the case of the UV/ $\text{H}_2\text{O}_2$  and UV/ $\text{K}_2\text{S}_2\text{O}_8$  systems, these results confirm that the presence of high amounts of NOM in water enhances BPA photooxidation. The percentage BPA degradation in ground water was higher with UV/ $\text{Na}_2\text{CO}_3$  than with UV/ $\text{H}_2\text{O}_2$  and UV/ $\text{K}_2\text{S}_2\text{O}_8$  systems, which may be attributable to the high bicarbonate content of this type of water (Table 1). This increases the generation of  $\text{CO}_3^{\bullet-}/\text{HCO}_3^{\bullet}$  radicals with UV/ $\text{Na}_2\text{CO}_3$ , whereas  $\text{HCO}_3^-$  acts as a scavenger of the  $\text{HO}^\bullet$  and  $\text{SO}_4^{\bullet-}$  radicals generated with the UV/ $\text{H}_2\text{O}_2$  and UV/ $\text{K}_2\text{S}_2\text{O}_8$  systems, respectively.

The BPA degradation by-products with the UV/ $\text{Na}_2\text{CO}_3$  system were similar to those detected with the UV/ $\text{H}_2\text{O}_2$  system.

### 3.3. Time course of TOC and toxicity.

Figure 4 depicts TOC values as a function of treatment time, showing a marked reduction in the TOC concentration during the first five minutes of treatment with all three systems used. The reduction in TOC for 60 min of treatment was 57% with the UV/ $\text{H}_2\text{O}_2$  system, 76% with UV/ $\text{K}_2\text{S}_2\text{O}_8$ , and 38% with UV/ $\text{Na}_2\text{CO}_3$ . Hence, UV/ $\text{K}_2\text{S}_2\text{O}_8$  was the most effective system to mineralize the organic matter present in the medium.

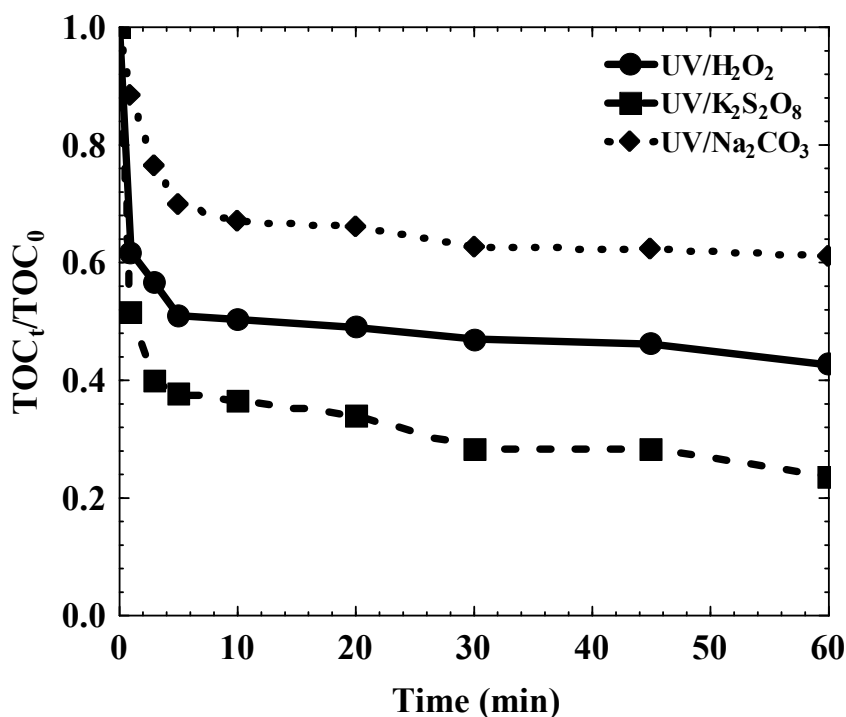


**Figure 4.** Evaluation of TOC with treatment time.  $[BPA]_0 = 20$  mg/L,  $[H_2O_2]_0 = [K_2S_2O_8]_0 = [Na_2CO_3]_0 = 500$   $\mu$ M,  $T = 25^\circ$ C.

Figure 5 depicts the percentage inhibition of *Vibrio Fischeri* bacteria as a function of treatment time with the UV/H<sub>2</sub>O<sub>2</sub>, UV/K<sub>2</sub>S<sub>2</sub>O<sub>8</sub>, and UV/Na<sub>2</sub>CO<sub>3</sub> systems. The highest percentage was obtained with the UV/H<sub>2</sub>O<sub>2</sub> system, indicating the formation of degradation byproducts that are more toxic than BPA. Moreover, the remaining H<sub>2</sub>O<sub>2</sub> is toxic and may contribute to increasing the percentage inhibition of *Vibrio Fischeri* bacteria. In the case of the UV/K<sub>2</sub>S<sub>2</sub>O<sub>8</sub> system, the percentage inhibition increased during the first ten minutes of treatment and then started to decrease with longer treatment time. These results indicate that the degradation byproducts generated by the treatment are less toxic than BPA. With the UV/Na<sub>2</sub>CO<sub>3</sub> system, percentage inhibition values remained virtually constant throughout the treatment time.

According to these results, the UV/K<sub>2</sub>S<sub>2</sub>O<sub>8</sub> system is the most appropriate for reducing both the medium toxicity and TOC.

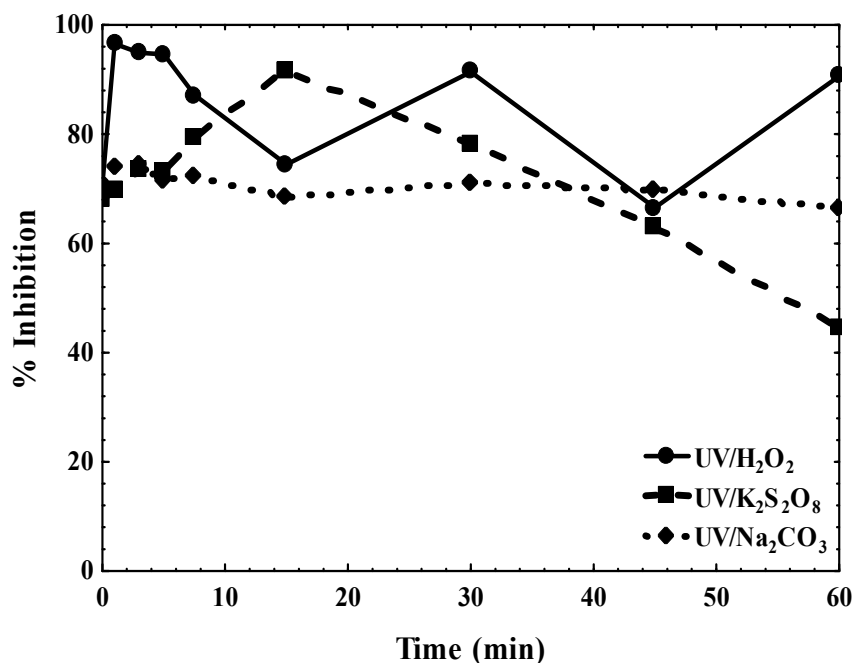


**Figure 5.** Time course of medium toxicity during treatment with UV/H<sub>2</sub>O<sub>2</sub>, UV/K<sub>2</sub>S<sub>2</sub>O<sub>8</sub>, or UV/Na<sub>2</sub>CO<sub>3</sub>. [BPA]<sub>0</sub> = 20 mg/L, [H<sub>2</sub>O<sub>2</sub>]<sub>0</sub> = [K<sub>2</sub>S<sub>2</sub>O<sub>8</sub>]<sub>0</sub> = [Na<sub>2</sub>CO<sub>3</sub>]<sub>0</sub> = 500 μM, T = 25°C.

### 3.4. Comparisons among UV/H<sub>2</sub>O<sub>2</sub>, UV/K<sub>2</sub>S<sub>2</sub>O<sub>8</sub>, and UV/Na<sub>2</sub>CO<sub>3</sub> systems

Figure 6a) depicts the BPA photodegradation kinetics with UV/H<sub>2</sub>O<sub>2</sub>, UV/K<sub>2</sub>S<sub>2</sub>O<sub>8</sub>, and UV/Na<sub>2</sub>CO<sub>3</sub> systems in ultrapure water. The results show that the degradation was most effective with the UV/K<sub>2</sub>S<sub>2</sub>O<sub>8</sub> system, followed by the UV/H<sub>2</sub>O<sub>2</sub> and UV/Na<sub>2</sub>CO<sub>3</sub> systems, which may be attributable to its formation of both HO• and SO<sub>4</sub><sup>•-</sup> radicals. The UV/Na<sub>2</sub>CO<sub>3</sub> system also had the lowest BPA degradation rate constant, because CO<sub>3</sub><sup>•-</sup>/HCO<sub>3</sub><sup>•</sup> has a lower radical reaction rate constant,  $k_{\text{CO}_3^{\bullet-}/\text{HCO}_3^{\bullet}\text{BPA}} = 3.89 \pm 0.09 \times 10^6 \text{ M}^{-1} \text{ s}^{-1}$ , and oxidizing power ( $E^\circ = 1.78 \text{ V}$ ) in comparison to the oxidizing power of HO• ( $E^\circ = 2.80 \text{ V}$ ) and SO<sub>4</sub><sup>•-</sup> ( $E^\circ = 2.05 \text{ V}$ ).

The solution pH and temperature proved to be key determinants of the efficacy of the systems used to oxidize BPA. The optimum solution pH for BPA photooxidation was 7, 2, and 7 for UV/H<sub>2</sub>O<sub>2</sub>, UV/K<sub>2</sub>S<sub>2</sub>O<sub>8</sub>, and UV/Na<sub>2</sub>CO<sub>3</sub>, respectively. Hence, the UV/K<sub>2</sub>S<sub>2</sub>O<sub>8</sub> system, the most effective process to remove BPA from aqueous solution, was most effective at acidic solution pH, whereas the UV/H<sub>2</sub>O<sub>2</sub> and UV/Na<sub>2</sub>CO<sub>3</sub> systems were more effective at neutral solution pH. Temperature also played an

important role in the degradation of BPA with these systems, reducing BPA photooxidation by the UV/H<sub>2</sub>O<sub>2</sub>, and UV/Na<sub>2</sub>CO<sub>3</sub> systems when it was increased and enhancing BPA photooxidation with the UV/K<sub>2</sub>S<sub>2</sub>O<sub>8</sub> system when it was increased.

In relation to the application of these systems, Figures 6b), c), and d) depict BPA photodegradation values with UV/H<sub>2</sub>O<sub>2</sub>, UV/K<sub>2</sub>S<sub>2</sub>O<sub>8</sub>, and UV/Na<sub>2</sub>CO<sub>3</sub> systems in wastewater, surface water, and ground water, respectively. As shown in Figure 6b), all three oxidation systems proved to be adequate for removing BPA from wastewater, showing an efficacy of 100 % after 30 minutes of treatment. This may be related to its high content of NOM, which can absorb UV radiation and generate excited triplet states (<sup>3</sup>NOM\*) and various reactive oxygen species [31-33]. The trend for surface water was similar to that for ultrapure water, but the effectiveness of both UV/K<sub>2</sub>S<sub>2</sub>O<sub>8</sub> and UV/H<sub>2</sub>O<sub>2</sub> systems was higher in surface water, whereas the effectiveness of the UV/Na<sub>2</sub>CO<sub>3</sub> system was lower. As depicted in Figure 6d), all three oxidation systems showed lower BPA degradation in groundwater than in the other water types, which may be attributable to its high content of metal species and bicarbonate ions, which act as HO• and SO<sub>4</sub>•<sup>-</sup> radical scavengers [26]. The highest BPA degradation rate with the UV/Na<sub>2</sub>CO<sub>3</sub> system was obtained in ground water, which may be attributable to an increase in carbonate radicals due to the presence of bicarbonate.

According to the results of this study, the selection of one of these BPA degradation systems depends on the water type. UV/K<sub>2</sub>S<sub>2</sub>O<sub>8</sub> is a good option to treat both ultrapure water and surface water, reducing the TOC and producing less toxic byproducts. The UV/Na<sub>2</sub>CO<sub>3</sub> system is the best choice for ground water, whereas all three systems are effective for treating wastewater. However, from an economic standpoint of view, the higher cost of K<sub>2</sub>S<sub>2</sub>O<sub>8</sub> (30-35 \$/kg) than of H<sub>2</sub>O<sub>2</sub> (0.6-1.3 \$/kg) and Na<sub>2</sub>CO<sub>3</sub> (0.2- 0.5 \$/kg) systems may play an important role in the system selection.

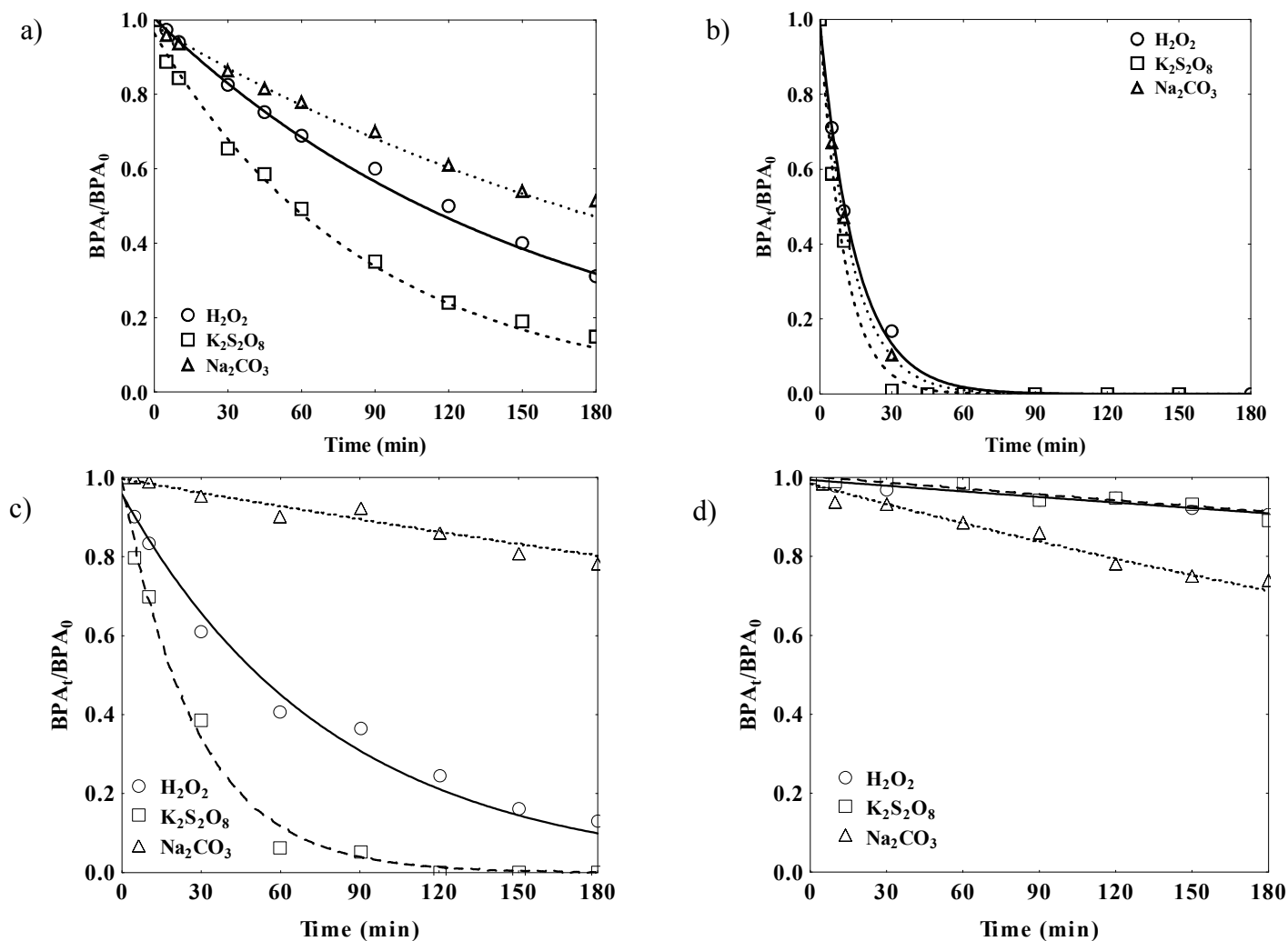


**Figure 6.** Photodegradation of BPA with UV/ $H_2O_2$ , UV/ $K_2S_2O_8$ , and UV/ $Na_2CO_3$  systems in a) ultrapure water b) wastewater, c) surface water, and d) ground water.  $[BPA]_0 = 10$  mg/L,  $[H_2O_2]_0 = [K_2S_2O_8]_0 = [Na_2CO_3]_0 = 500$   $\mu$ M,  $T = 25^\circ$ C.

#### 4. CONCLUSIONS

UV light has inadequate energy to degrade Bisphenol A, and the quantum yield of this system was close to zero, demonstrating its low effectiveness.

The UV/H<sub>2</sub>O<sub>2</sub> system was adequate to degrade BPA, yielding a reaction rate constant of BPA with HO• radicals of  $k_{\text{HO}\cdot\text{BPA}} = 1.70 \pm 0.21 \times 10^{10} \text{ M}^{-1} \text{ s}^{-1}$ . The percentage BPA degradation depended on the solution pH. The photooxidation process of BPA with UV/H<sub>2</sub>O<sub>2</sub> was slightly exothermic.

The UV/K<sub>2</sub>S<sub>2</sub>O<sub>8</sub> system was more effective than UV/H<sub>2</sub>O<sub>2</sub> to degrade BPA, achieving a higher percentage removal in a shorter time due to the generation of SO<sub>4</sub>•<sup>-</sup> and HO• radicals. Moreover, both removal of TOC and reduction of toxicity were the highest when using the UV/K<sub>2</sub>S<sub>2</sub>O<sub>8</sub> system. The reaction rate constant of BPA with SO<sub>4</sub>•<sup>-</sup> radicals was  $k_{\text{SO}_4\cdot\text{BPA}} = 1.37 \pm 0.15 \times 10^9 \text{ M}^{-1} \text{ s}^{-1}$ . The solution pH had a major influence on BPA degradation in the UV/K<sub>2</sub>S<sub>2</sub>O<sub>8</sub> system, and the lowest degradation percentage was at pH = 9. The photooxidation of BPA with UV/K<sub>2</sub>S<sub>2</sub>O<sub>8</sub> was endothermic.

The UV/Na<sub>2</sub>CO<sub>3</sub> system was less effective to degrade BPA in comparison to the UV/H<sub>2</sub>O<sub>2</sub> and UV/K<sub>2</sub>S<sub>2</sub>O<sub>8</sub> systems. The reaction rate constant of BPA with CO<sub>3</sub>•<sup>-</sup>/HCO<sub>3</sub>• radicals was  $k_{\text{CO}_3\cdot/\text{HCO}_3\cdot\text{BPA}} = 3.89 \pm 0.09 \times 10^6 \text{ M}^{-1} \text{ s}^{-1}$ . This reaction was exothermic.

BPA oxidation varied as a function of the water type when the UV/H<sub>2</sub>O<sub>2</sub>, UV/K<sub>2</sub>S<sub>2</sub>O<sub>8</sub>, and UV/Na<sub>2</sub>CO<sub>3</sub> systems were used, decreasing in order: wastewater > surface water > ultrapure water > ground water. The high degradation of BPA in wastewater may be related to its large content of organic matter, which generates additional hydroxyl radicals from the photolysis of organic matter. BPA degradation was lowest in ground water, due to its high content of metallic species and bicarbonate ions, which act as radical scavengers for both HO• and SO<sub>4</sub>•<sup>-</sup> radicals.

With regard to their application, UV/K<sub>2</sub>S<sub>2</sub>O<sub>8</sub> was the most effective to remove BPA and TOC from the different water types with the exception of ground water, for which the UV/Na<sub>2</sub>CO<sub>3</sub> system was the most suitable.



## 5. REFERENCES

- [1] Asakura, H., Matsuto, T., Tanaka, N. (2004). Behavior of endocrine-disrupting chemicals in leachate from MSW landfill sites in Japan. *Waste Management*, 24(6), 613-622.
- [2] Laganá, A., Bacaloni, A., De Ieva, I., Faberi, A., Fago, G., Marino, A. (2004). Analytical methodologies for determining the occurrence of endocrine disrupting chemicals in sewage treatment plant and natural waters. *Analytica Chimica Acta*, 501, (1), 79- 88.
- [3] Yamamoto, T., Yasuhara, A., Shiraishi, H., Nakasugi, O. (2001). Bisphenol A in hazardous waste landfill leachates. *Chemosphere*, 42(4), 415-418.
- [4] Liu, G., Ma, J., Li, X., Qin, Q. (2009). Adsorption of bisphenol A from aqueous solution onto activated carbons with different modification treatments. *Journal of Hazardous Materials*, 164, (2-3), 1275-1280.
- [5] Ministry of health, labour and welfare of Japan. (2000). Exposure and behavior researches of endocrine disrupting chemicals in tap water.
- [6] Nakanishi, A., Tamai, M., Kawasaki, N., Nakamura, T., Tanada, S. (2002). Adsorption characteristics of bisphenol A onto carbonaceous materials produced from wood chips as organic waste. *Journal of Colloid and Interface Science*, 252, (2), 393-396.
- [7] Bautista- Toledo, I., Ferro-García, M.A., Rivera-Utrilla, J., Moreno-Castilla, C., Vegas Fernández, F.J. (2005). Bisphenol A removal from water by activated carbon. Effects of carbon characteristics and solution chemistry. *Environmental Science and Technology*, 38, (16), 6246-6250.
- [8] Lobos, J.H., Leib, T.K., Su, T.M. (1992). Biodegradation of Bisphenol A by a gramnegative aerobic bacterium. *Applied and Environmental Microbiology*, 58, 1823-1831.

- [9] Spivack, J., Leib, T.K., Lobos, J.H. (1994). Novel pathway for bacterial metabolism of Bisphenol A. *Journal of Biological Chemistry*, 269, 7323–7329.
- [10] Ronen, Z., Abeliovich, A. (2000). Anaerobic–aerobic process for microbial degradation of tetrabromobisphenol *Applied and Environmental Microbiology*. 66, 2372–2377.
- [11] Rosenfeldt, E.J., Linden, K.G. (2004). Degradation of Endocrine Disrupting Chemicals Bisphenol A., Ethinyl Estradiol, and Estradiol during UV photolysis and advanced oxidation processes. *Environmental Science and Technology*, 38, 5476-5483.
- [12] Rivas, F. J., Encinas, Á., Acedo, B., Beltrán, F. J. (2009). Mineralization of bisphenol A by advanced oxidation processes. *Journal of Chemical Technology Biotechnology*, 84, (4), 589-594.
- [13] Katsumata, H., Kawabe, S., Kaneco, S., Suzuki, T., Ohta, K. (2004). Degradation of Bisphenol A in water by the photo-Fenton reaction. *Journal Photochemistry Photobiology A*, 162, 297–305.
- [14] Wu, C., Linden, K. G. (2010). Phototransformation of selected organophosphorus pesticides: Roles of hydroxyl and carbonate radicals. *Water Research*, 44, (12), 3585-3594.
- [15] Canonica, S., Kohn, T., Mac, M., Real, F. J., Wirz, J., Gunten, U. V. (2005). Photosensitizer Method to Determine Rate Constants for the Reaction of Carbonate Radical with Organic Compounds. *Environmental Science and Technology*, 39, (23), 9182-9188.
- [16] Méndez-Díaz, J., Sánchez-Polo, M., Rivera-Utrilla, J., Canonica, S., von Gunten, U. (2010). Advanced oxidation of the surfactant SDBS by means of hydroxyl and sulphate radicals. *Chemical Engineering Journal*, 163, (3), 300-306.
- [17] Ocampo-Pérez, R., Sánchez-Polo, M., Rivera-Utrilla, J., Leyva-Ramos, R. (2010). Degradation of antineoplastic cytarabine in aqueous phase by advanced oxidation

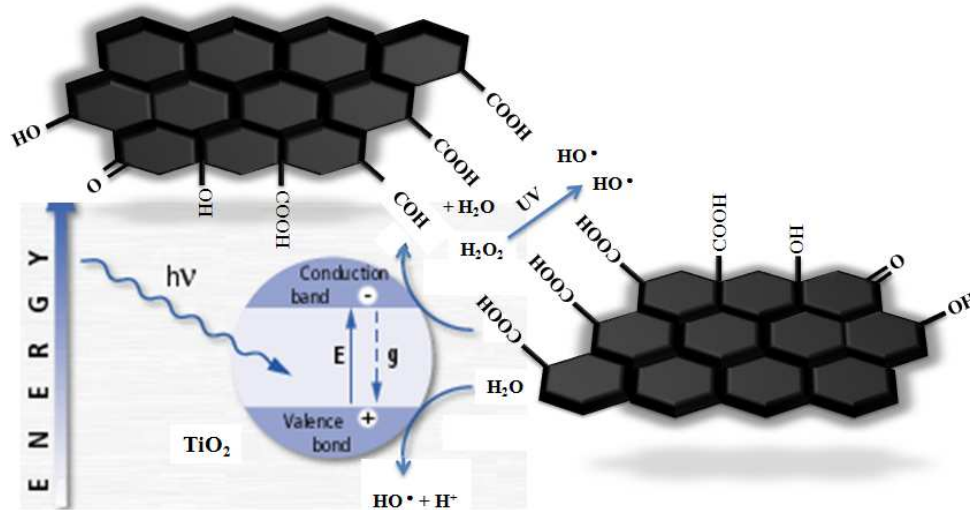
- processes based on ultraviolet radiation. *Chemical Engineering Journal*, 165, (2), 581-588.
- [18] Huang, J., Mabury, S.A. (2000). A new method for measuring carbonate radical reactivity toward pesticides, *Environmental Toxicology and Chemistry* 19, 1501-1507.
- [19] Canonica, S., Meunier, L., von Gunten, U. (2008). Phototransformation of selected pharmaceuticals during UV treatment of drinking water, *Water Research*, 42, 121-128.
- [20] Beltran, F.J., Ovejero, G., Acedo, B. (1993). Oxidation of atrazine in water by ultraviolet radiation combined with hydrogen peroxide, *Water Research*, 27, 1013-1021.
- [21] Azenha, M.E.D.G., Burrows, H.D., Canle L, M., Coimbra, R., Fernández, M.I., García, M.V., Peiteado, M.A., Santaballa, J.A. (2003). On the kinetics and energetics of one-electron oxidation of 1,3,5-triazines. *Chemical Communications*, 112-113.
- [22] APHA, AWWA and WPCF. (1998). Standard method for the examination of water and wastewater, 20th edition. american public health association; american water works association; and water pollution control federation. Washington DC.
- [23] Jennings, V.L.K., Rayner-Brandes, M.H., Bird, D.J. (2001). Assessing chemical toxicity with the bioluminescent photobacterium (*vibrio fischeri*): a comparison of three commercial systems, *Water Research*, 35, 3448-3456.
- [24] Cousins, I.T., Staples, C. A., Klecka, G.M., Mackay, D. (2002). A multimedia assessment of the environmental fate of bisphenol a. *Human and Ecological Risk Assessment*, 8, (5), 1107-1135.
- [25] M. Chang, C. Chung, J. Chern, T. Chen, Dye decomposition kinetics by UV/H<sub>2</sub>O<sub>2</sub>: Initial rate analysis by effective kinetic modeling methodology, *Chemical Engineering Science*, 65 (2010) 135-140.

- [26] Buxton BR, Greenstock CL, Helman WP, Ross AB (1988) Critical review of rate constants for reactions hydrated electrons, hydrogen atoms and hydroxyl radicals ( $\bullet\text{OH}/\bullet\text{O}^-$ ) in aqueous solution. *Journal of Physical and Chemistry Reference Data* 17:513-886.
- [27] Yavuz, Ö., Altunkaynak, Y., Güzel, F. (2003). Removal of copper, nickel, cobalt and manganese from aqueous solution by kaolinite. *Water Research*, 37, (4), 948-952.
- [28] Basfar, A.A., Mohamed, K.A., Al-Abduly, A.J., Al-Shahrani, A.A (2009) Radiolytic degradation of atrazine aqueous solution containing humic substances, *Ecotoxicology and Environmental Safety*, 72, 948-953.
- [29] Hoigne, J., Bader, H (1983) Rate constants of reactions of ozone with organic and inorganic compounds in water. II. Dissociating organic compounds, *Water Research*, 17, 185-194.
- [30] Hoigne, J., Bader, H (1983) Rate constants of reactions of ozone with organic and inorganic compounds in water. I. Non-dissociating organic compounds, *Water Research*, 17, 173-183.
- [31] Grannas, A.M., Martin, C.B., Chin, Y., Platz, M (2006) Hydroxyl radical production from irradiated Arctic dissolved organic matter, *Biogeochemistry*, 78, 51-66.
- [32] Mopper, K., Zhou, X (1990) Hydroxyl radical photoproduction in the sea and its potential impact on marine processes, *Science*, 250, 661-664.
- [33] Vaughan, P.P., Blough, N.V (1998) Photochemical formation of hydroxyl radical by constituents of natural waters, *Environmental Science and Technology*, 32, 2947-2953.
- [34] Khataee, A.R., Mirzajani, O (2010) UV/peroxydisulfate oxidation of C. I. Basic Blue 3: Modeling of key factors by artificial neural network, *Desalination*, 251, 64-69.

- [35] Lau, T.K., Chu, W., Graham, N.J.D (2007) The aqueous degradation of butylated hydroxyanisole by UV/S<sub>2</sub>O<sub>8</sub><sup>2-</sup>: Study of reaction mechanisms via dimerization and mineralization, *Environmental Science and Technology*, 41, 613-619.
- [36] Manoj, K.P. Prasanthkumar., Manjo, V.M., Aravind, U.K., Manojkumar, T.K., Aravindakumar, C.T. (2007). Oxidation of substituted triazines by sulfate radical anion (SO<sub>4</sub><sup>-</sup>) in aqueous medium: A laser flash photolysis and steady state radiolysis study. *Journal of Physical Organic Chemistry*, 20, 122-129.
- [37] Huie, R.E., Clifton, C.L. (1990). Temperature dependence of the rate constants for reactions of the sulfate radical, SO<sub>4</sub><sup>-</sup>, with anions. *Journal of Physical Chemistry*, 94, (23), 8561–8567
- [38] Siegrist, R. L., Crimi, M., Simpkin, T. J. (2011). *In situ* chemical oxidation for ground water remediation. Springer New York Heidelberg Dordrecht London.
- [39] David G. P. M., Bosio G. N., Gonzalez M. C., Russo N., Michelini M. C., Diez R. P., Mártire D. O. (2009). A combination theoretical and experimental study on the oxidation of fluvic acid by the sulfate radical anion. *Photochemistry Photobiology Science*, 8, 992-997.
- [40] Busset, C., Mazellier, P., Sarakha, M., De Laat, J. (2007). Photochemical generation of carbonate radicals and their reactivity with phenol. *Journal of Photochemistry and Photobiology A: Chemistry*, 185(2-3), 127-132.
- [41] Haygarth, K. S., Marin, T. W., Janik, T., Kanjana, K., Stanisky, C. M., Bartels, D. M. (2010). Carbonate Radical Formation in Radiolysis of Sodium Carbonate and Bicarbonate Solutions up to 250 °C and the Mechanism of its Second Order Decay. *Journal of Physical Chemistry A*, 114, (5), 2142–2150

## CAPÍTULO 5

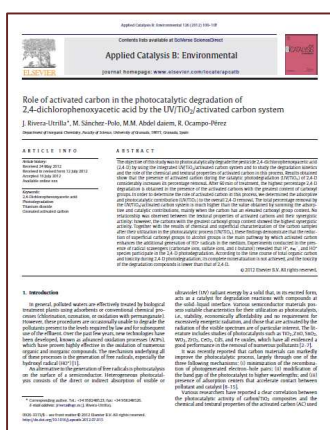
# PAPEL DEL CARBÓN ACTIVADO EN LA DEGRADACIÓN FOTOCATALÍTICA DEL ÁCIDO 2,4-DICLOROFENOXIACÉTICO MEDIANTE EL SISTEMA UV/TiO<sub>2</sub>/CARBÓN ACTIVADO





# ROLE OF ACTIVATED CARBON IN THE PHOTOCATALYTIC DEGRADATION OF 2, 4-DICHLOROPHENOXYACETIC ACID BY THE UV/TiO<sub>2</sub>/ACTIVATED CARBON SYSTEM

Article published in Applied Catalysis B: Environmental 126, 100-107 (2012)



## Highlights

- The degradation of 2,4-D with the UV/TiO<sub>2</sub>/activated carbon (AC) system was studied.
- The presence of ozonated AC enhances 2,4-D photodegradation by the UV/TiO<sub>2</sub> system.
- Carboxyl groups of AC participate in the additional generation of OH<sup>•</sup> radicals.
- The UV/TiO<sub>2</sub>/AC-ozonated system mineralized 40 % of the organic matter.
- The toxicity of the degradation byproducts was much lower than that of 2,4-D.

## ABSTRACT

The objective of this study was to photocatalytically degrade the pesticide 2,4-dichlorophenoxyacetic acid (2,4-D) by using the integrated UV/TiO<sub>2</sub>/activated carbon system and to study the degradation kinetics and the role of the chemical and textural properties of activated carbon in this process. Results obtained show that the presence of activated carbon during the catalytic photodegradation (UV/TiO<sub>2</sub>) of 2,4-D considerably increases its percentage removal. After 60 min of treatment, the highest percentage 2,4-D degradation is obtained in the presence of the activated carbons with the greatest content of carboxyl groups. In order to determine the role of activated carbon in this process, we determined the adsorptive and photocatalytic contribution (UV/TiO<sub>2</sub>) to the overall 2,4-D removal. The total percentage removal by the UV/TiO<sub>2</sub>/activated carbon system is much higher than the value obtained by summing the adsorptive and catalytic contributions, mainly when the carbon has an elevated carboxyl group content. No relationship was observed between the textural properties of activated carbons and their synergistic activity; however, the carbons with the greatest carboxyl group content showed the highest synergistic activity. Together with the results of chemical and superficial characterization of the carbon samples after their utilization in the photocatalytic process (UV/TiO<sub>2</sub>), these findings demonstrate that the reduction of superficial carboxyl groups to alcohol groups is the main pathway by which activated carbon enhances the additional generation of HO<sup>•</sup> radicals in the medium. Experiments conducted in the presence of radical scavengers (carbonate ions, sulfate ions, and t-butanol) revealed that H<sup>•</sup>, e<sub>aq</sub><sup>-</sup>, and HO<sup>•</sup> species participate in the 2,4-D photodegradation. According to the time course of total organic carbon and toxicity during 2,4-D photodegradation, its complete mineralization is not achieved, and the toxicity of the degradation compounds is lower than that of 2,4-D.





## 1. INTRODUCTION

In general, polluted waters are effectively treated by biological treatment plants using adsorbents or conventional chemical processes (chlorination, ozonation, or oxidation with permanganate). However, these procedures are occasionally unable to degrade the pollutants present to the levels required by law and for subsequent use of the effluent. Over the past few years, new technologies have been developed, known as advanced oxidation processes (AOPs), which have proven highly effective in the oxidation of numerous organic and inorganic compounds. The mechanism underlying all of these processes is the generation of free radicals, especially the hydroxyl radical ( $\text{HO}^\bullet$ ) [1].

An alternative to the generation of free radicals is photocatalysis on the surface of a semiconductor. Heterogeneous photocatalysis consists of the direct or indirect absorption of visible or ultraviolet (UV) radiant energy by a solid that, in its excited form, acts as a catalyst for degradation reactions with compounds at the solid-liquid interface. Various semiconductor materials possess suitable characteristics for their utilization as photocatalysts, i.e., stability, economic affordability and no requirement for excessively energetic radiation, and those that are activated by the radiation of the visible spectrum are of particular interest. The literature includes studies of photocatalysts such as  $\text{TiO}_2$ ,  $\text{ZnO}$ ,  $\text{SnO}_2$ ,  $\text{WO}_3$ ,  $\text{ZrO}_2$ ,  $\text{CeO}_2$ ,  $\text{CdS}$ , and Fe oxides, which have all evidenced a good performance in the removal of numerous pollutants [2-7].

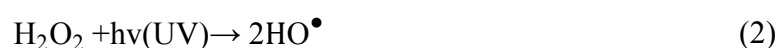
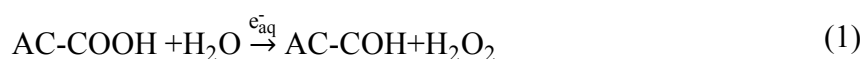
It was recently reported that carbon materials can markedly improve the photocatalytic process, largely through one of the three following mechanisms: i) minimization of the recombination of photogenerated electron-hole pairs; ii) modification of the band gap of the photocatalyst to higher wavelengths; and iii) presence of adsorption centers that accelerate contact between pollutant and catalyst [8-15].

Various researchers have reported a clear correlation between the photocatalytic activity of carbon/ $\text{TiO}_2$  composites and the chemical and textural properties of the activated carbon (AC) used as support [16]. The variation in degradation rate as a function of the

properties of the carbon material has been described as a synergistic effect in the literature. Thus, Matos et al. [16] studied the photocatalytic degradation of phenol, 4-chlorophenol, and 2,4-D in the presence of TiO<sub>2</sub> and two commercial activated carbons (L and H) and found that the presence of carbon H improved the photocatalytic degradation of pollutants with a synergistic factor of 2.5, 2.4, and 1.3, respectively. Cordero et al. [17] used a carbon prepared from *Tabebuia pentaphyla* wood and activated with CO<sub>2</sub> at 450-1000°C and reported that it exerted a synergistic effect on the catalytic activity of TiO<sub>2</sub>, enhancing the degradation of 4-chlorophenol.

A possible mechanism by which activated carbon increases the photocatalytic activity of TiO<sub>2</sub> was proposed by Silva et al. [10], who reported that the presence of mild concentrations of oxygen-containing surface groups, mainly carboxylic acids and phenols, may improve the photocatalytic activity of multi-walled carbon nanotubes–TiO<sub>2</sub> composite catalysts in the photocatalytic oxidation of benzene derivatives in aqueous suspensions.

In a previous study, Ocampo-Perez et al. [8] investigated the photocatalytic degradation of cytarabine in aqueous phase (UV/TiO<sub>2</sub>) in the presence of activated carbon with different chemical and textural properties. Results obtained suggested that the reaction of e<sub>aq</sub><sup>-</sup>, from the UV-TiO<sub>2</sub> interaction, with the activated carbon carboxylic acids are responsible for the increased photocatalytic activity of TiO<sub>2</sub>. We therefore hypothesized that the interaction between e<sub>aq</sub><sup>-</sup> and surface carboxylic acids on oxidized carbons reduces carboxylic acids to aldehydes, generating H<sub>2</sub>O<sub>2</sub> that can be decomposed into HO• radicals, and that these aldehydes can be transformed into a surface alcohol group that generates additional HO• radicals. The proposed mechanism is given by the following reactions.



With this background, the main aim of the present study was to experimentally confirm this mechanism, thereby advancing knowledge of the UV/TiO<sub>2</sub>/activated carbon system and assisting selection of the most appropriate carbons for obtaining the maximum degradation and mineralization of pollutants. For this purpose, we photocatalytically degraded herbicide 2,4-D, selected as model compound, using the UV/TiO<sub>2</sub>/activated carbon system and determined the degradation kinetics, the influence of operational variables, the effect of the chemical nature of the carbon, and the modifications of the carbon surface chemistry during the photooxidation process.

2,4-D is a herbicide in extensive use worldwide [18], thanks to its low cost and good selectivity [19], and it has been detected in waters in various regions [20]. It is considered moderately toxic, with a maximum allowed concentration in drinking water of 100 µg/L. 2,4-D has been eliminated from aqueous solutions with varying degrees of success by means of microbial, chemical, and photochemical processes [21, 22]. Photocatalysis has been reported as a good alternative for the degradation of recalcitrant compounds [23] and represents another potential technology for removing 2,4-D.

## 2. EXPERIMENTAL METHOD

### 2.1. Reagents

All chemical reagents used in this study (2,4-D, acetonitrile, *t*-butanol, sodium sulfate, and sodium carbonate) were high-purity analytical grade reagents supplied by Sigma-Aldrich. All solutions were prepared with ultrapure water obtained from Milli-Q<sup>®</sup> equipment (Millipore). Figure 1 depicts the molecular structure of 2,4 D and the species diagram of 2,4-D as a function of pH.

### 2.2. Activated carbons

Three commercial powdered activated carbons were used: Sorbo (S), Merck (M), and Witcot (W). The particle size range was 0.05-0.08 mm. Activated carbon W was oxidized with ozone (W<sub>O<sub>3</sub></sub>) in an OZOKAV ozonator with a maximum capacity of 76 mg/min, placing 0.50 g of activated carbon W in a column with upward O<sub>3</sub> flow and keeping the activated carbon in suspension to ensure its homogeneous oxidation. Two

carbon samples were obtained after ozone exposure of 30 min ( $W_{O_3-30}$ ) and 120 min ( $W_{O_3-120}$ ). All activated carbon samples were stored in a sealed container and placed in an oven at 110°C before their use.

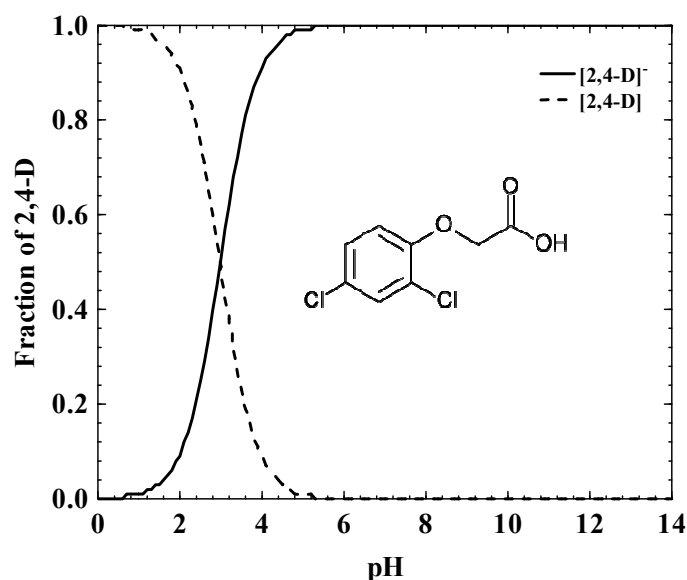


**Figure 1.** Molecular structure and species diagram of 2,4-D as a function of pH.

The physical characterization (surface area from adsorption of  $N_2$  at 77 K) and chemical characterization (functional groups and pH of the point of zero charge) of the five carbon samples were previously reported [8], and some of these characteristics are given in Table 1.

**Table 1.** Textural and chemical characteristics of the activated carbons

| Activated carbon | $S_{BET}^a)$<br>( $m^2/g$ ) | $pH_{PZC}^b)$ | Basic groups<br>( $meq/g$ ) | Carboxyl groups<br>( $meq/g$ ) | Phenol groups<br>( $meq/g$ ) | Lactone groups<br>( $meq/g$ ) | Total acid groups<br>( $meq/g$ ) |
|------------------|-----------------------------|---------------|-----------------------------|--------------------------------|------------------------------|-------------------------------|----------------------------------|
| S                | 1225                        | 10            | 1.08                        | 0.00                           | 0.24                         | 0.060                         | 0.30                             |
| M                | 1301                        | 7.7           | 0.44                        | 0.04                           | 0.16                         | 0.120                         | 0.32                             |
| W                | 1110                        | 6.5           | 0.76                        | 0.32                           | 0.42                         | 0.035                         | 0.78                             |
| $W_{O_3-30}$     | 670                         | 3.3           | 0.05                        | 1.42                           | 0.15                         | 0.99                          | 2.56                             |
| $W_{O_3-120}$    | 655                         | 2.9           | 0.03                        | 1.55                           | 0.11                         | 1.86                          | 3.52                             |

a) Surface area

b) pH of the point of zero charge

After the photocatalytic process, the carbon samples were again physically and chemically characterized to determine the chemical changes undergone by the activated carbons during 2,4-D degradation by the UV/TiO<sub>2</sub>/activated carbon system. A detailed description of the characterization methods was previously published [8, 24, 25].

### **2.3. Titanium dioxide**

TiO<sub>2</sub> used in this study was supplied by Degussa. X-ray diffraction (XRD) analysis revealed 93% anatase content and 7% rutile content. The surface area of TiO<sub>2</sub> was 60.9 m<sup>2</sup>/g. After the photocatalysis, the TiO<sub>2</sub> sample was again analyzed by XRD in order to determine changes in its crystal structure.

### **2.4. Adsorption isotherms of 2,4-D on both activated carbon and TiO<sub>2</sub>**

The experimental data for the adsorption equilibrium of 2,4-D on activated carbon or TiO<sub>2</sub> were obtained as follows. A mass of 10 mg of activated carbon or TiO<sub>2</sub> and 30 mL of 2,4-D solution at T = 25°C and pH=7 were added in the batch adsorber; the 2,4-D solution, at initial 2,4-D concentrations of 10-100 mg/L, remained in contact with the activated carbon or TiO<sub>2</sub> particles until equilibrium was reached. Preliminary experiments revealed that two days were sufficient to attain equilibrium. After reaching equilibrium, the solutions were centrifuged and filtered with Millipore disc filters (0.2 μm) to remove activated carbon or TiO<sub>2</sub>, and the final 2,4-D concentration was determined. The mass of 2,4-D adsorbed at equilibrium was calculated by a mass balance method.

### **2.5. Photoreactor design**

2,4-D degradation experiments in the presence of activated carbon and/or TiO<sub>2</sub> were conducted in a photoreactor formed by concentric tubes: a stainless steel outer tube (inner diameter [i.d.] of 13 cm x height of 18 cm) and quartz inner tube (i.d. of 5.5 cm x height of 45 cm). The inner tube contained a low-pressure Hg lamp (Heraeus Noblelight model TNN 15/32, nominal power 15 W, I<sub>0</sub> = 1.027×10<sup>-4</sup> Einstein s<sup>-1</sup> m<sup>-2</sup> at λ = 254 nm). The annular space of the photoreactor contained a sample holder with a capacity for six quartz reaction tubes (i.d. of 1.6 cm × height of 20 cm). Solutions in reaction tubes were kept at constant temperature by using a Frigiterm ultrathermostat, and the

suspension within reaction tubes was maintained in agitation by means of a magnetic agitation system.

## **2.6. Photocatalytic degradation of 2,4-D in the presence of activated carbon and/or TiO<sub>2</sub>**

Experimental 2,4-D photodegradation data were obtained as follows. A concentrated solution of 2,4-D (1000 mg/L) was prepared by adding 0.1 g of 2,4-D to a 100 mL flask with ultrapure water; 28.5 mL of ultrapure water were placed in the reaction tubes and different masses of activated carbon and TiO<sub>2</sub> were added. The suspension was homogenized by manual agitation and placed inside the photoreactor, where agitation continued. An aliquot (1.5, 0.75, or 0.30 mL) of 2,4-D solution was added to the reaction tubes to obtain an initial 2,4-D concentration of 50, 25, or 10 mg/L, respectively, simultaneously activating the photoreactor lamp. For all experiments the solutions were in anoxic conditions which were achieved by bubbling N<sub>2</sub>, and the solution pH was 7. Photocatalytic degradation of 2,4-D was monitored by taking 1.0-mL samples at regular time intervals for 2,4-D concentration measurement. After samples were withdrawn, they were immediately filtered with Millipore disc filters (0.20 µm- GSWP) to remove the activated carbon and TiO<sub>2</sub>.

Photocatalytic degradation of 2,4-D in the presence of radical scavengers was carried out using the same methodology but adding an aliquot of t-BuOH, Na<sub>2</sub>SO<sub>4</sub>, or Na<sub>2</sub>CO<sub>3</sub>/Na<sub>2</sub>SO<sub>4</sub> solutions to reaction tubes to obtain the desired concentration of 1 M of each radical scavenger.

## **2.7. Determination of 2,4-D concentration in aqueous solution**

The 2,4-D concentration in aqueous solution was determined by reverse-phase high performance liquid chromatography (HPLC) using a liquid chromatograph (Thermo-Fisher) equipped with a visible UV detector and an autosampler with capacity for 120 vials. A Nova-Pak® C<sub>18</sub> chromatographic column was used (4µm particle size; 3.9×150 mm). The mobile phase was 20 % acetonitrile and 80 % water in isocratic mode at a flow of 1.0 mL/min; the detector wavelength was 280 nm, and the injection volume was 100 µL.

## 2.8. Determination of total organic carbon

Total organic carbon (TOC) present in the system was determined by using a Shimadzu V-CSH analyzer with ASI-V autosampler.

## 2.9. Determination of degradation byproduct toxicity

Degradation byproduct toxicity was determined by using the LUMIStox 300 system and LUMIStherm incubator (Dr. Lange GmbH), based on the normalized biotest (UNE/EN/ISO 11348-2) of luminescent inhibition of *Vibrio Fischeri* bacteria (NRRL B-11177) [26, 27]. Toxicity was expressed as percentage inhibition at 15 min of exposure with reference to a stock saline solution (control).

## 3. RESULTS AND DISCUSSION

### 3.1. Adsorption isotherms and adsorption kinetics of 2,4-D on activated carbon

We first determined the adsorptive capacity of the activated carbons to enable subsequent interpretation of the results of catalytic photooxidation of 2,4-D in their presence. Figure 2a depicts the adsorption isotherms of 2,4-D on the five carbon samples.

The experimental data were interpreted with the Langmuir adsorption isotherm, which is mathematically represented as follows:

$$q = \frac{q_m K C_e}{1 + K C_e} \quad (4)$$

where  $C_e$  is 2,4-D concentration at equilibrium (mg/L),  $q$  is the mass of 2,4-D adsorbed per mass unit of carbon (mg/g),  $q_m$  is the maximum amount of 2,4-D adsorbed per adsorbent mass unit (mg/g), and  $K$  is the Langmuir constant (L/mg).

Table 2 lists the values of the above parameters and the percentage mean absolute deviation, %D, which was estimated from the following equation:



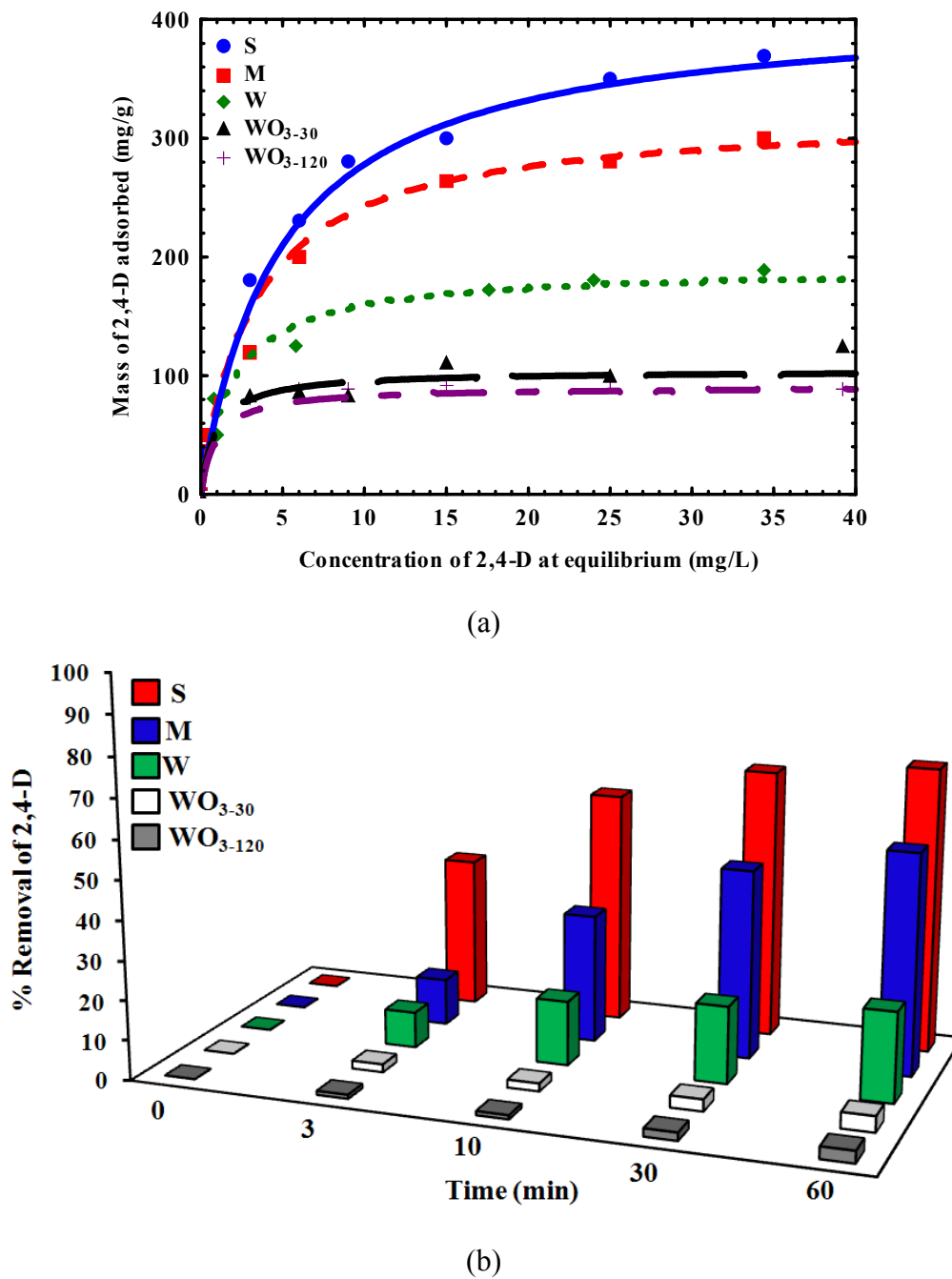


**Figure 2.** Adsorption of 2,4-D on activated carbons, (a) adsorption isotherms, (b) adsorption kinetics.  $T = 25^{\circ}\text{C}$  and  $\text{pH} = 7$ .

$$\%D = \frac{1}{N} \sum_{i=1}^N \left| \frac{q_{\text{exp}} - q_{\text{pred}}}{q_{\text{exp}}} \right| \times 100\% \quad (5)$$

where  $N$  is the number of experimental data points,  $q_{\text{exp}}$  (mg/g) is the experimental mass of 2,4-D adsorbed, and  $q_{\text{pred}}$  (mg/g) is the mass of adsorbed 2,4-D predicted with the Langmuir adsorption isotherm.

**Table 2.** Results obtained by applying the Langmuir equation to the equilibrium adsorption data.

| Activated carbon    | $q_m$<br>(mg/g) | $K$<br>(L/mg) | %D   |
|---------------------|-----------------|---------------|------|
| S                   | 412.1           | 0.207         | 11.1 |
| M                   | 321.1           | 0.307         | 3.1  |
| W                   | 190.8           | 0.507         | 5.1  |
| W <sub>O3-30</sub>  | 104.1           | 1.074         | 14.5 |
| W <sub>O3-120</sub> | 90.3            | 1.074         | 8.2  |

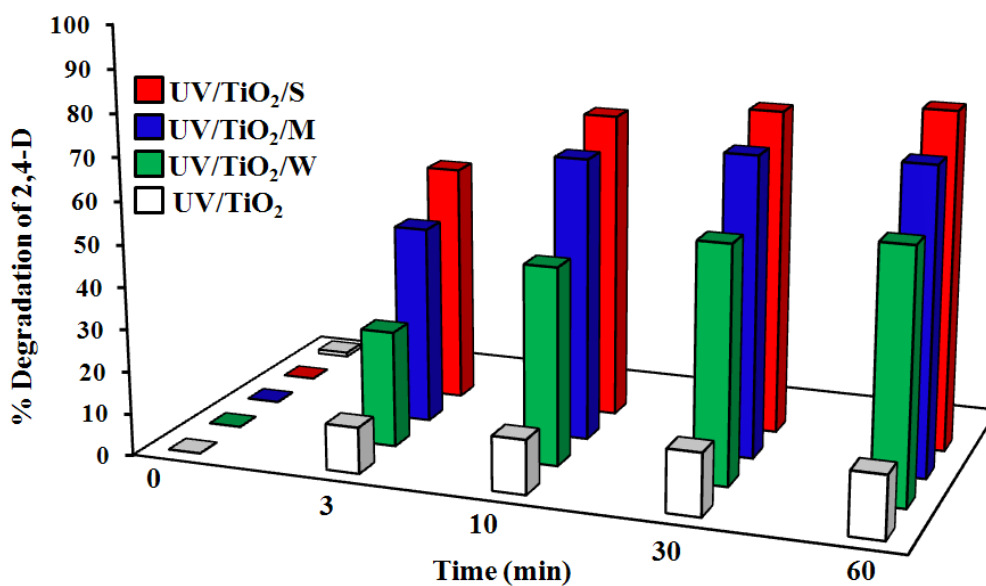
According to the data in Table 2, the highest adsorption capacity was obtained with sample S, followed by samples M, W, W<sub>O3-30</sub>, and W<sub>O3-120</sub>, with  $q_m$  values ranging from 412.1 mg/g (sample S) to 90.3 mg/g (sample W<sub>O3-120</sub>). The low adsorption capacity of ozonated carbons W<sub>O3-30</sub> and W<sub>O3-120</sub> is explained by two factors: a) under the experimental conditions used in this study ( $\text{pH} = 7$ ,  $T = 25$  °C), there is an increase in repulsive electrostatic interactions between 2,4-D and carbon surface, because 2,4-D is in deprotonated form (Figure 1) with a negative charge ( $\text{pK}_a = 2.85$ ) and the carbon surface is negative ( $\text{pH}_{\text{solution}} > \text{pH}_{\text{PZC}}$ ) and becomes more negative with lower  $\text{pH}_{\text{PZC}}$  (Table 1); and b) oxidation of the activated carbons increases the number of surface carboxyl groups (electronic deactivators of aromatic rings) and reduces the concentration of phenol groups (electronic activators of these rings), weakening  $\pi$ - $\pi$  adsorbate-adsorbent dispersion interactions through a reduction in the electronic density of carbon graphene planes [28-31].

Figure 2b shows the percentage 2,4-D removal as a function of time over a 60-min contact period with the different activated carbons at an initial 2,4-D concentration of 50 mg/L and carbon mass of 10 mg. This figure demonstrates that the percentage 2,4-D

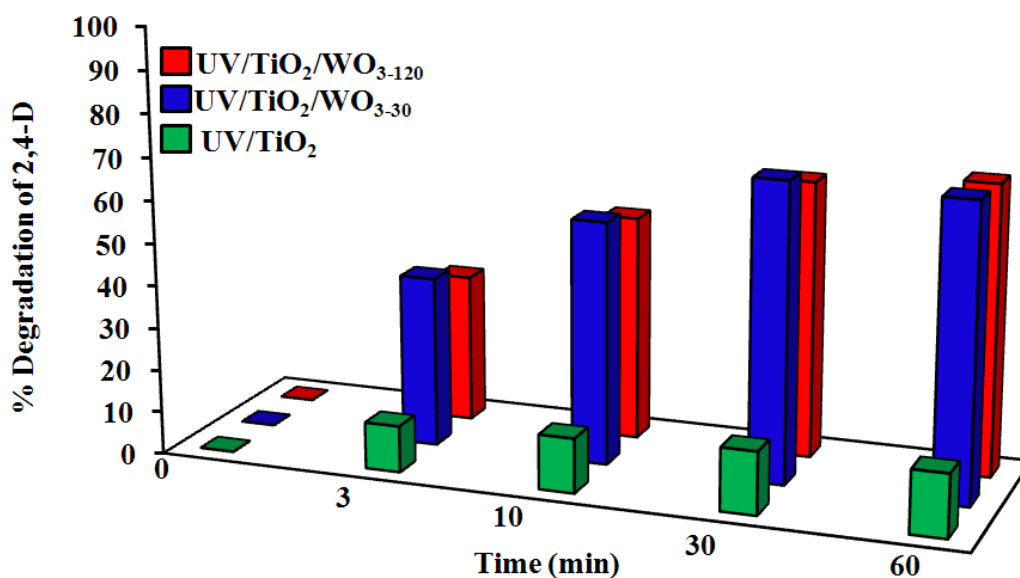
removal markedly increased after longer contact times with carbons S, M, and W and remains almost constant over time with samples  $WO_{3-30}$  and  $WO_{3-120}$ . After 60 min of contact, the highest percentage removal (72%) was with carbon S, followed by carbons M (56%), W (23%),  $WO_{3-30}$  (3%), and  $WO_{3-120}$  (4%). Hence, carbon S has the highest adsorption capacity and removal rate. It should be noted that the adsorption rate of organic compounds on granular activated carbon is generally controlled by intraparticle diffusion (diffusion in pore volume or superficial diffusion) [32, 33]; however, external mass transport was more important in the present study, in which a very small particle size (0.05-0.08 mm) was used in order to achieve a maximum reduction in diffusion effects, considerably reducing the intraparticle trajectory of 2,4-D molecules.

### 3.2. Photocatalytic degradation of 2,4-D in the presence of the activated carbons

Figure 3a depicts the variation in percentage 2,4-D degradation as a function of treatment time with the UV/TiO<sub>2</sub> system in the presence of carbons S, M, and W, while Figure 3b depicts this variation in the presence of carbons  $WO_{3-30}$  and  $WO_{3-120}$ . Figure 3a shows that the highest percentage 2,4-D removal after 60 min of treatment was obtained with carbon S (80%), followed by carbons M (72%) and W (59%). Comparing with the results in Figure 2b, the removal of 2,4-D was 1.1, 1.38, and 2.57-fold higher, respectively, with the combined UV/TiO<sub>2</sub>/activated carbon process than with the adsorption process. The role of activated carbon in the UV/TiO<sub>2</sub>/activated carbon system was analyzed by determining the contributions of adsorption and photocatalysis (UV/TiO<sub>2</sub>) to the removal of 2,4-D at 60 min of the combined treatment. The results in Table 3 show that: i) the greatest adsorptive contribution to the global removal process is made with carbons S and M ; ii) with these two carbons (S and M), the contribution of the photocatalytic process (UV/TiO<sub>2</sub>) is very low in comparison to the contribution of the adsorptive process, and iii) with carbon W, the total percentage removal obtained by the UV/TiO<sub>2</sub>/activated carbon system is markedly higher than the result of summing the adsorptive and catalytic contributions, indicating that its presence has a synergistic effect on the 2,4-D removal process.



(a)



(b)

**Figure 3.** 2,4-D photodegradation by means of the UV/TiO<sub>2</sub> system in the presence of different activated carbons. T = 25° C, pH = 7, [2,4-D]= 50 mg/L, mass of TiO<sub>2</sub> and activated carbon = 5 mg, and V = 30 mL.

The results in Table 3 were compared with the chemical and textural properties of the activated carbons. No clear relationship was observed between the surface area and the synergistic contribution to the global removal process, given that the three activated

carbons have a similar surface area ( $\cong 1200 \text{ m}^2/\text{g}$ ). However, the content of carboxyl and phenol groups is higher in carbon W than in carbons S or M (Table 1). Hence, the synergistic activity of carbon W in the removal of 2,4-D by the UV/TiO<sub>2</sub>/activated carbon system may be related to the elevated carboxyl group content on its surface (0.32 meq/g vs. 0.00 meq/g on carbon S and 0.04 meq/g on carbon M), as proposed in a previous study [8].

**Table 3.** Adsorptive and photocatalytic contributions to the removal of 2,4-D with the UV/TiO<sub>2</sub>/activated carbon system.

| <b>Activated Carbon</b>   | <b>Total (%)</b> | <b>Adsorption (%)</b> | <b>UV/TiO<sub>2</sub> (%)</b> | <b>Synergistic contribution (%)</b> |
|---------------------------|------------------|-----------------------|-------------------------------|-------------------------------------|
| <b>S</b>                  | 80               | 72                    | 14                            | 0                                   |
| <b>M</b>                  | 72               | 56                    | 14                            | 2                                   |
| <b>W</b>                  | 59               | 23                    | 14                            | 22                                  |
| <b>W<sub>O3-30</sub></b>  | 70               | 3                     | 14                            | 53                                  |
| <b>W<sub>O3-120</sub></b> | 70               | 4                     | 14                            | 52                                  |

The role of carboxyl groups in the photocatalytic process was examined by increasing the carboxyl group content of carbon W through oxidation with ozone for 30 min (W<sub>O3-30</sub>) and 120 min (W<sub>O3-120</sub>) and then texturally and chemically characterizing these samples (Table 1). The ozone treatment reduced the surface area value by 50%, increased the content of carboxyl and lactone groups, and reduced the content of phenol groups. The mechanism by which ozone interacts with the activated carbon surface has been reported in various publications [25, 34].

Figure 3b depicts the photocatalytic degradation of 2,4-D in the presence of these ozonated samples (W<sub>O3-30</sub> and W<sub>O3-120</sub>), demonstrating that the degradation was markedly enhanced by their presence, achieving 70% removal of 2,4-D after 60 min in both cases. This is much higher than the percentage removal obtained with the untreated carbon (W). As shown in Table 3, i) these ozonated carbon samples (W<sub>O3-30</sub> and W<sub>O3-</sub>

120) make a very low adsorptive contribution (<4%) to the global 2,4-D removal process, and ii) they make the highest synergistic contribution to this global process (>50 %).

In order to identify the mechanism by which ozonated carbon samples enhance 2,4-D photocatalysis, we chemically characterized sample  $W_{O3-30}$  by exposing it to UV and UV/TiO<sub>2</sub> radiation in the absence of 2,4-D. The results in Table 4 show: i) similar values of surface acid groups between UV-treated and untreated samples, and ii) a lower concentration of carboxyl groups and markedly higher content of phenol and lactone groups in the UV/TiO<sub>2</sub>-treated *versus* untreated samples.

**Table 4.** Chemical characteristics of the  $W_{O3-30}$  sample after treatment with UV or UV/TiO<sub>2</sub>.

| Activated carbon treatment         | pH <sub>PZ</sub><br>c | Basic groups<br>(meq/g) | Carboxyl groups<br>(meq/g) | Phenol groups<br>(meq/g) | Lactone groups<br>(meq/g) | Acid groups<br>(meq/g) |
|------------------------------------|-----------------------|-------------------------|----------------------------|--------------------------|---------------------------|------------------------|
| $W_{O3-30}$                        | 3.3                   | 0.05                    | 1.42                       | 0.15                     | 0.99                      | 2.56                   |
| UV/ $W_{O3-30}$                    | 3.2                   | 0.02                    | 1.40                       | 0.11                     | 0.97                      | 2.48                   |
| UV/ TiO <sub>2</sub> / $W_{O3-30}$ | 3.8                   | 0.05                    | 1.12                       | 0.23                     | 1.21                      | 2.61                   |

These results verify the proposed mechanism (reactions 1-3), indicating that the main pathway by which activated carbons enhance 2,4-D removal by the UV/TiO<sub>2</sub>/carbon system is the reduction of superficial carboxyl groups to aldehyde groups and finally to alcohol groups. Alcohol groups formed on the carbon surface may in turn react with adjacent carboxyl groups in the graphene planes of the activated carbon, generating lactone groups. This would explain the increase in lactone groups in sample  $W_{O3-30}$  with the UV/TiO<sub>2</sub>/ $W_{O3-30}$  system. The increase in phenol groups in sample  $W_{O3-30}$  would result from the decarboxylation of carboxyl groups to CO<sub>2</sub> by HO• radicals, followed by oxidation of the nascent surface carbons to phenol groups.

Figure 4 depicts the results from XRD analysis of the crystallinity of TiO<sub>2</sub> before and after photocatalysis. The crystallinity phases (anatase and rutile) were computed by using the following equation [35]

$$R(T) = 0.679 \left( \frac{I_R}{I_R + I_A} \right) + 0.312 \left( \frac{I_R}{I_R + I_A} \right)^2 \quad (6)$$

where  $R(T)$  is the rutile percentage,  $I_A$  is the intensity of the main anatase peak ( $2\theta=25.30^\circ$ ), and  $I_R$  is the intensity of the main rutile peak ( $2\theta=27.44^\circ$ ). The content of both samples was 93% anatase and 7% rutile. Hence, the crystallinity of  $\text{TiO}_2$  is not modified by interactions between the species generated in  $\text{TiO}_2$  photoactivation and the acid sites on the activated carbon.

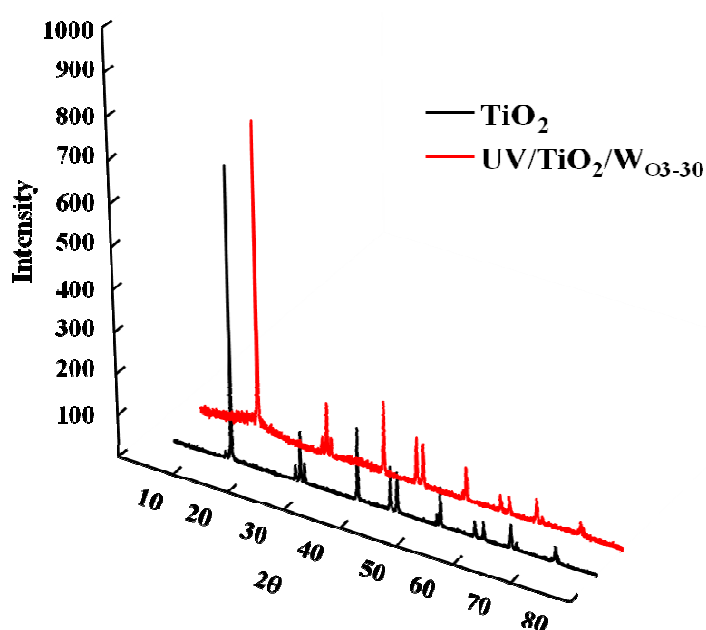


**Figure 4.** XRD of  $\text{TiO}_2$  before and after treatment.

The 2,4-D degradation by-products obtained by using both  $\text{UV}/\text{TiO}_2$  and  $\text{UV}/\text{TiO}_2/\text{WO}_3$  systems were determined by means of an ultra-pressure liquid chromatograph (UPLC) coupled to a mass spectrometer. In both cases the by-products detected were: 2-(2-chloro-4-hydroxyphenoxy) acetic acid, 2-(2,4-dihydroxyphenoxy) acetic acid, 5-chloro-2-methylphenol, and 4-methoxybenzene-1,3-diol.

### 3.3. Effect of the mass of activated carbon and $\text{TiO}_2$ on 2,4-D photocatalytic degradation

The effect of the mass of  $\text{TiO}_2$  and activated carbon on the percentage 2,4-D degradation was assessed by using a three-level full factorial design with one center

point. A total of 9 experiments were generated, taking the percentage degradation as response and the masses of carbon and  $\text{TiO}_2$  as independent variables. The initial concentration of 2,4-D was 50 mg/L and the masses of carbon and  $\text{TiO}_2$  were 0, 5, and 10 mg. The experimental response was fitted to the following equation:

$$\% \text{ Degradation} = \beta_1 x + \beta_2 x^2 + \beta_3 y + \beta_4 y^2 + \beta_5 xy + \beta_6 xy^2 + \beta_7 x^2 y + \beta_8 x^2 y^2 \quad (7)$$

where,  $\beta_1 \dots \beta_8$  are constants,  $x$  represents the carbon mass, and  $y$  is the  $\text{TiO}_2$  mass. Carbon  $\text{W}_{\text{O3-30}}$  was selected for these experiments. Figure 5 depicts the variation in percentage 2,4-D degradation as a function of the mass of  $\text{TiO}_2$  and activated carbon. The percentage 2,4-D degradation in the presence of carbon or  $\text{TiO}_2$  is very low and is markedly enhanced by increases in the mass of  $\text{TiO}_2$  and carbon. Figure 5 also shows that the highest percentage degradation was achieved with the addition of around 8 mg of both carbon and  $\text{TiO}_2$ .

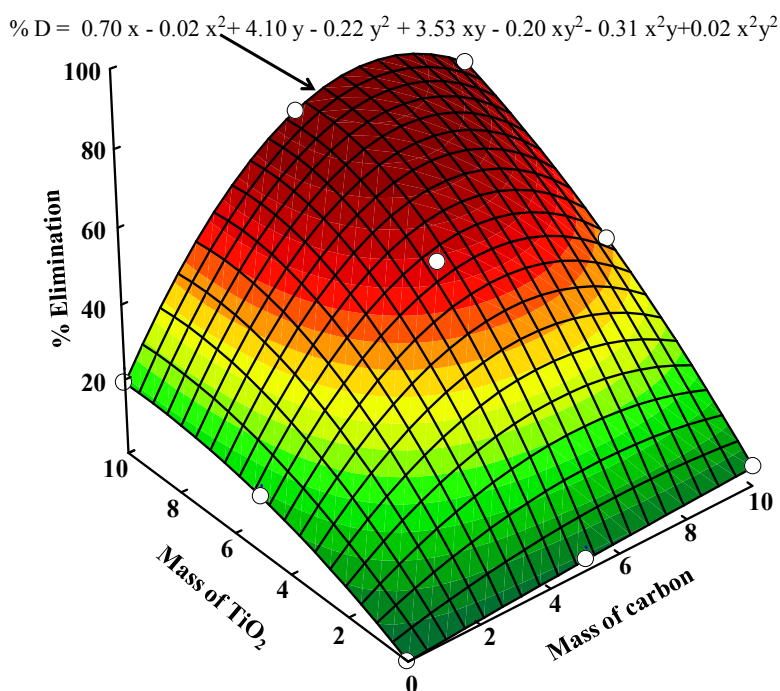
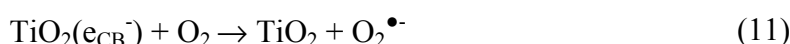
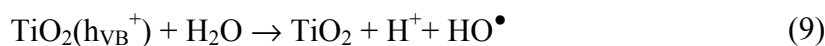
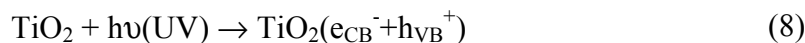


**Figure 5.** Variation in percentage 2,4 D degradation by the UV/ $\text{TiO}_2$ / $\text{W}_{\text{O3-30}}$  system with different masses of  $\text{TiO}_2$  and activated carbon.  $T = 25^\circ\text{C}$  and  $\text{pH} = 7$ ,  $[\text{2,4-D}]_0 = 50$  mg/L.



### 3.4. 2,4-D photocatalytic degradation in the presence of radical scavengers

Radical species generated in the UV activation of TiO<sub>2</sub> may give rise to oxidation or reduction reactions.



In order to study which of these species are involved in 2,4-D degradation, experiments were conducted in the presence of radical scavengers (t-BuOH, CO<sub>3</sub><sup>2-</sup>, or SO<sub>4</sub><sup>2-</sup>). The reaction rate constant of these scavengers with e<sub>aq</sub><sup>-</sup>, H<sup>•</sup> and HO<sup>•</sup> are given in Table 5.

**Table 5.** Reaction rate constant of radical scavengers with e<sub>aq</sub><sup>-</sup>, H<sup>•</sup> or HO<sup>•</sup> radicals [36]

| Scavengers                    | k <sub>e<sub>aq</sub><sup>-</sup></sub><br>(M <sup>-1</sup> s <sup>-1</sup> ) | k <sub>H<sup>•</sup></sub><br>(M <sup>-1</sup> s <sup>-1</sup> ) | k <sub>HO<sup>•</sup></sub><br>(M <sup>-1</sup> s <sup>-1</sup> ) |
|-------------------------------|---|--|---|
| CO <sub>3</sub> <sup>2-</sup> | 3.5×10 <sup>5</sup>   | ----   | 3.9×10 <sup>8</sup>   |
| SO <sub>4</sub> <sup>2-</sup> | 1.0×10 <sup>6</sup>   | ----   | ----  |
| t-BuOH                        | 4.0×10 <sup>5</sup>   | 1.7×10 <sup>5</sup>  | 6.0×10 <sup>8</sup>   |

Figure 6 depicts the percentage 2,4-D degradation as a function of time with the UV/TiO<sub>2</sub>/W<sub>O3-30</sub> system in the presence of t-BuOH (1M), SO<sub>4</sub><sup>2-</sup>/CO<sub>3</sub><sup>2-</sup> ions (1M/1M) and SO<sub>4</sub><sup>2-</sup> ions (1M). The percentage 2,4-D degradation after 60 min of treatment was 4%, 12%, and 38%, respectively. This figure also demonstrates that i) radical H<sup>•</sup> participates in the 2,4-D photodegradation process, and ii) the reduction in 2,4-D degradation rate is greater in the presence of t-BuOH (HO<sup>•</sup>, e<sub>aq</sub><sup>-</sup>, and H<sup>•</sup> scavenger) than in the presence of SO<sub>4</sub><sup>2-</sup>/CO<sub>3</sub><sup>2-</sup> (HO<sup>•</sup> and e<sub>aq</sub><sup>-</sup> scavenger) or SO<sub>4</sub><sup>2-</sup> (e<sub>aq</sub><sup>-</sup> scavenger) ions.

Based on the results in Figure 6, we calculated the contribution of each radical species to the global 2,4-D degradation by the UV/TiO<sub>2</sub>/W<sub>O3-30</sub> system as a function of

treatment time by subtracting the degradation kinetics corresponding to each radical from the overall degradation kinetics obtained by using the UV/TiO<sub>2</sub>/W<sub>03-30</sub> system. The results are depicted in Figure 7 and show that i) the three radical species participate in the decomposition of 2,4-D throughout the treatment period, ii) the contribution of H<sup>•</sup> to the global removal process increases initially and then remains constant after 30 min of treatment, iii) the contribution of HO<sup>•</sup> radicals reduces initially and then remains constant after 30 min, and iv) the contribution of e<sub>aq</sub><sup>-</sup> increases initially and then remains virtually constant after 30 min.

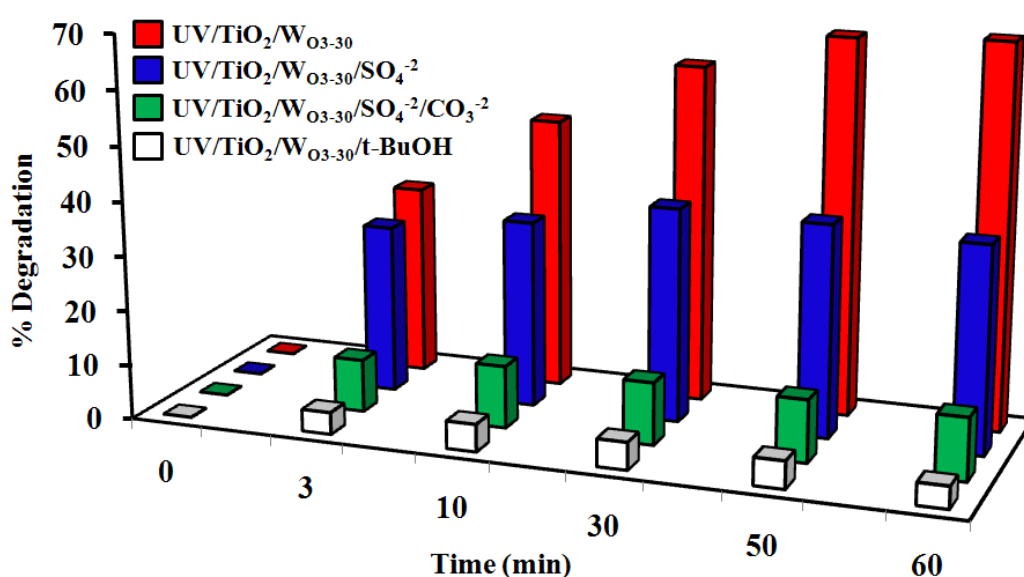


**Figure 6.** 2,4-D degradation by the UV/TiO<sub>2</sub>/W<sub>03-30</sub> system in the presence of radical scavengers, [t-BuOH]<sub>0</sub> = 1M, [SO<sub>4</sub><sup>2-</sup>]<sub>0</sub> = 1M, and [SO<sub>4</sub><sup>2-</sup>/CO<sub>3</sub><sup>2-</sup>]<sub>0</sub> = 1M/1M. T = 25° C, pH= 7, [2,4-D] = 50 mg/L, mass of TiO<sub>2</sub> and activated carbon = 5 mg, and V = 30 mL.

Following the method reported above and using the same radical scavengers, we also studied the contribution of the different radicals to 2,4-D degradation with the UV/TiO<sub>2</sub> system, i.e., in the absence of activated carbon (results in Figure 8). In contrast to observations in the presence of carbon W<sub>03-30</sub>, 70% of 2,4-D degradation was due to the contribution of electrons during the first 3 minutes, and this percentage gradually decreased until it reached 20 % after 60 min, due to the higher contribution of HO<sup>•</sup> radicals.

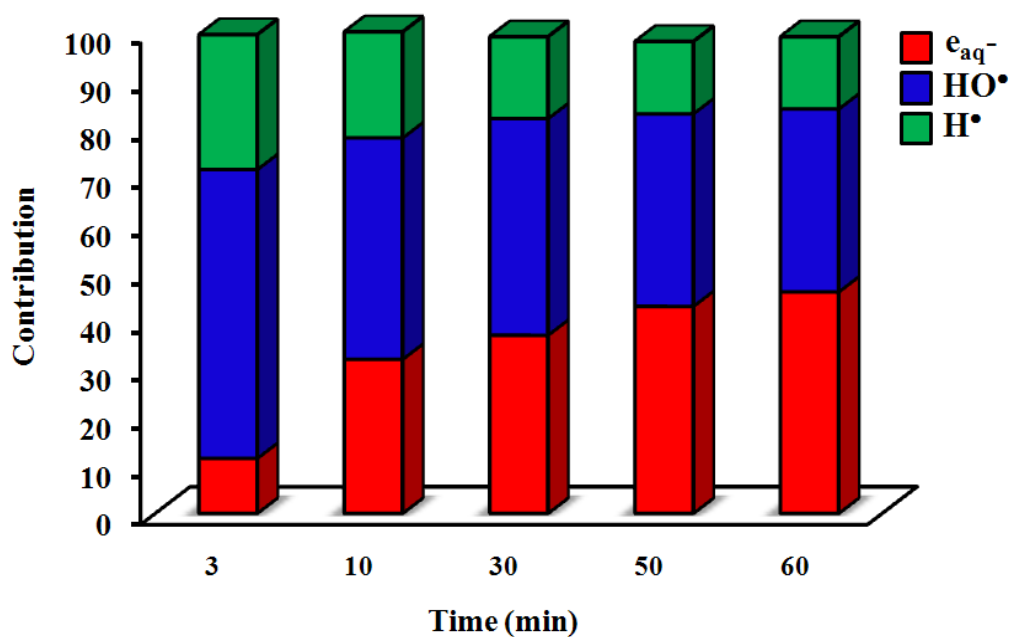


**Figure 7.** Contribution of radical species to 2,4-D removal by the UV/TiO<sub>2</sub>/W<sub>O3-30</sub> system. T = 25° C, pH = 7, [2,4-D] = 50 mg/L, mass of TiO<sub>2</sub> and activated carbon = 5 mg.

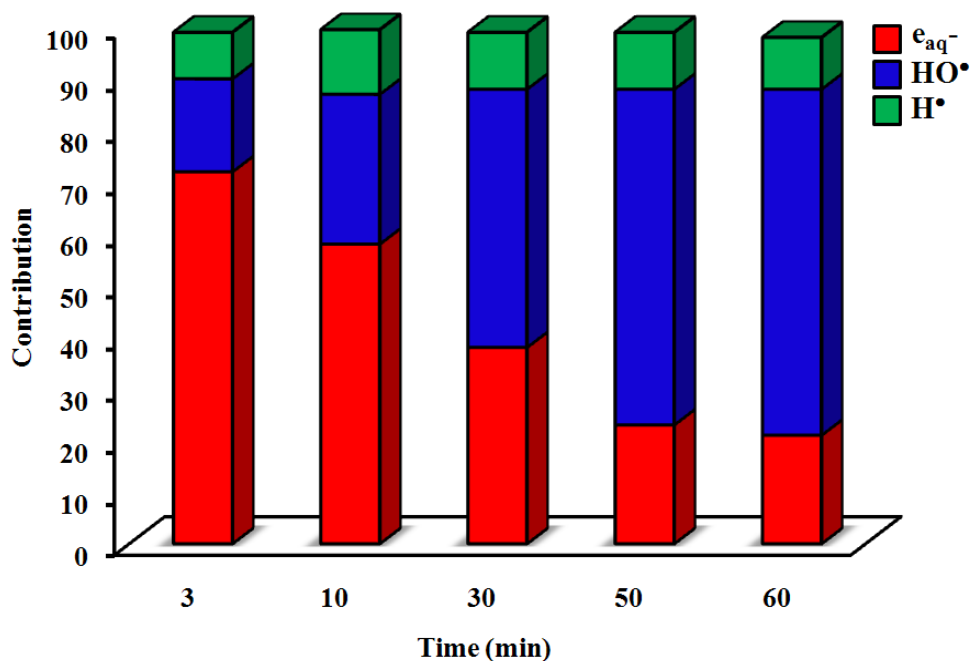


**Figure 8.** Contribution of radical species to 2,4-D removal by the UV/TiO<sub>2</sub> system. T = 25° C, pH = 7, [2,4-D] = 50 mg/L, mass of TiO<sub>2</sub> and activated carbon = 5 mg.

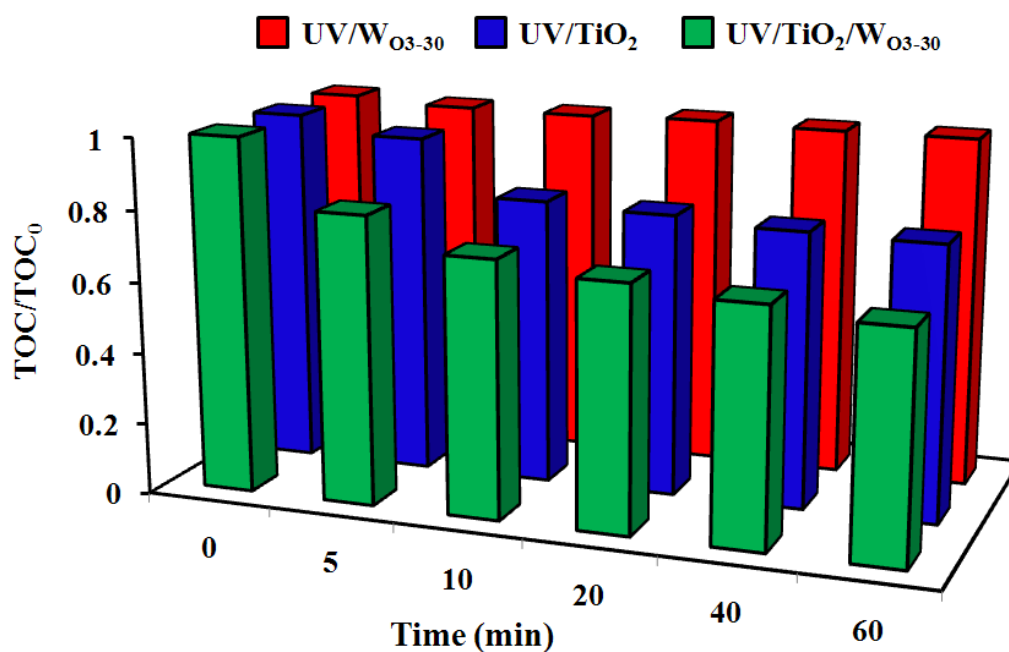
The results shown in Figures 7 and 8 again verify the action mechanism of ozonated carbons (reactions 1-3) in the UV/TiO<sub>2</sub>/activated carbon system, confirming the participation of the electrons initially generated in the production of HO• radicals when the UV/TiO<sub>2</sub>/W<sub>O3-30</sub> system was used.

### 3.5. Time course of TOC and toxicity during 2,4-D degradation

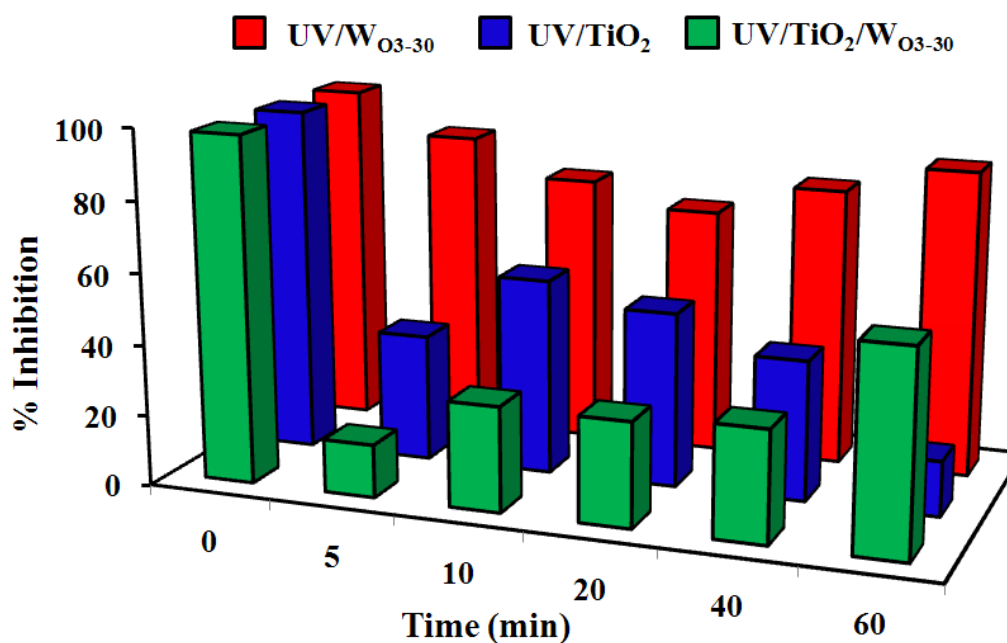
Key aspects of the effectiveness of treatments of organic compound-polluted water are (i) the transformation of dissolved organic carbon into CO<sub>2</sub>, and (ii) the toxicity of the degradation byproducts. We therefore studied these parameters during 2,4-D photodegradation.

Figure 9a depicts the variation in TOC concentration as a function of treatment time. According to these results: i) the UV/W<sub>O3-30</sub> system does not markedly reduce the TOC, confirming the low adsorption capacity of the ozone-treated carbon; and ii) the greatest percentage removal was achieved with the UV/TiO<sub>2</sub>/W<sub>O3-30</sub> system, due to the higher concentration in the medium of radical species, mainly HO• radicals.

Figure 9b depicts the percentage inhibition of *Vibrio Fischeri* bacteria during 2,4-D photodegradation with UV/W<sub>O3-30</sub>, UV/TiO<sub>2</sub>, and UV/TiO<sub>2</sub>/W<sub>O3-30</sub> treatments. This percentage was 97 % for the 2,4-D aqueous solution, demonstrating the high toxicity of 2,4-D, but it was drastically diminished with the UV/TiO<sub>2</sub>, and UV/TiO<sub>2</sub>/W<sub>O3-30</sub> systems for 5 min o treatment, indicating that the degradation byproducts obtained have a lower toxicity in comparison to 2,4-D; however for longer treatment times the byproducts toxicity increased



(a)



(b)

**Figure 9.** Variation in (a) TOC and (b) toxicity during 2,4-D photodegradation with UV/TiO<sub>2</sub>, UV/W<sub>03-30</sub>, and UV/TiO<sub>2</sub>/W<sub>03-30</sub> systems. T = 25° C, pH = 7, [2,4-D]=50 mg/L, mass of TiO<sub>2</sub> and activated carbon = 5 mg.

#### 4. CONCLUSIONS

The presence of ozonated activated carbons with a high carboxyl groups content enhances 2,4-D photodegradation by the UV/TiO<sub>2</sub> system.

Carboxyl groups in the graphene planes of the activated carbon participate in the additional generation of HO• radicals by interacting with the electrons produced by the UV/TiO<sub>2</sub> system. Consequently, the contribution of HO• radicals to the global 2,4-D degradation process is greater at the beginning of the photocatalytic treatment.

The UV/TiO<sub>2</sub>/W<sub>O3-30</sub> system mineralized 40 % of the organic matter present in the medium, and the toxicity of the degradation byproducts was considerably lower than that of 2,4-D.

## 5. REFERENCES

- [1] J. Hoigné, H. Bader, *Water Res.*, 10 (1976) 377-386.
- [2] S.K. Kim, H. Chang, K. Cho, D.S. Kil, S.W. Cho, H.D. Jang, J. Choi, J. Choi, *Mater. Lett.*, 65 (2011) 3330-3332.
- [3] J. Gao, X. Luan, J. Wang, B. Wang, K. Li, Y. Li, P. Kang, G. Han, *Desalination*, 268 (2011) 68-75.
- [4] A.A. Ashkarran, S.A.A. Afshar, S.M. Aghigh, M. kavianipour, *Polyhedron.*, 29 (2010) 1370-1374.
- [5] T. Ohno, F. Tanigawa, K. Fujihara, S. Izumi, M. Matsumura, *J. Photochem. Photobiol. A.*, 118 (1998) 41-44.
- [6] M. Faisal, S.B. Khan, M.M. Rahman, A. Jamal, K. Akhtar, M.M. Abdullah, *J. Mater. Sci. Technol.*, 27 (2011) 594-600.8.
- [7] M. Antoniadou, V.M. Daskalaki, N. Balis, D.I. Kondarides, C. Kordulis, P. Lianos, *Appl. Catal. B: Environ.*, 107 (2011) 188-196.
- [8] R. Ocampo-Pérez, M. Sánchez-Polo, J. Rivera-Utrilla, R. Leyva-Ramos, *Appl. Catal. B: Environ.*, 104 (2011) 177-184.
- [9] R. Sellappan, J. Zhu, H. Fredriksson, R.S. Martins, M. Zäch, D. Chakarov, *J. Mol. Catal. A: Chem.*, 335 (2011) 136-144.
- [10] C.G. Silva, J.L. Faria, *Appl. Catal. B: Environ.*, 101 (2010) 81-89.
- [11] F.J. Maldonado-Hódar, C. Moreno-Castilla, J. Rivera-Utrilla, *Appl. Catal. A: Gen.*, 203 (2000) 151-159.
- [12] X. Wang, Y. Liu, Z. Hu, Y. Chen, W. Liu, G. Zhao, *J. Hazard. Mater.*, 169 (2009) 1061-1067.

- 
- [13] G. Xue, H. Liu, Q. Chen, C. Hills, M. Tyrer, F. Innocent, J. Hazard. Mater., 186 (2011) 765-772.
- [14] W. Wang, C.G. Silva, J.L. Faria, Appl. Catal. B: Environ., 70 (2007) 470-478.
- [15] Y. Li, X. Li, J. Li, J. Yin, Catal. Commun., 6 (2005) 650-655.
- [16] J. Matos, J. Laine, J. Herrmann, J. Catal., 200 (2001) 10-20.
- [17] T. Cordero, C. Duchamp, J. Chovelon, C. Ferronato, J. Matos, J. Photochem. Photobiol. A, 191 (2007) 122-131.
- [18] D. Han, W. Jia, H. Liang, J. Environ. Sci., 22 (2010) 237-241.
- [19] Z. Aksu, E. Kabasakal, Sep. Purif. Technol., 35 (2004) 223-240.
- [20] A.J. Gold, T.G. Morton, W.M. Sullivan, J. Mcclory, Water Air Soil Poll., 37 (1988) 121-129.
- [21] D.D. Leavitt, M.A. Abraham, Environ. Sci. Technol., 24 (1990) 566-571.
- [22] W.A. Jury, D.D. Focht, W.J. Farmer, J. Environ. Qual., 16 (1987) 422-428.
- [23] E. Piera, J.C. Calpe, E. Brillas, X. Domènech, J. Peral, Appl. Catal. B: Environ., 27 (2000) 169-177.
- [24] M.I. Bautista-Toledo, J.D. Méndez-Díaz, M. Sánchez-Polo, J. Rivera-Utrilla, M.A. Ferro-García, J. Colloid Interface Sci., 317 (2008) 11-17.
- [25] M. Sánchez-Polo, J. Rivera-Utrilla, Carbon, 41 (2003) 303-307.
- [26] V.L.K. Jennings, M.H. Rayner-Brandes, D.J. Bird, Water Res., 35 (2001) 3448-3456
- [27] I.T. Cousins, C.A. Staples, G.M. Kelecka, G.M. Mackay, Hum. Ecol. Risk Assess., 8 (2002) 1107-1135.



- 
- [28] M. Sánchez-Polo, J. Rivera-Utrilla, G. Prados-Joya, M.A. Ferro-García, I. Bautista-Toledo, *Water Res.*, 42 (2008) 4163-4171.
- [29] J. Rivera-Utrilla, *Water Res.*, 41 (2007) 2480.
- [30] M. Sánchez-Polo, J. Rivera-Utrilla, J.D. Méndez-Díaz, S. Canonica, U. von Gunten, *Chemosphere*, 68 (2007) 1814-1820.
- [31] J. Rivera-Utrilla, M. Sánchez-Polo, *Carbon*, 40 (2002) 2685-2691.
- [32] R. Ocampo-Perez, R. Leyva-Ramos, J. Mendoza-Barron, R.M. Guerrero-Coronado, *J. Colloid Interface Sci.*, 364 (2011) 195-204.
- [33] R. Ocampo-Perez, R. Leyva-Ramos, P. Alonso-Davila, J. Rivera-Utrilla, M. Sanchez-Polo, *Chem. Eng. J.*, 165 (2010) 133-141.
- [34] H. Valdés, M. Sánchez-Polo, J. Rivera-Utrilla, C.A. Zaror, *Langmuir*, 18 (2002) 2111-2116.
- [35] L.E. Depero, L. Sangaletti, B. Allieri, E. Botempi, R. Salari, M. Zocchi, C. Casale, M. Notaro, *J. Mater. Res.*, 13 (1998) 1644-1649.
- [36] B.R. Buxton, C.L. Greenstock, W.P. Helman, A.B. Ross, *J. Phys. Chem. Ref. Data*, 17 (1988) 513-886

## CAPÍTULO 6

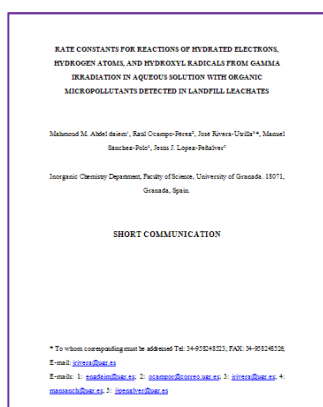
# CONSTANTES DE VELOCIDAD DE REACCIÓN DEL ELECTRÓN HIDRATADO, ÁTOMO DE HIDRÓGENO Y RADICAL HIDROXILO GENERADOS MEDIANTE RADIACIÓN GAMMA EN DISOLUCIÓN ACUOSA CON MICROCONTAMINANTES ORGÁNICOS DETECTADOS EN LIXIVIADOS DE VERTEDEROS





# RATE CONSTANTS FOR REACTIONS OF HYDRATED ELECTRONS, HYDROGEN ATOMS, AND HYDROXYL RADICALS FROM GAMMA IRRADIATION IN AQUEOUS SOLUTION WITH ORGANIC MICROPOLLUTANTS DETECTED IN LANDFILL LEACHATES

Manuscript submitted for publication



## Highlights

- Gamma radiation is effective for degradation of pollutants from landfill leachates.
- The efficiency of the radiation process decreases with longer exposure time.
- The highest efficiencies are achieved time
- The degradation of the micropollutants mainly takes place via oxidation pathway

## ABSTRACT

Gamma radiation has been used to induce the degradation of phthalic acid (PA), bisphenol A (BPA), diphenolic acid (DPA), 2,4- dichlorophenoxy-acetic acid (2,4-D), and 4-chloro-2-methylphenoxyacetic acid (MCPA) in aqueous solution, determining the dose constants, removal percentages, and radiation-chemical yields. Moreover, the determination of the reaction rate constants of these compounds with  $\text{HO}^\bullet$ ,  $\text{e}_{\text{aq}}^-$ , and  $\text{H}^\bullet$  was carried out. The reaction rate constants of hydroxyl radical ( $\text{HO}^\bullet$ ), hydrated electron ( $\text{e}_{\text{aq}}^-$ ) and hydrogen atom ( $\text{H}^\bullet$ ) with these pollutants were determined by means of competition kinetics, using 3-aminopyridine and atrazine as reference compounds. The rate constant values of  $k_{\text{HO}^\bullet}$ ,  $k_{\text{e}^-}$  and  $k_{\text{H}^\bullet}$  were;  $4.8 \pm 0.12 \times 10^{10}$ ,  $9.3 \pm 0.03 \times 10^9$ , and  $5.5 \pm 0.25 \times 10^7 \text{ M}^{-1} \text{ s}^{-1}$  for PA;  $1.7 \pm 0.21 \times 10^{10}$ ,  $7.0 \pm 0.07 \times 10^9$ , and  $4.7 \pm 0.18 \times 10^7 \text{ M}^{-1} \text{ s}^{-1}$  for BPA;  $4.5 \pm 0.08 \times 10^{10}$ ,  $7.6 \pm 0.12 \times 10^9$ , and  $3.1 \pm 0.31 \times 10^7 \text{ M}^{-1} \text{ s}^{-1}$  for DPA;  $6.6 \pm 0.13 \times 10^{10}$ ,  $9.8 \pm 0.35 \times 10^9$ , and  $6.8 \pm 0.01 \times 10^7 \text{ M}^{-1} \text{ s}^{-1}$  for 2,4-D; and  $3.3 \pm 0.02 \times 10^{10}$ ,  $1.5 \pm 0.17 \times 10^9$ , and  $5.3 \pm 0.09 \times 10^7 \text{ M}^{-1} \text{ s}^{-1}$  for MCPA, respectively. These results indicated that the elimination of these pollutants with gamma radiation mainly follows the oxidative pathway through reaction with  $\text{HO}^\bullet$  radical. These rate constant values have been related to the chemical composition of the pollutant molecules.



## 1. INTRODUCTION

Industrial and commercial growth in many countries around the world in the past decades has been accompanied by rapid generation of municipal and industrial solid waste, which creates the most serious environmental problems related to landfill such as the generation of leachates during the decomposition process [1, 2]. Among the emerging contaminants that have been detected in landfill leachates are plastic additives and herbicides [3-5]. All these pollutants have potential toxicity towards humans and animals and are suspected mutagens and carcinogens [6].

Recently, advanced oxidation processes (AOPs) have been demonstrated as potential alternative processes for the treatment of effluents containing toxic organic chemicals [7]. AOPs act as source of free radicals, principally hydroxyl radical ( $\text{HO}^\bullet$ ). An excellent source of free radicals for water treatment is ionizing radiation. The use of gamma radiolysis in the environmental remediation of drinking and wastewater is a promising technology, since it simultaneously generates oxidizing ( $\text{HO}^\bullet$ ) and reductive ( $e_{\text{aq}}^-$  and  $\text{H}^\bullet$ ) radical species, allowing to degrade a wide variety of compounds [8-10].

The determination of the reaction rate constants  $k_{\text{HO}^\bullet}$ ,  $k_{e_{\text{aq}}^-}$  and  $k_{\text{H}^\bullet}$  is very important for the good design of a treatment system based on the simultaneous generation of these radicals. There are few studies related to the determination of these constants for pollutants from landfill leachates [11-16]; hence, more effort is necessary to get the constants data and, thus, to improve the radiation technology for water treatment.

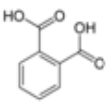
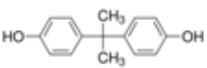
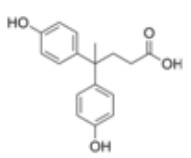
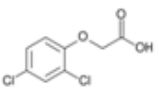
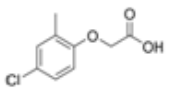
With this background, the objective of this study was to investigate the elimination of plastic additives (phthalic acid (PA), bisphenol A (BPA), and diphenolic acid (DPA)) and herbicides (2, 4- dichlorophenoxyacetic acid (2,4-D) and 4-chloro-2-methylphenoxyacetic acid (MCPA)) by using gamma irradiation and to determine the reaction rate constants of these compounds with  $\text{HO}^\bullet$ ,  $e_{\text{aq}}^-$  and  $\text{H}^\bullet$  radicals by using competitive kinetic. These five compounds have been selected as model organic micropollutants from landfill leachates.

## 2. MATERIAL AND METHODS

### 2.1. Reagents

All chemical reagents used in this study (phthalic acid, bisphenol A, diphenolic acid, 2,4-dichlorophenoxyacetic acid, 4-chloro-2-methylphenoxyacetic acid, 3-aminopyridine, atrazine, potassium nitrate, potassium chloride, potassium bromide, and hydrochloric acid) were high purity analytical grade reagents supplied by Sigma-Aldrich. All solutions were prepared with ultrapure water obtained from Milli-Q<sup>®</sup> equipment (Millipore). Table 1 presents the physiochemical characteristics of the selected organic pollutants from landfill leachates.

**Table 1.** Properties of the selected landfill leachate contaminants.

| Pollutant | Molecular         | Molecular<br>formula  | Solubility in  |                  |                  |                  |
|-----------|-------------------|---|----------------|------------------|------------------|------------------|
|           | Weight<br>(g/mol) |   | water<br>(g/L) | pK <sub>a1</sub> | pK <sub>a2</sub> | pK <sub>a3</sub> |
| PA        | 166.13            |  | 12.50          | 2.90             | 5.40             | --               |
| BPA       | 228.29            |  | 0.09           | 9.59             | 11.30            | --               |
| DPA       | 286.33            |  | 0.40           | 4.66             | 9.70             | 10.45            |
| 2,4-D     | 221.00            |  | 2.16           | 2.98             | --               | --               |
| MCPA      | 200.62            |  | 1.38           | 3.14             | --               | --               |

### 2.2. Irradiation sources

Irradiation studies were performed using a J.L. Shepherd & Associates MARK-I, model 30J, gamma irradiator in the Experimental Radiology Unit of the Biomedical Research Center of the University of Granada (Spain). The equipment includes four self-contained sources of <sup>137</sup>Cs with a total combined activity of 3.70×10<sup>13</sup> Bq (1000 Ci).

The irradiation chamber has a useful volume of 8.25 L and is equipped with a rotation system to ensure a uniform dose throughout the irradiation volume. All samples were irradiated in 2 mL vials sealed with screw caps to prevent the entry of air. The experiments were performed at room temperature ( $25 \pm 2$  °C). The samples were bubbled with N<sub>2</sub>, previously to be irradiated, to avoid the presence of dissolved O<sub>2</sub>.

### 2.3. Analytical methods

The concentrations of the five pollutants, as well as of atrazine and 3-aminopyridine, in aqueous solution were determined by high performance liquid chromatography (HPLC) in reverse phase, using a liquid chromatograph (Thermo-Fisher) equipped with a UV-detector and autosampler with capacity for 120 vials. The chromatographic column was a Nova-Pak<sup>®</sup> C<sub>18</sub> (4 µm particle size; 3.9×150 mm). Table 2 presents the experimental conditions used to determine the concentration of these compounds.

**Table 2.** Experimental conditions used to determine the concentration of the selected compounds.

| Compound                            | Mobile phase                    | Wavelength<br>(nm) | Flow<br>(mL/min) |
|-------------------------------------|---------------------------------|--------------------|------------------|
| <b>PA</b>                           | 10% acetonitrile                | 280                | 1.0              |
|                                     | 90% water                       |                    |                  |
| <b>BPA</b>                          | 50% of 0.4% phosphoric acid     | 270                | 1.5              |
|                                     | 50% methanol                    |                    |                  |
| <b>DPA</b>                          | 50% of 0.4% phosphoric acid     | 270                | 1.50             |
|                                     | 50% methanol                    |                    |                  |
| <b>2,4-D</b>                        | 20% acetonitrile                | 280                | 1.0              |
|                                     | 80% water                       |                    |                  |
| <b>MCPA</b>                         | 50% of 0.4% phosphoric acid     | 270                | 1.0              |
|                                     | 50% methanol                    |                    |                  |
| <b>Atrazine<br/>(Atr)</b>           | 50% 1 mM ammonium acetate       | 226                | 1.0              |
|                                     | 50% acetonitrile                |                    |                  |
| <b>3-Aminopyridine<br/>(3-Ampy)</b> | 20% of 10% orthophosphoric acid | 270                | 0.5              |
|                                     | 80% water                       |                    |                  |



## 2.4. Determination of radiation-chemical yields and dose constants

The effectiveness of the irradiation process is given by the radiation-chemical yield (G-value) which is calculated by using the following equation.

$$G = \frac{[C_0 - C] N_A}{D \times 6.24 \times 10^{16}} \quad (1)$$

where  $C_0$  is the initial contaminant concentration (mol/L),  $C$  is the contaminant concentration at dose  $D$  (mol/L),  $D$  is the absorbed dose (Gy),  $N_A$  is the Avogadro number ( $6.023 \times 10^{23}$  molecules/mol) and  $6.24 \times 10^{16}$  is the conversion factor of Gy at 100 eV/L. G-values are expressed in  $\mu\text{mol/J}$ , considering  $1 \text{ molecules} \times (100 \text{ eV})^{-1} = 0.10364 \mu\text{mol/J}$ .

The dose constant,  $k$ , was determined by considering that solute degradation kinetic data fit a pseudo-first order kinetics. The model of pseudo-first order is given by the following equation:

$$C = C_0 \times e^{-kD} \quad (2)$$

Furthermore, the doses required to degrade 50%,  $D_{50}$ , and 90%,  $D_{90}$ , of the initial contaminant concentration were calculated using Eqs. (3) and (4), respectively.

$$D_{50} = \frac{\text{Ln}(2)}{k} \quad (3)$$

$$D_{90} = \frac{\text{Ln}(10)}{k} \quad (4)$$

## 2.5. Determination of reaction rate constants ( $k_{H^\bullet}$ , $k_{HO^\bullet}$ and $k_{e_{aq}^-}$ )

### 2.5.1. Determination of $k_{H^\bullet}$

Reaction rate constants of each pollutant with  $H^\bullet$  radical were determined by competitive kinetic experiments using 3-Aminopyridine (3-Ampy)  $k_{H^\bullet, 3\text{-Ampy}} = 2.20 \times 10^9$

$M^{-1}s^{-1}$  as reference compound using the procedure reported elsewhere [17]. In a vial of 2 mL solutions of each compound at pH 1 (HCl 1 M) were added to obtain the desired concentrations (20 mg/L for each pollutant and 10, 20 and 40 mg/L for each reference compound) [18]. At pH 1, the G-value of  $e_{aq}^-$  tends to zero and, therefore, the radiation-chemical yield of  $H^\bullet$  is increased. Besides, an aliquot of potassium chloride was added to achieve a concentration of  $Cl^-$  ions of 1000 mg/L since  $Cl^-$  ions act as  $HO^\bullet$  scavenger. Table 3 summarizes the reaction constants of each radical scavenger used in this study.

**Table 3.** Radical scavenger reaction rate constants [18].

| Scavenger | $k_{e_{aq}^-}$<br>( $M^{-1} s^{-1}$ ) | $k_{H^\bullet}$<br>( $M^{-1} s^{-1}$ ) | $k_{HO^\bullet}$<br>( $M^{-1} s^{-1}$ ) |
|-----------|---------------------------------------|--|---|
| $Cl^-$    | ----                                  | ----                                   | $4.3 \times 10^9$                       |
| $Br^-$    | ----                                  | $2.8 \times 10^7$                      | $1.6 \times 10^{10}$                    |
| $NO_3^-$  | $9.7 \times 10^9$                     | $1.4 \times 10^6$                      | ----                                    |

The concentration of both compounds (pollutant and reference) was obtained at different time intervals and the rate constant  $k_{H^\bullet}$  was calculated using the following equation:

$$k_{H^\bullet, \text{pollutant}} = k_{H^\bullet, 3\text{-Ampy}} \times \frac{\left[ \text{Ln} \left( \frac{[\text{Pollutant}]_t}{[\text{Pollutant}]_0} \right) \right]}{\left[ \text{Ln} \left( \frac{[3\text{-Ampy}]_t}{[3\text{-Ampy}]_0} \right) \right]} \quad (5)$$

### 2.5.2. Determination of reaction rate constants ( $k_{HO^\bullet}$ and $k_{e_{aq}^-}$ )

The same methodology indicated in section 2.5.1 was used to determine the reaction rate constants  $k_{HO^\bullet}$  and  $k_{e_{aq}^-}$  except that the reference compounds were 3-Ampy  $k_{e_{aq}^-} = 6.10 \times 10^9 M^{-1}s^{-1}$  and  $k_{HO^\bullet, \text{Atr}} = 1.80 \times 10^{10} M^{-1}s^{-1}$  [17, 19]. Potassium nitrate or potassium bromide were added to the solution and the medium pH was 5.2 or 7.5, respectively. Nitrate anions act as an  $e_{aq}^-$  and  $H^\bullet$  scavenger with rate constants of  $9.7 \times 10^9$  and  $1.4 \times 10^6 M^{-1}s^{-1}$ , respectively (Table 3) [18, 20]. Therefore, the effective

concentration of HO• radical is increased by minimizing recombination of e<sub>aq</sub><sup>-</sup> and HO• radicals and enhanced the oxidative reactions [21]. On the other hand, Br<sup>-</sup> ions can react with HO• and H• radicals with rate constants of 1.60×10<sup>10</sup> M<sup>-1</sup>s<sup>-1</sup> and 2.8×10<sup>7</sup> M<sup>-1</sup>s<sup>-1</sup>, respectively [22, 23], removing them from the medium and leaving free e<sub>aq</sub><sup>-</sup> in the aqueous solution.

### 3. RESULTS AND DISCUSSION

#### 3.1. Degradation induced by gamma irradiation

Highly reactive radical species, mainly HO•, H• and e<sub>aq</sub><sup>-</sup> are produced in water radiolysis (Eq. (6)). The extent of their production depends on various factors, including solution pH, temperature, energy emitted per unit of distance travelled by the incident radiation in aqueous medium, absorbed dose, dose rate, and presence of dissolved gases.

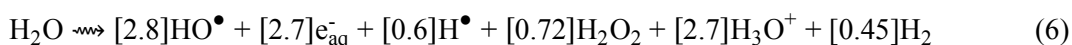
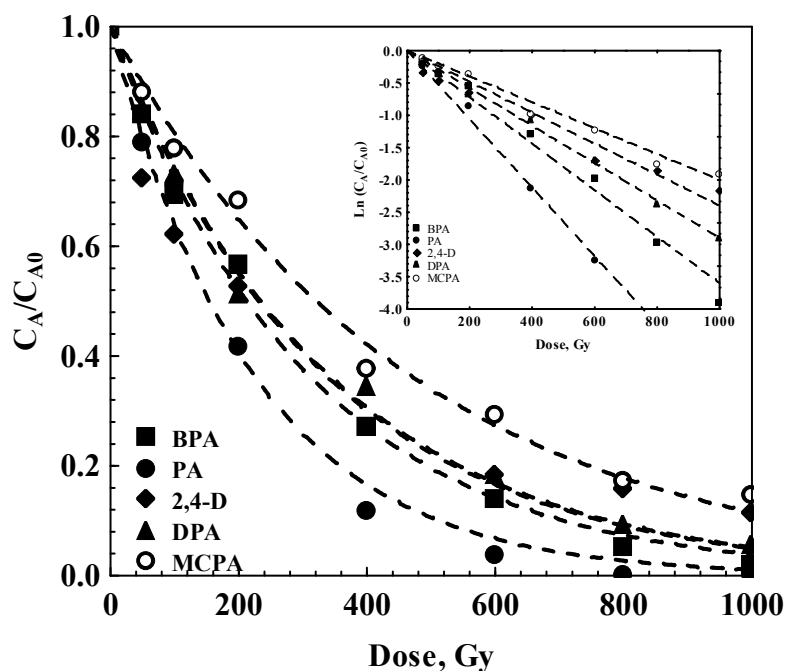


Figure 1 shows the degradation kinetics of the five pollutants by gamma irradiation as a function of the dose absorbed, at initial concentrations of 20 mg/L and at a dose rate of 1.66 Gy/min. As shown in this figure, the relative concentration ( $C_A/C_{A0}$ ) decreased with the increase in the absorbed dose for all compounds, and it is noticed that the degradation kinetic of these compounds exponentially decreases with higher absorbed dose which can be well represented by Eq. (2). Thus, the dose constant,  $k$ , for each experiment was obtained from the slope of the plot of  $\ln(C_A/C_{A0})$  versus adsorbed dose. The  $k$  values obtained are given in Table 4, where it is observed that PA presented the highest values of  $k$  and MCPA the lowest ones. Furthermore,  $k$  values markedly decreased with higher initial pollutant concentration. An explanation of this behavior is that a rise in the initial solute concentration increases the byproducts produced, which compete to react with the radicals species formed in radiolysis and, therefore, the number of radical species available to react with the pollutant is reduced.

The dose constant,  $k$ , was used to calculate the dose required to produce 50% and 90% pollutant degradation ( $D_{50}$  and  $D_{90}$  values) by means of Eqs. (3) and (4).  $D_{50}$  and  $D_{90}$

values (Table 4) were different for all pollutants studied, which confirms the high influence of the chemical structure of compounds on their degradation by gamma radiation.



**Figure 1.** Degradation of all contaminants as a function of radiation dose.  $[C_{A0}] = 20$  mg/L. Dose rate = 1.66 Gy/min,  $T = 25^\circ\text{C}$ , and  $\text{pH} = 4.0$ .

The efficiency of gamma radiation in the degradation of the pollutants was studied evaluating both degradation percentage and G-values. As an example, the results obtained for PA (Table 4, Exp. No. 2) are plotted in Figure 2. The G-values for the radiolytic decomposition of PA were in the range from 0.57 to 0.05 for absorbed doses lower than 1000 Gy. Interestingly, the G-value diminished with augmenting accumulated radiation dose but the removal percentage increased. According to these results, the efficiency of the gamma irradiation process decreases with longer exposure time. This trend can be explained by (i) the competition for solute molecules between the reactive radicals produced by water radiolysis, (ii) the competition for reactive radicals between parent compound and reaction by-products and (iii) radical–radical recombination reactions, including  $\text{HO}^\bullet$ ,  $e_{\text{aq}}^-$  and  $\text{H}^\bullet$  [10]. Because the radical species increase at higher radiation dose rates, the absolute rates for radical–radical

recombination reactions also increase, reducing the effective radical concentrations for reaction with PA. Similar results were obtained for the rest of pollutants, whose corresponding plots showed a cross point of both curves for dose values in between 100-150 Gy; therefore, gamma radiation is an efficient process for degradation of these pollutants when using doses of around 100 Gy, because, for these doses high degradation percentages and radiation-chemical yield are obtained.

### 3.2. Determination of the radical reaction rate constants $k_{HO^\bullet}$ , $k_{e_{aq}^-}$ and $k_{H^\bullet}$

Figure 3 shows, as an example, a typical graph of a competitive kinetics where  $\ln([PA]_t/[PA]_0)$  is plotted versus  $\ln([3\text{-Ampy}]_t/[3\text{-Ampy}]_0)$ . As described in the experimental section, from this type of figures, the corresponding reaction rate constants were determined. Table 5 shows the reaction rate constants of the five pollutants with hydroxyl radical  $HO^\bullet$ , hydrated electron  $e_{aq}^-$ , and hydrogen atom  $H^\bullet$ . The values of these constants are similar to those reported by other authors [11-16] for organic compounds of analogous characteristics to these studied in the present work. It is noteworthy that the highest rate constant for the degradation of these compounds is  $k_{HO^\bullet}$ . Thus, the order found was  $k_{HO^\bullet} > k_{e_{aq}^-} > k_{H^\bullet}$ , which indicates that the elimination process of these pollutants by gamma radiation mainly follows an oxidative pathway through reaction with  $HO^\bullet$  radical.

**Table 4.** Experimental conditions and kinetic parameters obtained by gamma radiation at a dose rate of 1.66 Gy/min.

| Exp. No | [PA] <sub>0</sub> (mg/L) | [BPA] <sub>0</sub> (mg/L) | [DPA] <sub>0</sub> (mg/L) | [2,4-D] <sub>0</sub> (mg/L) | [MCPA] <sub>0</sub> (mg/L) | G <sub>0</sub> ×10 (μmol/J) | k×10 <sup>3</sup> (Gy <sup>-1</sup> ) | D <sub>50</sub> (Gy) | D <sub>90</sub> (Gy) | % Degradation |
|---------|--------------------------|---------------------------|---------------------------|-----------------------------|----------------------------|-----------------------------|---------------------------------------|----------------------|----------------------|---------------|
| 1       | 10                       | -                         | -                         | -                           | -                          | 5.7                         | 12.1±0.6                              | 57.1                 | 189.7                | 100.0         |
| 2       | 20                       | -                         | -                         | -                           | -                          | 5.7                         | 4.5±0.3                               | 154.0                | 511.7                | 100.0         |
| 3       | 50                       | -                         | -                         | -                           | -                          | 6.7                         | 2.9±0.2                               | 239.8                | 796.7                | 98.0          |
| 4       | -                        | 10                        | -                         | -                           | -                          | 1.7                         | 4.3±0.3                               | 162.3                | 539.3                | 100.0         |
| 5       | -                        | 20                        | -                         | -                           | -                          | 2.8                         | 3.3±0.2                               | 212.6                | 706.3                | 98.1          |
| 6       | -                        | 50                        | -                         | -                           | -                          | 2.5                         | 1.4±0.1                               | 481.4                | 1599.0               | 76.5          |
| 7       | -                        | -                         | 10                        | -                           | -                          | 1.9                         | 5.4±0.2                               | 129.1                | 428.8                | 100.0         |
| 8       | -                        | -                         | 20                        | -                           | -                          | 2.2                         | 3.0±0.1                               | 233.4                | 775.3                | 94.6          |
| 9       | -                        | -                         | 50                        | -                           | -                          | 4.9                         | 2.3±0.2                               | 304.0                | 1009.9               | 86.7          |
| 10      | -                        | -                         | -                         | 10                          | -                          | 5.4                         | 6.7±1.3                               | 103.8                | 344.7                | 99.8          |
| 11      | -                        | -                         | -                         | 20                          | -                          | 5.0                         | 3.0±0.4                               | 233.4                | 775.3                | 88.7          |
| 12      | -                        | -                         | -                         | 50                          | -                          | 5.3                         | 1.2±0.1                               | 572.9                | 1903.0               | 64.0          |
| 13      | -                        | -                         | -                         | -                           | 10                         | 1.5                         | 3.2±0.2                               | 220.1                | 731.0                | 99.5          |
| 14      | -                        | -                         | -                         | -                           | 20                         | 2.4                         | 2.2±0.1                               | 319.4                | 1061.1               | 85.6          |
| 15      | -                        | -                         | -                         | -                           | 50                         | 2.4                         | 0.9±0.0                               | 761.7                | 2530.3               | 55.5          |

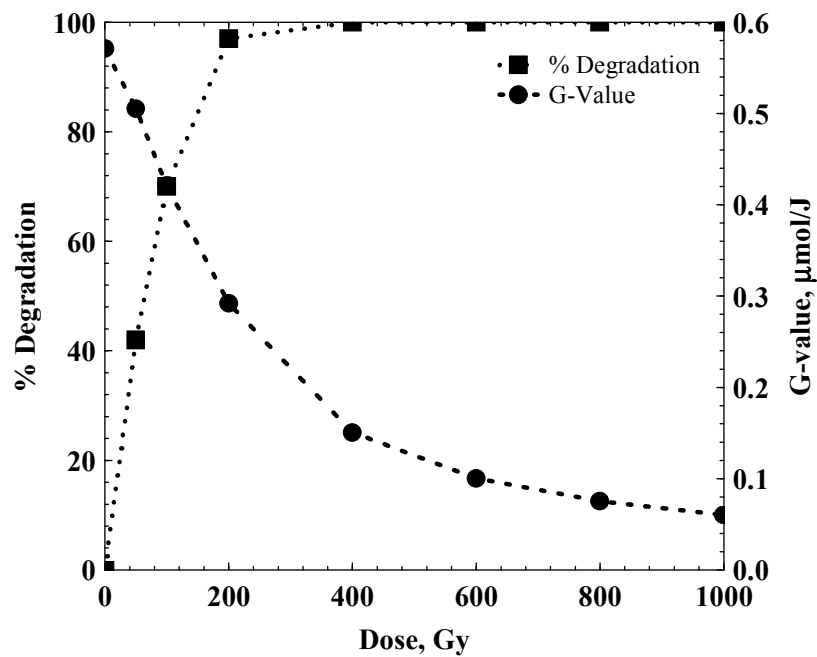


**Figure 2.** G-values and degradation percentage of PA as a function of radiation dose.

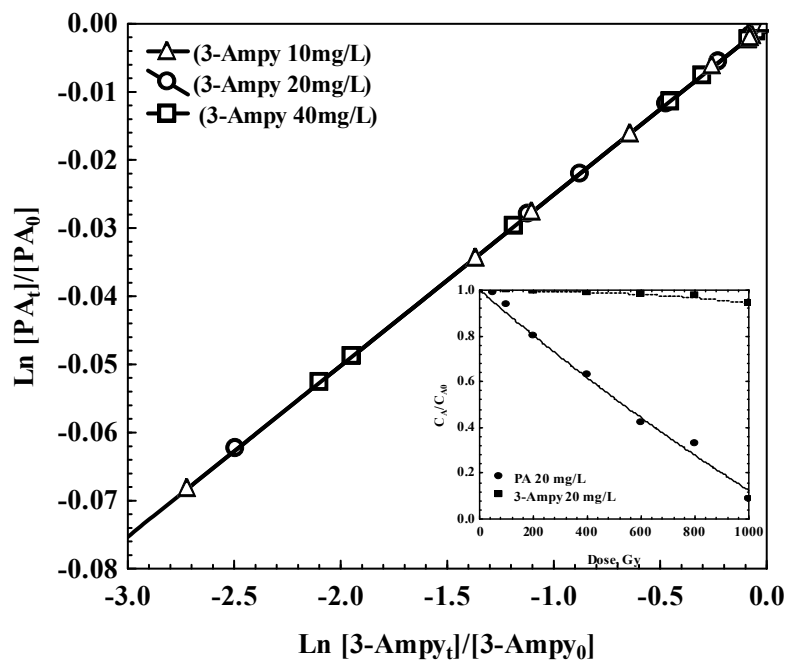


**Figure 3.** Competitive kinetics data obtained for PA [20 mg/L] and 3-Ampy [10, 20 and 40 mg/L]. Dose rate = 1.66 Gy/min, T = 25°C, and pH=1.0.

**Table 5.** Rate constants for the reaction of the selected compounds with species from water radiolysis.

| Pollutant | $k_{HO\bullet}$<br>( $M^{-1} s^{-1}$ ) | $k_{e_{aq}^-}$<br>( $M^{-1} s^{-1}$ ) | $k_{H\bullet}$<br>( $M^{-1} s^{-1}$ ) |
|-----------|--|---------------------------------------|---------------------------------------|
| PA        | $4.8 \pm 0.12 \times 10^{10}$          | $9.3 \pm 0.03 \times 10^9$            | $5.5 \pm 0.25 \times 10^7$            |
| BPA       | $1.7 \pm 0.21 \times 10^{10}$          | $7.0 \pm 0.07 \times 10^9$            | $4.7 \pm 0.18 \times 10^7$            |
| DPA       | $4.5 \pm 0.08 \times 10^{10}$          | $7.6 \pm 0.12 \times 10^9$            | $3.1 \pm 0.31 \times 10^7$            |
| 2,4-D     | $6.6 \pm 0.13 \times 10^{10}$          | $9.8 \pm 0.35 \times 10^9$            | $6.8 \pm 0.01 \times 10^7$            |
| MCPA      | $3.3 \pm 0.02 \times 10^{10}$          | $1.5 \pm 0.17 \times 10^9$            | $5.3 \pm 0.09 \times 10^7$            |

The  $k_{HO\bullet}$  values follow the order 2,4-D > PA > DPA > MCPA > BPA, which is similar to the order found for  $k_{e_{aq}^-}$  and  $k_{H\bullet}$ . This trend could be explain assuming that the radical reactions of these pollutants started with the attack of the radical electron to the benzylic positions of the pollutant molecules, in such a way that C atom in the benzylic position stabilizes the radicals initially formed. For 2,4-D this possibility does not exist because there is not C atoms in that position, and, therefore, the reaction progress will be more rapid than in the rest of pollutants. In the case of BPA, the presence of two aromatic rings stabilizes the benzylic radicals formed after the attack to the pollutant molecules, and, therefore, the reaction progress will be slower.

#### 4. CONCLUSIONS

Gamma radiation is an effective treatment for degradation of PA, BPA, DPA, 2,4-D and MCPA in aqueous solutions. The efficiency of these processes decreases with longer exposure time. The highest efficiencies are achieved using radiation doses of around 100 Gy.

The reaction rate constants  $k_{HO\bullet}$ ,  $k_{e_{aq}^-}$  and  $k_{H\bullet}$  were determined for these compounds by using competition kinetics. The reaction rate constants values obtained are very high and they demonstrated that the degradation process of these micropollutants mainly takes place via oxidation pathway.



The order followed by the reaction rate constants of these pollutants with  $\text{HO}^\bullet$ , hydrated electron  $e_{\text{aq}}^-$ , and hydrogen atom  $\text{H}^\bullet$  can be explained by the stability of the benzylic radicals formed after the attack of these species.

## 5. REFERENCES

- [1] O. Primo, M.J. Rivero, I. Ortiz, Photo-Fenton process as an efficient alternative to the treatment of landfill leachates, *J. Hazard. Mater.* 153 (2008) 834-842.
- [2] S. Renou, J.G. Givaudan, S. Poulain, F. Dirassouyan, P. Moulin, Landfill leachate treatment: Review and opportunity, *J. Hazard. Mater.* 150 (2008) 468-493.
- [3] C. Fang, Y. Long, Y. Lu, D. Shen, Behavior of dimethyl phthalate (DMP) in simulated landfill bioreactors with different operation modes, *Int. Biodeterior. Biodegrad.* 63 (2009) 732-738.
- [4] S.K. Marttinen, R.H. Kettunen, J.A. Rintala, Occurrence and removal of organic pollutants in sewages and landfill leachates, *Sci. Total Environ.* 301 (2003) 1-12.
- [5] A. Yasuhara, H. Shiraishi, M. Nishikawa, T. Yamamoto, T. Uehiro, O. Nakasugi, T. Okumura, K. Kenmotsu, H. Fukui, M. Nagase, Y. Ono, Y. Kawagoshi, K. Baba, Y. Noma, Determination of organic components in leachates from hazardous waste disposal sites in Japan by gas chromatography–mass spectrometry, *J. Chromatogr. A* 774 (1997) 321-332.
- [6] A. Bojanowska-Czajka, P. Drzewicz, Z. Zimek, H. Nichipor, G. Nałęcz-Jawecki, J. Sawicki, C. Kozyra, M. Trojanowicz, Radiolytic degradation of pesticide 4-chloro-2-methylphenoxyacetic acid (MCPA)—Experimental data and kinetic modelling, *Radiat. Phys. Chem.* 76 (2007) 1806-1814.
- [7] R.F. Dantas, S. Contreras, C. Sans, S. Esplugas, Sulfamethoxazole abatement by means of ozonation, *J. Hazard. Mater.* 150 (2008) 790-794.
- [8] J.W.T. Sprinks, R.J. Wood, *Introduction to radiation chemistry.*, Willey, New York, 1990.
- [9] R. Ocampo-Pérez, J. Rivera-Utrilla, M. Sánchez-Polo, J.J. López-Peñalver, R. Leyva-Ramos, Degradation of antineoplastic cytarabine in aqueous solution by gamma radiation, *Chem. Eng. J.* 174 (2011) 1-8.

- [10] M. Sánchez-Polo, J. López-Peñalver, G. Prados-Joya, M.A. Ferro-García, J. Rivera-Utrilla, Gamma irradiation of pharmaceutical compounds, nitroimidazoles, as a new alternative for water treatment, *Water Res.* 43 (2009) 4028-4036.
- [11] W.R. Haag, C.C.D. Yao, Rate Constants for Reaction of Hydroxyl Radicals with Several Drinking Water Contaminants, *Environ. Sci. Technol.* 26 (1992) 1005-1013.
- [12] S.A. Mabury, D.G. Crosby, Pesticide Reactivity toward Hydroxyl and Its Relationship to Field Persistence, *J. Agric. Food Chem.* 44 (1996) 1920-1924.
- [13] J. Peller, P.V. Kamat, Radiolytic transformations of chlorinated phenols and chlorinated phenoxyacetic acids, *J. Phys. Chem. A* 109 (2005) 9528-9535.
- [14] A. Szutka, J.K. Thomas, S. Gordon, E.J. Hart, Rate Constants of hydrated electron reactions with some aromatic acid, alkyl halides, heterocyclic compounds, and wener complexes, *J. Phys. Chem.* 69 (1965) 289-292.
- [15] M. Wu, N. Liu, G. Xu, J. Ma, L. Tang, L. Wang, H. Fu, Kinetics and mechanisms studies on dimethyl phthalate degradation in aqueous solutions by pulse radiolysis and electron beam radiolysis, *Radiat. Phys. Chem.* 80 (2011) 420-425.
- [16] R. Zona, S. Solar, K. Sehested, OH-radical induced degradation of 2,4,5-trichlorophenoxyacetic acid (2,4,5-T) and 4-chloro-2-methylphenoxyacetic acid (MCPA): A pulse radiolysis and gamma-radiolysis study, *Radiat. Phys. Chem.* 81 (2012) 152-159.
- [17] G.R. Dey, P. Dwibedy, D.B. Naik, K. Kishore, Nature of the transient species formed by the reactions of reducing radicals with 2- and 3-aminopyridines: A pulse radiolysis study, *Radiat. Phys. Chem.* 64 (2002) 123-130.
- [18] B.R. Buxton, C.L. Greenstock, W.P. Helman, A.B. Ross, Critical review of rate constants for reactions hydrated electrons, hydrogen atoms and hydroxyl radicals ( $\bullet\text{OH}/\bullet\text{O}^-$ ) in aqueous solution, *J. Phys. Chem.* 17 (1988) 513-886.

- 
- [19] F.J. Beltran, G. Ovejero, B. Acedo, Oxidation of atrazine in water by ultraviolet radiation combined with hydrogen peroxideP, *Water Res.* 27 (1993) 1013-1021.
- [20] S.P. Mezyk, D.M. Bartels, Temperature Dependence of Hydrogen Atom Reaction with Nitrate and Nitrite Species in Aqueous Solution, *J. Phys. Chem. A* 101 (1997) 6233-6237.
- [21] M.A. Tarr, The Electron Beam Process for the Radiolytic Degradation of Pollutants, in: B.J. Mincher, W.J. Cooper, *Chemical Degradation method for wastes and pollutants, Environmental and industrial application*, Publishing Inc., Marcel Dekker, New York, 2009, Chapter7.
- [22] E. Atinault, V. De Waele, U. Schmidhammer, M. Fattahi, M. Mostafavi, Scavenging of and OH radicals in concentrated HCl and NaCl aqueous solutions, *Chemical Physics Letters* 460 (2008) 461-465.
- [23] D. Zehavi, J. Rabani, The Oxidation of aqueous bromide ions by hydroxyl radicals. Pulse radiolytic investigation. *J. Phys. Chem.* 76 (1972) 312-319.



## CAPÍTULO 7

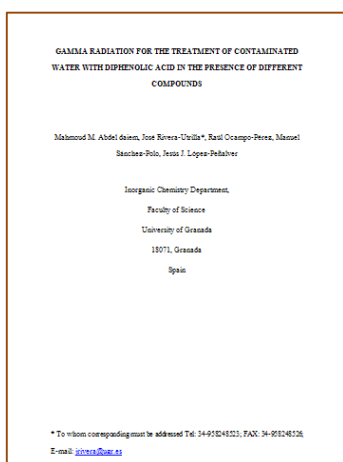
# TRATAMIENTO DE AGUA CONTAMINADA CON ÁCIDO DIFENÓLICO MEDIANTE RADIACIÓN GAMMA EN PRESENCIA DE DIFERENTES COMPUESTOS





# TREATMENT OF WATER CONTAMINATED WITH DIPHENOLIC ACID BY GAMMA RADIATION IN THE PRESENCE OF DIFFERENT COMPOUNDS

Manuscript submitted for publication



## Highlights

- Gamma radiation was effective to remove diphenolic acid (DPA) from aqueous solution.
- The solution pH had a major influence on DPA degradation, which was highest at pH 7.
- DPA degradation was reduced in the presence of  $\text{Br}^-$ ,  $\text{Cl}^-$ ,  $\text{CO}_3^{2-}$ ,  $\text{NO}_2^-$ ,  $\text{NO}_3^-$ , and  $\text{SO}_4^{2-}$ .
- Lower degradation rate were obtained with wastewater than with ultrapure water.
- Both TOC and toxicity decreased during DPA degradation in all water types studied.
- 

## ABSTRACT

The elimination of diphenolic acid (DPA) from contaminated water is an urgent challenge. The aim of this study was to investigate DPA degradation by gamma radiation, studying the influence of the dose rate, initial DPA concentration, solution pH, the presence of  $\text{O}_2$ , and the presence of different additives (e.g.,  $\text{Br}^-$ ,  $\text{Cl}^-$ ,  $\text{CO}_3^{2-}$ ,  $\text{NO}_2^-$ ,  $\text{NO}_3^-$ , and  $\text{SO}_4^{2-}$ ). A further objective was to study the effect of the water matrix (ultrapure water, surface water, and wastewater) and the variation in total organic carbon and toxicity as a function of absorbed dose. Results obtained showed that: gamma radiation was effective to remove DPA from aqueous solution; the dose constant was slightly dependent on the dose rate; and the solution pH had a major influence on DPA degradation, which was highest at pH 7. DPA degradation was reduced in the presence of  $\text{Br}^-$ ,  $\text{Cl}^-$ ,  $\text{CO}_3^{2-}$ ,  $\text{NO}_2^-$ ,  $\text{NO}_3^-$ , and  $\text{SO}_4^{2-}$  and was lower with higher concentrations of these species, largely due to their competition with DPA for the reactive radicals generated, especially  $\text{HO}^\bullet$ . Lower degradation rate constants were obtained with wastewater and surface water than with ultrapure water due to the presence of organic matter and  $\text{HCO}_3^-$ ,  $\text{Cl}^-$ ,  $\text{SO}_4^{2-}$ , and  $\text{NO}_3^-$  ions, which react with the reactive radical species ( $\text{HO}^\bullet$ ,  $\text{H}^\bullet$  and  $\text{e}_{\text{aq}}^-$ ). The TOC and toxicity of the medium decreased during DPA degradation in all water types studied.



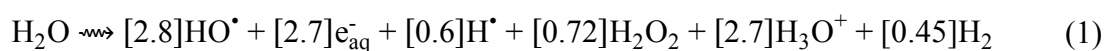


## 1. INTRODUCTION

Endocrine-disrupting compounds (EDCs) are natural and synthetic chemicals that cause adverse effects in humans and animals by influencing the endocrine system. They are considered to be a significant cause of reproductive and sexual disorders in animals [1]. Various EDCs are released into the aquatic environment, mainly *via* the effluent of sewage treatment plants [2]. EDC concentrations detected in the aquatic environment range from ng/L to µg/L [3, 4]. Even at low concentrations, EDCs can pose a serious threat to the endocrine system of humans and animals.

The widespread presence of EDCs in waters indicates that they are inadequately removed by conventional wastewater treatment processes and are eventually released into surface waters [2]. Advanced oxidation processes (AOPs) have been proposed as alternative methods for the treatment of EDCs [5-9]. They are based on the generation of species with high oxidizing power (e.g., HO• radicals), which interact with the pollutant, degrading it into byproducts with lower molecular weight and even achieving its complete mineralization. However, the oxidative pathway is very slow for some pollutants, for which reductive radicals (e.g., electrons, e<sub>aq</sub><sup>-</sup>, or hydrogen radicals, H•) are more effective [10].

Ionizing radiation is a promising water treatment option because it simultaneously generates oxidizing and reductive radical species (HO•, H• and e<sub>aq</sub><sup>-</sup>) from water radiolysis (Equation (1)) [11], allowing the degradation of a wide variety of compounds. Guo et al. [12] found that bisphenol A (BPA) degradation with gamma radiation was a feasible and effective to remove BPA from aqueous solution, which was largely attributed to HO• radical oxidation. Other authors have used gamma radiation to degrade EDCs [12- 14], pesticides [15, 16], nitroaromatic compounds [17], herbicides [18], and pharmaceutical compounds [10, 19, 20].



The values in square brackets in Equation (1) are the number of molecules formed with the absorption of 100 eV of energy in an air-free medium at pH 7.0 [11].

Few studies have been published on the removal of diphenolic acid (DPA), a typical EDC, from aqueous phase by adsorption and photocatalytic processes. Guo et al. [13] studied the photocatalytic degradation of DPA in the presence of  $\beta$ -cyclodextrin ( $\beta$ -CD) under UV radiation, reporting its enhancement in the presence of  $\beta$ -CD. Likewise, Guo et al. [14] investigated the photochemical behavior of DPA in the presence of  $\beta$ -CD and  $\text{TiO}_2$  suspensions and found that DPA degradation was increased in their presence, mainly due to the adsorption of DPA on  $\text{TiO}_2$  surface, which facilitates DPA degradation in the presence of hydroxyl radicals photoproduced by  $\text{TiO}_2$ .

With this background, the aim of this study was to determine the effectiveness of gamma radiation to degrade DPA in aqueous solution, studying: i) the effect of operational variables such as: initial concentration, dose rate, medium pH, and the presence of  $\text{O}_2$ ; ii) the effect of the presence of  $\text{Br}^-$ ,  $\text{Cl}^-$ ,  $\text{CO}_3^{2-}$ ,  $\text{NO}_2^-$ ,  $\text{NO}_3^-$ , and  $\text{SO}_4^{2-}$ ; iii) the influence of the chemical composition of the water, using natural water samples (surface water and wastewater); and iv) determining the variation in total organic carbon (TOC) and toxicity of DPA byproducts.

In this study, DPA was selected as a model EDC pollutant because of its frequent detection in the aquatic environment [21]. Over the past decade, considerable attention has been paid by researchers to DPA as a replacement for bisphenol A (BPA) in the synthesis of new polyesters and polycarbonates [22-27]. DPA is now commercially available at a much cheaper price than BPA and can be utilized to introduce functional carboxyl groups into the polymer structure [28]. However, DPA poses the same environmental risks as BPA, of which it is a derivative. Both compounds exert a strong estrogenic endocrine disrupting effect and have been associated with cancer, liver damage, and obesity-promotion, among other adverse health effects. It is therefore important to remove DPA from waters before their domestic utilization [22].

## 2. MATERIAL AND METHODS

### 2.1. Reagents

All chemical reagents used (diphenolic acid, potassium chloride, sodium nitrite, sodium carbonate, sodium nitrate, sodium sulfate, potassium bromide, hydrochloric acid, sodium hydroxide, phosphoric acid, and methanol) were high-purity analytic grade reagents supplied by Sigma-Aldrich. All solutions were prepared with ultrapure water obtained with Milli-Q<sup>®</sup> equipment (Millipore). Figure 1 presents the chemical structure and species distribution diagram of DPA as a function of solution pH.

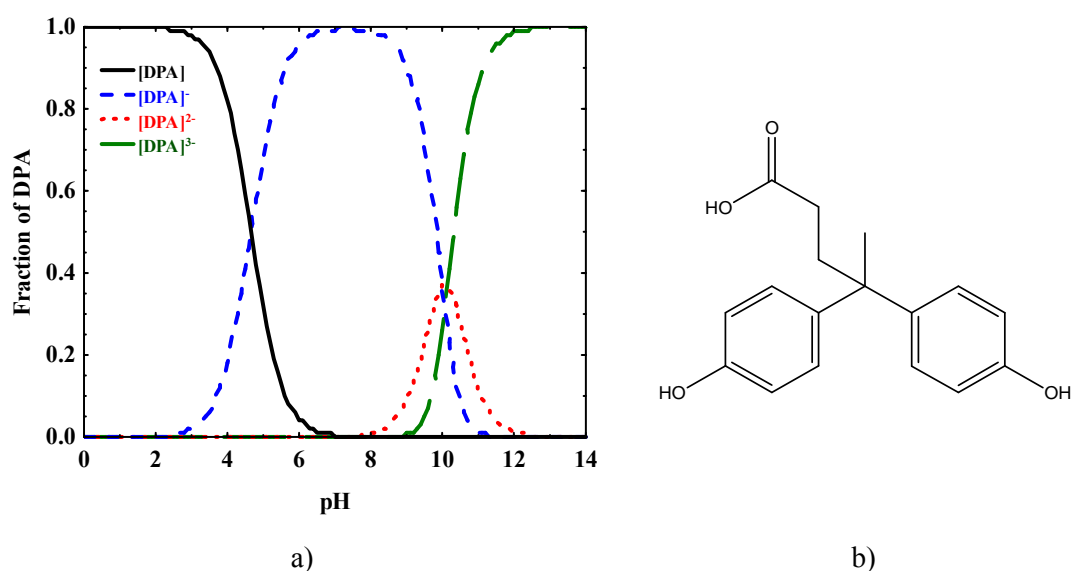


**Figure 1.** a) Species distribution diagram of DPA as a function of solution pH, b) Molecular structure of DPA.

### 2.2. Irradiation sources

Irradiation studies were performed using a J. L. Shepherd & Associates MARK-I model 30J gamma irradiator in the Experimental Radiology Unit of the Biomedical Research Center of the University of Granada (Spain). The equipment includes four sources of <sup>137</sup>Cs with a total combined activity of  $3.70 \times 10^{13}$  Bq (1,000 Ci). The equipment has three irradiation positions for different dose rates: position 1, 3.83 Gy/min; position 2, 1.66 Gy/min; and position 3: 1.06 Gy/min. DPA samples were irradiated in 2 mL vials sealed with screw caps to prevent air entry. The experiments were performed at room

temperature ( $25 \pm 2$  °C). Samples were bubbled with  $N_2$ , before irradiation to avoid the presence of dissolved  $O_2$ .

### 2.3. Collection and characterization of water samples

Surface water samples were collected from a drinking water treatment plant and wastewater samples from a wastewater treatment plant. Both types of waters were supplied by *Aguas y Servicios de la Costa Tropical de Granada* in Motril (Granada, Spain). Standard methods [29] were used to determine their characteristics, which are listed in Table 1. After their characterization, samples were filtered and stored in cold until their use.

**Table 1.** Chemical characteristics of different water types.

| Water           | pH  | TOC<br>(mg/L) | [HCO <sub>3</sub> <sup>-</sup> ]<br>(mg/L) | [Cl <sup>-</sup> ]<br>(mg/L) | [SO <sub>4</sub> <sup>2-</sup> ]<br>(mg/L) | [NO <sub>3</sub> <sup>-</sup> ]<br>(mg/L) |
|-----------------|-----|---------------|--|------------------------------|--|---|
| Ultrapure water | 6.8 | 0.0           | 0.0  | 0.0                          | 0.0  | 0.0                                       |
| Surface water   | 8.2 | 14.9          | 3.6  | 1.7                          | 59.8                                       | 4.28                                      |
| Wastewater      | 8.0 | 103.2         | 9.2  | 3.6                          | 88.9                                       | 5.99                                      |

### 2.4. Analytical methods

DPA concentration in aqueous solution was determined by high performance liquid chromatography (HPLC) in reverse phase, using a liquid chromatograph (Thermo-Fisher) equipped with a UV-detector and autosampler with a capacity for 120 vials. The chromatographic column was a Nova-Pak® C<sub>18</sub> (4 µm particle size; 3.9×150 mm). The mobile phase was 50% of 0.4% phosphoric acid solution v/v and 50% methanol in isocratic mode at flow of 0.5 mL/min; detector wavelength was 270 nm, and injection volume was 100 µL.

The total organic carbon (TOC) concentration of solutions was determined by using a Shimadzu V-CSH equipment with an ASI-V autosampler. The toxicity of DPA byproducts was determined by using a standardized biotest (DIN/EN/ISO 11348-2) of the inhibition of *Vibrio Fischeri* bacteria (NRRL B-11177) [30]. Bioluminescence was

measured with LUMISTOX 300 equipment [31], and results were expressed as percentage luminescence inhibition at 15 min of exposure.

Degradation byproducts were determined at different irradiation doses (0 to 1000 Gy) with an initial DPA concentration of 50 mg/L at 25 °C and pH = 7. DPA degradation by-products were separated from water by means of an ultra-pressure liquid chromatograph (UPLC, Waters, USA) equipped with a C<sub>18</sub> analytical column (2.1×100 mm, 1.7 μm) and coupled to a mass spectrometer (Waters, USA). The mobile phase was 50 % water and 50 % methanol and it was run in isocratic mode. The column temperature was kept at 25°C and the injection volume was 50 μL.

## 2.5. Determination of radiation-chemical yields and dose constant

The effectiveness of the irradiation process is given by the radiation-chemical yield (G-value) which is calculated by using the following equation [32]:

$$G = \frac{[C_0 - C] N_A}{D \times 6.24 \times 10^{16}} \quad (2)$$

where  $C_0$  is the initial DPA concentration (mol/L),  $C$  is the DPA concentration at dose  $D$  (mol/L),  $D$  is the absorbed dose (Gy),  $N_A$  is the Avogadro number ( $6.023 \times 10^{23}$  molecules/mol), and  $6.24 \times 10^{16}$  is the conversion factor of Gy at 100 eV/L. G-values are expressed in μmol/J, considering  $1 \text{ molecule} \times (100 \text{ eV})^{-1} = 0.10364 \text{ μmol/J}$ .

The initial radiation-chemical yield ( $G_0$ ) was estimated by fitting the equation (3) to the experimental data (G vs. D), where  $d$  is the rate of variation of G against D.

$$G = G_0 \times e^{-dD} \quad (3)$$

The dose constant,  $k$ , was determined by considering that pollutant degradation kinetic data fit a pseudo-first order kinetics. The pseudo-first order model is given by the following equation:

$$C=C_0 \times e^{-kD} \quad (4)$$

Furthermore, the doses required to degrade 50%,  $D_{50}$ , and 90%,  $D_{90}$ , of the initial contaminant concentration were calculated using Eqs. (5) and (6), respectively.

$$D_{50} = \frac{\text{Ln}(2)}{k} \quad (5)$$

$$D_{90} = \frac{\text{Ln}(10)}{k} \quad (6)$$

### 3. RESULTS AND DISCUSSION

#### 3.1. Radiolytic degradation of DPA in aqueous solution

Figure 2 depicts the degradation kinetics of DPA by gamma irradiation as a function of the dose adsorbed, for initial concentrations of 20, 50, and 100 mg/L at a dose rate of 1.66 Gy/min (Table 2, Exp. Nos. 1-3). As shown in this figure, DPA removal increased with higher absorbed dose, and this effect was more marked at lower initial concentrations. Table 2 shows the  $k$  values obtained and the doses required to degrade 50% and 90% of the initial DPA concentration. As can be observed, the  $k$  value markedly decreased from  $3.37 \pm 0.00 \times 10^{-3}$  to  $1.21 \pm 0.01 \times 10^{-3} \text{ Gy}^{-1}$  for initial concentrations of 20 mg/L and 100 mg/L, respectively. One explanation is that a rise in the initial DPA concentration produces an increase in byproducts, which react with the radicals species formed in radiolysis and reduce the number of radical species available to react with DPA.

G-values were calculated for different initial DPA concentrations at a radiation dose of 1.66 Gy/min. They increased with higher initial DPA concentrations (Figure 2), as previously observed for nitroimidazoles by Sánchez-Polo et al. [20]. This is because the reactive radicals produced by water radiolysis at higher DPA concentrations had a greater opportunity to react with DPA molecules, yielding a higher removal efficacy, as shown by the G-value obtained (Table 2).

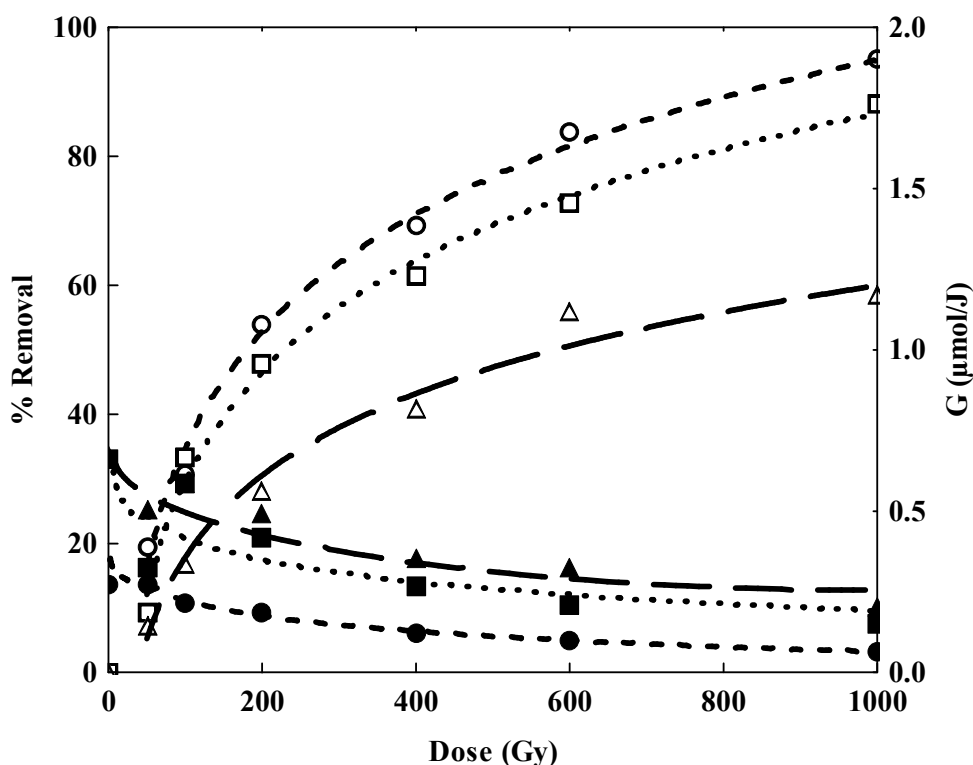


**Figure 2.** G-values (black symbols) and % DPA removal (white symbols) during gamma radiation. Initial concentration of DPA: 20 mg/L (○, ●), 50 mg/L (□, ■), and 100 mg/L (△, ▲), Dose rate = 1.66 Gy/min, pH = 7.0, and T = 25°C.

The effect of the irradiation dose rate on DPA degradation was investigated by conducting the degradation kinetics under the same experimental conditions, with an initial DPA concentration of 50 mg/L, at dose rates of 1.06, 1.66, and 3.83 Gy/min (Figure 3). There was a slight increase in dose constant with higher irradiation dose rates, with values of  $2.29 \pm 0.02 \times 10^{-3}$ ,  $2.74 \pm 0.03 \times 10^{-3}$ , and  $3.20 \pm 0.01 \times 10^{-3} \text{ Gy}^{-1}$  for 1.06, 1.66, and 3.83 Gy/min, respectively (Table 2, Exp. Nos. 2, 4, 5), indicating that gamma radiation is more effective at elevated dose rates. The G-value for the three dose rates was lower at higher irradiation doses. To facilitate study of the influence of operational variables on the effectiveness of DPA irradiation, a dose rate of 1.66 Gy/min and an initial DPA concentration of 50 mg/L were selected for the experiments.



**Table 2.** Gamma radiation of DPA-contaminated water: experimental conditions and kinetic parameters.

| Exp. N° | [DPA] <sub>0</sub> (mg/L) | pH   | Dose rate (Gy/min) | [Br <sup>-</sup> ] (mg/L) | [Cl <sup>-</sup> ] (mg/L) | [CO <sub>3</sub> <sup>2-</sup> ] (mg/L) | [NO <sub>2</sub> <sup>-</sup> ] (mg/L) | [NO <sub>3</sub> <sup>-</sup> ] (mg/L) | [SO <sub>4</sub> <sup>2-</sup> ] (mg/L) | G <sub>0</sub> ×10 (μmol/J) | k ×10 <sup>3</sup> (Gy <sup>-1</sup> ) | D <sub>50</sub> (Gy) | D <sub>90</sub> (Gy) |
|---------|---------------------------|------|--------------------|---------------------------|---------------------------|---|--|--|---|-----------------------------|--|----------------------|----------------------|
| 1       | 20                        | 7.0  | 1.66               | -                         | -                         | -                                       | -                                      | -                                      | -                                       | 2.75                        | 3.37±0.00                              | 205.6                | 683.0                |
| 2       | 50                        | 7.0  | 1.66               | -                         | -                         | -                                       | -                                      | -                                      | -                                       | 6.61                        | 2.74±0.03                              | 252.6                | 839.3                |
| 3       | 100                       | 7.0  | 1.66               | -                         | -                         | -                                       | -                                      | -                                      | -                                       | 6.72                        | 1.21±0.01                              | 572.9                | 1903.3               |
| 4       | 50                        | 7.0  | 1.06               | -                         | -                         | -                                       | -                                      | -                                      | -                                       | 6.19                        | 2.29±0.02                              | 303.1                | 1006.7               |
| 5       | 50                        | 7.0  | 3.83               | -                         | -                         | -                                       | -                                      | -                                      | -                                       | 6.05                        | 3.20±0.01                              | 216.5                | 719.2                |
| 6       | 50                        | 2.0  | 1.66               | -                         | -                         | -                                       | -                                      | -                                      | -                                       | 0.84                        | 0.48±0.05                              | 1454.7               | 4832.3               |
| 7       | 50                        | 12.0 | 1.66               | -                         | -                         | -                                       | -                                      | -                                      | -                                       | 5.50                        | 1.93±0.01                              | 359.9                | 1195.7               |
| 8       | 50                        | 7.0  | 1.66               | 5                         | -                         | -                                       | -                                      | -                                      | -                                       | 2.94                        | 2.35±0.02                              | 294.7                | 979.8                |
| 9       | 50                        | 7.0  | 1.66               | 20                        | -                         | -                                       | -                                      | -                                      | -                                       | 2.66                        | 1.25±0.01                              | 552.4                | 1834.9               |
| 10      | 50                        | 7.0  | 1.66               | 50                        | -                         | -                                       | -                                      | -                                      | -                                       | 1.42                        | 0.84±0.02                              | 822.6                | 2732.6               |
| 11      | 50                        | 7.0  | 1.66               | 100                       | -                         | -                                       | -                                      | -                                      | -                                       | 0.90                        | 0.58±0.01                              | 1207.9               | 4012.5               |
| 12      | 50                        | 7.0  | 1.66               | 1000                      | -                         | -                                       | -                                      | -                                      | -                                       | 1.40                        | 0.59±0.01                              | 1178.9               | 3916.2               |
| 13      | 50                        | 5.1  | 1.66               | -                         | 5                         | -                                       | -                                      | -                                      | -                                       | 3.92                        | 2.55±0.11                              | 271.8                | 903.0                |
| 14      | 50                        | 5.1  | 1.66               | -                         | 20                        | -                                       | -                                      | -                                      | -                                       | 3.65                        | 1.95±0.01                              | 356.5                | 1184.1               |
| 15      | 50                        | 5.2  | 1.66               | -                         | 50                        | -                                       | -                                      | -                                      | -                                       | 3.32                        | 1.74±0.14                              | 339.3                | 1326.5               |
| 16      | 50                        | 5.6  | 1.66               | -                         | 100                       | -                                       | -                                      | -                                      | -                                       | 3.02                        | 1.30±0.06                              | 532.4                | 1768.6               |
| 17      | 50                        | 5.7  | 1.66               | -                         | 1000                      | -                                       | -                                      | -                                      | -                                       | 1.93                        | 0.97±0.03                              | 715.7                | 2377.6               |
| 18      | 50                        | 8.2  | 1.66               | -                         | -                         | 5                                       | -                                      | -                                      | -                                       | 3.62                        | 2.60±0.07                              | 266.6                | 885.6                |
| 19      | 50                        | 8.2  | 1.66               | -                         | -                         | 20                                      | -                                      | -                                      | -                                       | 3.17                        | 2.08±0.15                              | 333.1                | 1106.4               |
| 20      | 50                        | 8.5  | 1.66               | -                         | -                         | 50                                      | -                                      | -                                      | -                                       | 3.33                        | 1.84±0.14                              | 377.7                | 1254.6               |
| 21      | 50                        | 9.2  | 1.66               | -                         | -                         | 100                                     | -                                      | -                                      | -                                       | 2.78                        | 1.46±0.01                              | 475.3                | 1578.9               |
| 22      | 50                        | 9.9  | 1.66               | -                         | -                         | 1000                                    | -                                      | -                                      | -                                       | 2.60                        | 1.09±0.06                              | 633.4                | 2104.0               |
| 23      | 50                        | 6.4  | 1.66               | -                         | -                         | -                                       | 5                                      | -                                      | -                                       | 3.87                        | 2.38±0.05                              | 291.2                | 967.5                |
| 24      | 50                        | 6.4  | 1.66               | -                         | -                         | -                                       | 20                                     | -                                      | -                                       | 3.52                        | 1.97±0.09                              | 351.3                | 1167.1               |
| 25      | 50                        | 7.2  | 1.66               | -                         | -                         | -                                       | 50                                     | -                                      | -                                       | 2.40                        | 1.34±0.04                              | 516.3                | 1715.7               |
| 26      | 50                        | 7.6  | 1.66               | -                         | -                         | -                                       | 100                                    | -                                      | -                                       | 1.42                        | 0.84±0.02                              | 822.6                | 2732.6               |
| 27      | 50                        | 7.9  | 1.66               | -                         | -                         | -                                       | 1000                                   | -                                      | -                                       | 1.20                        | 0.60±0.01                              | 1157.9               | 3846.6               |

**Table 2.** Gamma radiation of DPA-contaminated water: experimental conditions and kinetic parameters (continued).

| Exp. N° | [DPA] <sub>0</sub> (mg/L) | pH  | Dose rate (Gy/min) | [Br <sup>-</sup> ] (mg/L) | [Cl <sup>-</sup> ] (mg/L) | [CO <sub>3</sub> <sup>2-</sup> ] (mg/L) | [NO <sub>2</sub> <sup>-</sup> ] (mg/L) | [NO <sub>3</sub> <sup>-</sup> ] (mg/L) | [SO <sub>4</sub> <sup>2-</sup> ] (mg/L) | G <sub>0</sub> ×10 (μmol/J) | k ×10 <sup>3</sup> (Gy <sup>-1</sup> ) | D <sub>50</sub> (Gy) | D <sub>90</sub> (Gy) |
|---------|---------------------------|-----|--------------------|---------------------------|---------------------------|---|--|--|---|-----------------------------|--|----------------------|----------------------|
| 28      | 50                        | 7.0 | 1.66               | -                         | -                         | -                                       | -                                      | 5                                      | -                                       | 3.41                        | 2.60±0.02                              | 266.6                | 885.6                |
| 29      | 50                        | 7.0 | 1.66               | -                         | -                         | -                                       | -                                      | 20                                     | -                                       | 3.09                        | 2.01±0.05                              | 344.8                | 1145.6               |
| 30      | 50                        | 7.0 | 1.66               | -                         | -                         | -                                       | -                                      | 50                                     | -                                       | 1.91                        | 1.61±0.03                              | 430.5                | 1430.2               |
| 31      | 50                        | 7.0 | 1.66               | -                         | -                         | -                                       | -                                      | 100                                    | -                                       | 1.16                        | 1.10±0.09                              | 630.1                | 2093.3               |
| 32      | 50                        | 7.0 | 1.66               | -                         | -                         | -                                       | -                                      | 1000                                   | -                                       | 1.30                        | 0.80±0.01                              | 866.4                | 2878.2               |
| 33      | 50                        | 7.0 | 1.66               | -                         | -                         | -                                       | -                                      | -                                      | 5                                       | 4.05                        | 2.65±0.05                              | 106.6                | 354.2                |
| 34      | 50                        | 7.0 | 1.66               | -                         | -                         | -                                       | -                                      | -                                      | 20                                      | 3.55                        | 2.12±0.04                              | 327.0                | 1086.1               |
| 35      | 50                        | 7.0 | 1.66               | -                         | -                         | -                                       | -                                      | -                                      | 50                                      | 3.73                        | 2.01±0.10                              | 344.8                | 1145.6               |
| 36      | 50                        | 7.0 | 1.66               | -                         | -                         | -                                       | -                                      | -                                      | 100                                     | 3.11                        | 1.64±0.03                              | 422.7                | 1404.0               |
| 37      | 50                        | 7.0 | 1.66               | -                         | -                         | -                                       | -                                      | -                                      | 1000                                    | 2.91                        | 1.20±0.08                              | 577.6                | 1918.8               |

The effect of the irradiation dose rate on DPA degradation was investigated by conducting the degradation kinetics under the same experimental conditions, with an initial DPA concentration of 50 mg/L, at dose rates of 1.06, 1.66, and 3.83 Gy/min (Figure 3). There was a slight increase in dose constant with higher irradiation dose rates, with values of  $2.29 \pm 0.02 \times 10^{-3}$ ,  $2.74 \pm 0.03 \times 10^{-3}$ , and  $3.20 \pm 0.01 \times 10^{-3} \text{ Gy}^{-1}$  for 1.06, 1.66, and 3.83 Gy/min, respectively (Table 2, Exp. Nos. 2, 4, 5), indicating that gamma radiation is more effective at elevated dose rates. The G-value for the three dose rates was lower at higher irradiation doses. To facilitate study of the influence of operational variables on the effectiveness of DPA irradiation, a dose rate of 1.66 Gy/min and an initial DPA concentration of 50 mg/L were selected for the experiments.

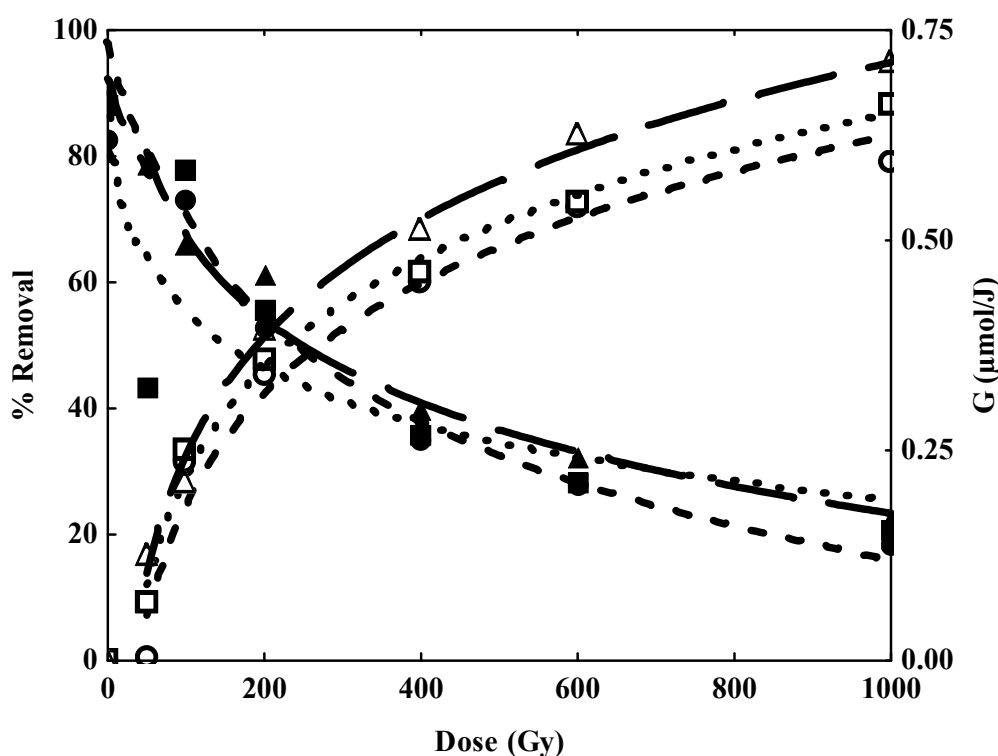


**Figure 3.** G-values (black symbols) and % DPA removal (white symbols) during gamma radiation. Initial DPA concentration of 50 mg/L; dose rate: 1.06 Gy/min ( $\circ$ ,  $\bullet$ ), 1.66 Gy/min ( $\square$ ,  $\blacksquare$ ), and 3.83 Gy/min ( $\Delta$ ,  $\blacktriangle$ ), pH = 7.0, and T = 25°C.

The radiation-chemical yield of species generated in water radiolysis is a function of the medium pH [33, 34]. Therefore, the irradiation was studied in acidic and basic media (Figure 4), irradiating DPA aqueous solutions at pH = 2.0, 7.0, and 12.0 (Table 2, Exp.

Nº 2, 6, 7). The lowest DPA degradation was observed at pH = 2.0, with a marked reduction in the dose constant,  $k = 0.48 \pm 0.05 \times 10^{-3} \text{ Gy}^{-1}$ , which was not observed at the other pH values studied. One explanation for this drastic decrease in DPA degradation rate is that reaction (7) is favored at pH = 2.0 and the G-value of  $e_{\text{aq}}^-$  tends to zero, increasing the radiation-chemical yield of  $\text{H}^\bullet$ ; this supports the hypothesis that  $\text{H}^\bullet$  radicals are not involved in DPA degradation. Moreover, an increase in the  $\text{H}^\bullet$  concentration favors the recombination of radicals (reaction (8)) and reduces the concentration of  $\text{HO}^\bullet$  radicals in the medium, which contributes to decreasing the  $k$  value.

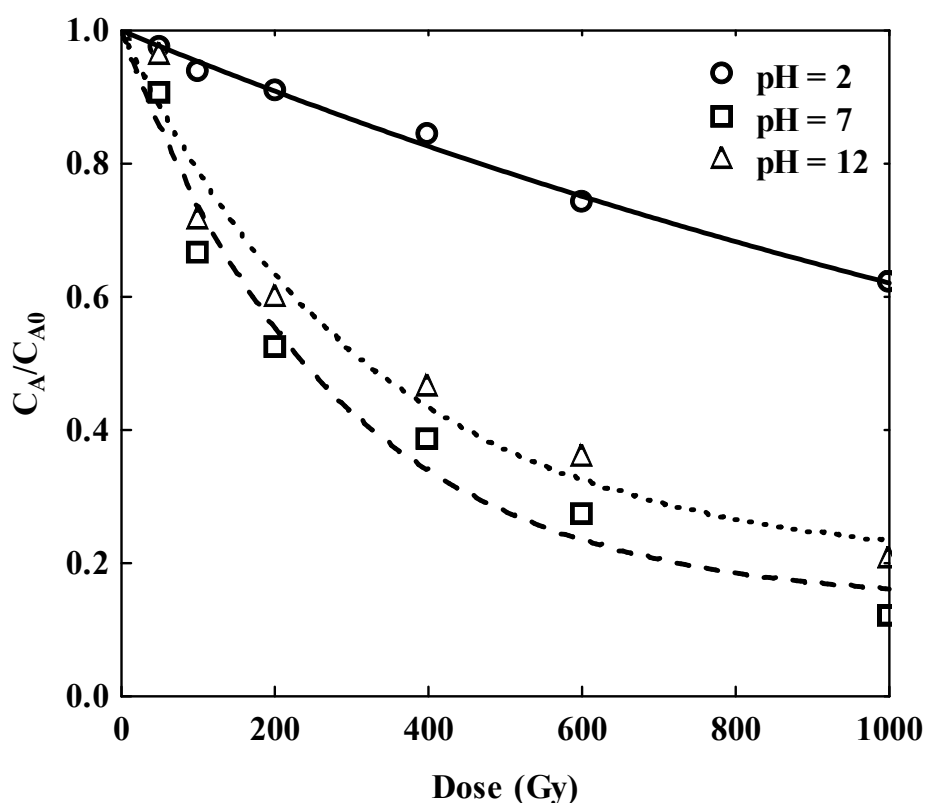
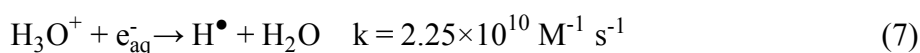
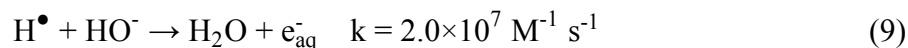


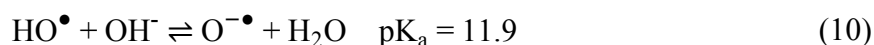
**Figure 4.** Effect of solution pH on DPA degradation during gamma radiation. Dose rate = 1.66 Gy/min,  $[\text{DPA}]_0 = 50 \text{ mg/L}$ , and  $T = 25^\circ\text{C}$ .



Joseph et al. [34] established that the concentration of  $e_{aq}^-$  increases between pH = 6.0 and pH = 8.0 by reaction (9), explaining why the highest dose constant ( $k = 2.74 \pm 0.03 \times 10^{-3} \text{ Gy}^{-1}$ ) was observed at pH = 7.0.



Finally, the equilibrium in reaction (10) gains in importance at a pH value of 12.0, when  $\text{HO}^\bullet$  radicals transform into the less reactive  $\text{O}^{\bullet-}$  species [34], explaining the lower dose constant ( $k = 1.93 \pm 0.01 \times 10^{-3} \text{ Gy}^{-1}$ ) at this pH.



DPA degradation byproducts were determined at pH = 7 using different irradiation doses, with an initial DPA concentration of 50 mg/L (see Experimental section). The results obtained showed that the only stable byproduct found was monohydroxylated diphenolic acid, whose concentration gradually increased with the absorbed dose.

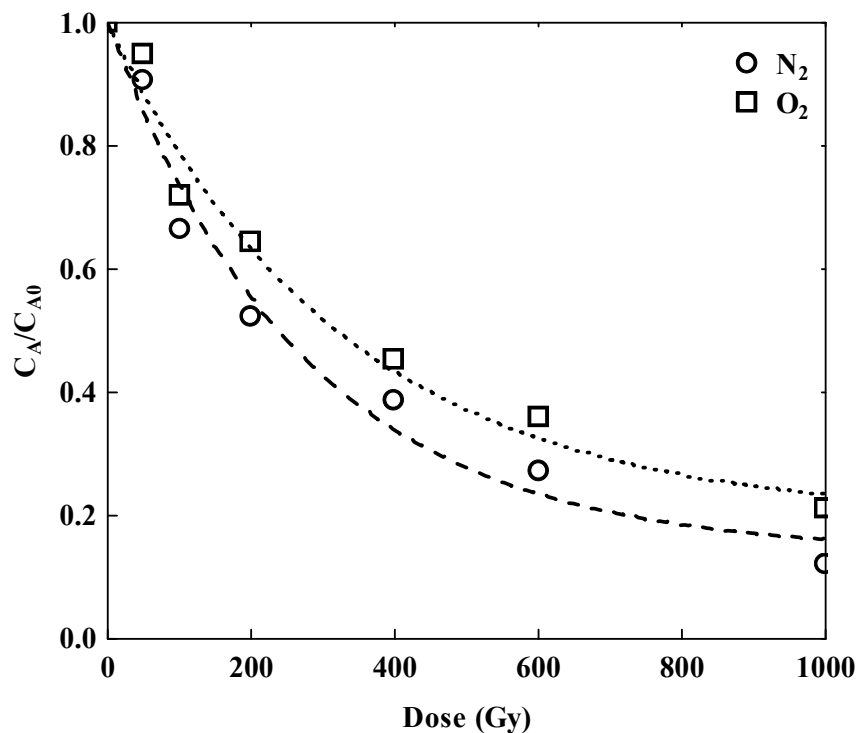
### 3.2. Effect of the presence of $\text{O}_2$ on DPA degradation

Two sets of experiments were performed to examine the influence of  $\text{O}_2$  on DPA degradation: one with no initially dissolved  $\text{O}_2$  in the solution (samples were bubbled with  $\text{N}_2$ ), and another with a fully aerated solution. Results obtained are shown in Figure 5. The slightly reduction in DPA degradation observed in the presence of  $\text{O}_2$  may be due to the reaction of  $\text{O}_2$  with  $e_{aq}^-$  species, which shows a reaction rate constant,  $k = 1.9 \times 10^{10} \text{ M}^{-1} \text{ s}^{-1}$  [35].

### 3.3. Effect of the presence of $\text{Br}^-$ , $\text{Cl}^-$ , $\text{CO}_3^{2-}$ , $\text{NO}_2^-$ , $\text{NO}_3^-$ , or $\text{SO}_4^{2-}$ , on DPA degradation

Natural waters are complex matrixes containing anions that can interfere with the radiolytic degradation of DPA by reacting with radical species formed during the process (Table 3). To study the effect of the presence of anions on DPA degradation, common anions found in natural water and industrial wastewater ( $\text{Br}^-$ ,  $\text{Cl}^-$ ,  $\text{CO}_3^{2-}$ ,  $\text{NO}_2^-$ ,

$\text{NO}_3^-$ , and  $\text{SO}_4^{2-}$ ) were each added to different 50 mg/L DPA solutions before their irradiation. Table 2, Exp. Nos. 8-37, and Figure 6 show the results obtained.



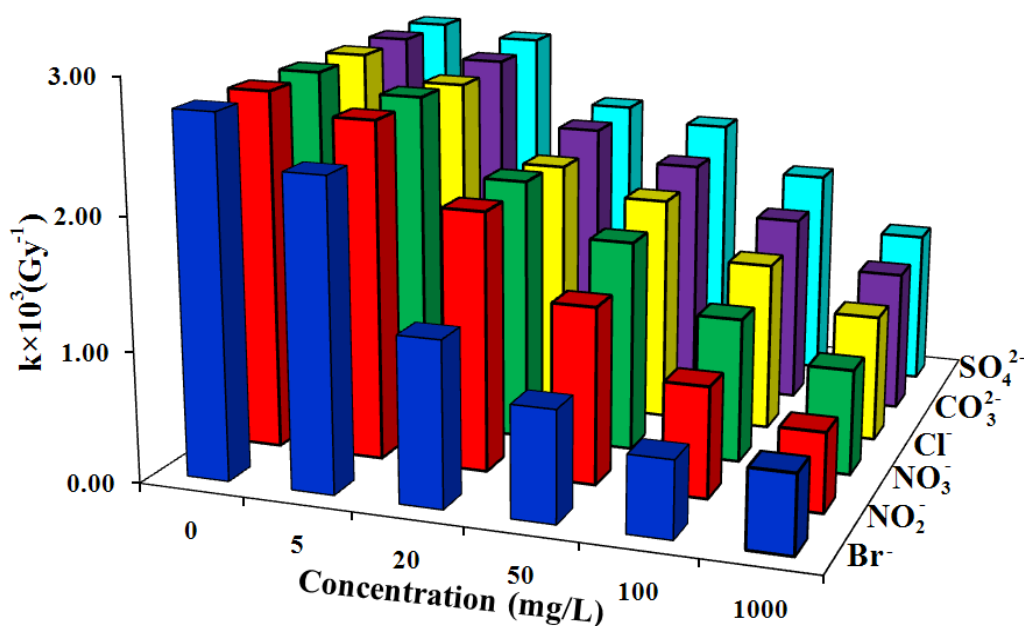
**Figure 5.** Effect of the presence of  $\text{O}_2$  on DPA degradation during gamma radiation. Dose rate = 1.66 Gy/min,  $[\text{DPA}]_0 = 50$  mg/L,  $\text{pH} = 7.0$ , and  $T = 25^\circ\text{C}$ .

Figure 6 depicts the variation in dose constant,  $k$ , as a function of the concentration of species added to the DPA aqueous solution, showing a decrease in dose constant at higher concentrations of each anion ( $\text{Br}^-$ ,  $\text{Cl}^-$ ,  $\text{CO}_3^{2-}$ ,  $\text{NO}_2^-$ ,  $\text{NO}_3^-$ , and  $\text{SO}_4^{2-}$ ). The reduction in  $k$  varied among anions in the order:  $\text{Br}^- > \text{NO}_2^- > \text{NO}_3^- > \text{Cl}^- > \text{CO}_3^{2-} > \text{SO}_4^{2-}$ . These results can be explained by the reactions shown in Table 3.

$\text{Br}^-$  ions can act as  $\text{HO}^\bullet$  radical scavengers (reaction 11), forming  $\text{BrOH}^{\bullet-}$ , which is involved in reactions 12 and 13 to form  $\text{Br}_2^{\bullet-}$  radicals, which can contribute to remove  $\text{H}^\bullet$  and  $e_{\text{aq}}^-$  species from the medium by reactions 14 and 15. However, the addition of more than 100 mg/L of  $\text{Br}^-$  does not have an appreciably greater effect on the dose constant (Table 2, Exp. Nos. 11, 12), indicating that this concentration is adequate to remove all reactive radicals present in the medium.

**Table 3.** Reactions of anions  $\text{Br}^-$ ,  $\text{Cl}^-$ ,  $\text{CO}_3^{2-}$ ,  $\text{NO}_2^-$ ,  $\text{NO}_3^-$ , and  $\text{SO}_4^{2-}$  with the radiolytic species  $\text{HO}^\bullet$ ,  $\text{H}^\bullet$ , and  $\text{e}_{\text{aq}}^-$ .

| Reaction number | Chemical Reaction   | Rate Constant ( $\text{M}^{-1} \text{s}^{-1}$ ) | Reference |
|-----------------|---|---|-----------|
| (11)            | $\text{HO}^\bullet + \text{Br}^- \rightarrow \text{BrOH}^{\bullet-}$                                | $1.1 \times 10^{10}$                            | [35]      |
| (12)            | $\text{BrHO}^{\bullet-} \rightarrow \text{Br}^\bullet + \text{HO}^-$                                | $4.2 \times 10^6$                               | [36]      |
| (13)            | $\text{Br}^\bullet + \text{Br}^- \leftrightarrow \text{Br}_2^{\bullet-}$                            | $1.0 \times 10^{10}$                            | [36]      |
| (14)            | $\text{e}_{\text{aq}}^- + \text{Br}_2^{\bullet-} \rightarrow 2\text{Br}^-$                          | -----   | [37]      |
| (15)            | $\text{H}^\bullet + \text{Br}_2^{\bullet-} \rightarrow 2\text{Br}^- + \text{H}^+$                   | -----   | [37]      |
| (16)            | $\text{Cl}^- + \text{HO}^\bullet \rightarrow \text{ClOH}^{\bullet-}$                                | $4.3 \times 10^9$                               | [38]      |
| (17)            | $\text{ClOH}^{\bullet-} \rightarrow \text{Cl}^- + \text{HO}^\bullet$                                | $6.1 \times 10^9$                               | [38]      |
| (18)            | $\text{ClOH}^{\bullet-} + \text{e}_{\text{aq}}^- \rightarrow \text{Cl}^- + \text{HO}^-$             | $1.0 \times 10^{10}$                            | [38]      |
| (19)            | $\text{ClOH}^{\bullet-} + \text{H}_3\text{O}^+ \rightarrow \text{Cl}^\bullet + 2\text{H}_2\text{O}$ | $2.1 \times 10^{10}$                            | [38]      |
| (20)            | $\text{Cl}^\bullet + \text{H}^\bullet \rightarrow \text{Cl}^- + \text{H}^+$                         | $1.0 \times 10^{10}$                            | [38]      |
| (21)            | $\text{Cl}^\bullet + \text{Cl}^- \rightarrow \text{Cl}_2^{\bullet-}$                                | $2.1 \times 10^{10}$                            | [38]      |
| (22)            | $\text{Cl}_2^{\bullet-} + \text{e}_{\text{aq}}^- \rightarrow 2\text{Cl}^-$                          | $1.0 \times 10^{10}$                            | [38]      |
| (23)            | $\text{Cl}_2^{\bullet-} + \text{H}^\bullet \rightarrow 2\text{Cl}^- + \text{H}^+$                   | $8.0 \times 10^9$                               | [38]      |
| (24)            | $\text{HO}^\bullet + \text{CO}_3^{2-} \rightarrow \text{CO}_3^{\bullet-} + \text{HO}^-$             | $3.9 \times 10^8$                               | [38]      |
| (25)            | $\text{HO}^\bullet + \text{HCO}_3^- \rightarrow \text{CO}_3^{\bullet-} + \text{H}_2\text{O}$        | $8.5 \times 10^6$                               | [38]      |
| (26)            | $\text{e}_{\text{aq}}^- + \text{CO}_3^{2-} \rightarrow \text{CO}_3^{\bullet-}$                      | $3.9 \times 10^5$                               | [39]      |
| (27)            | $\text{e}_{\text{aq}}^- + \text{HCO}_3^- \rightarrow \text{HCO}_3^{\bullet-}$                       | $6.0 \times 10^5$                               | [38]      |
| (28)            | $\text{H}^\bullet + \text{HCO}_3^- \rightarrow \text{CO}_3^{\bullet-} + \text{H}_2$                 | $4.0 \times 10^4$                               | [38]      |
| (29)            | $\text{HO}^\bullet + \text{NO}_2^- \rightarrow \text{NO}_2^\bullet + \text{HO}^-$                   | $6.0 \times 10^9$                               | [40]      |
| (30)            | $\text{HO}^\bullet + \text{NO}_2^\bullet \rightarrow \text{HNO}_3$                                  | $1.3 \times 10^9$                               | [41]      |
| (31)            | $\text{H}^\bullet + \text{NO}_2^- \rightarrow \text{NO} + \text{HO}^-$                              | $7.1 \times 10^8$                               | [42]      |
| (32)            | $\text{NO}_2^\bullet + \text{H}^\bullet \rightarrow \text{HNO}_2$                                   | $1.0 \times 10^{10}$                            | [40]      |
| (33)            | $\text{e}_{\text{aq}}^- + \text{NO}_2^- \rightarrow \text{NO}_2^{\bullet 2-}$                       | $3.5 \times 10^9$                               | [43]      |
| (34)            | $\text{H}^+ + \text{NO}_3^- \rightarrow \text{HNO}_3$   | $(4.4-6.0) \times 10^8$                         | [44]      |
| (35)            | $\text{HO}^\bullet + \text{HNO}_3 \rightarrow \text{H}_2\text{O} + \text{NO}_3^\bullet$             | $(0.88-1.2) \times 10^8$                        | [45]      |
| (36)            | $\text{H}^\bullet + \text{HNO}_3 \rightarrow \text{H}_2 + \text{NO}_3^\bullet$                      | $\leq 1.0 \times 10^7$                          | [46]      |
| (37)            | $\text{NO}_3^\bullet + \text{H}_2\text{O} \rightarrow \text{HNO}_3 + \text{HO}^\bullet$             | $3.0 \times 10^2$                               | [45]      |
| (38)            | $\text{e}_{\text{aq}}^- + \text{NO}_3^- \rightarrow \text{NO}_3^{\bullet 2-}$                       | $9.7 \times 10^9$                               | [20]      |
| (39)            | $\text{NO}_3^{\bullet 2-} + \text{H}^+ \rightarrow \text{NO}_2 + \text{HO}^-$                       | $4.5 \times 10^{10}$                            | [47]      |
| (40)            | $\text{H}^\bullet + \text{NO}_3^- \rightarrow \text{NO}_2^\bullet + \text{HO}^-$                    | $4.4 \times 10^6$                               | [42]      |
| (41)            | $\text{NO}_2^\bullet + \text{H}^\bullet \rightarrow \text{HNO}_2$                                   | $1.0 \times 10^{10}$                            | [40]      |
| (42)            | $\text{HO}^\bullet + \text{NO}_3^\bullet \rightarrow \text{HONO}_3$                                 | $1.0 \times 10^{10}$                            | [46]      |
| (43)            | $\text{H}^\bullet + \text{NO}_3^\bullet \rightarrow \text{HNO}_3$                                   | $1.0 \times 10^{10}$                            | [46]      |
| (44)            | $\text{e}_{\text{aq}}^- + \text{SO}_4^{2-} \rightarrow \text{SO}_4^{\bullet-}$                      | $1.0 \times 10^6$                               | [15]      |



**Figure 6.** Variation in dose constant as a function of the species concentration present in the water. Dose rate = 1.66 Gy/min,  $[DPA]_0 = 50$  mg/L, and  $T = 25^\circ\text{C}$ .

The presence of  $\text{Cl}^-$  ions (5-1000 mg/L) significantly reduced the dose constant (Table 2, Exp. N° 13-17). Chloride ions react with  $\text{HO}^\bullet$  radicals, as shown in reaction 16, but the radical formed ( $\text{ClOH}^\bullet$ ) may again generate  $\text{HO}^\bullet$  radicals by reaction 17.  $\text{ClOH}^\bullet$  may also react with  $e^-_{\text{aq}}$  or with  $\text{H}_3\text{O}^+$  ions (reactions 18 and 19) forming  $\text{Cl}^\bullet$  radicals, which are involved in reactions 20-23 and thereby contribute to removing  $\text{H}^\bullet$  and  $e^-_{\text{aq}}$  species from the medium. In most of the present cases, the decrease in dose constant was lower with the addition of  $\text{Cl}^-$  ions *versus*  $\text{Br}^-$  ions, attributable to the higher reaction rate constant between  $\text{HO}^\bullet$  radicals and  $\text{Br}^-$  *versus*  $\text{Cl}^-$  ( $k = 1.1 \times 10^{10} \text{ M}^{-1} \text{ s}^{-1}$  vs.  $k = 4.3 \times 10^9 \text{ M}^{-1} \text{ s}^{-1}$ , respectively).

$\text{CO}_3^{2-}$  ions act as  $\text{HO}^\bullet$  radical scavengers ( $k = 3.9 \times 10^8 \text{ M}^{-1} \text{ s}^{-1}$ ) and can also react with  $e^-_{\text{aq}}$ , although at a much lower reaction rate than with  $\text{HO}^\bullet$  radicals ( $k = 3.9 \times 10^5 \text{ M}^{-1} \text{ s}^{-1}$ ). The equilibrium established in aqueous solution is  $\text{HCO}_3^- \rightleftharpoons \text{CO}_3^{2-} + \text{H}^+$ , with  $\text{pK}_a = 10.33$ ; therefore, at the working pH solution (lower than 10.33), this equilibrium would shift to the left, with a predominance of  $\text{HCO}_3^-$  species, involving reactions 25, 27, and



28 (Table 3). Moreover,  $\text{CO}_3^{\bullet-}$  radicals formed by reactions 24 and 28 (Table 3) have a reduction potential of 1.58 V at pH = 12 and of 1.78 V at pH = 7; hence,  $\text{CO}_3^{\bullet-}$  radicals can oxidize numerous organic compounds [48], including DPA. This would explain the less marked decrease in dose constant in the presence of  $\text{CO}_3^{2-}$  than in the presence of the other anions.

The experimental results showed that low concentrations of  $\text{NO}_2^-$  ions in the medium produced a significant reduction in the dose constant, because  $\text{NO}_2^-$  ions acted as inhibitors of  $\text{HO}^\bullet$ ,  $\text{H}^\bullet$  radicals, and  $e_{\text{aq}}^-$  by reactions 29-33 (Table 3).  $\text{NO}_3^-$  ions act as scavengers of  $\text{H}^\bullet$  and  $e_{\text{aq}}^-$  radicals by reactions 34, 36-43 (Table 3) and can act as  $\text{HO}^\bullet$  radical inhibitors by reaction 35; although the rate constant is lower with  $\text{HO}^\bullet$  ( $k = 0.88\text{--}1.20 \times 10^8 \text{ M}^{-1}\text{s}^{-1}$ ) versus  $e_{\text{aq}}^-$  ( $k = 9.7 \times 10^9 \text{ M}^{-1}\text{s}^{-1}$ ) radicals (Table 3). The dose constant significantly decreased at higher  $\text{NO}_3^-$  ion concentrations, as depicted in Figure 6.

$\text{SO}_4^{2-}$  ions act as radical scavengers of only  $e_{\text{aq}}^-$  by reaction 44 (Table 3). Therefore, the presence of  $\text{SO}_4^{2-}$  ions has the least influence on DPA degradation, attributable to the presence of  $\text{HO}^\bullet$  radicals in the medium and demonstrating that DPA degradation largely takes place *via* the oxidation pathway.

The results in Table 2 and Figure 6 show that, in general, the reduction in dose constant was generally greater when the reaction rate constant of the anion with  $\text{HO}^\bullet$  radicals was higher, confirming the predominance of the oxidative pathway in DPA degradation through reaction with  $\text{HO}^\bullet$  radicals. Thus, the DPA degradation reduction was greater in the presence of  $\text{Br}^-$  ions versus the other radicals because  $\text{Br}^-$  has the highest reaction rate constant with  $\text{HO}^\bullet$  radicals.  $\text{SO}_4^{2-}$  ions are not  $\text{HO}^\bullet$  scavengers, explaining why they had the lowest impact on DPA degradation. To confirm this hypothesis, the rate constants of the reactions of DPA with  $\text{HO}^\bullet$ ,  $e_{\text{aq}}^-$ , and  $\text{H}^\bullet$  were determined (data not shown), yielding:  $k_{\text{HO}^\bullet\text{DPA}} = 4.50 \pm 0.08 \times 10^{10} \text{ M}^{-1} \text{ s}^{-1}$ ,  $k_{e_{\text{aq}}^-\text{DPA}} = 7.60 \pm 0.12 \times 10^9 \text{ M}^{-1} \text{ s}^{-1}$ , and  $k_{\text{H}^\bullet\text{DPA}} = 3.10 \pm 0.31 \times 10^7 \text{ M}^{-1} \text{ s}^{-1}$ , verifying the key role of the oxidation pathway in DPA degradation by gamma irradiation.

### 3.4. Effect of water matrix on DPA degradation

In order to analyze the applicability of the radiolysis system for DPA degradation in aqueous solutions, experiments were conducted with ultrapure water, surface water, and wastewater at an initial DPA concentration of 50 mg/L. Table 1 shows the main characteristics of these water samples. Concentrations of organic matter (TOC), bicarbonate, chloride, sulfate, and nitrate ions were higher in wastewater than in surface water and ultrapure water.

Table 4 lists the dose constants for DPA removal from the three water types, showing the appreciably lower values in wastewater and surface water than in ultrapure water in the order ultrapure water > surface water > wastewater ( $2.74 \pm 0.03 \times 10^{-3}$ ,  $1.20 \pm 0.11 \times 10^{-3}$ , and  $0.58 \pm 0.03 \times 10^{-3}$  Gy<sup>-1</sup>, respectively). One explanation for this decrease in dose constant is that the radiolysis-generated species also react with other solutes in the medium, including dissolved organic matter. This effect was tested by calculating the inhibition rates of the radical species as a function of their solution pH, organic matter content, and alkalinity, using the following equations:

$$r_{\text{HO}\cdot} = k_{\text{H}^+}[\text{H}^+] + k_{\text{TOC}}[\text{TOC}] + k_{\text{HCO}_3^-}[\text{HCO}_3^-] + k_{\text{Cl}^-}[\text{Cl}^-] + k_{\text{NO}_3^-}[\text{NO}_3^-] \quad (45)$$

where  $r_{\text{HO}\cdot}$  is the inhibition rate of HO• radicals in s<sup>-1</sup>.  $k_{\text{H}^+} = 7 \times 10^9$  M<sup>-1</sup> s<sup>-1</sup>,  $k_{\text{TOC}} = 2.0 \times 10^8$  M<sup>-1</sup> s<sup>-1</sup>,  $k_{\text{HCO}_3^-} = 8.5 \times 10^6$  M<sup>-1</sup> s<sup>-1</sup>,  $k_{\text{Cl}^-} = 4.3 \times 10^9$  M<sup>-1</sup> s<sup>-1</sup>, and  $k_{\text{NO}_3^-} = 1.04 \times 10^8$  M<sup>-1</sup> s<sup>-1</sup> [11, 15, 38]. [H<sup>+</sup>], [TOC], [HCO<sub>3</sub><sup>-</sup>], [Cl<sup>-</sup>], and [NO<sub>3</sub><sup>-</sup>] are the initial concentrations of each species present in the water.

$$r_{\text{e}_{\text{aq}}^-} = k_{\text{H}^+}[\text{H}^+] + k_{\text{TOC}}[\text{TOC}] + k_{\text{HCO}_3^-}[\text{HCO}_3^-] + k_{\text{SO}_4^{2-}}[\text{SO}_4^{2-}] + k_{\text{NO}_3^-}[\text{NO}_3^-] \quad (46)$$

where  $r_{\text{e}_{\text{aq}}^-}$  is the inhibition rate of aqueous electron e<sub>aq</sub><sup>-</sup> in s<sup>-1</sup>.  $k_{\text{H}^+} = 2.3 \times 10^{10}$  M<sup>-1</sup> s<sup>-1</sup>,  $k_{\text{TOC}} = 1.0 \times 10^7$  M<sup>-1</sup> s<sup>-1</sup>,  $k_{\text{HCO}_3^-} = 6.0 \times 10^5$  M<sup>-1</sup> s<sup>-1</sup>,  $k_{\text{SO}_4^{2-}} = 1.0 \times 10^6$  M<sup>-1</sup> s<sup>-1</sup>, and

$k_{\text{NO}_3^-} = 9.7 \times 10^9 \text{ M}^{-1} \text{ s}^{-1}$  [11, 15].  $[\text{SO}_4^{2-}]$  is the initial concentrations of each species present in the water.

$$r_{\text{H}\cdot} = k_{\text{H}^+}[\text{H}^+] + k_{\text{TOC}}[\text{TOC}] + k_{\text{HCO}_3^-}[\text{HCO}_3^-] + k_{\text{Cl}^-}[\text{Cl}^-] + k_{\text{NO}_3^-}[\text{NO}_3^-] \quad (47)$$

where  $r_{\text{H}\cdot}$  is the inhibition rate of  $\text{H}\cdot$  radicals in  $\text{s}^{-1}$ .  $k_{\text{H}^+} = 7.8 \times 10^9 \text{ M}^{-1} \text{ s}^{-1}$ ,  $k_{\text{TOC}} = 1.7 \times 10^7 \text{ M}^{-1} \text{ s}^{-1}$ ,  $k_{\text{HCO}_3^-} = 4.0 \times 10^4 \text{ M}^{-1} \text{ s}^{-1}$ ,  $k_{\text{Cl}^-} = 1.0 \times 10^{10} \text{ M}^{-1} \text{ s}^{-1}$ , and  $k_{\text{NO}_3^-} = 4.4 \times 10^6 \text{ M}^{-1} \text{ s}^{-1}$  [11, 15, 38, 42].

Table 4 shows the results obtained for the inhibitory capacity of the three water types studied.  $\text{HO}\cdot$ ,  $\text{e}_{\text{aq}}^-$ , and  $\text{H}\cdot$  radical inhibition rates were much higher in wastewater than in surface water and especially ultrapure water, explaining the markedly decreased dose constant in wastewater.

### 3.5 Time course of TOC and toxicity during DPA degradation

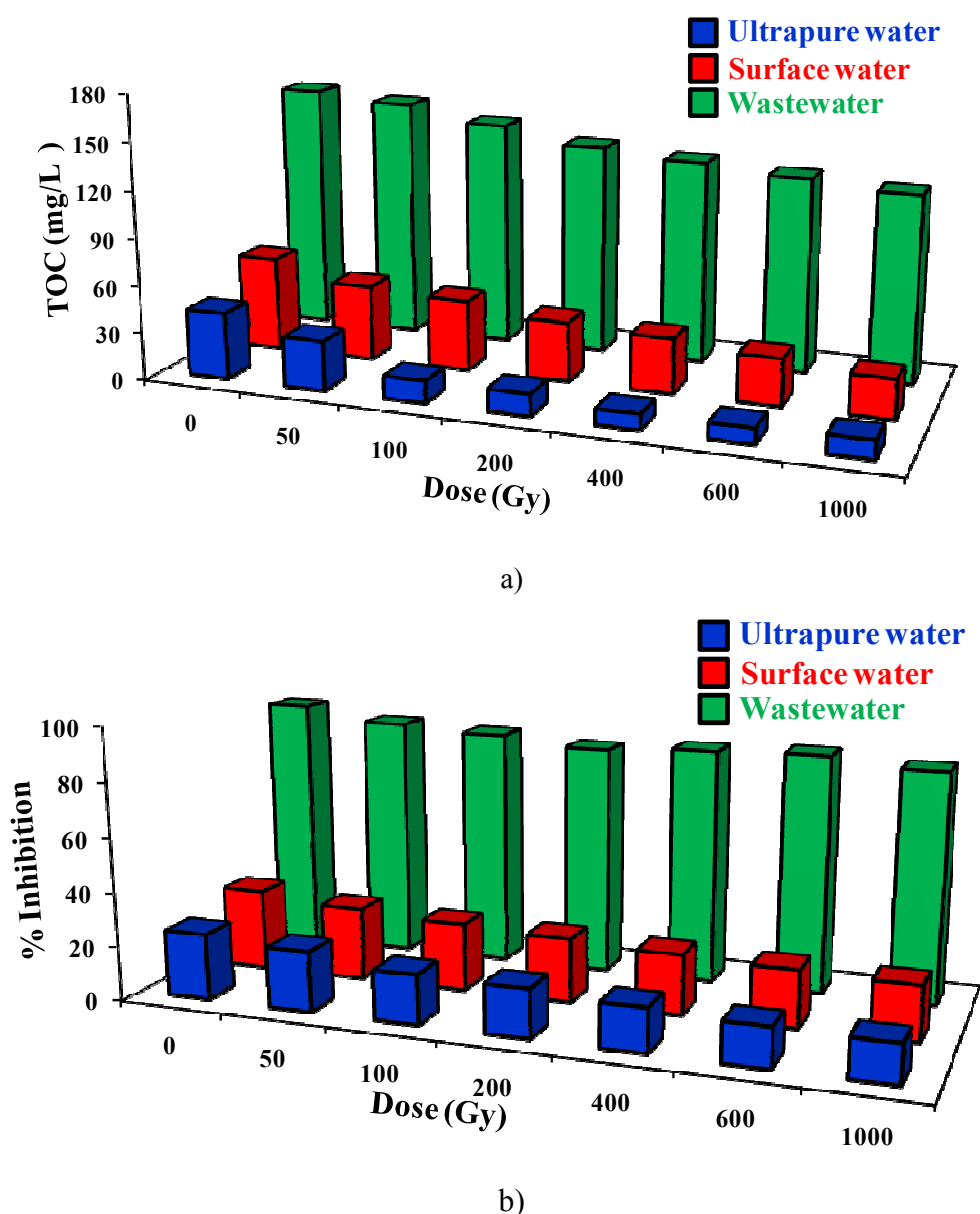
Radiolytic treatment of water polluted with organic products changes the structure of the original compounds, generating byproducts with a lower molecular weight. These can be mineralized to  $\text{CO}_2$ , producing a corresponding decrease in TOC. The usefulness of radiolysis to treat DPA in water depends not only on the effectiveness of the degradation but also on the mineralization of organic matter present and the reduction in toxicity. Therefore, variations in TOC and toxicity were analyzed as a function of the irradiation dose.

Figure 7 a) depicts TOC values in ultrapure water, surface water, and wastewater as a function of the irradiation dose. TOC concentrations decreased at higher doses in all water types. Thus, at a dose of 1000 Gy, the highest percentage mineralization (73%) was obtained in ultrapure water, followed by surface water (58%), and wastewater (25%), as expected given the latter's high concentration of dissolved organic matter.

**Table 4.** Dose constants for the removal of DPA from different water types with the HO•, e<sub>aq</sub><sup>-</sup>, H•, and total radical inhibition rates.

| Type of water          | G <sub>0</sub> ×10<br>(μmol/J) | k x10 <sup>3</sup><br>(Gy <sup>-1</sup> ) | D <sub>50</sub><br>(Gy) | D <sub>90</sub><br>(Gy) | r <sub>HO•</sub><br>(s <sup>-1</sup> ) | r <sub>e-</sub><br>(s <sup>-1</sup> ) | r <sub>H•</sub><br>(s <sup>-1</sup> ) | r <sub>Total</sub><br>(s <sup>-1</sup> ) |
|------------------------|--------------------------------|---|-------------------------|-------------------------|--|---------------------------------------|---------------------------------------|--|
| <b>Ultrapure water</b> | 6.61                           | 2.74±0.03                                 | 252.64                  | 839.26                  | 1.11×10 <sup>3</sup>                   | 3.65×10 <sup>3</sup>                  | 1.24×10 <sup>3</sup>                  | 5.99×10 <sup>3</sup>                     |
| <b>Surface water</b>   | 3.15                           | 1.20±0.11                                 | 557.62                  | 1918.82                 | 4.65×10 <sup>8</sup>                   | 6.83×10 <sup>8</sup>                  | 5.07×10 <sup>8</sup>                  | 1.65×10 <sup>9</sup>                     |
| <b>Wastewater</b>      | 1.67                           | 0.58±0.03                                 | 1195.08                 | 3969.97                 | 2.17×10 <sup>9</sup>                   | 1.02×10 <sup>9</sup>                  | 1.18×10 <sup>9</sup>                  | 4.37×10 <sup>9</sup>                     |

Figure 7 b) depicts the inhibition percentage of *Vibrio Fischeri* bacteria in ultrapure water, surface water, and wastewater as a function of the irradiation dose. Percentage bacteria inhibition values were lower after than before the treatment; thus, at a dose of 1000 Gy, the toxicity was reduced by around 42%, 32%, and 10% in ultrapure water, surface water, and wastewater, respectively. These results confirm that the radiolytic treatment of DPA is most effective in ultrapure water because of the presence of radical scavengers in natural water samples.



**Figure 7.** Variation in TOC (a) and toxicity (b) during DPA degradation with gamma radiation. Dose rate = 1.66 Gy/min,  $[DPA]_0 = 50$  mg/L, pH = 7, and T = 25°C.

#### 4. CONCLUSIONS

Gamma radiation is a feasible and effective treatment to remove DPA from aqueous solutions. DPA degradation increases at higher irradiation doses.

The dose constant shows a slight dependence on the dose rate, while the solution pH exerts a major influence on the DPA degradation rate, whose maximum values is observed at  $\text{pH} = 7$ .

DPA degradation is reduced in the presence of  $\text{Br}^-$ ,  $\text{Cl}^-$ ,  $\text{CO}_3^{2-}$ ,  $\text{NO}_2^-$ ,  $\text{NO}_3^-$ , or  $\text{SO}_4^{2-}$ , and this decrease is greater at high concentrations of these anions, largely due to their competition with DPA for the reactive radicals generated, particularly  $\text{HO}^\bullet$

Dose constants are lower in wastewater and surface water than in ultrapure water because they contain organic matter and  $\text{HCO}_3^-$ ,  $\text{Cl}^-$ ,  $\text{SO}_4^{2-}$ , and  $\text{NO}_3^-$  ions that react with the radiolytically generated reactive radical species ( $\text{HO}^\bullet$ ,  $\text{H}^\bullet$  and  $e_{\text{aq}}^-$ ).

The TOC and toxicity of the medium are reduced during the DPA degradation, confirming the suitability of gamma irradiation to treat water contaminated with DPA.

## 5. REFERENCES

- [1] K.K. Samir, B. Xie, M.L. Thompson, S.W. Sung, S.K. Ong, J.V. Leeuwent, Fate, transport, and biodegradation of natural estrogens in the environment and engineered systems, *Environ. Sci. Technol.* 40 (2006) 6537-6546.
- [2] S. Yoon, S. Jeong, S. Lee, Oxidation of bisphenol A by UV/S<sub>2</sub>O<sub>8</sub><sup>2-</sup>: comparison with UV/H<sub>2</sub>O<sub>2</sub>, *Environ. Technol.* 40 (2012) 123-128.
- [3] D. Kolpin, E.D. Furlong, M.T. Meyer, E.M. Thurman, S. Zaugg, L.B. Barber, H.T. Buxton, Pharmaceutical, hormones, and other organic wastewater contaminants in U.S. streams, 1990-2000: A national reconnaissance, *Environ. Sci. Technol.* 36 (2002) 1202-1211.
- [4] P. Hohenblum, O. Gans, W. Moche, S. Scharf, G. Lorbeer, Monitoring of selected estrogenic hormones and industrial chemicals in ground waters and surface waters in Australia, *Sci. Total Environ.* 333 (2004) 185-193.
- [5] M.F. Brugnera, K. Rajeshwar, J.C. Cardoso, M.V.B. Zanoni, Bisphenol A removal from wastewater using self-organized TiO<sub>2</sub> nanotubular array electrodes, *Chemosphere* 78 (2010) 569-575.
- [6] M. Deborde, S. Rabouan, P. Mazellier, J. Duguet, B. Legube, Oxidation of bisphenol A by ozone in aqueous solution, *Water Res.* 42 (2008) 4299-4308.
- [7] P. He, Z. Zheng, H. Zhang, L. Shao, Q. Tang, PAEs and BPA removal in landfill leachate with Fenton process and its relationship with leachate DOM composition, *Sci. Total Environ.* 407 (2009) 4928-4933.
- [8] F.J. Rivas, Á. Encinas, B. Acedo, F.J. Beltrán, Mineralization of bisphenol A by advanced oxidation processes, *J. Chem. Technol. Biot.* 84 (2009) 589-594..
- [9] E.M. Rodríguez, G. Fernández, N. Klammerth, M.I. Maldonado, P.M. Álvarez, S. Malato, Efficiency of different solar advanced oxidation processes on the oxidation of bisphenol A in water, *Appl. Catal. B-Environ.* 95 (2010) 228-237.

- [10] R. Ocampo-Pérez, J. Rivera-Utrilla, M. Sánchez-Polo, J.J. López-Peñalver, R. Leyva-Ramos, Degradation of antineoplastic cytarabine in aqueous solution by gamma radiation, *Chem. Eng. J.* 174 (2011) 1-8.
- [11] J.W.T. Spinks, R.J. Wood, *Introduction to radiation chemistry*, Willey, New York, 1990.
- [12] Z. Guo, Q. Dong, D. He, C. Zhang, Gamma radiation for treatment of bisphenol A solution in presence of different additives, *Chem. Eng. J.* 183 (2012) 10-14
- [13] L. Guo, B. Wang, W. Huang, F. Wu, J. Huang, Photocatalytic degradation of diphenolic acid in the Presence of beta-Cyclodextrin under UV Light. *E. S. I. A. T.* (2009) 322-324.
- [14] L. Guo, Y. Liu, B. Wang, F. Wu, Y. Li, Photochemical behavior of diphenolic acid in  $\beta$ -Cyclodextrin and  $\text{TiO}_2$  suspensions. *I. C. B. B. E.* (2012) 1-4.
- [15] K.A. Mohamed, A.A. Basfar, A.A. Al-Shahrani, Gamma-ray induced degradation of diazinon and atrazine in natural groundwaters, *J. Hazard. Mater.* 166 (2009) 810-814.
- [16] R. Zhao, H. Bao, L. Xia,  $\square$ -Irradiation degradation of methamidophos, *Chin. J. Chem.* 27 (2009) 1749-1754.
- [17] H. Bao, J. Gao, Y. Liu, Y. Su, A study of biodegradation/ $\square$ -irradiation on the degradation of p-chloronitrobenzene, *Radiat. Phys. Chem.* 78 (2009) 1137-1139.
- [18] A. Bojanowska-Czajka, P. Drzewicz, C. Kozyra, G. Nałęcz-Jawecki, J. Sawicki, B. Szostek, M. Trojanowicz, Radiolytic degradation of herbicide 4-chloro-2-methyl phenoxyacetic acid (MCPA) by  $\square$ -radiation for environmental protection, *Ecotoxicol. Environ. Saf.* 65 (2006) 265-277.
- [19] B. Razavi, W. Song, W.J. Cooper, J. Greaves, J. Jeong, Free-radical-induced oxidative and reductive degradation of fibrate pharmaceuticals: Kinetic studies and degradation mechanisms, *J. Phys. Chem. A* 113 (2009) 1287-1294.



- [20] M. Sánchez-Polo, J. López-Peñalver, G. Prados-Joya, M.A. Ferro-García, J. Rivera-Utrilla, Gamma irradiation of pharmaceutical compounds, nitroimidazoles, as a new alternative for water treatment, *Water Res.* 43 (2009) 4028-4036.
- [21] Y.H. Guo, K.X. Li, J.H. Clark, The synthesis of diphenolic acid using the periodic mesoporous  $H_3PW_{12}O_{40}$ -silica composite catalysed reaction of levulinic acid, *Green chem.* 9 (2007) 839-841.
- [22] R.F. Zhang, J.A. Moore, Synthesis, characterization and properties of polycarbonate containing diphenolic acid, *Polym. Prepr.* 43 (2002) 1007–1008.
- [23] R. Zhang, J.A. Moore, Synthesis, Characterization and properties of polycarbonate containing carboxyl side groups, *Macromol. Sympos.* 199 (2003) 375-390.
- [24] P. Fischer, G.R. Hartraxft, Diphenolic acid ester polycarbonates, *J. Appl. Polym. Sci.* 10 (1966) 245–252.
- [25] B. Cerbai, R. Solaro, E. Chiellini, Synthesis and characterization of functional polyesters tailored for biomedical applications, *J. Polym. Sci. Part A* 46 (2008) 2459-2476.
- [26] C.H. Wang, S. Nakamura, Synthesis of aromatic polyesters having pendant carboxyl groups in the side chains and conversion of the carboxyl groups to other reactive group, *J. Polym. Sci. Part A-Polym. Chem.* 33 (1995) 2157–2163.
- [27] F.K. Chu, C.J. Hawker, P.J. Pomery, D.J.T. Hill, Intramolecular cyclization in hyperbranched polyesters, *J. Polym. Sci. Part A-Polym. Chem.* 35 (1997) 1627–1633.
- [28] Z. Ping, W. Linbo, L. Bo-Geng, Thermal stability of aromatic polyesters prepared from diphenolic acid and its esters, *Polym. Degrad. Stab.* 94 (2009) 1261-1266.
- [29] APHA, AWWA and WPCF, Standard method for the examination of water and wastewater, 20<sup>th</sup> edition. american public health association; american water works association; and water pollution control federation, Washington DC, 1998.

- [30] K. Froehner, T. Backhaus, L.H. Grimme, Bioassays with *Vibrio fischeri* for the assessment of delayed toxicity, *Chemosphere* 40 (2000) 821-828.
- [31] V.L.K. Jennings, M.H. Rayner-Brandes, D.J. Bird, Assessing chemical toxicity with the bioluminescent photobacterium (*vibrio fischeri*): a comparison of three commercial systems, *Water Res.* 35 (2001) 3448-3456.
- [32] A.A. Basfar, K.A. Mohamed, A.J. Al-Abduly, A.A. Al-Shahrani, Radiolytic degradation of atrazine aqueous solution containing humic substances, *Ecotoxicol. Environ. Saf.* 72 (2009) 948-953.
- [33] B.G. Ershov, A.V. Gordeev, A model for radiolysis of water and aqueous solutions of H<sub>2</sub>, H<sub>2</sub>O<sub>2</sub> and O<sub>2</sub>, *Radiat. Phys. Chem.* 77 (2008) 928-935.
- [34] J.M. Joseph, B.S. Choi, P. Yakabuskie, J.C. Wren, A combined experimental and model analysis on the effect of pH and O<sub>2</sub>(aq) on  $\square$ -radiolytically produced H<sub>2</sub> and H<sub>2</sub>O<sub>2</sub>, *Radiat. Phys. Chem.* 77 (2008) 1009-1020.
- [35] B.R. Buxton, C.L. Greenstock, W.P. Helman, A.B. Ross, Critical review of rate constants for reactions hydrated electrons, hydrogen atoms and hydroxyl radicals ( $\bullet\text{OH}/\bullet\text{O}$ ) in aqueous solution, *J. Phys. Chem.* 17 (1988) 513-886.
- [36] Y.B. Tripathi, V. Tripathi, S.N. Tripathi, Beta-blocking activity of inularacemosa, paper presented to 13<sup>th</sup> international congress of biochemistry, Amsterdam, The Netherlands (1985) 25–30
- [37] J.A. LaVerne, M.R. Ryan, T. Mu, Hydrogen production in the radiolysis of bromide solutions. *Radiat. Phys. Chem.* 78 (2009) 1148-1152.
- [38] E. Atinault, V. De Waele, U. Schmidhammer, M. Fattahi, M. Mostafavi, Scavenging of and OH radicals in concentrated HCl and NaCl aqueous solutions, *Chem. Phys. Lett.* 460 (2008) 461-465.
- [39] K. Nash, W. Mulac, M. Noon, S. Fried, J.C. Sullivan, Pulse radiolysis studies of U(VI) complexes in aqueous media, *J. Inorg. Nucl. Chem.* 43 (1981) 897-899.

- [40] T. Løgager, K. Sehested, Formation and decay of peroxyntic acid: A pulse radiolysis study, *J. Phys. Chem.* 97 (1993) 10047-10052.
- [41] M.V. Shankar, S. Nélieu, L. Kerhoas, J. Einhorn, Photo-induced degradation of diuron in aqueous solution by nitrites and nitrates: kinetics and pathways, *Chemosphere* 66 (2007) 767-774.
- [42] S.P. Mezyk, D.M. Bartels, Temperature dependence of hydrogen atom reaction with nitrate and nitrite species in aqueous solution, *J. Phys. Chem. A* 101 (1997) 6233-6237.
- [43] A.J. Elliot, D.R. McCracken, G.V. Buxton, N.D. Wood, Estimation of rate constants for near-diffusion-controlled reactions in water at high temperatures, *J. Chem. Soc., Faraday Trans.* 86 (1990) 1539-1547.
- [44] O. Redlich, R.W. Duerst, A. Merbach, Ionization of strong electrolytes. XI. The molecular states of nitric acid and perchloric acid, *J. Chem. Phys.* 49 (1968) 2986-2994.
- [45] G.A. Poskrebyshev, P. Neta, R.E. Huie, Equilibrium constant of the reaction  $\bullet\text{OH} + \text{HNO}_3 \longleftrightarrow \text{H}_2\text{O} + \text{NO}_3\bullet$  in aqueous solution, *J. Geophys. Res.-Atmos.* 106 (2001) 4995-5004.
- [46] G.A. Poskrebyshev, R.E. Huie, P. Neta, The rate and equilibrium constants for the reaction  $\text{NO}_3\bullet + \text{Cl}^- \longleftrightarrow \text{NO}_3^- + \text{Cl}\bullet$  in aqueous solutions, *J. Phys. Chem. A* 107 (2003) 1964-1970.
- [47] A.R. Cook, N. Dimitrijevic, B.W. Dreyfus, D. Meisel, L.A. Curtiss, D.M. Camaioni, Reducing radicals in nitrate solutions. The  $\text{NO}_3^{2-}$  system revisited, *J. Phys. Chem. A* 105 (2001) 3658-3666.
- [48] R.E. Huie, L.C.T. Shoute, P. Neta, Temperature dependence of the rate constants for reactions of the carbonate radical with organic and inorganic reductants, *Int. J. Chem. Kinet.* 23 (1991) 541-552



## **CONCLUSIONES GENERALES**



## CONCLUSIONES GENERALES

La revisión bibliográfica realizada en esta Tesis Doctoral describe la relevancia ambiental, así como los procesos más recientes aplicados para llevar a cabo la eliminación del ácido ftálico, bisfenol A, ácido difenólico, ácido 2,4-diclorofenoxiacético y ácido 4-cloro-2-metilfenoxiacético del agua destinada al consumo humano, aguas residuales, lodos y suelos. En general, los compuestos seleccionados se suelen encontrar en un amplio rango de concentraciones en los distintos sistemas considerados, siendo, la mayoría de ellos, disruptores endocrinos. La revisión realizada muestra también que hay numerosos procesos utilizados para la eliminación de estos compuestos de los diferentes medios, destacando los procesos químicos y biológicos, sin embargo, son los procesos de oxidación avanzada y las diferentes combinaciones de los mismos los más eficaces en la eliminación de los compuestos estudiados.

El estudio de las cinéticas de adsorción de ácido ftálico, bisfenol A, ácido difenólico, ácido 2,4-diclorofenoxiacético y ácido 4-cloro-2-metilfenoxiacético sobre carbones activados comerciales mostró que el uso de modelos difusionales permite una mejor simulación de la velocidad de adsorción de los contaminantes sobre los carbones, ya que los supuestos considerados en estos modelos se aproximan en mayor medida al proceso real de adsorción. Los carbones activados seleccionados presentan una elevada capacidad de adsorción de ácido ftálico, lo cual puede ser atribuido al establecimiento de interacciones electrostáticas entre la superficie del carbón activado y el adsorbato. El proceso de adsorción del ácido ftálico es altamente dependiente del pH de la disolución, sin embargo, la fuerza iónica no tiene una influencia importante en el proceso de adsorción de este contaminante. Es interesante destacar el papel de los microorganismos en el proceso de adsorción, ya que la presencia de los mismos incrementó considerablemente la capacidad de adsorción de los carbones activados para extraer ácido ftálico. La composición química del agua es otra variable importante en el proceso de adsorción del ácido ftálico; así, la mayor capacidad de adsorción se produjo al utilizar agua residual, lo cual es debido a la precipitación de los ftalatos orgánicos y

la formación de complejos entre el anión ftalato y los cationes metálicos presentes en el agua residual. Además, los resultados obtenidos en régimen dinámico confirmaron la existencia de fenómenos difusionales en el proceso de adsorción del ácido ftálico sobre el carbón activado.

La eliminación del bisfenol A mediante procesos de oxidación avanzada basados en el uso de radiación ultravioleta puso de manifiesto que la radiación ultravioleta no es eficiente en la degradación de este compuesto, determinándose un rendimiento cuántico próximo a cero. Los estudios realizados con los sistemas UV/H<sub>2</sub>O<sub>2</sub>, UV/K<sub>2</sub>S<sub>2</sub>O<sub>8</sub> y UV/Na<sub>2</sub>CO<sub>3</sub> demostraron la gran reactividad del bisfenol A con los radicales hidroxilo ( $k_{\text{HO}\cdot\text{BPA}} = 1.70 \times 10^{10} \text{ M}^{-1} \text{ s}^{-1}$ ), sulfato ( $k_{\text{SO}_4\cdot\text{BPA}} = 1.37 \times 10^9 \text{ M}^{-1} \text{ s}^{-1}$ ) y carbonato/bicarbonato ( $k_{\text{CO}_3\cdot^-/\text{HCO}_3\cdot\text{BPA}} = 3.89 \times 10^6 \text{ M}^{-1} \text{ s}^{-1}$ ). La velocidad de eliminación depende, al igual que en el proceso de adsorción, de la matriz química del agua, del pH de la disolución y de la temperatura. En este proceso, la mayor velocidad de eliminación se observó en aguas residuales, lo cual es debido a una mayor generación de radicales en el proceso de fotooxidación de la materia orgánica disuelta. La mineralización de la materia orgánica disuelta fue más eficiente utilizando el sistema UV/K<sub>2</sub>S<sub>2</sub>O<sub>8</sub>, donde se obtuvo 76% de mineralización a los 60 min de tratamiento, comparado con el 57 y 38% obtenido con los sistemas UV/H<sub>2</sub>O<sub>2</sub> y UV/Na<sub>2</sub>CO<sub>3</sub>, respectivamente. La aplicación del sistema UV/K<sub>2</sub>S<sub>2</sub>O<sub>8</sub> redujo la toxicidad del medio, indicando que los subproductos de degradación generados son menos tóxicos que el compuesto original. Por otro lado, la aplicación del sistema UV/H<sub>2</sub>O<sub>2</sub> incrementó la toxicidad del medio después del tratamiento, lo cual representa una desventaja para su aplicación en sistemas de tratamiento de aguas.

Los resultados obtenidos en el proceso de fotocatalisis (UV/TiO<sub>2</sub>/carbón activado) del ácido 2,4-diclorofenoxiacético han permitido dilucidar el papel que presenta el carbón activado en este proceso. Los datos obtenidos han mostrado que las propiedades químicas del carbón activado son las principales responsables del aumento de la actividad catalítica del proceso combinado UV/TiO<sub>2</sub>/carbón activado. Así, la reducción de los grupos carboxílicos presentes en la superficie del carbón activado por los

electrones generados en el proceso fotocatalítico (UV/TiO<sub>2</sub>) favorece la generación de radicales hidroxilo en el medio, incrementando, de este modo, la eliminación del 2,4-D. Además, la optimización del proceso ha permitido deducir que la variable más importante en el proceso basado en el uso simultáneo de UV/TiO<sub>2</sub>/carbón activado es la dosis de carbón activado adicionada al sistema. Más aun, el uso combinado de UV/TiO<sub>2</sub>/carbón activado conduce a un incremento en el porcentaje de mineralización de la materia orgánica y a una reducción de la toxicidad de los subproductos de degradación.

La determinación de las constantes de velocidad de reacción del ácido ftálico, bisfenol A, ácido difenólico, ácido 2,4-diclorofenoxiacético y ácido 4-cloro-2-metilfenoxiacético con el radical hidroxilo, el electrón y el átomo de hidrógeno (principales productos generados en el proceso radiolítico del agua) ponen de manifiesto que la radiólisis se presenta como una alternativa prometedora en la eliminación de contaminantes orgánicos de las aguas. El efecto de las variables operacionales sobre la eficiencia del proceso radiolítico se estudió usando como compuesto modelo el ácido difenólico. Los resultados obtenidos ponen de manifiesto que el pH de la disolución desempeña un papel fundamental en la velocidad de eliminación. Así, la máxima degradación se alcanza a pH 7. Además, los experimentos realizados en presencia de aniones comúnmente encontrados en las aguas naturales (Br<sup>-</sup>, Cl<sup>-</sup>, CO<sub>3</sub><sup>2-</sup>, NO<sub>2</sub><sup>-</sup>, NO<sub>3</sub><sup>-</sup> o SO<sub>4</sub><sup>2-</sup>) mostraron una reducción en la velocidad de degradación del ácido difenólico, especialmente con aquellos aniones que actúan como atrapadores de radicales hidroxilo. Es interesante destacar que, independientemente de las condiciones experimentales utilizadas, la concentración de la materia orgánica disuelta, así como la toxicidad de los subproductos de degradación se reducen durante el proceso radiolítico del ácido difenólico. Finalmente, los resultados obtenidos con aguas naturales muestran que la eficiencia del proceso radiolítico se ve reducida en aguas caracterizadas por presentar elevada concentración de materia orgánica disuelta, así como con aguas caracterizadas por presentar una elevada concentración salina, ya que ambos factores actúan como inhibidores de radicales.

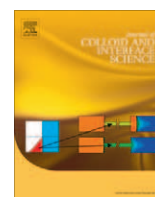






**PUBLICACIONES**





## Adsorption/bioadsorption of phthalic acid, an organic micropollutant present in landfill leachates, on activated carbons

José D. Méndez-Díaz, Mahmoud M. Abdel daiem, José Rivera-Utrilla\*, Manuel Sánchez-Polo, Isidora Bautista-Toledo

Departamento de Química Inorgánica, Facultad de Ciencias, Universidad de Granada, 18071 Granada, Spain

### ARTICLE INFO

#### Article history:

Received 3 October 2011

Accepted 27 November 2011

Available online 7 December 2011

#### Keywords:

Activated carbon

Adsorption

Phthalic acid

Microorganisms

### ABSTRACT

This study investigated the adsorption of phthalic acid (PA) in aqueous phase on two activated carbons with different chemical natures, analyzing the influence of: solution pH, ionic strength, water matrix (ultrapure water, ground water, surface water, and wastewater), the presence of microorganisms in the medium, and the type of regime (static and dynamic). The activated carbons used had a high adsorption capacity (242.9 mg/g and 274.5 mg/g), which is enhanced with their phenolic groups content. The solution pH had a major effect on PA adsorption on activated carbon; this process is favored at acidic pHs. PA adsorption was not affected by the presence of electrolytes (ionic strength) in solution, but was enhanced by the presence of microorganisms (bacteria) due to their adsorption on the carbon, which led up to an increase in the activated carbon surface hydrophobicity. PA removal varies as a function of the water type, increasing in the order: ground water < surface water  $\approx$  ultrapure water < wastewater. The effectiveness of PA adsorption was lower in dynamic than in static regime due to the shorter adsorbent–adsorbate contact time in dynamic regime.

© 2011 Elsevier Inc. All rights reserved.

### 1. Introduction

Industrial activity has led to the release of a large number of synthetic organic chemicals into the environment [1], including plasticizers and organic esters, which are added to polymers to facilitate their processing and increase the flexibility and toughness of the final product by internal modification of the polymer molecules [2,3].

The extensive use of plasticizers worldwide has resulted in the presence of phthalates in multiple environments, with evidence of phthalic acid esters (PAEs) in soils, natural water, and wastewater [4]. Due to their very large production and wide distribution, PAEs have become ubiquitous environmental pollutants [5], and some of them are suspected to be mutagens [6] or carcinogens [7]. They are also considered to be endocrine disruptors, a group of contaminants causing special concern [8].

Large amounts of PAEs are leached from plastics dumped at municipal landfills [9]. PAE concentrations in wastewater from chemical plants and nearby rivers ranged from 10 to 300  $\mu\text{g/L}$ , reaching 30 mg/L in wastewater near plasticizer-producing factories [10].

Adsorption on activated carbon is proved to be the most effective and reliable physicochemical non-destructive technique for landfill leachate treatment, achieving a higher reduction in dissolved organ-

ic carbon in comparison to chemical methods [11–13]. In fact, the USA Environmental Protection Agency has acknowledged that adsorption on activated carbon, one of the oldest water treatments, is one of the best methods available to remove organic and inorganic pollutants from water intended for human consumption [14].

Despite its high effectiveness to remove leachate-derived contaminants, few data have been published on the use of adsorption on activated carbon to eliminate PAEs from waters [13,15]. Furthermore, there have been no studies on the effect of the aqueous medium (i.e., natural waters) or of the presence of bacteria on this process, which are highly relevant issues in the real-life treatment of waters polluted with PAEs.

With this background, the objective of this study was to examine the adsorption of phthalic acid (PA), used as model PAE compound, on two activated carbons with different chemical characteristics, analyzing the influence of the medium pH and ionic strength on the adsorption yield. The influence of water type was studied by means of experiments in ultrapure, superficial, subterranean, and waste waters. The effect on PA adsorption of the presence of bacteria in the medium was also investigated.

### 2. Experimental

#### 2.1. Reagents

All chemical reagents used in this study (phthalic acid, potassium phosphates, hydrochloric acid, and sodium chloride) were

\* Corresponding author. Fax: +34 958248526.

E-mail addresses: ppmendez@ugr.es (J.D. Méndez-Díaz), engdaim@ugr.es (M.M. Abdel daiem), jrivera@ugr.es (J. Rivera-Utrilla), mansanch@ugr.es (M. Sánchez-Polo), bautista@ugr.es (I. Bautista-Toledo).





## Review

## Environmental impact of phthalic acid esters and their removal from water and sediments by different technologies – A review

Mahmoud M. Abdel daiem, José Rivera-Utrilla\*, Raúl Ocampo-Pérez, José D. Méndez-Díaz, Manuel Sánchez-Polo

*Inorganic Chemistry Department, Faculty of Science, University of Granada, 18071 Granada, Spain*

## ARTICLE INFO

## Article history:

Received 12 March 2012

Received in revised form

8 May 2012

Accepted 16 May 2012

Available online

## Keywords:

Review

Phthalic acid esters

PAEs in the environment

PAEs removal

Water treatments

Endocrine disrupting chemicals

## ABSTRACT

This article describes the most recent methods developed to remove phthalic acid esters (PAEs) from water, wastewater, sludge, and soil. In general, PAEs are considered to be endocrine disrupting chemicals (EDCs), whose effects may not appear until long after exposure. There are numerous methods for removing PAEs from the environment, including physical, chemical and biological treatments, advanced oxidation processes and combinations of these techniques. This review largely focuses on the treatment of PAEs in aqueous solutions but also reports on their treatment in soil and sludge, as well as their effects on human health and the environment.

© 2012 Elsevier Ltd. All rights reserved.

### 1. Introduction

Legislation on the quality of wastewater discharged into the environment has become increasingly strict and wastewater reutilization more widespread over recent years, leading to the development of novel technologies for treating wastewater and removing new and emerging pollutants (Arévalo et al., 2009). There is a constant generation of new contaminants with unknown short-, medium-, or long-term effects on human health and the environment, whose maximum permissible concentrations have yet to be established. Industrial and pharmaceutical pollutants are causing particular concern due to their continuous discharge into water and their persistence, even at low concentrations (Klavarioti et al., 2009).

Industrial waste has been poorly managed and is becoming a major problem in industrialized regions. Agriculture, chemical, textile and metallurgic industries consume large amounts of water that are released into the environment after processing and contain dissolved toxic substances such as acids, bases, toxic chemical

compounds and heavy metals, all potentially harmful to the environment (Navarro and Font, 1993).

Industrial activity has led to the release of a large number of synthetic organic chemicals into the environment, including plasticizers and organic esters, which are added to polymers to facilitate their processing and increase the flexibility and toughness of the final product by internal modification of the polymer molecules (Bauer and Herrmann, 1997; Nascimento Filho et al., 2003). They are widely used in numerous products, such as medical equipment, food film, upholstery, flooring, mouldings, gaskets, piping, rain-wear, electrical wire insulation, roofing systems, vehicle trim/undercoating, and pond liners, among others. They also serve to endow paints with special coating properties.

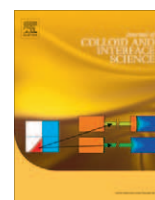
The most widely used primary plasticizers have a low molecular weight and are designated monomeric plasticizers, distinguishing them from polymeric plasticizers, which are generally saturated polyesters. The most common monomeric plasticizers are esters derived from phthalic acid, although others are derived from different organic acids, such as phosphates, trimellitates, citrates, sebacates, and adipates, among others (Titow, 1990; Wickson, 1993). The content of phthalate in a finished plastic product ranges from 10 to 60% by weight (IARC, 2000).

Polyvinylchloride (PVC) is an excellent example of the industrial importance of plasticizers (Horn et al., 2004). PVC is one of the most

\* Corresponding author. Tel.: +34 958248523; fax: +34 958248526.

E-mail addresses: [engdaim@ugr.es](mailto:engdaim@ugr.es) (M.M. Abdel daiem), [jrivera@ugr.es](mailto:jrivera@ugr.es) (J. Rivera-Utrilla), [ocampor@correo.ugr.es](mailto:ocampor@correo.ugr.es) (R. Ocampo-Pérez), [ppmendez@ugr.es](mailto:ppmendez@ugr.es) (J.D. Méndez-Díaz), [mansanch@ugr.es](mailto:mansanch@ugr.es) (M. Sánchez-Polo).





## Modeling adsorption rate of organic micropollutants present in landfill leachates onto granular activated carbon

Raúl Ocampo-Pérez, Mahmoud M. Abdel daiem, José Rivera-Utrilla\*, José D. Méndez-Díaz, Manuel Sánchez-Polo

*Inorganic Chemistry Department, Faculty of Science, University of Granada, 18071 Granada, Spain*

### ARTICLE INFO

#### Article history:

Received 9 May 2012

Accepted 3 July 2012

Available online 16 July 2012

#### Keywords:

Activated carbon

Organic micropollutants

Adsorption rate

Pore volume diffusion

### ABSTRACT

The overall adsorption rate of single micropollutants present in landfill leachates such as phthalic acid (PA), bisphenol A (BPA), diphenolic acid (DPA), 2,4-dichlorophenoxy-acetic acid (2,4-D), and 4-chloro-2-methylphenoxyacetic acid (MCPA) on two commercial activated carbons was studied. The experimental data obtained were interpreted by using a diffusional model (PVSDM) that considers external mass transport, intraparticle diffusion, and adsorption on an active site. Furthermore, the concentration decay data were interpreted by using kinetics models. Results revealed that PVSDM model satisfactorily fitted the experimental data of adsorption rate on activated carbon. The tortuosity factor of the activated carbons used ranged from 2 to 4. The contribution of pore volume diffusion represented more than 92% of intraparticle diffusion confirming that pore volume diffusion is the controlling mechanism of the overall rate of adsorption and surface diffusion can be neglected. The experimental data were satisfactorily fitted the kinetic models. The second-order kinetic model was better fitted the experimental adsorption data than the first-order model.

© 2012 Elsevier Inc. All rights reserved.

### 1. Introduction

Among organic micropollutants detected in wastewater are those from landfill leachates such as: phthalic acid (PA), bisphenol A (BPA), diphenolic acid (DPA), 2,4-dichlorophenoxy-acetic acid (2,4-D) and 4-chloro-2-methylphenoxyacetic acid (MCPA) [1–3]. PA, BPA, and DPA are used as plasticizers, flame retardants, fungicides, antioxidants, and rubber chemicals, as well as in the production of epoxy and unsaturated polyesters-styrene resins. They are considered endocrine disruptor pollutants [4,5]. 2,4-D is a widely used herbicide in the world [6]; it is commonly preferred because of its low cost and good selectivity [7], and MCPA is frequently utilized for control of a wide variety of broadleaf weeds in cornfield, grasses, orchards, grapes, flax, sugarcane, pulses and non-crop areas. Both herbicides have been frequently detected in drinking water [8].

Activated carbon is the most commonly employed adsorbent for industrial applications, especially to eliminate organic compounds from aqueous solution due to its chemical and textural properties. Adsorption on activated carbon has been recommended by the USA Environmental Protection Agency as the best available technology for removing non-biodegradable toxic organic compounds from drinking water and industrial wastewater [9].

In previous works [10,11], the adsorption of PA and BPA in aqueous solution on activated carbons with different chemical nature were investigated. It was found that the activated carbons used had a high capacity to adsorb PA due to their phenolic groups content; moreover, the adsorption capacity was favored at acidic pHs and it was not significantly affected by the presence of electrolyte. The adsorption of BPA fundamentally depends on the chemical nature of the carbon surface and the solution pH. Furthermore, the presence of electrolytes in solution favored the adsorption process due to a screen effect; however, the presence of mineral matter in carbons reduced their adsorption capacity because of the hydrophilic nature of this matter. Ayranci and Bayram [12] studied the adsorption behavior of PA and its three esters: dimethyl phthalate, diethyl phthalate, and diallyl phthalate onto activated carbon cloth, and they found that the adsorption process of these phthalate species followed the first-order kinetic rate. Liu et al. [13] investigated the adsorption of BPA on granular activated carbon modified with nitric acid and thermal treatment. They reported that the experimental kinetic data were well described by the pseudo-second order kinetic model, as well as that the adsorbed amount of BPA decreased by increasing temperature and pH. Aksu and Kabasakal [7] studied the adsorption of 2,4-D on activated carbon. The adsorption equilibrium data were satisfactorily fitted by the Freundlich and Koble–Corrigan isotherm models, and the adsorption rate data were interpreted with a pseudo first-order kinetic model.

\* Corresponding author. Fax: +34 958248526.

E-mail address: jriversa@ugr.es (J. Rivera-Utrilla).







## Role of activated carbon in the photocatalytic degradation of 2,4-dichlorophenoxyacetic acid by the UV/TiO<sub>2</sub>/activated carbon system

J. Rivera-Utrilla\*, M. Sánchez-Polo, M.M. Abdel daiem, R. Ocampo-Pérez

Department of Inorganic Chemistry, Faculty of Science, University of Granada, 18071, Granada, Spain

### ARTICLE INFO

#### Article history:

Received 24 May 2012

Received in revised form 12 July 2012

Accepted 16 July 2012

Available online xxx

#### Keywords:

2,4-Dichlorophenoxyacetic acid

Photodegradation

Titanium dioxide

Ozonated activated carbon

### ABSTRACT

The objective of this study was to photocatalytically degrade the pesticide 2,4-dichlorophenoxyacetic acid (2,4-D) by using the integrated UV/TiO<sub>2</sub>/activated carbon system and to study the degradation kinetics and the role of the chemical and textural properties of activated carbon in this process. Results obtained show that the presence of activated carbon during the catalytic photodegradation (UV/TiO<sub>2</sub>) of 2,4-D considerably increases its percentage removal. After 60 min of treatment, the highest percentage 2,4-D degradation is obtained in the presence of the activated carbons with the greatest content of carboxyl groups. In order to determine the role of activated carbon in this process, we determined the adsorptive and photocatalytic contribution (UV/TiO<sub>2</sub>) to the overall 2,4-D removal. The total percentage removal by the UV/TiO<sub>2</sub>/activated carbon system is much higher than the value obtained by summing the adsorptive and catalytic contributions, mainly when the carbon has an elevated carboxyl group content. No relationship was observed between the textural properties of activated carbons and their synergistic activity; however, the carbons with the greatest carboxyl group content showed the highest synergistic activity. Together with the results of chemical and superficial characterization of the carbon samples after their utilization in the photocatalytic process (UV/TiO<sub>2</sub>), these findings demonstrate that the reduction of superficial carboxyl groups to alcohol groups is the main pathway by which activated carbon enhances the additional generation of HO• radicals in the medium. Experiments conducted in the presence of radical scavengers (carbonate ions, sulfate ions, and *t*-butanol) revealed that H<sup>+</sup>, e<sub>aq</sub><sup>-</sup>, and HO• species participate in the 2,4-D photodegradation. According to the time course of total organic carbon and toxicity during 2,4-D photodegradation, its complete mineralization is not achieved, and the toxicity of the degradation compounds is lower than that of 2,4-D.

© 2012 Elsevier B.V. All rights reserved.

### 1. Introduction

In general, polluted waters are effectively treated by biological treatment plants using adsorbents or conventional chemical processes (chlorination, ozonation, or oxidation with permanganate). However, these procedures are occasionally unable to degrade the pollutants present to the levels required by law and for subsequent use of the effluent. Over the past few years, new technologies have been developed, known as advanced oxidation processes (AOPs), which have proven highly effective in the oxidation of numerous organic and inorganic compounds. The mechanism underlying all of these processes is the generation of free radicals, especially the hydroxyl radical (HO•) [1].

An alternative to the generation of free radicals is photocatalysis on the surface of a semiconductor. Heterogeneous photocatalysis consists of the direct or indirect absorption of visible or

ultraviolet (UV) radiant energy by a solid that, in its excited form, acts as a catalyst for degradation reactions with compounds at the solid–liquid interface. Various semiconductor materials possess suitable characteristics for their utilization as photocatalysts, i.e., stability, economical affordability and no requirement for excessively energetic radiation, and those that are activated by the radiation of the visible spectrum are of particular interest. The literature includes studies of photocatalysts such as TiO<sub>2</sub>, ZnO, SnO<sub>2</sub>, WO<sub>3</sub>, ZrO<sub>2</sub>, CeO<sub>2</sub>, CdS, and Fe oxides, which have all evidenced a good performance in the removal of numerous pollutants [2–7].

It was recently reported that carbon materials can markedly improve the photocatalytic process, largely through one of the three following mechanisms: (i) minimization of the recombination of photogenerated electron–hole pairs; (ii) modification of the band gap of the photocatalyst to higher wavelengths; and (iii) presence of adsorption centers that accelerate contact between pollutant and catalyst [8–15].

Various researchers have reported a clear correlation between the photocatalytic activity of carbon/TiO<sub>2</sub> composites and the chemical and textural properties of the activated carbon (AC) used

\* Corresponding author. Tel.: +34 958248523; fax: +34 958248526.  
E-mail address: [jrivera@ugr.es](mailto:jrivera@ugr.es) (J. Rivera-Utrilla).





